FURTHERING THE REACTIVITY OF LOW-NUCLEARITY N-HETEROCYCLIC CARBENE SUPPORTED COPPER(I) COMPLEXES

A Dissertation
Presented to
The Academic Faculty

by

Abraham J. Jordan

In Partial Fulfillment
of the Requirements for the Degree
Doctor of Philosophy in the
School of Chemistry and Biochemistry

Georgia Institute of Technology
August 2019

FURTHERING THE REACTIVITY OF LOW-NUCLEARITY N-HETEROCYCLIC CARBENE SUPPORTED COPPER(I) COMPLEXES

Approved by:

Dr. Joseph P. Sadighi, Advisor
School of Chemistry and Biochemistry
Georgia Institute of Technology

Dr. Jake D. Soper
School of Chemistry and Biochemistry
Georgia Institute of Technology

Dr. Angus P. Wilkinson
School of Chemistry and Biochemistry
Georgia Institute of Technology

Dr. Stefan France
School of Chemistry and Biochemistry
Georgia Institute of Technology

Dr. Christopher W. Jones
School of Chemical and Biomolecular Engineering
Georgia Institute of Technology

Date Approved: June 28th, 2019

To mom and dad.

ACKNOWLEDGEMENTS

It would be impossible to thank all the people who have helped me reach this point, and I will inevitably leave someone out who deserves thanks. Throughout this process, I've been fortunate to come across many wonderful people who have helped along the way, and I would like to take this opportunity to thank them.

First, and foremost I would like to thank Joseph Sadighi. As my advisor, he has had the most direct involvement in my Ph.D. work and this thesis, but much more so, I am extremely grateful for his all his efforts in my development over the past five years. From him, I have learned innumerable lessons that have made me a better scientist, and I will no doubt look to these throughout my career.

I am extremely lucky to a have been a part of a fantastic research group and would like to thank, Chelsea Wyss, Brandon Tate, Wes Napoline, Nick Daugherty, Yu Cao, Kevin Omolo, Chris Sato, Neil Dodd, Percie Thompson, Kelly Schultz, Rebecca Walde, Sabrine Cypher, Andrew Royappa, Alyssa DeLucia, Chase Morey and David Hopkins for all being excellent lab mates. I owe Chelsea Wyss extra thanks for training me when I first joined the group, as well as Percie Thompson, Kelly Schultz, and Rebecca Walde who have all worked with me on my thesis work.

Additionally, I would like to thank the School of Chemistry and Biochemistry as whole for helping to provide a good graduate experience, and especially all the friends I've made here at Georgia Tech. I'd like to thank Leslie Gelbaum and Hanno Leisen for their assistance in the NMR facilities, David Bostwick for his help in performing mass

spectrometry experiments, and John Bacsa for his efforts in determining the crystallographic structures.

I would like to thank my committee, Jake Soper, Angus Wilkinson, Stefan France and Christopher Jones for their valuable insight and discussions about my thesis work and their kind allowance in borrowing chemicals and using instruments.

I would also like to thank my high school chemistry teachers, Kelly Halko and Ranald Bleakley. While I may not have appreciated it at the time, they first sparked a curiosity and interest in chemistry that has led me here. Furthermore, I would like to thank the Department of Chemistry at the Virginia Military Institute, especially Daren Timmons, Tappey Jones and Dan Harrison. Their encouragement and discussions about chemistry and life, both at VMI and throughout graduate school has been highly cherished.

Finally, I would like to thank my parents, Roger and Dawn. They've taught me countless lessons that were just as important to success in graduate school as what I learned in class or lab, and I am forever grateful for their continuous love and support.

Thank you all.

TABLE OF CONTENTS

LIST OF TABLES

LIST OF FIGURES

LIST OF SCHEMES

LIST OF SYMBOLS AND ABBREVIATIONS

5Dipp	1,3-bis-(2,6-diisopropylphenyl)imidazolin-2-ylidene
6Dipp	1,3-bis(2,6-diisopropylphenyl)-3,4,5,6-tetrahydropyrimidin-2-ylidene
6Mes	1,3-bis(2,4,6-trimethylphenyl)-3,4,5,6-tetrahydropyrimidin-2-ylidene
7Dipp	1,3-bis(2,6-diisopropyl-phenyl)-4,5,6,7-tetrahydro-1,3-diazepin-2-ylidene
α	alpha
Å	angstrom
Ar	aryl
aq	aqueous
atm	atmosphere(s)
ATR	attenuated total reflection
β	beta
^{11}B NMR	boron-11 nuclear magnetic resonance
$B_2(cat)_2$	bis(catecholato)diboron
$B_2(neo)_2$	bis(neopentylglycolato)diboron
$B_2(pin)_2$	bis(pinacolato)diboron
t-Bu	*tert*-butyl
br	broad
CAAC	Cyclic alkylamino carbene
calcd	calculated
C	Celsius
^{13}C NMR	carbon-13 nuclear magnetic resonance
CCDC	Cambridge Crystallographic Data Center

C_6D_6	deuterated benzene
C_6H_6	benzene
CD_2Cl_2	deuterated dichloromethane
CH_2Cl_2	dichloromethane
CD_3CN	deuterated acetonitrile
CH_3CN	acetonitrile
cm	centimeter
Cy	cyclohexyl
°	degree(s)
deg	degrees(s)
°C	degree(s) Celsius
δ	delta, chemical shift
d	day(s)
d	doublet
dd	doublet of doublets
dq	doublet of quartets
d	deuterated
D	deuterium
DCM	dichloromethane
DEPT-90	Distortionless Enhancement by Polarization Transfer, 90°
Dipp	diisopropylphenyl
DOSY	diffusion ordered spectroscopy
η	eta
Et	ethyl
etc	*et cetera* (and so forth)

Et_2O	diethyl ether
eq.	equivalents
F-TEDA-BF_4	1-Chloromethyl-4-fluoro-1,4-diazoniabicyclo[2.2.2]octane bis(tetrafluoroborate) or Selectfluor™
g	gram(s)
GC-MS	Gas-chromatography mass-spectrometry
^{1}H NMR	proton nuclear magnetic resonance
HB(pin)	4,4,5,5-tetramethyl-1,3,2-dioxaborolane, pinacolborane
Hz	hertz
HOMO	highest occupied molecular orbital
IDipp	1,3-bis(2,6-diisopropylphenyl)-imidazole-2-ylidene
IPr*	1,3-bis(2,6-(diphenylmethyl)-4-methylphenyl)imidazol-2-ylidene
IPr**	1,3-bis[2,6-bis[di(4-*tert*-butylphenyl)methyl]-4-methylphenyl]imidazol-2-ylidene
IR	infrared
K	Kelvin
M	Molar, or moles per liter
m	multiplet
μ	mu
μL	microliter
mg	milligrams
Me	methyl
MeOH	methanol
min	minute(s)
mL	milliliters
mm	millimeters

mmol	millimole
MHz	megahertz
m/z	mass-to-charge ration
neo	neopentylglycolate
NFSI	*N*-fluorobenzenesulfonimide
NHC	N-heterocyclic carbene
NMR	nuclear magnetic resonance
O-*t*-Bu	*tert*-butoxide
%	percent
Ph	phenyl
$PhCF_3$	trifluorotoluene
$PhCH_3$	toluene
pin	pinacolate
Ph_3P	triphenylphosphine
ppm	parts per million
π	pi
i-Pr	isopropyl
q	quartet
quin	quintet
rt	room temperature
σ	sigma
σ*	sigma-antibonding
s	singlet
SIDipp	see 5Dipp
SIPr	see 5Dipp

sept	septet
θ	theta, diffraction angle
t	triplet
TM	transition metal
THF	tetrahydrofuran
UV−vis	ultraviolet-visible
ν	wavenumber
1	$[(IDipp)CuH]_2$
2	$[(CAAC)CuH]_2$
3a	$[(6Dipp)CuH]_2$
3b	$[(7Dipp)CuH]_2$
4a	(6Dipp)copper(I) formate
4b	(7Dipp)copper(I) formate
5a	(6Dipp)copper(I) hexyl
6a	(6Dipp)copper(I) heptanoate
7a	6Dipp)copper(I) (*N*-benzyl)formimidoyl
8	(*E*)-3-fluorohex-3-ene
9	(*E*)-(2-fluorovinyl) benzene
10	(*E*)-(4-fluoro-3-hexen-3-yl) boronic acid neopentylglycolato ester
11	$(IDipp)CuN(SO_2Ph)_2$
12	*E*)-(2-fluoro-1,2-diphenylvinyl)boronic acid neopentyl glycolato ester
13a	Potassium (*E*)-(4-fluorohex-3-en-3-yl)trifluoroborate
13b	Potassium (*E*)-(2-fluoro-1,2-diphenylvinyl)trifluoroborate
13c	Potassium (*E*)-(2-fluoro-1-phenylprop-1-en-1-yl)trifluoroborate
13d	Potassium (*E*)-(1-fluorohex-1-en-2-yl)trifluoroborate

13e Potassium (*E*)-[2-fluoro-1-(4-methoxyphenyl)vinyl]trifluoroborate

13f Potassium (*E*)-[1-([1,1'-biphenyl]-4-yl)-2-fluorovinyl]trifluoroborate

13g Potassium (*E*)-(1-(cyclohex-1-en-1-yl)-2-fluorovinyl)trifluoroborate

13h Potassium (*E*)-[1-(4-(*tert*-butyl)phenyl)-2-fluorovinyl]trifluoroborate

13i Potassium (*E*)-(1-fluoro-1-phenylbut-1-en-2-yl)trifluoroborate (1-fl), potassium (*E*)-(2-fluoro-1-phenylbut-1-en-1-yl)trifluoroborate (2-fl)

13j Potassium (*E*)-(6-pthalimido-1-fluorohex-1-en-2-yl)trifluoroborate

14 2-Fluoro-1-(4-methoxyphenyl)ethenone

15 (2-Fluoroprop-1-ene-1,1-diyl)dibenzene

16 $[(7Dipp)Cu]_2S$

17 (7Dipp)CuSH

18 (7Dipp)CuO-*t*-Bu

19 $[(7Dipp)CuS]_2$

20 $(7Dipp)Cu(NCCD_3)BF_4$

SUMMARY

This thesis focuses on the synthesis of N-heterocyclic carbene (NHC) supported copper(I) complexes and their bond-breaking and bond-forming reactivity. The body of this work discusses new (NHC)copper(I) hydride dimers, the electrophilic fluorination of (NHC)copper(I) vinyls, and the nitrosylation of (NHC)copper(I) sulfide complexes.

First, the expanded-ring N-heterocyclic carbenes 6Dipp and 7Dipp (6Dipp = 1,3-bis(2,6-diisopropylphenyl)-3,4,5,6-tetra-hydropyrimidin-2-ylidene and 7Dipp = 1,3-bis(2,6-diisopropyl-phenyl)-4,5,6,7-tetrahydro-1,3-diazepin-2-ylidene) are shown to support isolable neutral copper hydride dimers. $[(6Dipp)CuH]_2$ reacts with 1-hexene to give (6Dipp)copper(I) hexyl by 1,2-insertion, and with benzyl isonitrile to afford an η^1-formimidoyl by 1,1-insertion.

Next, we show that the electrophilic fluorination of (NHC)copper(I) vinyls results in fluoroalkene formation. Alkynes can be converted to *cis*-(β-fluorovinyl)boronates by reaction with an (NHC)copper(I) boryl generated in situ, followed by *N*-fluorobenzenesulfonimide (NFSI). This sequence gives rise to anti-Markovnikov fluorination products from terminal alkynes. Oxidation of a *cis*-(β-fluorovinyl)trifluoroboronate yields an α-fluoroketone, whereas a palladium-catalyzed Suzuki-Miyuara coupling yields a tetrasubstituted monofluoroalkene.

Lastly, the reactivity of a series of copper(I) sulfide complexes stabilized by the expanded-ring N-heterocyclic carbene 7Dipp, towards nitrosonium (NO^+) is shown. 7Dipp is shown to support neutral sulfide- and disulfide-bridged dicopper(I) complexes, in

addition to a mononuclear copper(I) hydrosulfide. Addition of NO^+ to each of these results in the formation of NHC-supported copper(I) cations and elemental sulfur. Concomitant decomposition of copper(I) to Cu^0 upon reaction of NO^+ with the dicopper(I) sulfide or disulfide is observed, whereas ammonium ion formation is observed upon reaction of the copper(I) hydrosulfide with NO^+. Ammonium ion formation is likewise observed upon reaction of NO^+ with (7Dipp)copper(I) hydride.

INTRODUCTION

Part of this thesis chapter has been adapted with permission from an article co-written by the author:

Jordan, A. J.; Lalic, G.; Sadighi, J. P. Coinage Metal Hydrides: Synthesis, Characterization, and Reactivity. *Chem. Rev.* **2016**, *116*, 8318-8372.

1.1 Organometallic Transformations in Copper-Mediated Processes

As the most abundant and cheapest coinage metal, copper has a long and rich history in catalyzing and mediating organic transformations. In the early 1900s, the Ullmann and Goldberg cross-coupling reactions utilized copper metal for C–C and C–N bond formation.[1] Since then copper has been used in a diverse array of organic transformations, notably in the copper-catalyzed alkyne-azide cycloadditions known as "Click" chemistry.[2] More recently, numerous copper systems have been developed to catalyze the reductive functionalization of alkenes and alkynes, resulting in new C–B, C–C, C–N, or C–Si bonds.[3] These serve as a powerful set of tools to introduce molecular complexity. Moreover, many similar systems had been previously studied for the reduction of ketones and α,β-unsaturated ketones.[3d,3e,4] These overall transformations result in highly functionalized organic products, often in regio- and stereospecific fashion, and typically follow a general framework of fundamental organometallic transformations. These transformations were an important guide to the developments that are presented in this thesis and are outlined below.

Copper halides most often serve as starting complexes for these types of transformations. Ligated copper(I) halides are often stable to air and moisture and are sometimes commercially available. Alternatively, addition of free ligand and copper(I)

salts to the reaction mixture can be sufficient to generate the intended copper(I) complex. Copper(I) halides, or psuedohalides, can then undergo ligand substitution to generate a copper alkoxide, or fluoride (Scheme 1.1a). Copper alkoxides can readily react with dihydrogen, silanes, boranes, silylboranes or diboron reagents to form a corresponding copper hydride, copper silyl or copper boryl via transmetallation (Scheme 1.1b). In many copper-hydride-catalyzed reactions, copper(II) salts are used as an easily handled copper source; they are then reduced *in situ* to the active copper(I) species by the silane. The Cu–H, Cu–B or Cu–Si can add across carbon-carbon multiply bonded species, generating copper carbanion intermediates (Scheme 1.1c, Cupration). These carbanion nucleophiles will react with a number of electrophiles to incorporate a wide range of functionality. Concomitant release of the active copper hydride, boryl or silyl permits catalysis. If a copper halide or pseudohalide is released upon electrophilic functionalization, a promotor such as a group 1 alkoxide can regenerate the active catalytic species.

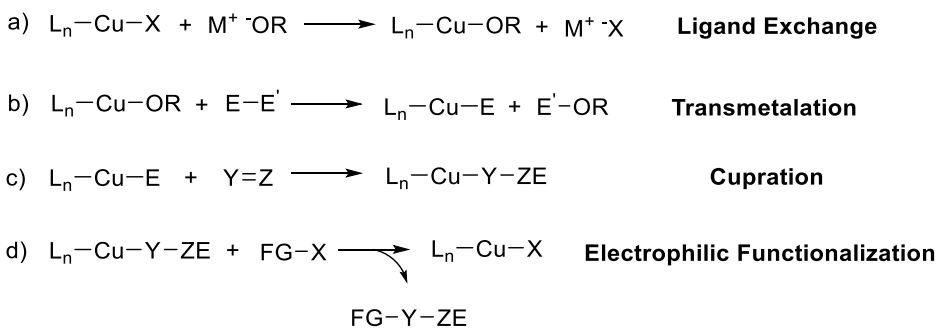

Scheme 1.1 General organometallic transformations of copper-catalyzed reductive functionalizations.

1.2 Mechanistic Considerations of General Transformations

The transmetalation step, forming the active copper-hydride, -boryl, or silyl species, (Cu–E) occurs via a σ-bond metathesis[5] mechanism that passes through a four-centered transition-state (Scheme 1.2). The driving force is derived from the formation a strong main-group–oxygen, or –fluorine bond. The cupration step is suggested to involve a π-complex intermediate between the copper and the C–C multiple bond prior to 1,2-insertion, and must occur in the *syn*-fashion, proceeding through a four-centered transition state.[6] It is worth noting that while the insertion of CO_2 into a copper–boron bond is calculated to involve a π-bound intermediate, the insertion of CO_2 into a copper–methyl or –vinyl does not.[6a,7] The electrophilic functionalization steps are less studied but thought to proceed via concerted σ-bond metathesis mechanisms, or oxidative-addition/reductive-elimination pathways for the hydroamination of alkynes utilizing hydroxylamine esters.[8] Interestingly, the proposed copper(III) intermediates have not been characterized.

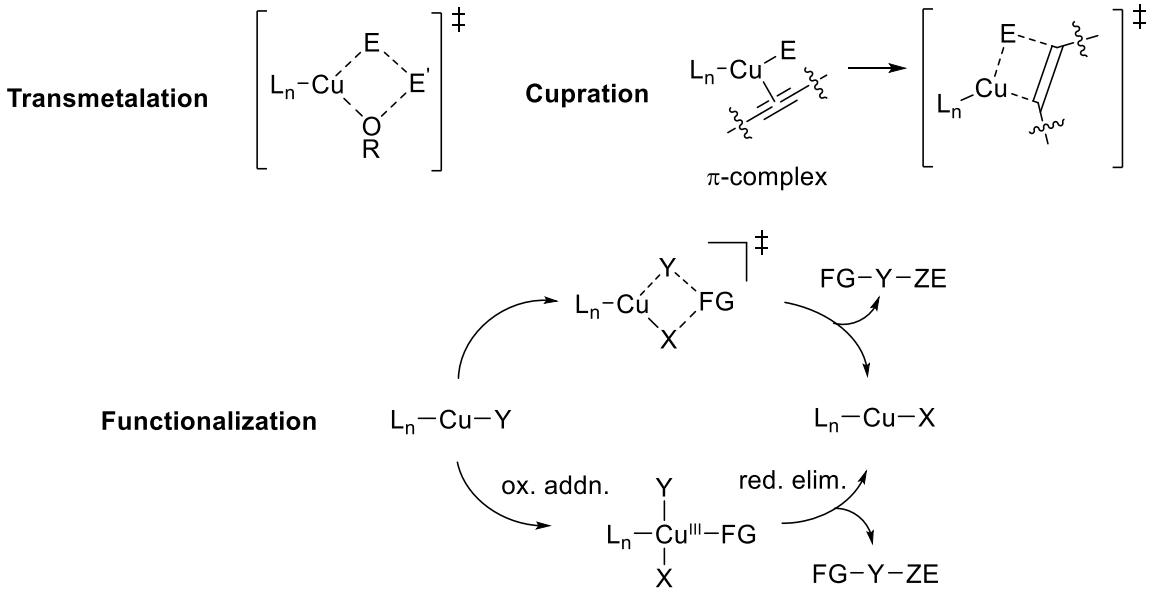

Scheme 1.2 Mechanism of individual transformations.

1.3 Oxidation State Considerations

In the steps presented above the copper center does not need to undergo any redox changes, with the exception of the proposed oxidative-addition/reductive-elimination functionalization pathway. Therefore, in these systems the copper is almost always monovalent. Copper(I) has a fully occupied 3d-subshell, distinct from most earlier transition metal complexes, and an empty 4s orbital which participates in much of the bonding and therefore reactivity. It is important to remember there are non-negligible contributions due to mixing with filled 3d- and empty 4p-orbitals[9] but to a first approximation it is valuable to use the spherically symmetric 4s-orbital to derive bonding motifs in copper(I) complexes. Copper, silver and gold also differ from the group 12 and later metals because their d-subshells remain energetically accessible, and thus the possibility of oxidation state changes must be considered.

The bulk of this thesis will focus on monovalent copper complexes, but copper is prone to one-electron processes that commonly involve the +2 or +3 oxidation states. Since copper(I) has a full d-subshell the complexes are diamagnetic, permitting the use of nuclear magnetic resonance (NMR) spectroscopy to study these complexes. NMR spectra of earlier first-row transition-metals are often not well-defined nor diagnostic due to paramagnetism. ^{1}H, ^{11}B, ^{13}C, ^{19}F and ^{31}P NMR spectroscopy were used extensively and the relevant spectra will be discussed where they lend insight into the chemistry discussed.

1.4 N-Heterocyclic Carbene Supporting Ligands for Copper(I) Complexes

To isolate, characterize and study proposed intermediates relevant to copper(I)-mediated and -catalyzed process, N-heterocyclic carbene (NHC) ligands were employed to stabilize these complexes. NHCs are modular, sterically demanding, strong two-electron σ-donor ligands that are commonly used as ancillary supporting ligands.[10] Phosphines, in addition to NHCs, are commonly employed ligands in copper-catalyzed reductive processes but we have found NHCs to be practical for isolating well-defined copper(I) complexes.

Modification of the NHC backbone and N-substituents affect the steric and electronic parameters of the ligand. We have found NHC ligands that incorporate N-diisopropylphenyl substituents, which provide added steric bulk, successful in stabilizing copper(I) complexes; the four that were most commonly employed throughout this thesis are depicted in Figure 1.1. An increased ring size for the NHC backbone, increases the N–C–N, bond angles influencing the steric and electronic properties.[11] IDipp (1,3-bis(2,6-diisopropylphenyl)-imidazole-2-ylidene, 5Dipp (1,3-bis-(2,6-diisopropylphenyl)imidaz-olein-2-ylidene), 6Dipp (1,3-bis(2,6-diisopropylphenyl)-3,4,5,6-tetrahydropyrimidin-2-ylidene) and 7Dipp (1,3-bis(2,6-diisopropylphenyl)-4,5,6,7-tetrahydro-1,3-diazepin-2-ylidene) have increasing ring size across the series; therefore 7Dipp is the most sterically demanding and the strongest σ-donor. While IDipp is a weakest donor and the least sterically demanding in the series, it is still a very bulky, strong donor.

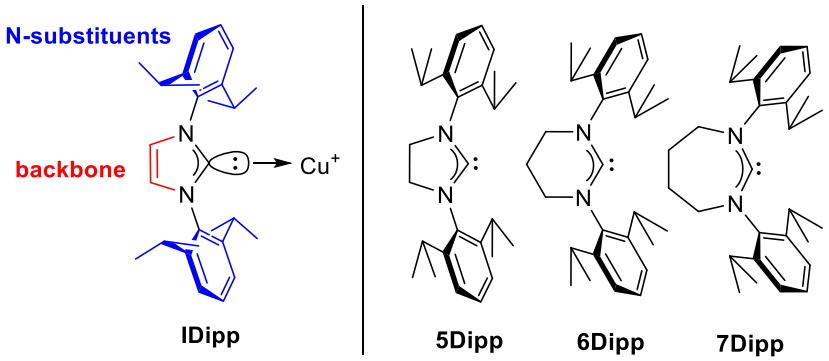

Figure 1.1. Diisopropylphenyl substituted NHCs employed in this work.

(NHC)copper(I) complexes are generally prepared by deprotonation of air-stable cyclic amidinium chloride salts in the presence of copper(I) chloride to give air-stable (NHC)copper(I) chlorides. The amidinium salts are typically readily isolated in two steps from inexpensive commercially available starting materials.[12] Some common amidinium salts, free NHCs and (NHC)copper(I) chloride salts are commercially available, but typically these were easily synthesized in good yield.

1.5 Three-Center Two-Electron Bonded Species

Hydride will often bridge two or more metal centers because its spherically symmetric 1s orbital can overlap well with the transition metal (TM) orbitals. There are a number of ways to classify three-center two-electron bonding in metal complexes[13] but once a bridge is formed the two electrons will reside in a bonding orbital delocalized across the three atoms. For hydride bridges of TMs, the 1s orbital typically interacts with the lobes of d-orbitals whereas the 1s orbital of a hydride bridging group 11 metals will overlap with metal orbitals that are majority s in character (Figure 1.2). The σ-donation of the bridging hydride into a formally empty Cu–Cu bonding orbital can be viewed as increasing the Cu–

Cu interaction.[14] Indeed, bridging hydrides,[15] boryls,[16] and silyls[17] complexes can show extremely short Cu···Cu contacts.

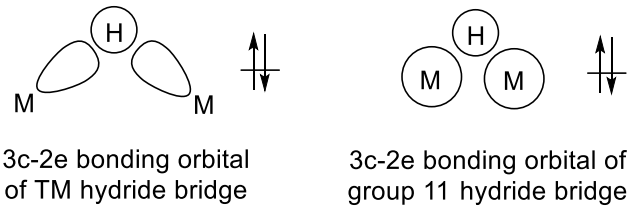

Figure 1.2 Orbital representation of TM hydride bridges.

Copper(I) hydride complexes tend to form oligomers[3e] that feature multiple hydride-bridges, and only recently has there been spectroscopic evidence for a monomeric copper(I) hydride, which is in equilibrium with a dimer.[18] For neutral copper(I) hydrides, the active species is considered to be monomeric that typically exists as a minor component as an equilibrium mixture with its oligomers. The consequences of this oligomeric nature of copper hydrides on the reactivity is not well studied.

The first dimeric copper(I) hydride, reported by Caulton and coworkers is a good example of the energetic favorability of Cu–H bridges.[19] In an attempt to make a 4-coordinate monomeric copper(I) hydride, by hydrogenolysis of $[Cu_4(O\text{-}t\text{-}Bu)_4]$ in the presence of a tripodal phoshine donor ligand, Caulton demonstrated a dimeric $[Cu_2(\mu\text{-}H)_2]$ structure, with a pendant phosphine, to be preferred over the expected four-coordinate monomer bearing a third P–Cu bond (Figure 1.3).

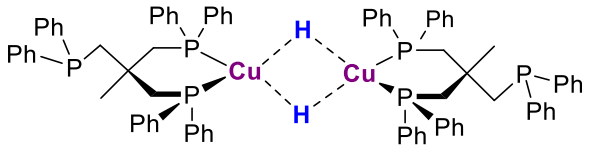

Figure 1.3 Phosphine supported copper hydride dimer bearing pendant phosphine.

Although they will not be the topic of discussion in this thesis it is worth noting that NHC-supported boryl- or silyl-bridged copper(I) complexes also feature three-center two-electron bonds between the boryl/silyl and copper centers.[16-17] Additionally, carbanions can form stable bridges between two copper(I) centers. For example, a vinyl sp^2-orbital can overlap with copper(I) orbitals with a majority 4s character, similarly to the interaction between bridging hydrides (Figure 1.4). Recently, NHCs have been shown to support a number of different bridging silver(I) carbanions.[20] In both neutral and cationic complexes, the hydride or carbon directly bonded to copper(I) centers shows considerable anionic character. This is evident by the insertion of CO_2 into the hydride-bridged dicopper(I) cation to yield a bridging formate (Figure 1.4).[21] A 1,2-insertion of phenyl acetylene yields a vinyl-bridged dicopper(I) cation, featuring a three-center-two-electron bond.[21]

Differing philosophies exist on how to represent three-center two-electron bonding. This thesis will use dashed line notation, as used in Figures 1.3 and 1.4, to indicate partial covalency between copper and hydrogen (or carbon), or between two copper centers. These systems often show short copper–copper distances that is suggestive of possible bonding interactions, but the bonding interaction is not required.

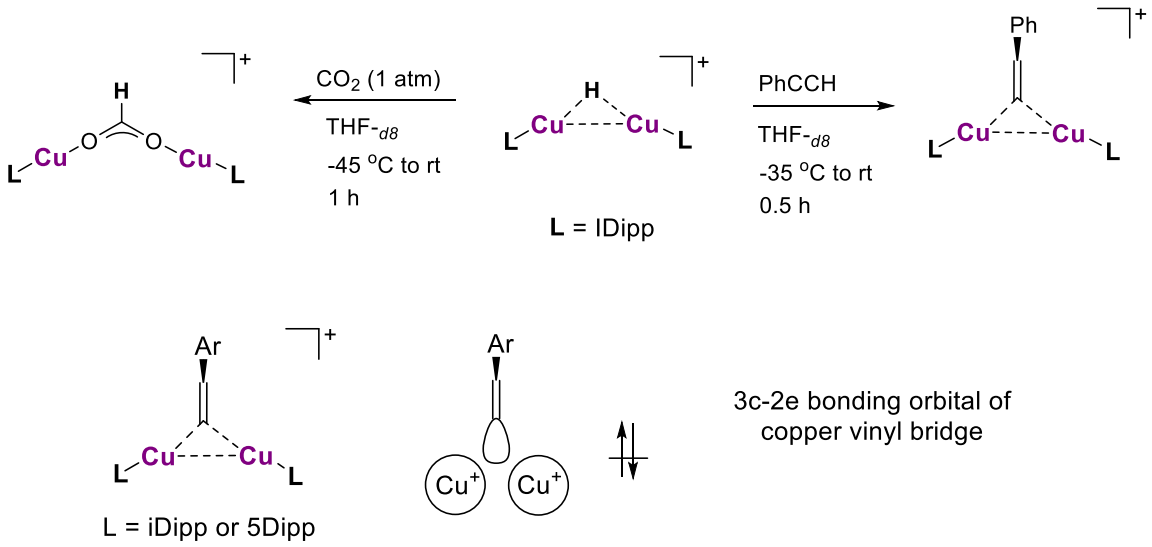

Figure 1.4 Vinyl-bridged dicopper cation bonding.

1.6 Bridged σ- and π-Donor Atoms

In cases which feature three-center two-electron bonding, the bridging atom is considered to be a purely σ-donor. Bridging atoms that also include π-donor capabilities, a halide for example, thus do not feature three-center two-electron bonding, but rather these have four electrons in bonding orbitals between the bridging atom and the metal centers. This bonding is evident in the 5Dipp-supported fluoride-bridged dicopper(I) cation, as well as the analogous fluoride-bridged disilver(I) and digold(I) cations (Figure 1.5).[22] The bent M–F–M core reveals significant covalent character. The fluoride-bridged dicopper(I) cation reacts readily with adventitious moisture to generate HF and the hydroxide-bridged dicopper(I) cation. Additionally, the fluoride-bridged digold(I) cation reacts with allene to generate a vinylic C–F bond.

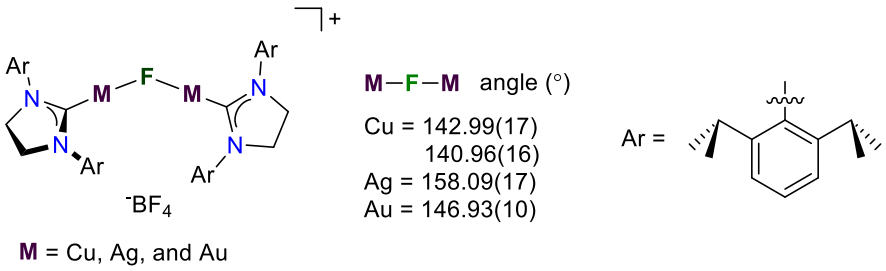

Figure 1.5 Dinuclear fluoride-bridged cations of copper, silver and gold.

In such complexes, a σ-bonding orbital is formed between a p-orbital of the bridging atom and a formal metal-metal bonding orbital, analogous to the three-center two-electron orbital described above. Additionally, a π-bonding orbital arises from overlap of a separate filled p-orbital of the bridging atom with a metal-metal antibonding orbital. This leaves the remaining p-orbital of the bridging atom non-bonding, and most likely the highest occupied molecular orbital (HOMO). Since the π-bonding interaction results in filling of the metal-metal antibonding orbital, no metal-metal interaction should be observed.[14e] This is evident by the increased Cu···Cu distance of the fluoride-bridged dicopper(I) cation compared to the hydride-bridged dicopper(I) cation. This orbital representation would also hold true for bridging chalcogenides such as sulfide (S^{2-}) or selenide (Se^{2-}).

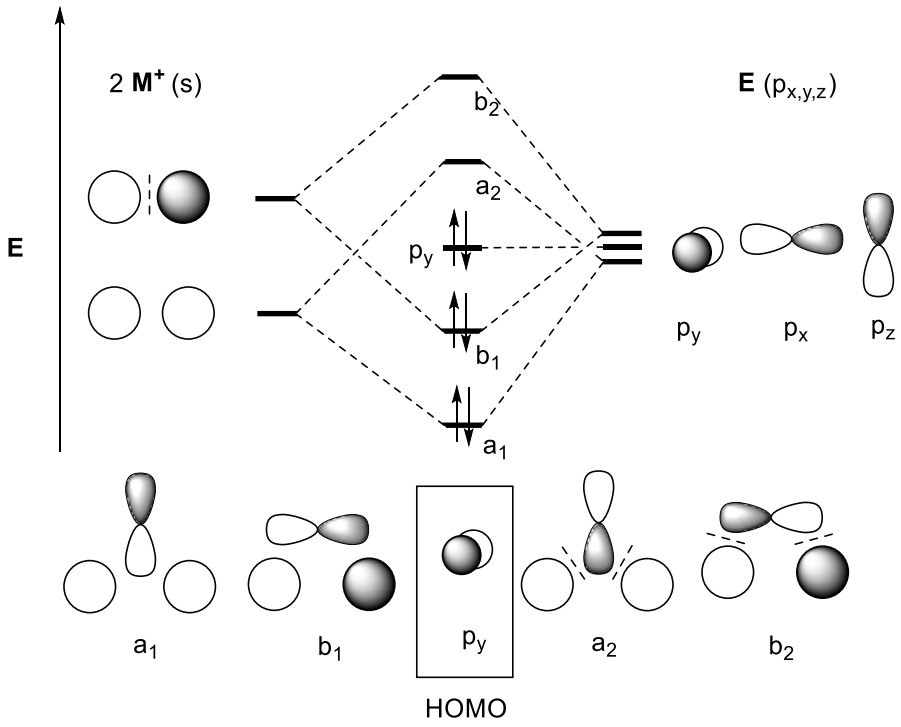

Figure 1.6 Frontier molecular orbital depiction of a bridging donor with two σ-acceptor metal centers.

1.7 Concluding Remarks

This thesis describes the synthesis and reactivity of many new N-heterocyclic carbene supported copper(I) complexes. Understanding the considerations discussed above was imperative to the development of the new organometallic chemistries shown throughout this thesis.

1.8 References

[1] (a) Ullmann, F.; Bielecki, J. *Berichte der deutschen chemischen Gesellschaft* **1901**, *34*, 2174-2185; (b) Ullmann, F.; Sponagel, P. *Berichte der deutschen chemischen Gesellschaft* **1905**, *38*, 2211-2212; (c)Goldberg, I. *Berichte der deutschen chemischen Gesellschaft* **1906**, *39*, 1691-1692.

[2] (a) Hein, J. E.; Fokin, V. V. *Chem. Soc. Rev.* **2010**, *39*, 1302-1315; (b)Liang, L.; Astruc, D. *Coord. Chem. Rev.* **2011**, *255*, 2933-2945; (c) Sletten, E. M.; Bertozzi, C. R. *Acc. Chem. Res.* **2011**, *44*, 666-676

[3] (a) Fujihara, T.; Semba, K.; Terao, J.; Tsuji, Y. *Catal. Sci. Technol.* **2014**, *4*, 1699-1709; (b) Suess, A. M.; Lalic, G. *Synlett* **2016**, *27*, 1165-1174; (c) Soradova, Z.; Sebesta, R. *ChemCatChem* **2016**, *8*, 2581-2588; (d) Mohr, J.; Oestreich, M. *Angew. Chem., Int. Ed.* **2016**, *55*, 12148-12149; (e) Jordan, A. J.; Lalic, G.; Sadighi, J. P. *Chem. Rev.* **2016**, *116*, 8318-8372.

[4] a) Deutsch, C.; Krause, N.; Lipshutz, B. H. *Chem. Rev.* **2008**, *108*, 2916-2927; (b) Rendler, S.; Oestreich, M. *Angew. Chem., Int. Ed.* **2007**, *46*, 498-504.

[5] Waterman, R. *Organometallics* **2013**, *32*, 7249-7263.

[6] (a) Fan, T.; Sheong, F. K.; Lin, Z. *Organometallics* **2013**, *32*, 5224-5230; (b) Semba, K.; Kameyama, R.; Nakao, Y. *Synlett* **2015**, *26*, 318-322; (c) Whittaker, A. M.; Lalic, G. *Org. Lett.* **2013**, *15*, 1112-1115; (d) Van Hoveln, R.; Hudson, B. M.; Wedler, H. B.; Bates, D. M.; Le Gros, G.; Tantillo, D. J.; Schomaker, J. M. *J. Am. Chem. Soc.* **2015**, *137*, 5346-5354; (e) Grigg, R. D.; Van Hoveln, R.; Schomaker, J. M. *J. Am. Chem. Soc.* **2012**, *134*, 16131-16134.

[7] Zhao, H.; Lin, Z.; Marder, T. B. *J. Am. Chem. Soc.* **2006**, *128*, 15637-15643.

[8] Tobisch, S. *Chem. Sci.* **2017**, *8*, 4410-4423.

[9] Mehrotra, P. K.; Hoffmann, R. *Inorg. Chem.* **1978**, *17*, 2187-2189.

[10] Hopkinson, M. N.; Richter, C.; Schedler, M.; Glorius, F. *Nature* **2014**, *510*, 485-496.

[11] a) Gusev, D. G. *Organometallics* **2009**, *28*, 6458-6461; (b) Magill, A. M.; Cavell, K. J.; Yates, B. F. *J. Am. Chem. Soc.* **2004**, *126*, 8717-8724; (c) Fructos, M. R.; Belderrain, T. R.; de Fremont, P.; Scott, N. M.; Nolan, S. P.; Diaz-Requejo, M. M.; Perez, P. J. *Angew. Chem., Int. Ed.* **2005**, *44*, 5284-5288; (d) De Fremont, P.; Scott, N. M.; Stevens, E. D.; Nolan, S. P. *Organometallics* **2005**, *24*, 2411-2418; (e) Dunsford, J. J.; Cavell, K. J.; Kariuki, B. M. *Organometallics* **2012**, *31*, 4118-4121.

[12] (a) Arduengo, A. J., III; Krafczyk, R.; Schmutzler, R.; Craig, H. A.; Goerlich, J. R.; Marshall, W. J.; Unverzagt, M. *Tetrahedron* **1999**, *55*, 14523-14534; (b) Kolychev,

E. L.; Portnyagin, I. A.; Shuntikov, V. V.; Khrustalev, V. N.; Nechaev, M. S. *J. Organomet. Chem.* **2009**, *694*, 2454-2462; (c) Kuhn, K. M.; Grubbs, R. H. *Org. Lett.* **2008**, *10*, 2075-2077.

[13] Green, J. C.; Green, M. L. H.; Parkin, G. *Chem. Commun.* **2012**, *48*, 11481-11503.

[14] (a) Alemany, P.; Alvarez, S. *Inorg. Chem.* **1992**, *31*, 4266-4275; (b)Mealli, C.; Godinho, S. S. M. C.; Calhorda, M. J. *Organometallics* **2001**, *20*, 1734-1742; (c) Koelmel, C.; Ahlrichs, R. *J. Phys. Chem.* **1990**, *94*, 5536-5542; (d)Hermann, H. L.; Boche, G.; Schwerdtfeger, P. *Chem. - Eur. J.* **2001**, *7*, 5333-5342; (e) Wyss, C. M., Ph.D. Thesis, Georgia Institute of Technology, **2015**. https://smartech.gatech.edu/handle/1853/54331 (Accessed June 2019)

[15] Mankad, N. P.; Laitar, D. S.; Sadighi, J. P. *Organometallics* **2004**, *23*, 3369-3371.

[16] Wyss, C. M.; Bitting, J.; Bacsa, J.; Gray, T. G.; Sadighi, J. P. *Organometallics* **2016**, *35*, 71-74.

[17] Plotzitzka, J.; Kleeberg, C. *Inorg. Chem.* **2016**, *55*, 4813-4823.

[18] Romero, E. A.; Olsen, P. M.; Jazzar, R.; Soleilhavoup, M.; Gembicky, M.; Bertrand, G. *Angew. Chem., Int. Ed.* **2017**, *56*, 4024-4027.

[19] Goeden, G. V.; Huffman, J. C.; Caulton, K. G. *Inorg. Chem.* **1986**, *25*, 2484-2485.

[20] Tate, B. K.; Jordan, A. J.; Bacsa, J.; Sadighi, J. P. *Organometallics* **2017**, *36*, 964-974.

[21] Wyss, C. M.; Tate, B. K.; Bacsa, J.; Gray, T. G.; Sadighi, J. P. *Angew. Chem., Int. Ed.* **2013**, *52*, 12920-12923.

[22] Wyss, C. M.; Tate, B. K.; Bacsa, J.; Wieliczko, M.; Sadighi, J. P. *Polyhedron* **2014**, *84*, 87-95.

CHAPTER 2. SYNTHESIS AND REACTIVITY OF NEW COPPER(I) HYDRIDE DIMERS

Part of this thesis chapter has been adapted with permission from an article co-written by the author:

Jordan, A. J.; Wyss, C. M.; Bacsa, J.; Sadighi, J. P. Synthesis and Reactivity of New Copper(I) Hydride Dimers. *Organometallics* **2016**, *35*, 613-616.

2.1 Background

Copper hydrides are key intermediates in transformations of a wide range of unsaturated organic subsrates.[1] The hexameric cluster $[(Ph_3P)CuH]_6$, first reported by Osborn et al.[2] and subsequently known as Stryker's reagent,[3–5] is among the most widely studied copper hydride complexes.[6] Various phosphine donors have provided excellent scaffolds for copper hydrides in numerous reduction processes,[1] with new applications appearing rapidly.[7–11] Exploring lower-nuclearity copper hydrides, Caulton and co-workers showed the hydride bridge in a dimeric $\{Cu_2(\mu\text{-}H_2)\}$ core to be stronger than a potential third P−Cu bond.[12] N-Heterocyclic carbenes (NHCs) also serve as excellent supporting ligands for copper-catalyzed reduction processes.[13–17] While the active (NHC)CuH species is typically generated *in situ*, the solid-state structure of $[(IDipp)CuH]_2$ (**1a**; Figure 2.1) also reveals a dimeric $\{Cu_2(\mu\text{-}H_2)\}$ core.[18]

Recently, Bertrand et al. showed that cyclic alkylaminocarbene (CAAC) ligands greatly improve the stability of the $\{Cu_2(\mu\text{-}H_2)\}$ core (**2**; Figure 2.1).[19] The authors attribute this stability to the increased steric bulk about the metal hindering the formation of larger oligomers. A slight increase in the stability of (NHC)copper(I) hydrides was achieved by

Schomaker et al. by changing the isopropyl groups of IDipp to 3-pentyl or 4-heptyl.[15] Diffusion NMR experiments (DOSY) revealed that the (NHC)copper(I) hydrides favor a dimeric form in solution as well as in the solid state.[15]

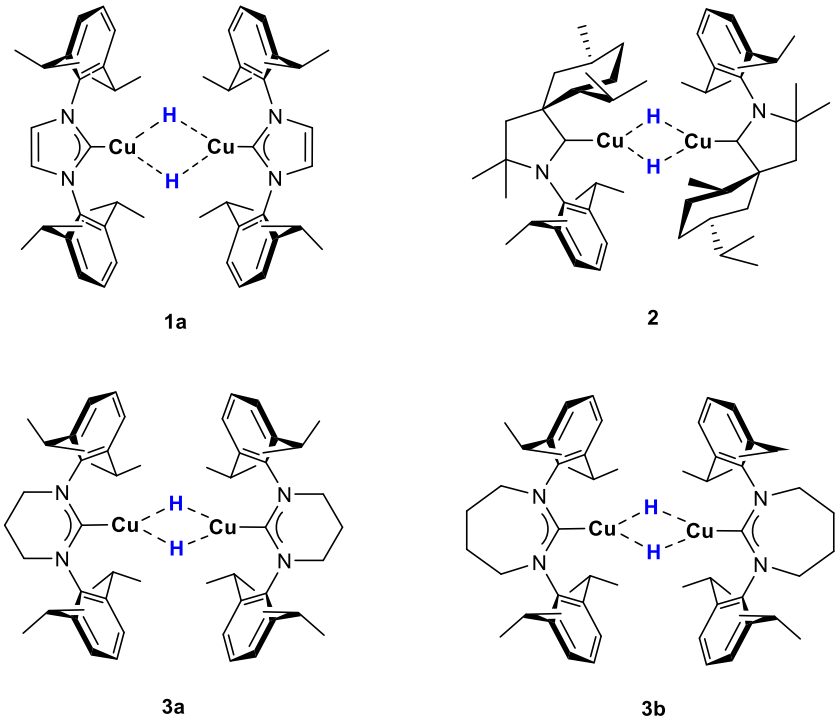

Figure 2.1 Isolable (carbene)copper hydrides: $[(IDipp)CuH]_2$ (**1a**), ref 18; $[(CAAC)CuH]_2$ (**2**), ref 19; **3a,b**, this work.

Expanded-ring NHCs, derived from six- and seven-membered cyclic amidinium salts, have been shown to increase the stability of other reactive metal species.[20–22] Recently, Whittlesey et al. reported that (6Mes)copper(I) hydride (6Mes = 1,3-bis(2,4,6-trimethylphenyl)-3,4,5,6-tetrahydropyrimidin-2-ylidene) proved too unstable to isolate but could be trapped efficiently with alkynes or ketones.[23] We now report the synthesis of $[(6Dipp)CuH]_2$ (**3a**) and $[(7Dipp)CuH]_2$ (**3b**) (6Dipp = 1,3-bis(2,6-diisopropylphenyl)-3,4,5,6-tetrahydropyrimidin-2-ylidene; 7Dipp =1,3-bis(2,6-diisopropylphenyl)- 4,5,6,7-

tetrahydro-1,3-diazepin-2-ylidene). These complexes are stable at ambient temperature, both in the solid state and in solution. Complex **3a** undergoes clean 1,2-insertion of an alkene substrate and 1,1-insertion of an isonitrile.

2.2 Results and Discussion

2.2.1 Synthesis of Expanded-Ring (NHC)Copper(I) Hydrides

The generation of **3a** or **3b** by addition of pinacolborane 4,4,5,5-tetramethyl-1,3,2-dioxaborolane [HB(pin)] to a solution of (6Dipp)CuO-*t*-Bu or (7Dipp)CuO-*t*-Bu is evidenced by the generation of an intense yellow or orange color (Scheme 2.1). The ^{1}H NMR spectra of these hydrides in C_6D_6 solution show characteristic hydride singlets at δ 0.77 ppm (**3a**) and at δ 0.47 ppm (**3b**). For comparison, the spectrum for the analogous $[(5Dipp)CuH]_2$ (1b; 5Dipp = 1,3-bis(2,6- diisopropylphenyl)imidazolin-2-ylidene)[24] shows a hydride resonance at δ 1.93 ppm[25] and that of $[(IDipp)CuH]_2$ at δ 2.67 ppm.[18] This upfield shift in the hydride resonances may be attributed not only to increased electron donation by the NHCs but also to anisotropic shielding by the aryl rings as they are brought closer to the hydrides by the wider N−C−N angle.[26,27]

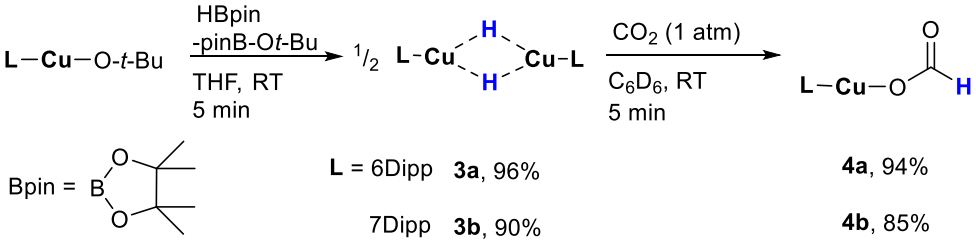

Scheme 2.1 Synthesis and Carboxylation of (NHC)CuH.

2.2.2 Oligomeric Nature of (NHC)Copper(I) Hydrides

The solid-state infrared spectra of **3a** and **3b** show absorptions assigned to bridging hydride−copper stretches at 909 and 912 cm^{-1}, respectively. These values fall between those of 881 cm^{-1} for **1b**[18] and 981 cm^{-1} for **2**.[19] Although stretching frequencies of terminal copper-hydride-complexes have not been reported, to the best of our knowledge, the IR spectrum of monomeric (IDipp)AuH displays a sharp Au−H stretch at 1976 cm^{-1}.[28] We therefore wondered whether dissociation in solution to form a terminal hydride might be observable by IR spectroscopy, but the solution IR spectrum of **3a** (Figure 2.2) displayed no absorption we would attribute to a terminal copper hydride. Moreover, the bridging hydride absorption remains, suggesting that the dimeric form is favored in solution, as it is for hydrides bearing five-membered NHCs.[15]

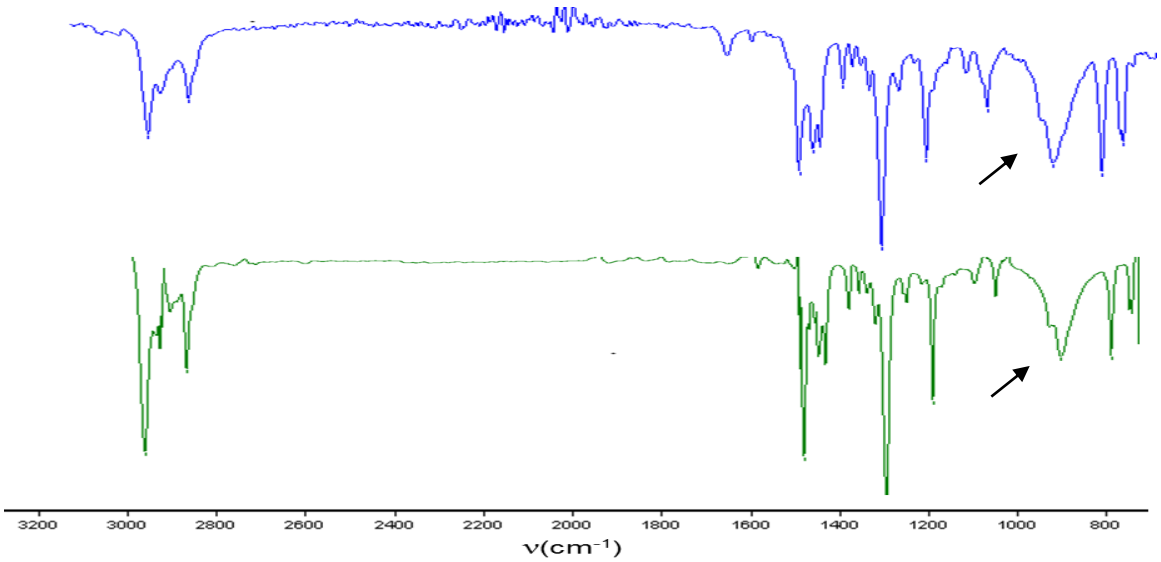

Figure 2.2 Infrared spectra of $[(6Dipp)CuH]_2$, solid state (top, blue) and solution cell (bottom, green). The solution cell IR spectrum of $[(6Dipp)CuH]_2$ was taken as a solution in toluene loaded into a 0.1mm path length cell using a Bruker Alpha-P infrared spectrometer.

The intense yellow color of copper hydride dimers, unusual for copper(I) complexes, is well documented.[18,19,29] The UV−vis absorption spectra of **3a,b** show strong absorptions at 453 and 476 nm, respectively (Figure 2.3). These electronic transitions have not been definitively assigned, but the close Cu···Cu contact[18,19] may allow a dσ* → pσ transition analogous to those identified by Gray et al. for d^8–d^8 and d^{10}–d^{10} complexes of Pd and Pt.[30–33]

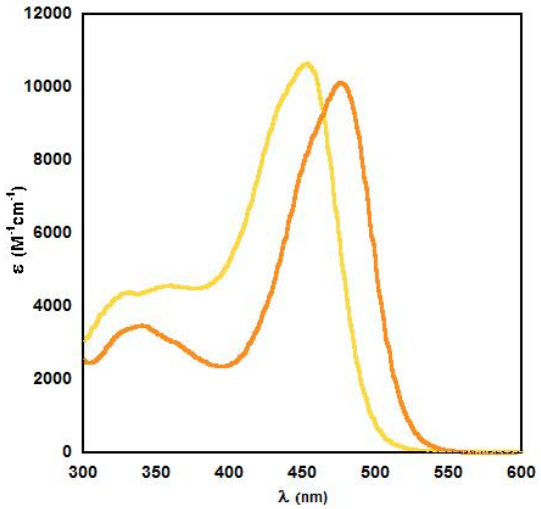

Figure 2.3 UV-Vis absorption spectra of **3a** (yellow) and **3b** (orange) in toluene.

Although the dimeric form is favored in solution, and neither the monomeric 6Dipp or 7Dipp supported copper(I) hydride is observed, we still suggest that a monomeric form exists as minor component of an equilibrium mixture with the dimer. To probe this question, we combined equimolar [(6Dipp)CuH)$_2$] and [(6Dipp)CuD)$_2$]. The ^{1}H NMR spectrum showed one new resonance at 0.81 ppm, corresponding to [(6Dipp)Cu]$_2$-(μ-H)-(μ-D). Formation of the mixed hydride-deuteride complex suggests that small concentrations of the terminal hydride and deuteride are at equilibrium, then recombine (Figure 2.4).

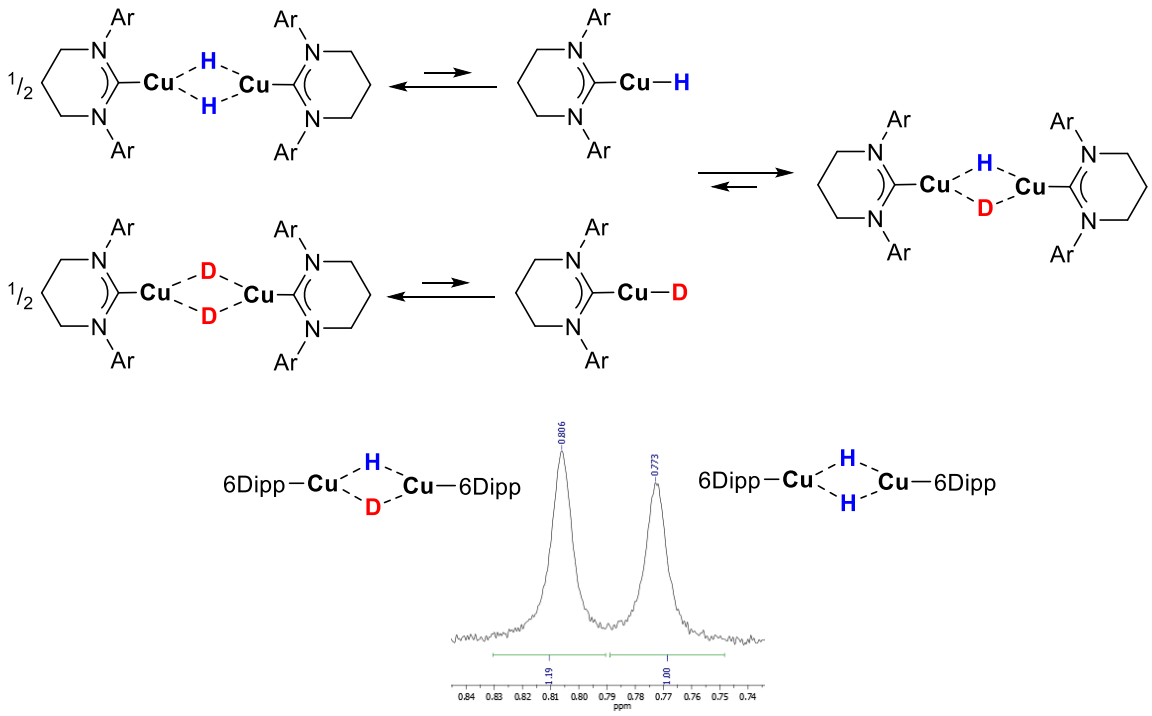

Figure 2.4 Hydride and Deuteride Exchange.

2.2.3 1,2-Insertion Chemistry of Expanded-Ring (NHC)Copper(I) Hydrides

Whereas decomposition of **1a** is evident after 1 h in solution at ambient temperature, the ligands 6Dipp and 7Dipp confer greatly improved stability. Complexes **3a,b** are stable for multiple days in solution and in the solid state. We attribute this increase in stability to the steric encumbrance enforced by the expanded NHC backbone through the *N*-aryl groups. Despite this increased stability, the hydride remains quite reactive: the rapid insertion of CO_2 into **3a,b** is discernible by an immediate loss of color when their solutions are exposed to an atmosphere of CO_2 (Scheme 2.1). The products are formates **4a,b**, analogous to those formed from copper hydrides supported by other NHCs.[34–37]

Hydrocupration of alkynes is well documented and is a key catalytic step in many reductive processes.[17,18,23,25] Until recently, the 1,2-insertion of unactivated alkenes into copper hydrides remained elusive. Buchwald et al. reported the insertion of unactivated alkenes into copper hydrides by bidentate phosphine ligands in the hydroamination of olefins.[11,38] Although (NHC)copper(I) alkyl systems are known, they are typically prepared via transmetalation.[39–42] After treatment of **3a** with 1-hexene, the ^{1}H NMR spectrum shows the growth of a triplet resonance at 0.12 ppm, assigned to a newly formed copper-bound methylene. In the reaction of 1-hexene with **3a** in THF solution, the yellow color disappears within 24 h to yield (6Dipp)copper(I) 1-hexyl (**5a**). Under 1 atm of CO_2, **5a** cleanly forms (6Dipp)copper(I) heptanoate (**6a**) within 40 min (Scheme 2.2). This reaction is consistent with the insertion of CO_2 into other (NHC)- copper−carbon bonds.[39,42] With 1 eq. of 1-hexene per Cu, insertion into $[(5Dipp)CuH]_2$ (generated *in situ*) was also evident by ^{1}H NMR spectroscopy but proceeded to the extent of only 20% after 48 h. Decomposition of $[(5Dipp)CuH]_2$ became apparent after 2 h and continued throughout the reaction period.

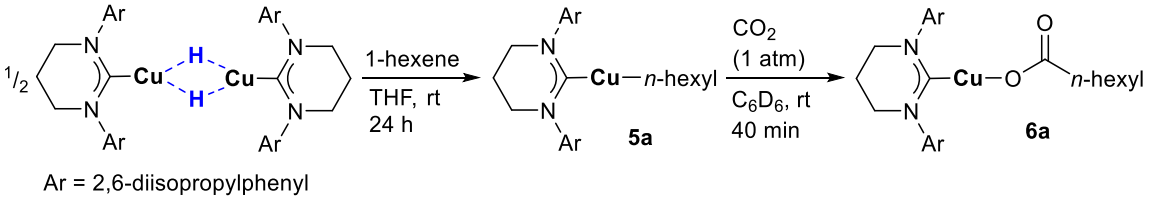

Scheme 2.2 Formation and Carboxylation of a Copper Alkyl.

2.2.4 1,1-Insertion Chemistry of Expanded- Ring (NHC)Copper(I) Hydrides

Discrete 1,1-insertion reactions of isonitriles with copper hydrides have not been reported, but isonitriles have been shown to insert into Cu−B bonds in the synthesis of 2-borylated indoles,[43] and the insertion of isonitriles into other M−H bonds is well

documented.[44] Benzyl isonitrile readily inserts into [(6Dipp)CuH]$_2$, yielding a new copper formimidoyl (**7a**; Scheme 2.3). Interestingly, Bertrand and coworkers treated **2** with *t*-BuNC and observed the net insertion of the supporting carbene, rather than the isonitrile, into the copper−hydride bond.[19]

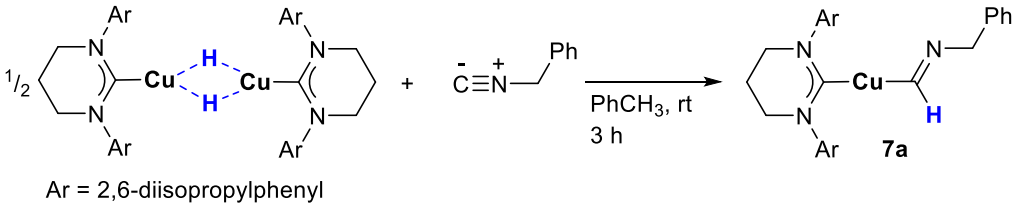

Scheme 2.3 Isonitrile Insertion into [(6Dipp)CuH]$_2$.

The ^{1}H NMR spectrum of **7a** in C_6D_6 solution shows a characteristic singlet resonance at δ 9.37 ppm, consistent with the formation of a formimidoyl moiety. Furthermore, the benzyl protons shift from δ 3.61 ppm for benzyl isonitrile to δ 4.53 ppm in **7a**. The ^{13}C NMR spectrum shows a new resonance at δ 209.9 ppm, characteristic of the metal-bound carbon of an η^1 -formimidoyl.[45,46] This resonance was confirmed to be that of a CH moiety by a DEPT 90 experiment (see Figure 2.39). Slow diffusion of pentane into a toluene solution of **7a** afforded yellow crystals suitable for X-ray diffraction (Figure 2.5). The structure shows a nearly linear geometry about copper, with an angle of 173.26(8)°, while the Cu−C−N angle of the formimidoyl is 120.4(2)°. The copper−carbon distances to both the NHC and formimidoyl are quite similar at 1.933(2) and 1.916(2) Å, respectively. The formimidoyl C−N distance is 1.291(3) Å, consistent with a C=N double bond. Benzyl isonitrile also reacts with **3b**, as judged by ^{1}H NMR spectroscopy, but the reaction is much slower, and subsequent insertion into the newly generated formimidoyl appears to compete with initial insertion into the hydride (see page 50).

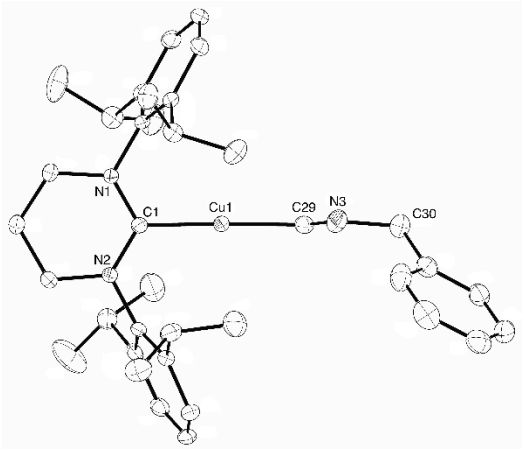

Figure 2.5 Thermal ellipsoid depiction (50% probability) of **7a**. Selected bond lengths (Å) and angles (deg): Cu1−C1 1.933(2), Cu1− C29 1.916(2), C29−N3 1.291(3); C1−Cu1−C29 173.26(8), Cu1− C29−N3 120.4(2), C29−N3−C30 118.57(19).

2.3 Conclusion

In summary, expanded-ring NHCs bearing a sterically encumbering *N*-aryl group stabilize the dimeric $\{Cu_2(\mu\text{-}H_2)\}$ core. The six-membered NHC in particular enables reactions such as the 1,2-insertion of an unactivated alkene and the 1,1-insertion of an isonitrile, and suppresses the competitive decomposition observed using five-membered NHCs as supporting ligands. We anticipate that these reactions will enable new copper-based catalytic processes.

2.4 Experimental

2.4.1 *General Considerations*

Unless otherwise indicated, manipulations were performed in an MBraun glovebox under an inert atmosphere of nitrogen, or in sealable glassware on a Schlenk line under an atmosphere of argon. Glassware and magnetic stir bars were dried in a ventilated oven at 160 °C and were allowed to cool under vacuum. Dichloromethane (BDH), hexane (EMD Millipore Omnisolv), tetrahydrofuran (THF, EMD Millipore Omnisolv), toluene (EMD Millipore Omnisolv) were sparged with ultra-high purity argon (NexAir) for 30 minutes prior to first use, dried using an MBraun solvent purification system, transferred to Straus flasks, degassed using three freeze-pump-thaw cycles, and stored under nitrogen or argon. Anhydrous benzene (EMD Millipore Drisolv) and, anhydrous pentane (EMD Millipore Drisolv, sealed under a nitrogen atmosphere) were used as received and stored in a glovebox. Tap water was purified in a Barnstead International automated still prior to use.

Benzene-d_6 (Cambridge Isotope Labs) was dried over sodium benzophenone ketyl, vacuum-transferred into oven-dried resealable flasks, and degassed by successive freeze-pump-thaw cycles. Dichloromethane-d_2 (Cambridge Isotope Laboratories) was dried over calcium hydride overnight, vacuum-transferred to an oven-dried resealable Schlenk flask, and degassed by successive freeze-pump-thaw cycles.

Sodium *tert*-butoxide (TCI America), copper(I) chloride (Alfa-Aesar), 4,4,5,5-tetramethyl-1,3,2-dioxaborolane (Sigma-Aldrich), benzyl isonitrile (Sigma-Aldrich), 2,6-diisopropylaniline (Sigma-Aldrich), *N*,*N*-diisopropylethylamine (Alfa-Aesar), acetic acid, (Alfa-Aesar), sodium metal (Alfa-Aesar), benzophenone (Alfa-Aesar), 1,2-dichloroethane

(EMD Millipore Omnisolv), 1,3-dichloropropane (TCI America), 1,4-dibromobutane (Sigma-Aldrich) 1,4- triethylorthoformate (Alfa-Aesar), sodium bis(trimethylsilyl)amide (NaHMDS, Sigma-Aldrich), nitrogen (NexAir), and argon (both industrial and ultra-high purity grades, NexAir) were used as received. Carbon dioxide (NexAir) was passed through P_2O_5 prior to use. 1-Hexene (Alfa-Aesar) was filtered over alumina (EMD) prior to use. 5Dipp·HCl,[47] (5Dipp)CuCl,[48] and (5Dipp)CuOtBu,[48] *N*,*N'*-bis(2,6-diisopropylphenyl)formamidine,[49] and 7Dipp·HBF_4[49] were prepared according to literature protocols and were characterized by ^{1}H NMR spectroscopy.

2.4.2 *Spectroscopic Measurements*

^{1}H and ^{13}C spectra were obtained using a Varian Vx 400 MHz spectrometer. ^{1}H and ^{13}C NMR chemical shifts are referenced with respect to solvent signals and reported relative to tetramethylsilane. Unless otherwise stated, infrared spectra were collected using microcrystalline samples on a Bruker Alpha-P infrared spectrometer equipped with an attenuated total reflection (ATR) attachment. Samples were exposed to air as briefly as possible prior to data collection. UV-visible absorption spectra were acquired using a Varian Cary 50 spectrophotometer. Unless otherwise noted, all electronic absorption spectra were recorded at ambient temperatures in 1 cm quartz cells.

2.4.3 *Elemental Analyses*

Elemental analyses were performed by Atlantic Microlab, Inc. in Norcross, Georgia.

2.4.4 *Synthetic Procedures*

2.4.4.1 Synthesis of 6Dipp•HCl

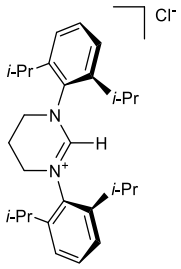

Figure 2.6 6Dipp•HCl

N,*N*-Diisopropylethylamine (1.95 mL, 15.0 mmol) was added to a mixture of *N*,*N*-bis(2,6-diisopropylphenyl)formamidine (5.0 g, 14 mmol), and 1,3-dichloropropane (6.5 mL, 69 mmol) The flask was equipped with a reflux condenser; the reaction mixture was heated to 120 ºC and allowed to stir for 16h. Excess 1,3-dichloropropane was then removed *in vacuo*. The resulting brown solid was dissolved in CH_2Cl_2 (20 mL), washed with saturated aqueous K_2CO_3 (3 x 10 mL) and H_2O (1 x 10 mL), dried over $MgSO_4$, and concentrated *in vacuo*. This resulting brown solid was dissolved in CH_2Cl_2 (30 mL) and toluene (10 mL) before the CH_2Cl_2 was removed *in vacuo*. The resulting colorless precipitate was collected on a frit, washed with 2 portions of toluene (5 mL), and dried overnight under vacuum to give a colorless solid (4.06 g, 67%). ^{1}H NMR (400 MHz, $CDCl_3$): δ (ppm) 7.54 (s, 1H, NC(*H)*N), 7.43 (t, $^3J_{HH}$ = 7.6 Hz, 2H, para-C*H*), 7.25 (d, $^3J_{HH}$ = 7.8 Hz, 4H, *meta*-C*H*), 4.22 (t, $^3J_{HH}$ = 5.6 Hz, 4H, NCH_2), 3.01 (sept, $^3J_{HH}$ = 6.8 Hz, 4H, C*H*$(CH_3)_2$), 2.81 (m, 2H, NCH_2CH_2), 1.37 (d, $^3J_{HH}$ = 6.8 Hz, 12H, $CH_2(CH_3)_2$), 1.22 (d, $^3J_{HH}$ =6.8 Hz, 12H, $CH_2(CH_3)_2$) $^{13}C\{^1H\}$ NMR (100 MHz,$CDCl_3$): δ (ppm) 152.9

(NC(*H*)N), 145.3 (*ortho*-C), 135.5 (*ipso*-*C*), 131.2 (*meta*-*C*), 125.0 (*para*-*C*), 48.9 (N*C*H_2), 28.8 (*C*H(CH_3)$_2$), 24.7 (CH(*C*H_3)$_2$), 24.7 (CH(*C*H_3)$_2$), 19.2 (NCH_2*C*H_2).

Note: This is a previously reported compound that was prepared via a different synthetic route.[50]

2.4.4.2 Synthesis of (6Dipp)CuCl

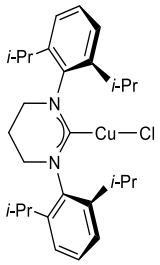

Figure 2.7 (6Dipp)CuCl

NaHMDS (0.411 g, 2.25 mmol) was added to a solution of 6Dipp•HCl (0.972 g, 2.20 mmol) in THF (10 mL) with stirring. After 2h, CuCl (0.222 g, 2.25 mmol) was added and the mixture was allowed to stir overnight before being filtered through Celite, washed with CH_2Cl_2 and concentrated *in vacuo* to give a colorless solid. This was dissolved in a minimal amount of CH_2Cl_2, layered with hexanes and placed in the freezer overnight. The resulting colorless solid was collected on a frit and, dried *in vacuo* to afford the title complex. (0.920 g, 83 %). ^{1}H NMR (400 MHz, $CDCl_3$): δ (ppm) 7.36 (t, $^3J_{HH}$ = 7.6 Hz, 2H, para-C*H*), 7.21 (d, $^3J_{HH}$ = 7.6 Hz, 4H, *meta*-C*H*), 3.43 (t, $^3J_{HH}$ = 6.0 Hz, 4H, NCH_2), 3.06 (sept, $^3J_{HH}$ = 6.8 Hz, 4H, C*H*(CH_3)$_2$), 2.37 (quin, $^3J_{HH}$ = 6.0 Hz, 2H, NCH_2CH_2), 1.34 (d, $^3J_{HH}$ = 7.2 Hz, 12H, CH_2(CH_3)$_2$), 1.31 (d, $^3J_{HH}$ = 7.2 Hz, 12H, CH_2(CH_3)$_2$). ^{13}C{^{1}H} NMR (100 MHz, $CDCl_3$): δ (ppm) 200.8 (N*C*Cu), 145.6 (*ortho*-C), 141.5 (*ipso*-*C*), 129.5

(*meta*-*C*), 124.8 (*para*-*C*), 46.3 (N*C*H_2), 28.8 (*C*H(CH_3)$_2$), 25.0 (CH(*C*H_3)$_2$), 24.8 (CH(*C*H_3)$_2$), 20.6 (NCH$_2$*C*H_2).

Note: This is a previously reported compound that was prepared via a different synthetic route.[51]

2.4.4.3 Synthesis of (7Dipp)CuCl

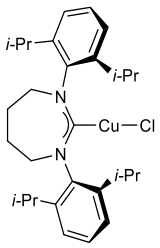

Figure 2.8 (7Dipp)CuCl

NaHMDS (0.379 g, 2.07 mmol) was added to a solution of 7Dipp•HBF_4 (1.00 g, 1.97 mmol) in THF (10 mL) with stirring. After 2h, CuCl (0.207 g, 2.09 mmol) was added and the mixture was allowed to stir overnight before being filtered through Celite, washed with CH_2Cl_2 and concentrated *in vacuo* to give colorless solid. This was dissolved in a minimal amount of CH_2Cl_2, layered with hexanes and placed in the freezer overnight. The resulting colorless solid was collected on a frit and, dried *in vacuo* to afford the title complex. (0.804 g, 79%). ^{1}H NMR (400 MHz, $CDCl_3$): δ (ppm) 7.32 (t, $^3J_{HH}$ = 7.6 Hz, 2H, para-C*H*), 7.18 (d, $^3J_{HH}$ = 7.6 Hz, 4H, *meta*-C*H*), 3.97 (m, 4H, NCH_2), 3.25 (sept, $^3J_{HH}$ = 6.8 Hz, 4H, C*H*(CH_3)$_2$), 2.33 (m, 4H, NCH$_2$CH_2), 1.35 (d, $^3J_{HH}$ = 6.8 Hz, 12H, CH$_2$(CH_3)$_2$), 1.32 (d, $^3J_{HH}$ = 6.8 Hz, 12H, CH$_2$(CH_3)$_2$). ^{13}C{^{1}H} NMR (100 MHz, $CDCl_3$): δ (ppm) 210.3 (N*C*Cu), 145.0 (*ortho*-C), 144.0 (*ipso*-*C*), 129.1 (*meta*-*C*), 124.9 (*para*-*C*), 54.0 (N*C*H_2),

28.9 (*C*H(CH$_3$)$_2$), 25.3 (NCH$_2$*C*H$_2$), 24.8 (CH(*C*H$_3$)$_2$), 24.8 (CH(*C*H$_3$)$_2$), IR: ν (cm^{-1}) 2960, 2873, 1496, 1447, 1385, 1362, 1311, 1290, 1177, 1056, 936, 904, 804, 785, 761, 573, 450 Anal. Calcd for $C_{29}H_{42}ClCuN_2$: C, 67.29; H, 8.18; N, 5.41. Found C, 67.35; H, 8.23; N, 5.42.

2.4.4.4 Synthesis of (6Dipp)CuO-*t*-Bu.

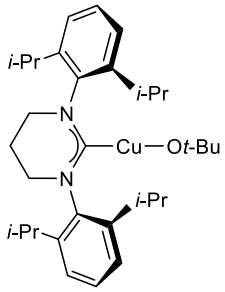

Figure 2.9 (6Dipp)CuO-*t*-Bu

Sodium *tert*-butoxide (0.033 g, 0.34 mmol) was added to a solution of (6Dipp)CuCl (0.170 g, 0.34 mmol) in THF (4 mL) with stirring. After 3 hours, the reaction mixture was filtered through Celite, and the filter pad was washed with 2 portions of THF (1 mL each). The filtrate was concentrated, and the residue was dried for 12 hours at 40ºC under vacuum, affording the product at a colorless powder (0.174 g, 96%). ^{1}H NMR (400 MHz, C_6D_6): δ (ppm) 7.13 (dd, $^3J_{HH}$ = 8.4, 6.8 Hz, 2H para-CH), 7.05 (d, $^3J_{HH}$ = 7.2 Hz, 4H, *meta*-CH), 3.03 (sept, $^3J_{HH}$ = 6.8 Hz, 4H, C*H*(CH$_3$)$_2$), 2.68 (t, *J* = 6.0 Hz, 4H, NC*H*$_2$), 1.57 (d, $^3J_{HH}$ = 7.2 Hz, 12H, CH$_2$(C*H*$_3$), 1.44 (quin, $^3J_{HH}$ = 6.0 Hz, 2H, NCH$_2$C*H*$_2$), 1.18 (d, $^3J_{HH}$ = 7.2 Hz, 12H, CH$_2$(C*H*$_3$), 1.16 (s, 9H, C(C*H*$_3$)$_3$). ^{13}C{^{1}H} NMR (100 MHz, C_6D_6): δ (ppm) 203.5 (N*C*Cu), 145.5 (*ortho*-C), 142.6 (*ipso*-*C*), 129.3 (*meta*-*C*), 124.8 (*para*-*C*), 68.8 (O*C*(CH$_3$)$_3$), 46.1 (N*C*H$_2$), 37.1 (OC(*C*H$_3$)$_3$), 28.9 (*C*H(CH$_3$)$_2$), 25.2 (CH(*C*H$_3$)$_2$), 24.8

(CH(CH_3)$_2$), 20.4 (NCH$_2$$CH_2$). IR: ν (cm^{-1}) 2957, 2869, 1492, 1473, 1385, 1363, 1323, 1307, 1291, 1195, 1094, 1057, 970, 803, 787, 760, 592, 551, 457 Anal. Calcd for $C_{32}H_{49}CuN_2O$: C, 71.00; H, 9.12; N, 5.18. Found C, 69.74; H, 9.19; N, 5.10.

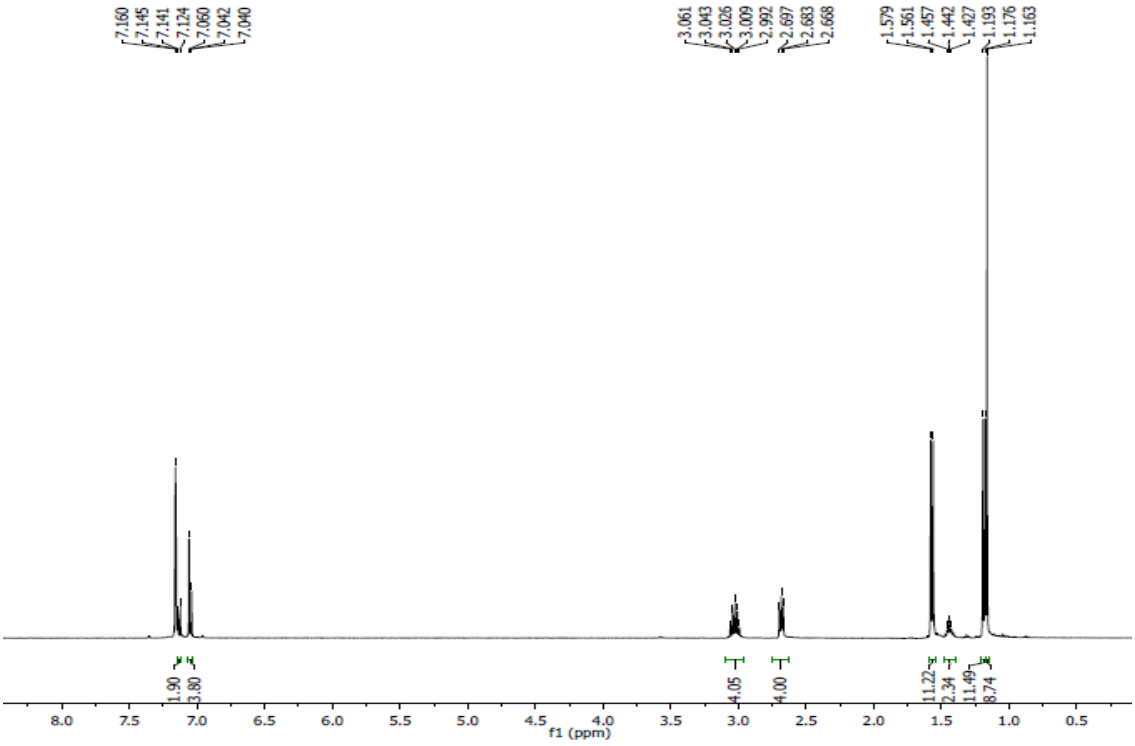

Figure 2.10. ^{1}H NMR spectrum of (6Dipp)CuO-*t*-Bu in C_6D_6.

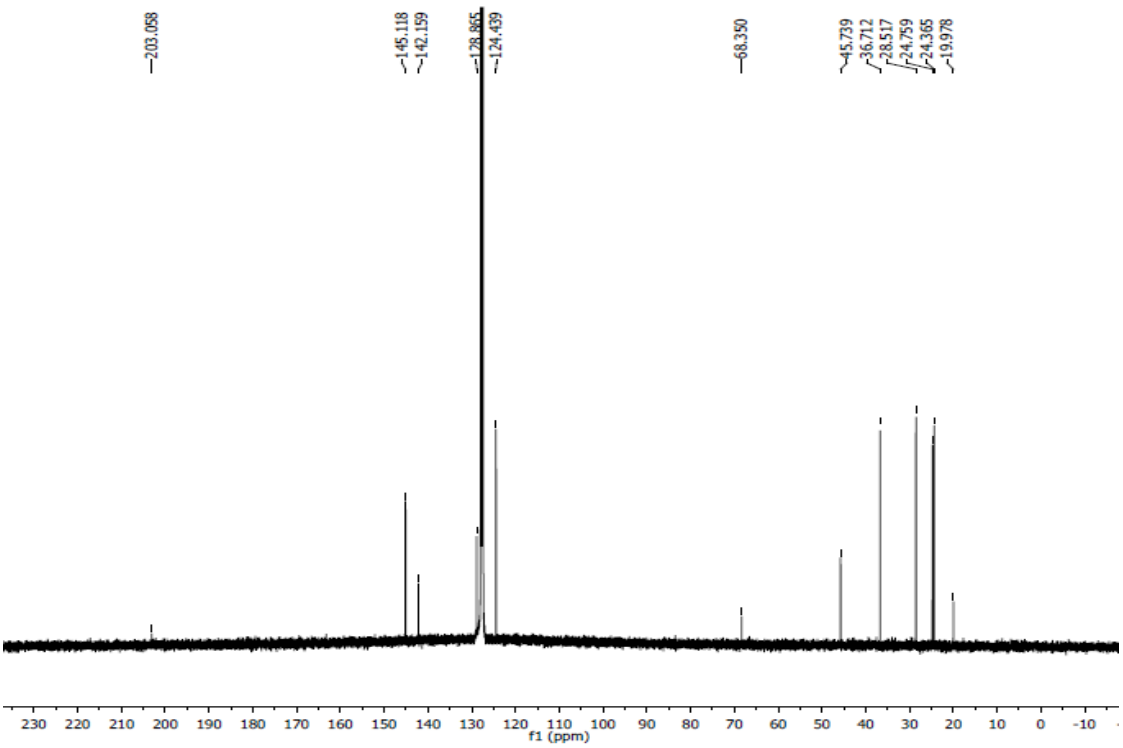

Figure 2.11. ^{13}C NMR spectrum of 6DippCuO-*t*-Bu in C_6D_6.

2.4.4.5 Synthesis of (7Dipp)CuO-*t*-Bu.

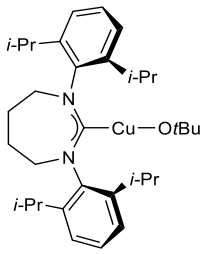

Figure 2.12 (7Dipp)CuO-*t*-Bu

Sodium *tert*-butoxide (0.059 g, 0.61 mmol) was added to a solution of (7Dipp)CuCl (0.313 g, 0.61 mmol) in THF (8 mL) with stirring. After 3 hours, the reaction mixture was filtered through Celite, and the filter pad was washed with 2 portions of THF (2 mL each). The filtrate was concentrated, and the residue was dried for 12 hours at 40 ºC under

vacuum, affording the product at a colorless powder (0.272 g, 81%). ^{1}H NMR (400 MHz, C_6D_6): δ (ppm) 7.13 (dd, $^{3}J_{HH}$ = 8.8, 7.2 Hz, 2H, para-C*H*), 7.05 (d, $^{3}J_{HH}$ = 7.6 Hz, 4H, *meta*-C*H*), 3.26 (m, 4H, NCH_2), 3.24 (sept, $^{3}J_{HH}$ = 6.8 Hz, 4H, C*H*(CH_3)$_2$), 1.60 (m, 16H, NCH_2CH_2, $CH_2(CH_3)_2$), 1.21 (d, $^{3}J_{HH}$ = 6.8 Hz, 12H, $CH_2(CH_3)_2$), 1.12 (s, 9H, C(CH_3)$_3$) ^{13}C{^{1}H} NMR (100 MHz, C_6D_6): δ (ppm) 213.1 (N*C*Cu), 145.02 (*ortho*-C), 144.99 (*ipso-C*), 128.9 (*meta-C*), 125.0 (*para-C*), 68.7 (O*C*(CH_3)$_3$), 53.7 (N*C*H_2), 37.0 (OC(*C*H_3)$_3$), 29.1 (*C*H(CH_3)$_2$), 25.1 (NCH_2CH_2), 24.7 (CH(*C*H_3)$_2$), IR: ν (cm^{-1}) 2957, 1493, 1448, 1385, 1363, 1308, 1291, 1194, 1094, 1057, 970, 803, 788, 760, 572, 552, 456.

Note: We have been unable to obtain satisfactory elemental analysis for (7Dipp)CuO-*t*-Bu. The complex is extremely moisture sensitive. While NMR-silent impurities cannot be ruled out, we believe the ^{1}H and ^{13}C NMRs spectra reflect the purity of the sample.

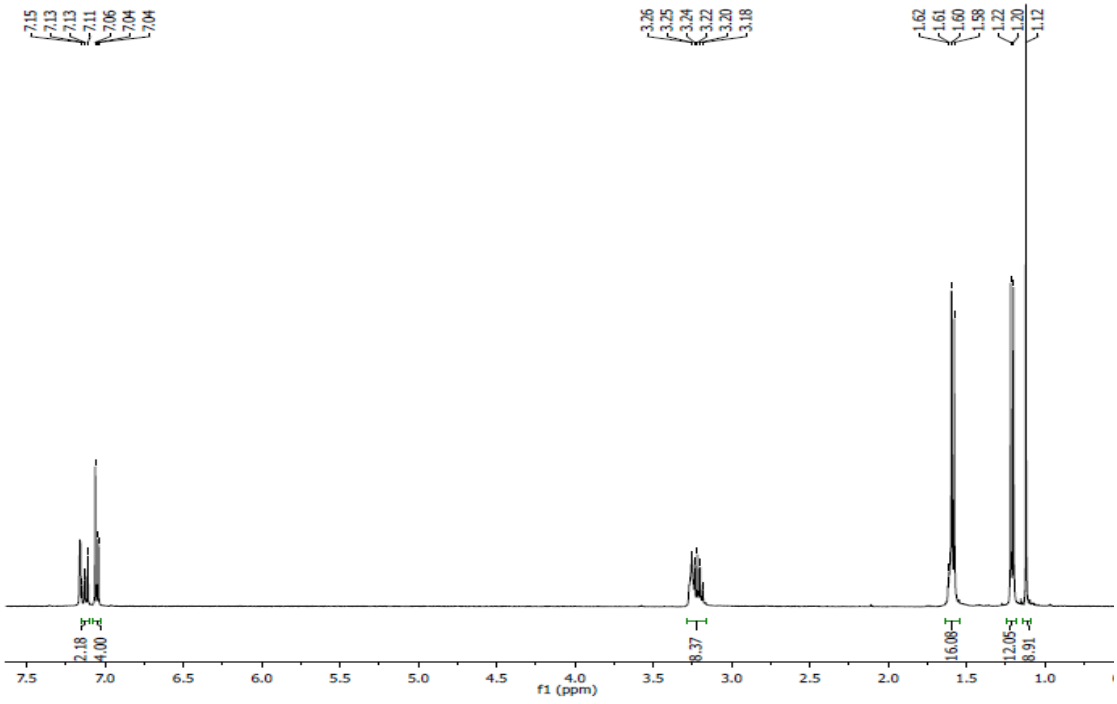

Figure 2.13. ^{1}H NMR spectrum of (7Dipp)CuO-*t*-Bu in C_6D_6.

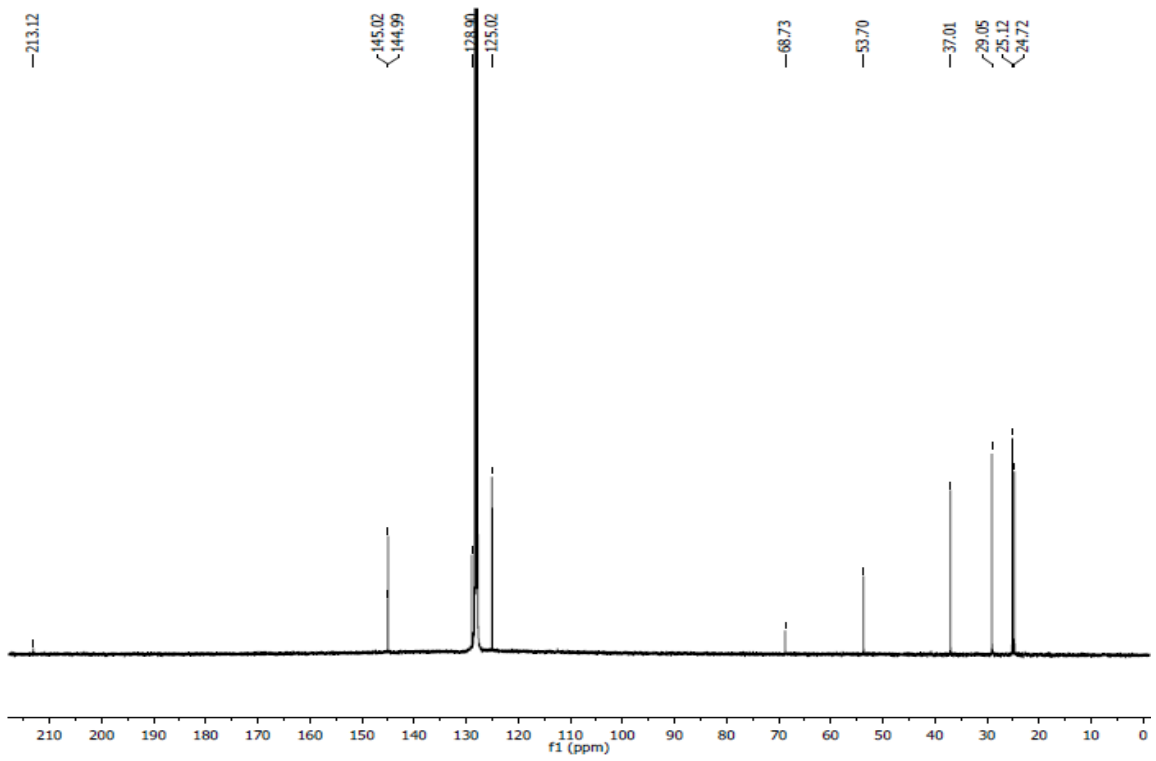

Figure 2.14. ^{13}C NMR spectrum of (7Dipp)CuO-*t*-Bu in C_6D_6.

2.4.4.6 Synthesis of $[(6Dipp)CuH]_2$

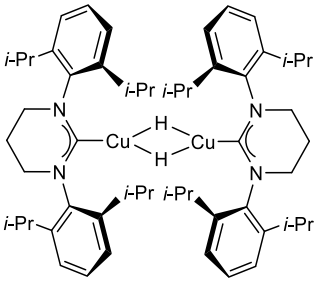

Figure 2.15 $[(6Dipp)CuH]_2$ (**3a**)

Pinacolborane 4,4,5,5,-tetramethyl-1,3,2-dioxaborolane [HB(pin)] (0.040 mL, 0.26 mmol) was added to a solution of (6Dipp)CuO-*t*-Bu (0.095 g, 0.18 mmol) in THF (1 mL) via syringe. The resulting yellow solution was layered with pentane (2 mL) and placed

in the freezer at –35º C for 12h. The supernatant was decanted by pipette, pentane (1 mL) was added and the mixture was placed back in the freezer for 4h. The supernatant was decanted and pentane (1 mL) was added again before being placed in the freezer for another 4h. The resulting yellow crystals were dried *in vacuo* for 1h to afford the title complex. (0.079 g, 96%). ^{1}H NMR (400 MHz, C_6D_6): δ (ppm) 7.21 (t, $^{3}J_{HH}$ = 7.6 Hz, 2H, para-C*H*), 7.00 (d, $^{3}J_{HH}$ = 7.6 Hz, 4H, *meta*-C*H*), 3.17 (sept, $^{3}J_{HH}$ = 6.8 Hz, 4H, C*H*$(CH_3)_2$), 2.88 (t, $^{3}J_{HH}$ = 6.0 Hz, 4H, NC*H*$_2$), 1.65 (quin, $^{3}J_{HH}$ = 6.0 Hz, 2H, NCH_2CH_2), 1.42 (d, $^{3}J_{HH}$ = 6.8 Hz, 12H, $CH_2(CH_3)_2$), 1.28 (d, $^{3}J_{HH}$ = 7.2 Hz, 12H, $CH_2(CH_3)_2$), 0.77 (s, 1H, Cu-*H*) ^{13}C{^{1}H} NMR (100 MHz, C_6D_6): δ (ppm) 213.5 (N*C*Cu), 146.2 (*ortho*-C), 142.4 (*ipso-C*), 124.3 (*para-C*), 45.9 (N*C*H$_2$), 28.7 (*C*H$(CH_3)_2$), 25.7 (CH(*C*H$_3)_2$), 25.4 (CH(*C*H$_3)_2$), 20.9 (NCH_2CH_2). We believe the *meta*-C resonance is overlapped by the solvent signal of C_6D_6. IR: ν (cm^{-1}) 2955, 2864, 1483, 1452, 1384, 1296, 1195, 1057, 909, 798, 749, 616, 549, 450

Note: We have been unable to obtain satisfactory elemental analysis for **3a**. The complex is extremely air and moisture-sensitive. After exposure of a benzene solution of **3a** to dry CO_2, and concentration *in vacuo*, the more stable formate complex **4a** was isolated without further purification and its elemental analysis was obtained (see page 35). We reasoned that only a sufficiently pure sample of **3a** would give rise to analytically pure **4a**.

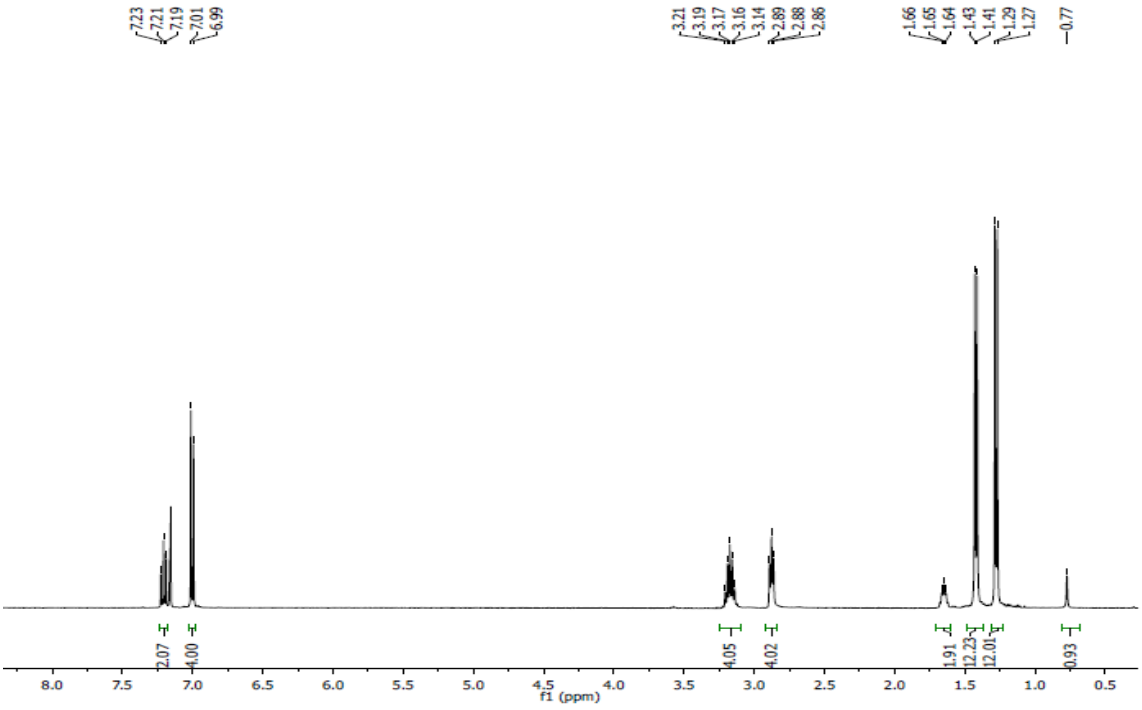

Figure 2.16. ^{1}H NMR spectrum of $[(6Dipp)CuH]_2$ in C_6D_6.

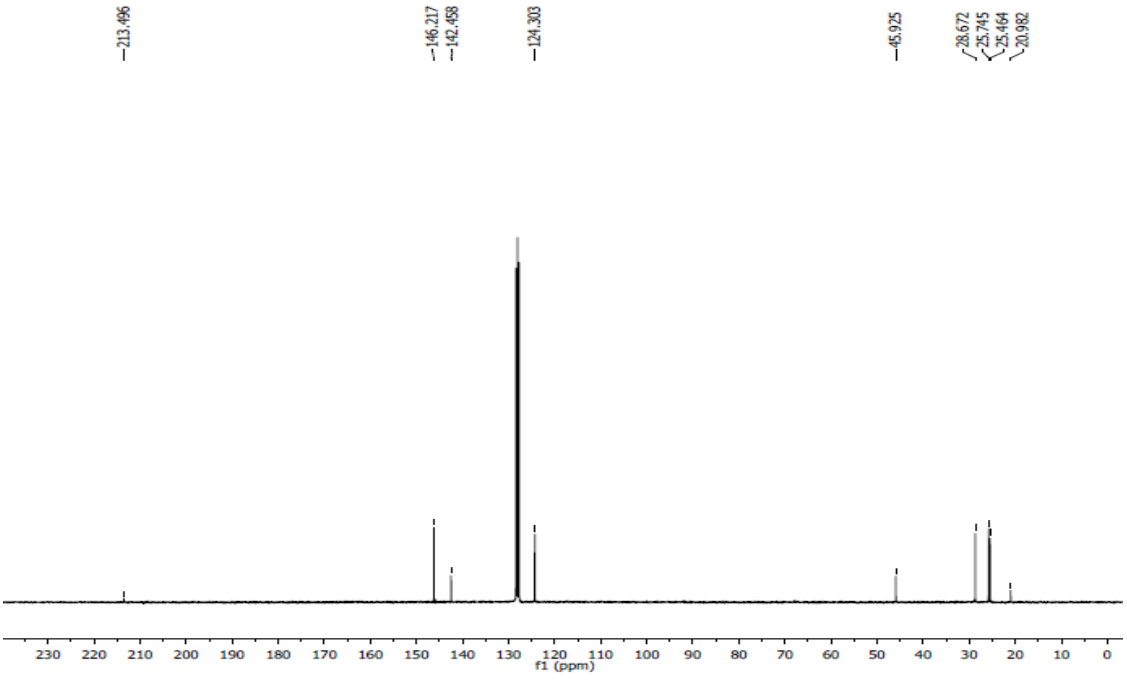

Figure 2.17. ^{13}C NMR spectrum of $[(6Dipp)CuH]_2$ in C_6D_6.

2.4.4.7 Synthesis of (6Dipp)copper(I) formate

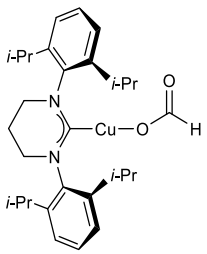

Figure 2.18 (6Dipp)copper(I) formate (**4a**)

In an oven dried 25-mL Schlenk flask under N_2, a solution of $[(6Dipp)CuH]_2$ (0.036 g, 0.038 mmol) in benzene (5 mL) was degassed by 3 freeze-pump-thaw cycles before being exposed to an atmosphere of CO_2. The bright yellow solution immediately became colorless, and deposited a white precipitate. The benzene was removed *in vacuo* and dried under vacuum for 12h affording the product as a colorless powder (0.036 g, 94 %). ^{1}H NMR (400 MHz, CD_2Cl_2): δ (ppm) 7.68 (s, 1H, OC(O)*H*) 7.39 (t, $^3J_{HH}$ = 7.6 Hz, 2H, para-C*H*), 7.25 (d, $^3J_{HH}$ = 7.6 Hz, 4H, *meta*-C*H*), 3.43 (t, $^3J_{HH}$ = 6.0 Hz, 4H, NCH_2) 3.05 (sept, $^3J_{HH}$ = 6.8 Hz, 4H, C*H*$(CH_3)_2$), 2.36 (quin, $^3J_{HH}$ = 6.0 Hz, 2H, NCH_2CH_2), 1.33 (d, $^3J_{HH}$ = 6.8 Hz, 12H, $CH_2(CH_3)_2$), 1.31 (d, $^3J_{HH}$ = 7.2 Hz, 12H, $CH_2(CH_3)_2$) ^{13}C{^{1}H} NMR (100 MHz, CD_2Cl_2): δ (ppm) 200.6 (N*C*Cu), 166.7 (O*C*(O)H) 146.2 (*ortho*-C), 142.1 (*ipso*-*C*), 129.5 (*meta*-*C*), 125.0 (*para*-*C*), 46.6 (NCH_2), 29.0 (*C*H$(CH_3)_2$), 24.9 (CH(*C*$H_3)_2$), 24.7 (CH(*C*$H_3)_2$), 20.8 (NCH_2CH_2). IR ν (cm^{-1}) 2961, 2926, 2866, 2794, 1621, 1509, 1455, 1309, 1255, 1206, 1180, 1149, 1108, 1078, 1058, 985, 938, 803, 758, 552, 516, 445. Anal. Calcd for $C_{29}H_{42}CuN_2O_2$: C, 67.87; H, 8.11; N, 5.46. Found C, 67.94; H, 8.11; N, 5.52.

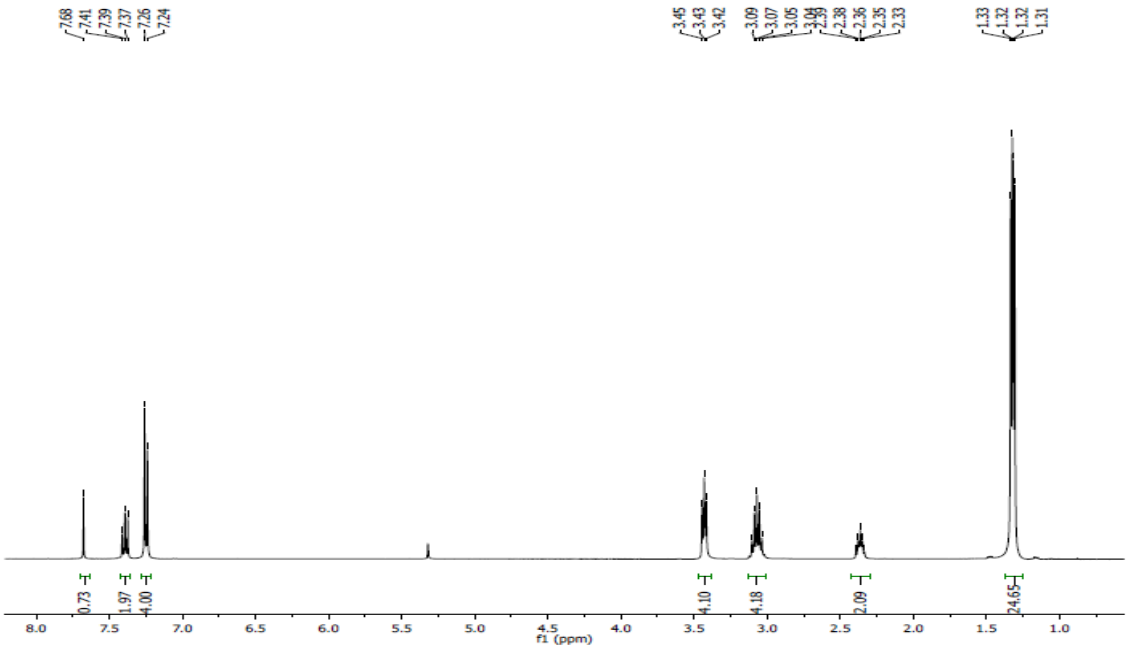

Figure 2.19. ^{1}H NMR spectrum of (6Dipp)copper(I) formate in CD_2Cl_2.

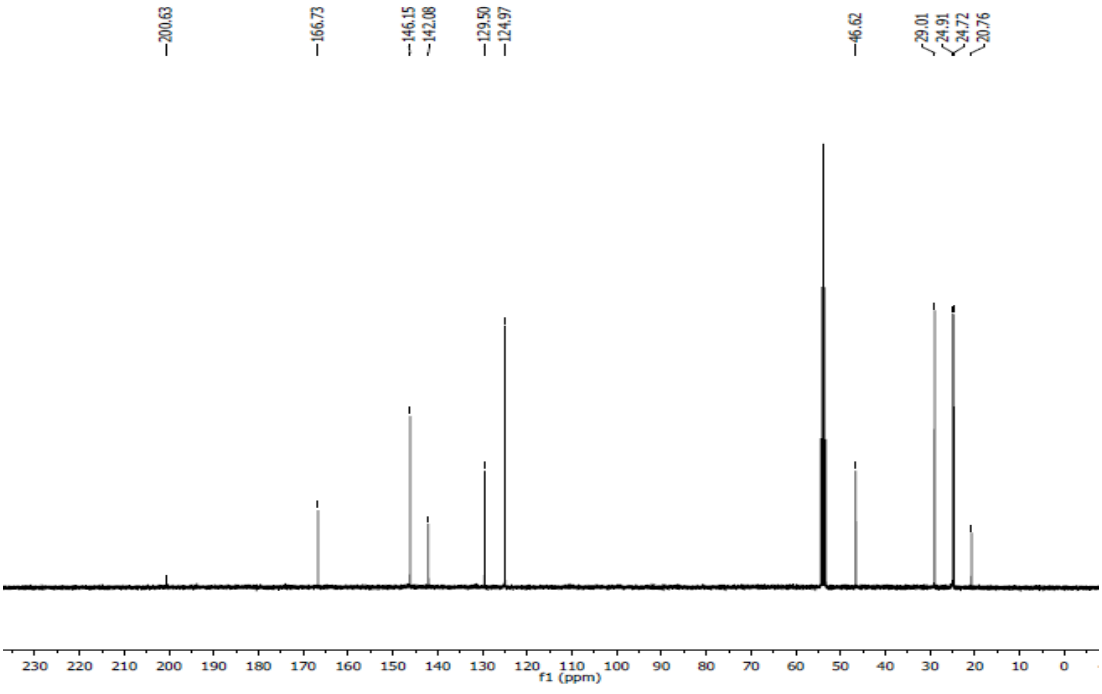

Figure 2.20. ^{13}C NMR spectrum of (6Dipp)copper(I) formate in CD_2Cl_2.

2.4.4.8 Synthesis of $[(7Dipp)CuH]_2$

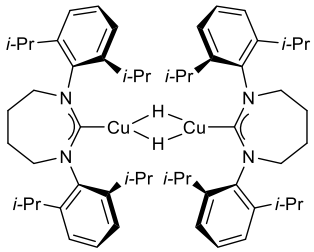

Figure 2.21 $[(7Dipp)CuH]_2$ (**3b**)

Pinacolborane 4,4,5,5,-tetramethyl-1,3,2-dioxaborolane [HB(pin)] (0.040 mL, 0.26 mmol) was added to a solution of (7Dipp)CuO-*t*-Bu (0.102 g, 0.184 mmol) in THF (2 mL) via syringe. The resulting yellow solution was layered with pentane (2 mL) and placed in the freezer at –35º C for 12h. The supernatant was decanted by pipette before pentane (2 mL) was added and placed back in the freezer for 4h. The supernatant was decanted and pentane (2 mL) was added again before being placed in the freezer for another 4h. The resulting orange crystals were dried *in vacuo* for 1h to afford the title complex (0.080 g, 90 %). ^{1}H NMR (400 MHz, C_6D_6): δ (ppm) 7.20 (t, $^3J_{HH}$ = 7.6 Hz, 2H, para-C*H*), 6.99 (d, $^3J_{HH}$ = 7.6 Hz, 4H, *meta*-C*H*), 3.41 (m, 4H, NCH_2), 3.31 (sept, $^3J_{HH}$ = 6.8 Hz, 4H, C*H*$(CH_3)_2$), 1.74 (m, 4H, NCH_2CH_2), 1.41 (d, $^3J_{HH}$ = 6.8 Hz, 12H, $CH_2(CH_3)_2$), 1.30 (d, $^3J_{HH}$ = 6.8 Hz, 12H, $CH_2(CH_3)_2$), 0.47 (s, 1H, Cu-*H*). ^{13}C{^{1}H} NMR (100 MHz, C_6D_6): δ (ppm) 223.9 (N*C*Cu), 145.4 (*ortho*-C), 144.8 (*ipso*-*C*), 127.7 (*meta*-*C*), 124.7 (*para*-*C*), 53.7 (NCH_2), 28.8 (*C*H$(CH_3)_2$), 26.0 (NCH_2CH_2), 25.7 (CH(*C*$H_3)_2$), 25.6 (CH(*C*$H_3)_2$), IR: ν (cm^{-1}) 2956, 2861, 1459, 1420, 1382, 1360, 1317, 1267, 1176, 1057, 936, 912, 798, 782, 752, 618, 550, 454, 401.

Note: We have been unable to obtain satisfactory elemental analysis for **3b**. The complex is extremely air and moisture-sensitive. After exposure of a benzene solution of **3b** to dry CO_2, and concentration *in vacuo*, the more stable formate complex **4b** was isolated without further purification and its elemental analysis was obtained (see page 40) We reasoned that only a sufficiently pure sample of **4b** would give rise to analytically pure **4b**.

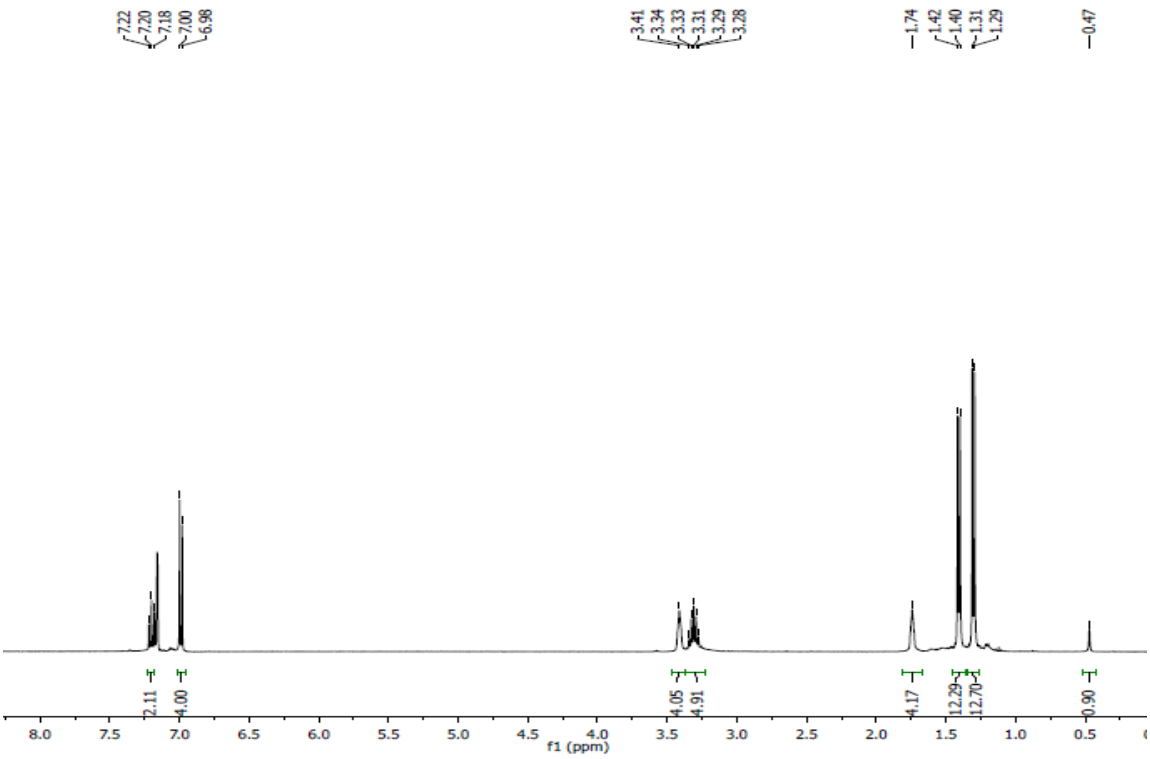

Figure 2.22 ^{1}H NMR spectrum of $[(7Dipp)CuH]_2$ in C_6D_6.

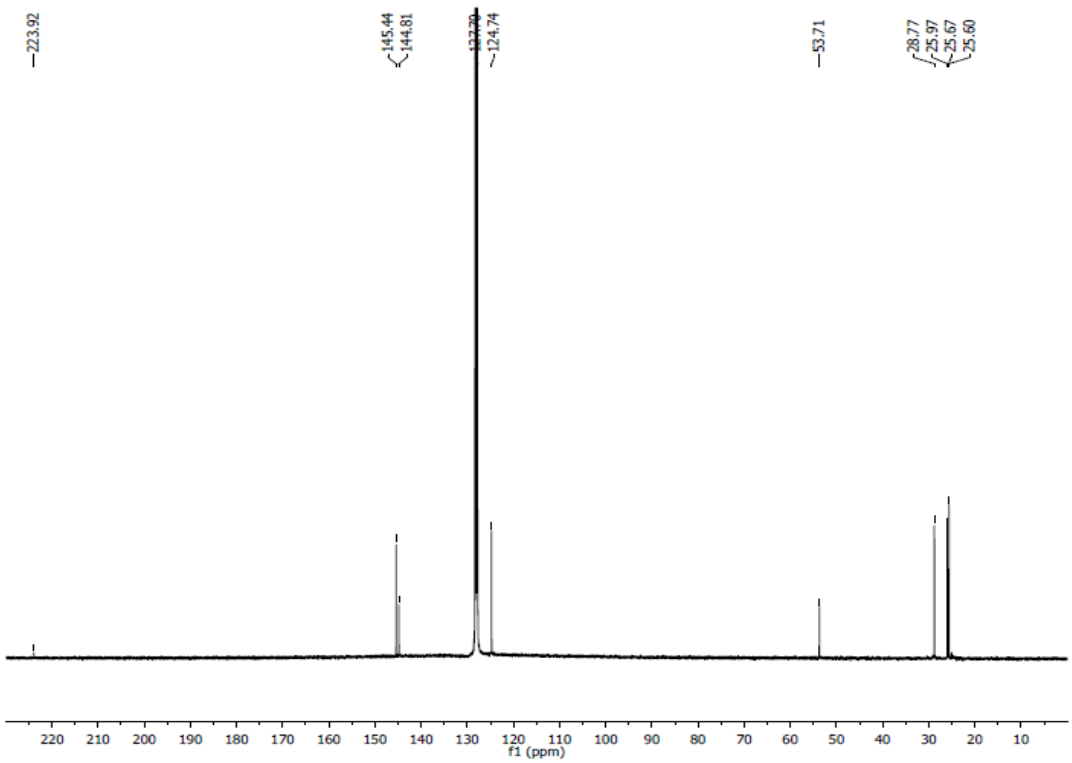

Figure 2.23 ^{13}C NMR spectrum of $[(7Dipp)CuH]_2$ in C_6D_6.

2.4.4.9 Synthesis of (7Dipp)copper(I) formate

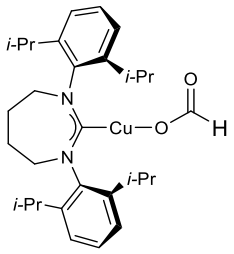

Figure 2.24 (7Dipp)copper(I) formate (**4b**)

In an oven dried 25-mL Schlenk flask under N_2, a solution of $[(7Dipp)CuH]_2$ (0.022 g, 0.023 mmol) in benzene (5 mL) was degassed by 3 freeze-pump-thaw cycles before being exposed to an atmosphere of CO_2. The bright orange solution immediately became colorless, and deposited a white precipitate. The benzene was removed *in vacuo* and dried

under vacuum for 12h affording the product as a colorless powder. (0.021 g, 85%) ^{1}H NMR (400 MHz, CD_2Cl_2): δ (ppm) 7.59 (s, 1H, OC(O)*H*) 7.35 (t, $^{3}J_{HH}$ = 7.6 Hz, 2H, para-C*H*), 7.23 (d, $^{3}J_{HH}$ = 7.6 Hz, 4H, *meta*-C*H*), 3.97 (m, 4H, NCH_2), 3.26 (sept, $^{3}J_{HH}$ = 6.8 Hz, 4H, C*H*(CH_3)$_2$), 2.33 (m, 4H, NCH_2CH_2), 1.33 (d, $^{3}J_{HH}$ = 7.2 Hz, 24H, CH_2(CH_3)$_2$). ^{13}C{^{1}H} NMR (100 MHz, CD_2Cl_2): δ (ppm) 210.1 (N*C*Cu), 166.7 (O*C*(O)H) 145.5 (*ortho*-C), 144.5 (*ipso*-*C*), 129.1 (*meta*-*C*), 125.1 (*para*-*C*), 54.4 (NCH_2), 37.0 (OC(*C*H_3)$_3$), 29.1 (*C*H(CH_3)$_2$), 25.1 (NCH_2CH_2), 24.74 (CH(*C*H_3)$_2$), 24.70 (CH(*C*H_3)$_2$). IR: ν (cm^{-1}) 2962, 2926, 2866, 2795, 1634, 1590, 1478, 1468, 1446, 1387, 1364, 1316, 1290, 1266, 1179, 1095, 1057, 949, 936, 805, 785, 762, 695, 496, 452. Anal. Calcd for $C_{30}H_{43}CuN_2O_2$: C, 68.34; H, 8.22; N, 5.31. Found C, 68.10; H, 8.37; N, 5.18.

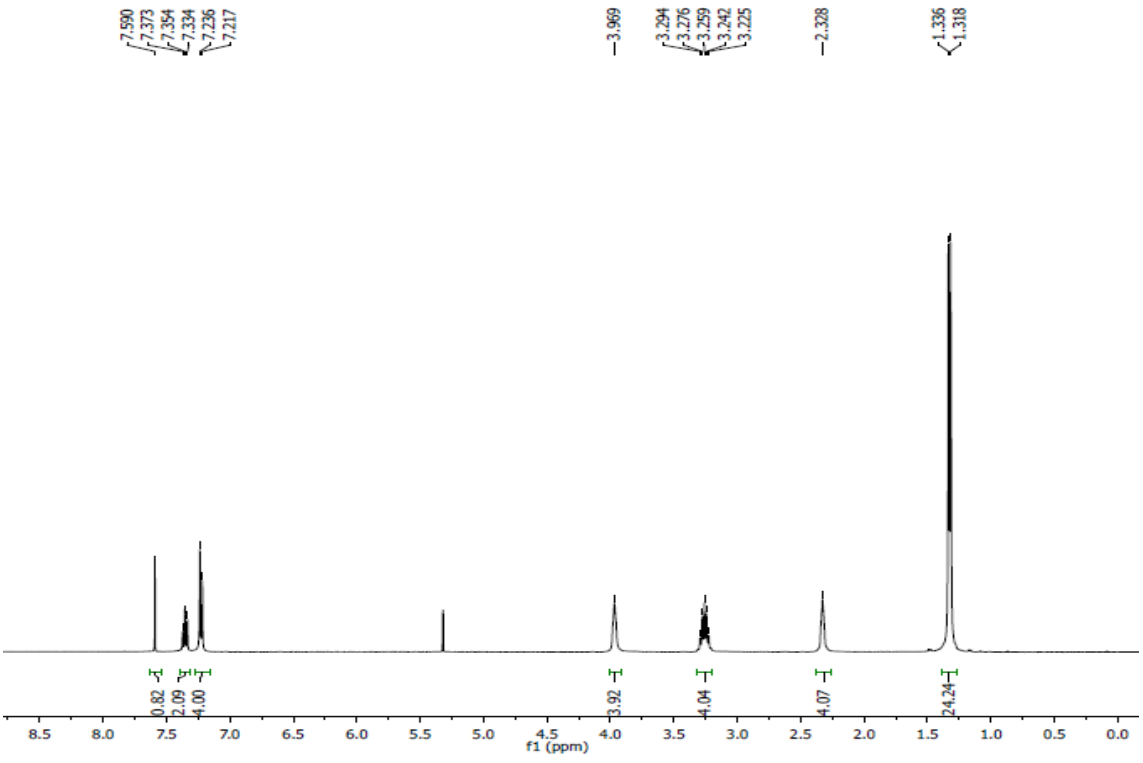

Figure 2.25 ^{1}H NMR spectrum of (7Dipp)copper(I) formate in CD_2Cl_2.

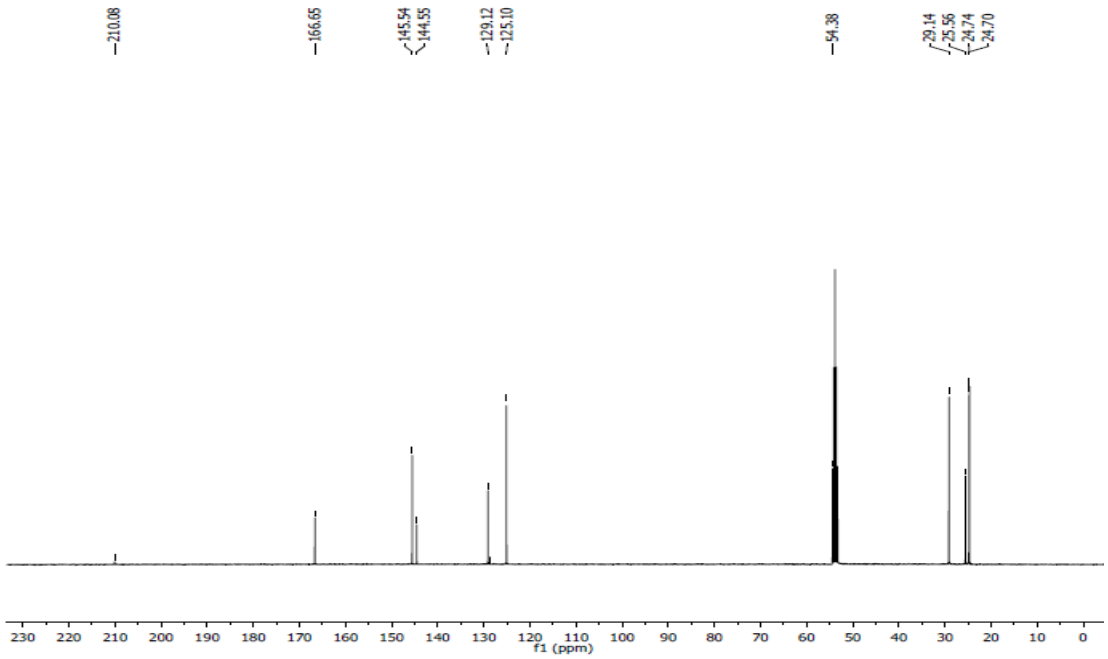

Figure 2.26. ^{13}C NMR spectrum of (7Dipp)copper(I) formate in CD_2Cl_2.

2.4.4.10 Synthesis of (6Dipp)copper(I) hexyl

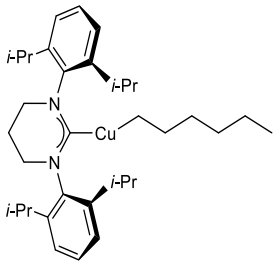

Figure 2.27 (6Dipp)copper(I) hexyl (**5a**)

1-Hexene (0.106 mL, 0.85 mmol) was added to a solution of $[(6Dipp)CuH]_2$ (0.020 g, 0.021 mmol) in THF (2 mL). After 24h the resulting solution was concentrated *in vacuo* to give a colorless solid (0.017 g, 72%). ^1H NMR (400 MHz, C_6D_6): δ (ppm) 7.21 (dd, $^3J_{HH}$ = 8.4, 7.2 Hz, 2H, para-C*H*), 7.10 (d, $^3J_{HH}$ = 7.6 Hz, 4H, *meta*-C*H*), 3.08 (sept, $^3J_{HH}$ = 6.8 Hz, 4H, C*H*$(CH_3)_2$), 2.70 (t, $^3J_{HH}$ = 6.0 Hz, 4H, NCH_2), 1.61 (quin, $^3J_{HH}$ = 7.6 Hz, 2H, Cu-

CH_2CH_2), 1.54 (d, $^3J_{HH}$ = 6.8 Hz, 12H, $CH_2(CH_3)_2$), 1.50 (m, 2H, NCH_2CH_2), 1.36 (m, 4H, Cu-$(CH_2)_2(CH_2)_2$), 1.22 (d, $^3J_{HH}$ = 6.8 Hz, 12H, $CH_2(CH_3)_2$), 1.09 (quin, $^3J_{HH}$ = 7.6 Hz, 2H, Cu-$(CH_2)_4(CH_2)CH_3$), 0.97 (t, $^3J_{HH}$ = 6.8 Hz, 3H, Cu-$(CH_2)_5CH_3$), 0.12 (t, $^3J_{HH}$ = 7.6 Hz, 2H, Cu-CH_2) $^{13}C\{^1H\}$ NMR (100 MHz, C_6D_6): δ (ppm) 204.7 (N*C*Cu), 145.8 (*ortho*-C), 142.1 (*ipso*-*C*), 129.0 (*meta*-*C*), 124.5 (*para*-*C*), 46.0 (NCH_2), 38.0 (Cu-CH_2CH_2), 33.1 (Cu-$(CH_2)_2CH_2$), 31.1 (Cu-$(CH_2)_3CH_2$), 28.9 ($CH(CH_3)_2$), 25.0 ($CH(CH_3)_2$), 24.7 ($CH(CH_3)_2$), 23.6 (Cu-$(CH_2)_4CH_2$), 20.5 (NCH_2CH_2), 14.9 (Cu-$(CH_2)_5CH_3$), 10.8 (Cu-CH_2). IR ν (cm^{-1}) 2960, 2867, 1645, 1628, 1506, 1452, 1303, 1203, 1056, 935, 803, 757, 556, 537, 492, 452, 420, 401.

Note: We have been unable to obtain satisfactory elemental analysis for **5a**. The complex is extremely air, moisture and light sensitive. While NMR-silent impurities cannot be ruled out, we believe the ^1H and ^{13}C NMR spectra provided reflect the purity of the sample.

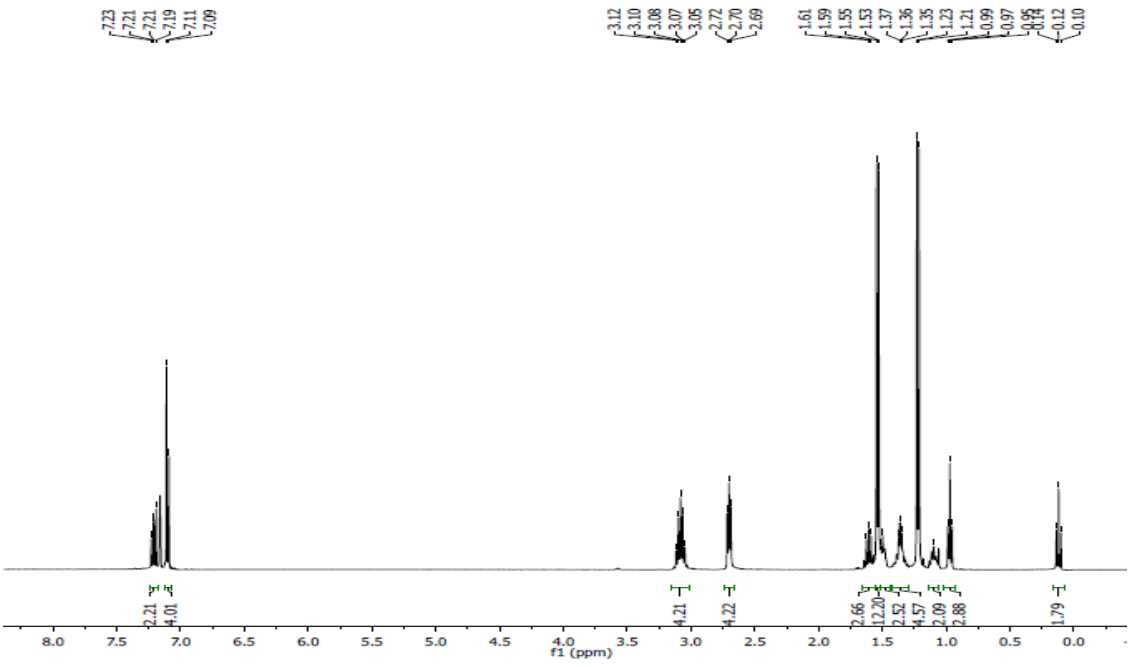

Figure 2.28 ^1H NMR spectrum of (6Dipp)copper(I) hexyl in C_6D_6.

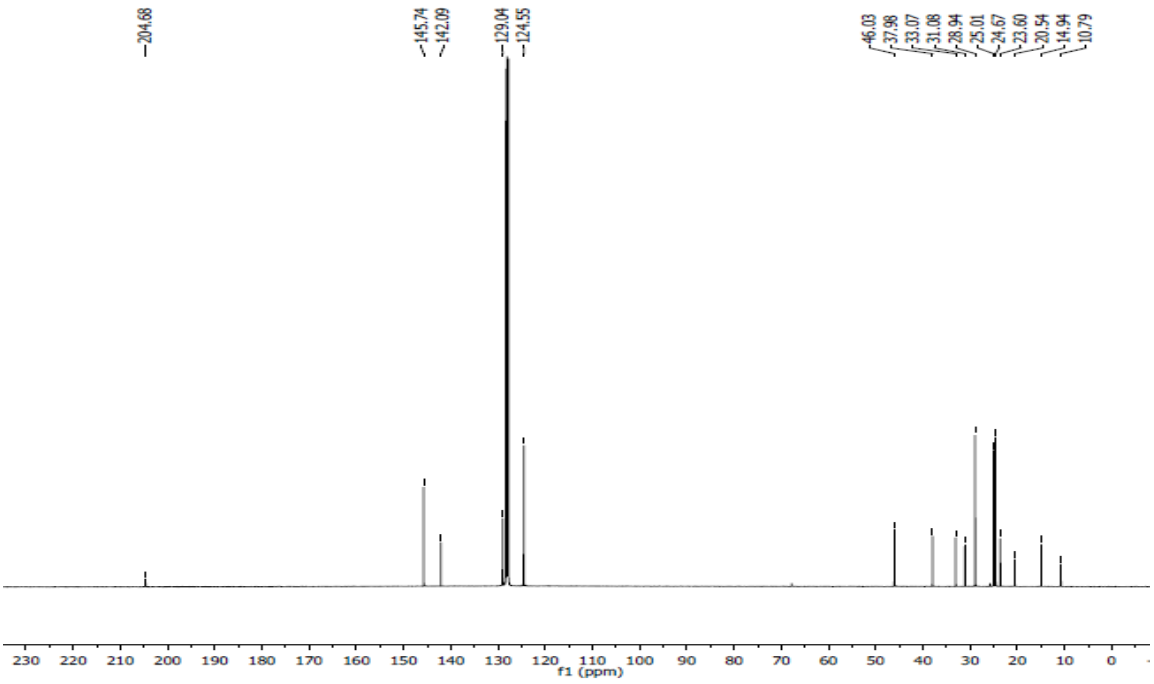

Figure 2.29. ^{13}C NMR spectrum of (6Dipp)copper(I) hexyl in C_6D_6.

2.4.4.11 Synthesis of (6Dipp)copper(I) heptanoate

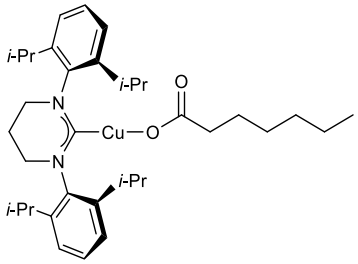

Figure 2.30 (6Dipp)copper(I) heptanoate (**6a**)

In an oven-dried J. Young NMR tube under N_2, a solution of (6Dipp)Cu-hexyl (0.030 g, 0.054 mmol) in C_6D_6 (0.7 mL) was degassed by 3 freeze-pump-thaw cycles before being exposed to an atmosphere of CO_2. After 40 min, the C_6D_6 was removed *in vacuo* and the residual solid was dried for 12h, affording the product as a colorless powder.

(0.029 g, 91%). ^{1}H NMR (400 MHz, C_6D_6): δ (ppm) 7.16 (t, $^{3}J_{HH}$ = 7.2 Hz, 2H, para-C*H*), 7.07 (d, $^{3}J_{HH}$ = 7.2 Hz, 4H, *meta*-C*H*), 3.04 (sept, $^{3}J_{HH}$ = 6.8 Hz, 4H, C*H*$(CH_3)_2$), 2.72 (t, $^{3}J_{HH}$ = 6.0 Hz, 4H, NC*H*$_2$), 2.12 (t, $^{3}J_{HH}$ = 7.2 Hz, 2H, OC(O)C*H*$_2$), 1.57 (d, $^{3}J_{HH}$ = 7.2 Hz, 12H, $CH_2(CH_3)_2$), 1.54 (m, 4H, $OC(O)CH_2CH_2$, NCH_2CH_2), 1.18 (d, $^{3}J_{HH}$ = 7.2 Hz, 12H, $CH_2(CH_3)_2$), 1.11 (m, 6H, OC(O) $(CH_2)_2(CH_2)_3$), 0.80 (t, $^{3}J_{HH}$ = 7.2 Hz, 3H, $OC(O)(CH_2)_5CH_3$). $^{13}C\{^{1}H\}$ NMR (100 MHz, C_6D_6): δ (ppm) 202.1 (N*C*Cu), 178.8 (Cu-O*C*(O), 145.7 (*ortho*-C), 142.1 (*ipso*-*C*), 129.5 (*meta*-*C*), 124.9 (*para*-*C*), 46.0 (NCH_2), 37.0 ($OC(O)CH_2CH_2$), 32.2 ($OC(O)CH_2CH_2$), 29.6 ($OC(O)(CH_2)_2CH_2$), 28.9 ($CH(CH_3)_2$), 26.9 ($OC(O)(CH_2)_3CH_2$), 25.1 ($CH(CH_3)_2$), 24.8 ($CH(CH_3)_2$), 23.0 ($OC(O)(CH_2)_4CH_2$), 14.4 (OC(O) $(CH_2)_5CH_3$). IR ν (cm^{-1}) 2959, 2925, 2866, 1607, 1509, 1554, 1371, 1342, 1306, 1235, 1205, 1152, 1057, 984, 935, 806, 762, 726, 638, 556, 502, 453.

Note: We have been unable to obtain satisfactory elemental analysis for **6a**. The complex is air- and moisture-sensitive. While NMR-silent impurities cannot be ruled out, we believe the ^{1}H and ^{13}C NMR spectra reflect the purity of the sample.

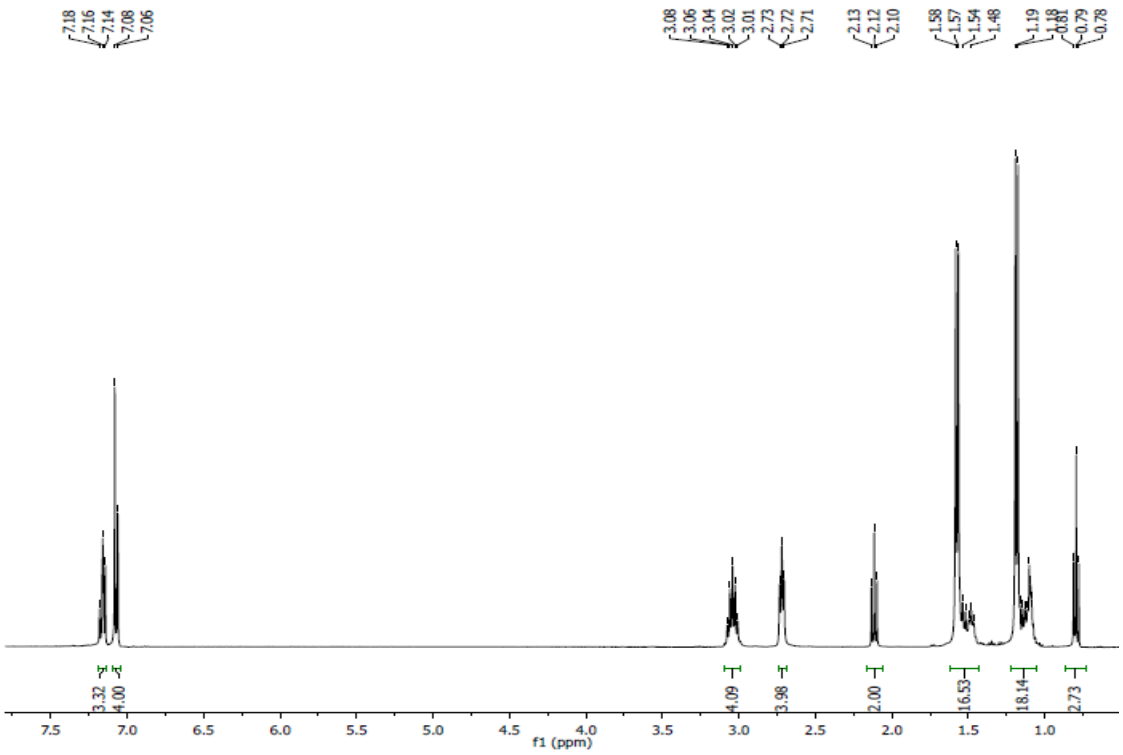

Figure 2.31 ^{1}H NMR spectrum of (6Dipp)copper(I) heptanoate in C_6D_6.

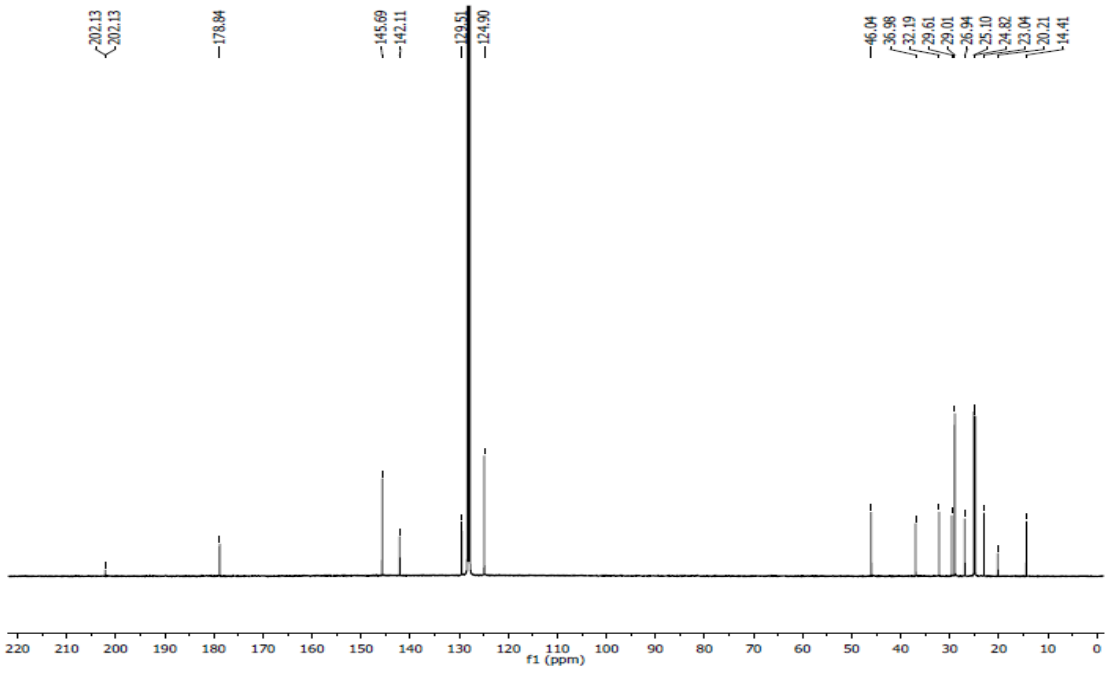

Figure 2.32 ^{13}C NMR spectrum of (6Dipp)copper(I) heptanoate in C_6D_6.

2.4.4.12 Synthesis of (6Dipp)copper(I) (*N*-benzyl)formimidoyl

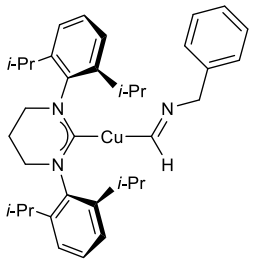

Figure 2.33 (6Dipp)copper(I) (*N*-benzyl)formimidoyl (**7a**)

Benzyl isocyanide (0.064 mL, 0.052 mmol) was added via syringe to a solution of $[(6Dipp)CuH]_2$ (0.025 g, 0.026 mmol) toluene (1.5 mL). After 3h the solution was layered with pentane (1 mL) and allowed to stand in the freezer at –35º C for 48h. The supernatant was decanted by pipette, the resulting crystals were redissolved in toluene (1 mL), layered with pentane (1 mL) and placed back in the freezer. After 48h, the supernatant was decanted by pipette. The resulting crystals were dried *in vacuo* for 12h to give a pale yellow solid. (0.018 g, 57%) ^{1}H NMR (400 MHz, C_6D_6): δ (ppm) 9.37 (s, 1H, Cu-C(N)*H*), 7.26 (m, 5H, -C_6H_5), 7.18 (t, $^3J_{HH}$ = 7.2 Hz, para-C*H*), 7.08 (d, $^3J_{HH}$ = 7.2 Hz, 4H, *meta*-C*H*), 4.53 (s, 2H, C(H)=NCH_2), 3.06 (sept, $^3J_{HH}$ = 6.8 Hz, 4H, C*H*$(CH_3)_2$), 2.70 (t, $^3J_{HH}$ = 6.0 Hz, 4H, NCH_2), 1.56 (d, $^3J_{HH}$ = 6.8 Hz, 12H, $CH_2(CH_3)_2$), 1.47 (quin, $^3J_{HH}$ = 5.6 Hz, 2H, NCH_2CH_2), 1.20 (d, $^3J_{HH}$ = 7.2 Hz, 12H, $CH_2(CH_3)_2$). $^{13}C\{^1H\}$ NMR (100 MHz, C_6D_6): δ (ppm) 209.9 (Cu-*C*(N)H), 204.8 (N*C*Cu), 145.8 (dipp-*ortho*-C), 144.1 (Bn-*ipso*-C), 141.7 (dipp-*ipso*-*C*), 129.3 (dipp-*meta*-*C*), 128.2 (Bn-*ortho*-C), 127.9 (Bn-*meta*-C), 125.4 (Bn-para-C), 124.7 (dipp-*para*-*C*), 77.1 (C(H)=N*C*H_2), 45.9 (N*C*H_2), 29.0 (*C*H$(CH_3)_2$), 25.2 (CH(*C*$H_3)_2$), 24.7 (CH(*C*$H_3)_2$), 20.4 (NCH_2CH_2). IR ν (cm^{-1}) 2959, 2923, 2866, 1582,

1509, 1451, 1400, 1384, 1254, 1204, 1056, 989, 934, 8789, 804, 754, 694, 618, 551, 512, 452.

Note: We have been unable to obtain satisfactory elemental analysis for **7a**. The complex is extremely air-, and moisture-sensitive. Although NMR-silent impurities cannot be ruled out, we believe the ^{1}H and ^{13}C NMR spectra reflect the purity of the sample.

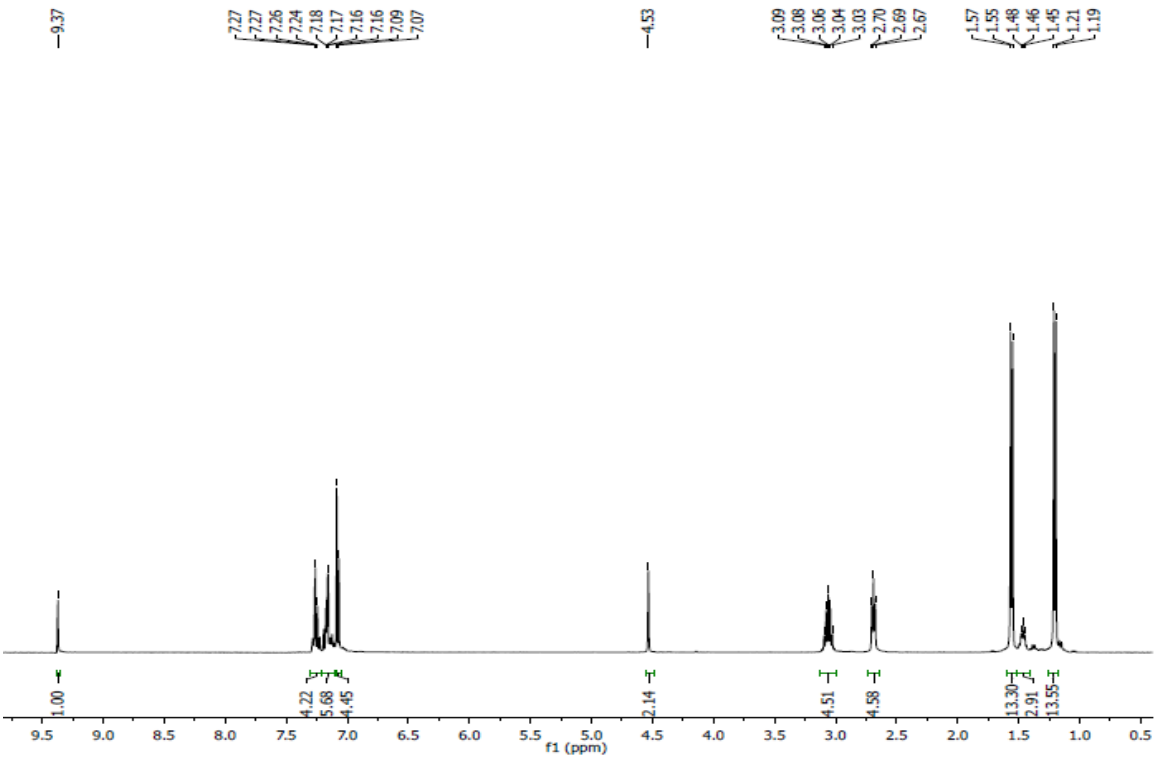

Figure 2.34 ^{1}H NMR spectrum of (6Dipp)copper(I) (*N*-benzyl)formimidoyl in C_6D_6.

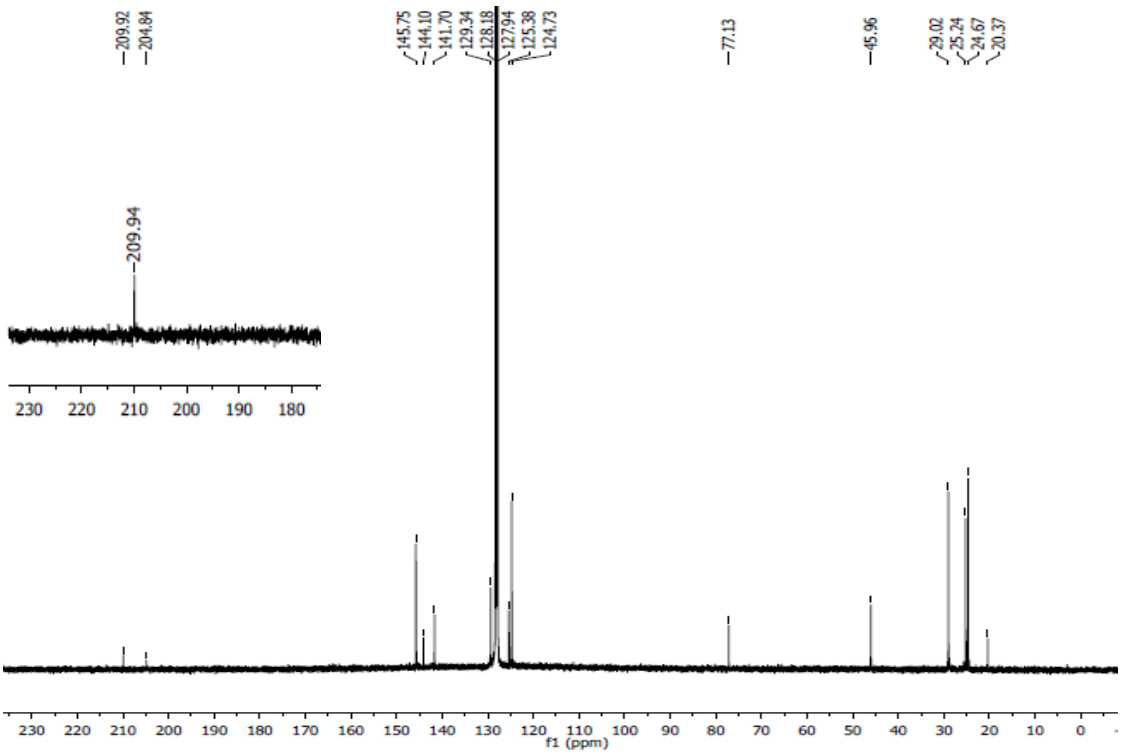

Figure 2.35 ^{13}C NMR spectrum of (6Dipp)copper(I) (*N*-benzyl)formimidoyl overlaid with the DEPT-90 in C_6D_6.

2.4.4.13 Reaction of $[(5Dipp)CuH]_2$ with 1-Hexene.

Pinacolborane [4,4,5,5,-tetramethyl-1,3,2-dioxaborolane; HB(pin)] (0.055 mL, 0.037 mmol) was added to a solution of (5Dipp)CuO-*t*-Bu (0.020 g, 0.037 mmol) and 1.4-dimethoxybenzene (0.005 g, 0.04 mmol; internal standard) in C_6D_6 (1 mL) via syringe. The solution immediately became bright yellow in color and 1-hexene (0.047 mL, 0.037 mmol) was then added via syringe. The solution was transferred to a J. Young NMR tube, and the reaction was monitored by ^{1}H NMR.

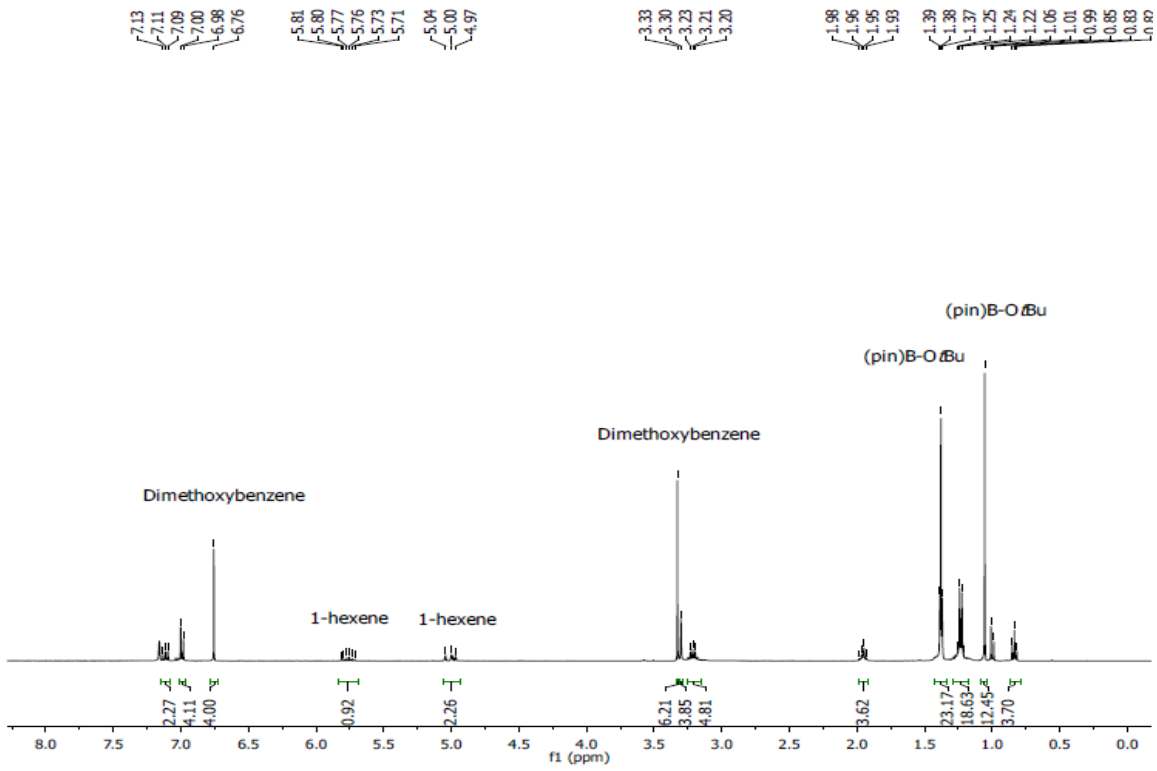

Figure 2.36 ^{1}H NMR spectrum of $[(5Dipp)CuH]_2$ with 1-hexene in C_6D_6 after 10 min.

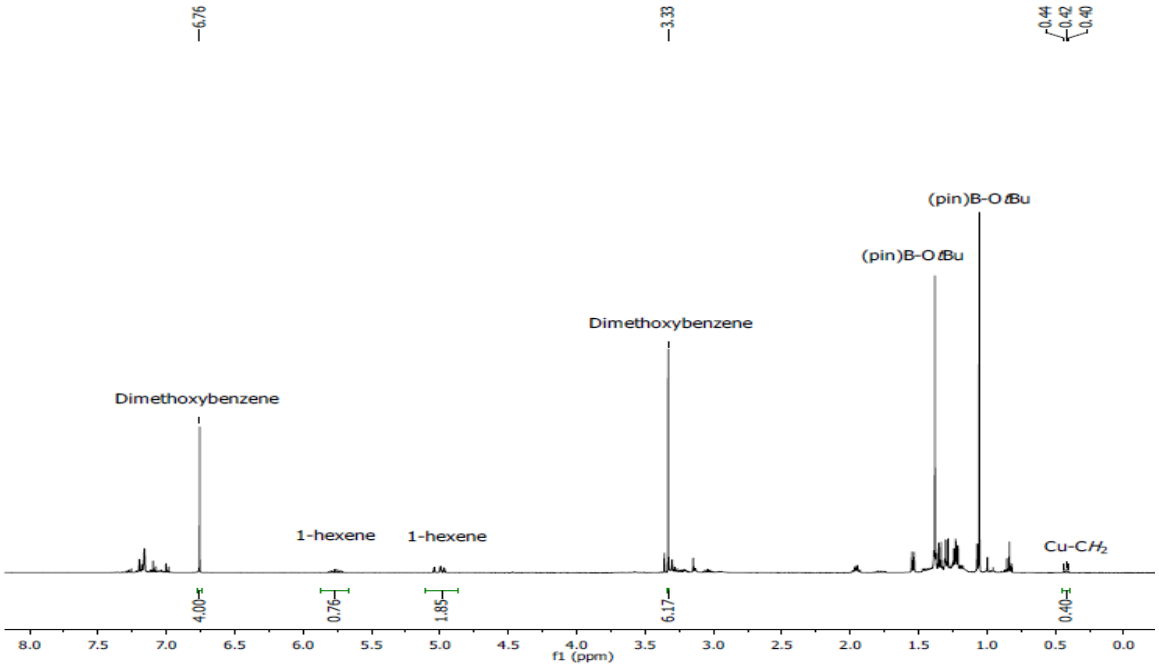

Figure 2.37 ^{1}H NMR spectrum of $[(5Dipp)CuH]_2$ with 1-hexene in C_6D_6 after 48h.

2.4.4.14 Reaction of $[(7Dipp)CuH]_2$ with benzyl isocyanide.

Benzyl isocyanide (0.027 mL, 0.023 mmol) was added to a solution of $[(7Dipp)CuH]_2$ (**4b**, 0.012 g, 0.021 mmol) in C_6D_6 (0.7 mL) via syringe. The solution was transferred to a J. Young NMR tube, and the reaction was monitored by ^1H NMR spectroscopy.

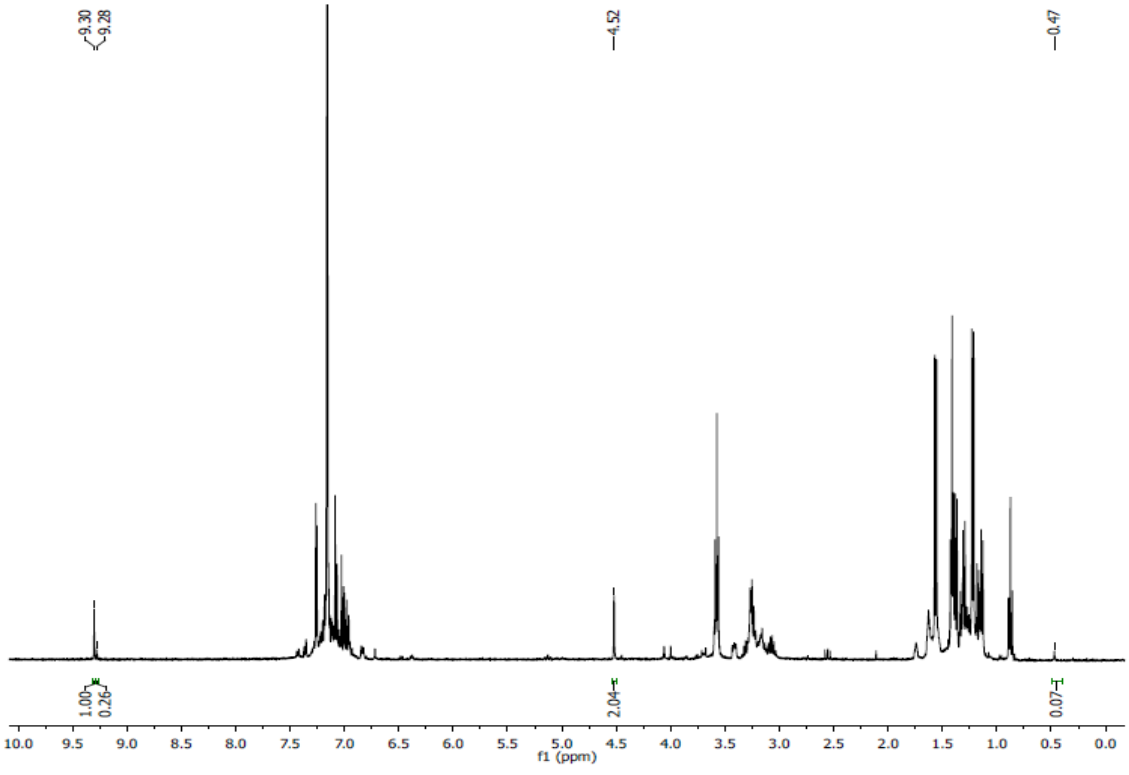

Figure 2.38 ^1H NMR spectrum of $[(7Dipp)CuH]_2$ with benzyl isocyanide in C_6D_6 after 5.5 h.

2.4.5 *X-ray diffraction studies.*

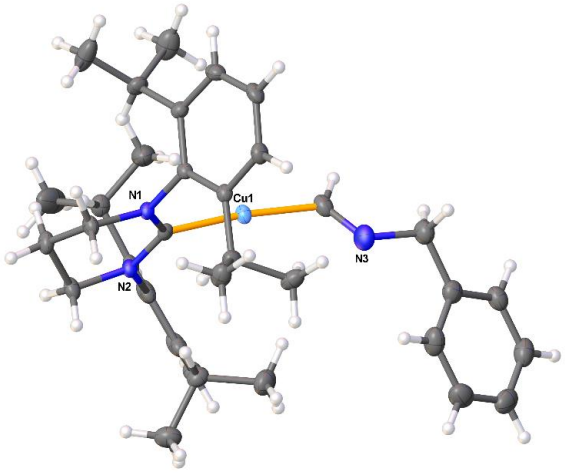

Figure 2.39 Thermal ellipsoid plot of **7a**.

Single yellow block-shaped crystals of **7a** were recrystallised from a mixture of toluene and pentane by vapor diffusion. A suitable crystal (0.64×0.31×0.22 mm) was selected and mounted on a loop with paratone oil on a Bruker APEX-II CCD diffractometer. The crystal was cooled to T = 100(2) K during the data collection. The structure was solved with **ShelXT**[52] using direct and dual-space solution methods and by using **Olex2**[53] as the graphical interface. The model was refined with **ShelXL-97**[54] using Least Squares minimisation.

Crystal Data. $C_{36}H_{48}CuN_3$, M_r = 586.31, monoclinic, $P2_1/c$ (No. 14), a = 10.5381(13) Å, b = 19.114(2) Å, c = 16.3664(19) Å, β = 97.200(2)°, α = γ = 90°, V = 3270.6(7) Å^3, T = 100(2) K, Z = 4, Z' = 1, μ(MoK$_\alpha$) = 0.695, 48654 reflections measured, 9194 unique (R_{int} = 0.0424) which were used in all calculations. The final wR_2 was 0.1280 (all data) and R_1 was 0.0491 (I > 2(I)).

Table 2.1 Crystal Data for **7a**

Compound	**7a**
Formula	$C_{36}H_{48}CuN_3$
$D_{calc.}$/ g cm^{-3}	1.191
μ/mm^{-1}	0.695
Formula Weight	586.31
Colour	yellow
Shape	block
Max Size/mm	0.64
Mid Size/mm	0.31
Min Size/mm	0.22
T/K	100(2)
Crystal System	monoclinic
Space Group	$P2_1/c$
a/Å	10.5381(13)
b/Å	19.114(2)
c/Å	16.3664(19)
α/°	90
β/°	97.200(2)
γ/°	90
V/Å^3	3270.6(7)
Z	4
Z'	1
Θ_{min}/°	1.646
Θ_{max}/°	29.632
Measured Refl.	48654
Independent Refl.	9194
Reflections Used	7470
R_{int}	0.0424
Parameters	369
Restraints	0
Largest Peak	1.075
Deepest Hole	-0.389
GooF	1.062
wR_2 (all data)	0.1280
wR_2	0.1180
R_1 (all data)	0.0654
R_1	0.0491

Table 2.2 Bond Lengths (Å) for **7a**

Atom	Atom	Length/Å
Cu1	C29	1.916(2)
Cu1	C1	1.9326(18)
N1	C14	1.475(2)
N1	C2	1.442(2)
N1	C1	1.339(2)
N2	C16	1.476(2)
N2	C17	1.441(2)
N2	C1	1.336(2)
N3	C29	1.292(3)
N3	C30	1.467(3)
C18	C26	1.516(3)
C18	C19	1.396(3)
C18	C17	1.405(3)
C3	C4	1.392(3)
C3	C11	1.519(3)
C3	C2	1.407(2)
C23	C24	1.530(3)
C23	C25	1.533(3)
C23	C22	1.518(3)
C4	C5	1.384(3)
C8	C9	1.527(3)
C8	C10	1.535(3)
C8	C7	1.521(3)
C21	C20	1.381(3)
C21	C22	1.396(3)
C6	C5	1.385(3)
C6	C7	1.400(3)
C15	C16	1.509(3)
C15	C14	1.515(3)
C26	C27	1.513(3)
C26	C28	1.523(3)
C19	C20	1.387(3)
C11	C12	1.521(3)
C11	C13	1.525(3)
C30	C31	1.513(3)
C31	C32	1.393(3)
C31	C36	1.394(3)
C34	C35	1.381(4)
C34	C33	1.372(4)
C32	C33	1.381(3)
C35	C36	1.388(4)
C2	C7	1.395(3)
C22	C17	1.400(3)

Table 2.3 Bond Angles (deg) for **7a**

Atom	Atom	Atom	Angle/°
C29	Cu1	C1	173.28(8)
C2	N1	C14	116.99(15)
C1	N1	C14	124.81(15)
C1	N1	C2	118.21(15)
C17	N2	C16	115.45(15)
C1	N2	C16	124.81(16)
C1	N2	C17	119.68(15)
C29	N3	C30	118.57(19)
C19	C18	C26	121.19(18)
C19	C18	C17	117.52(18)
C17	C18	C26	121.24(18)
C4	C3	C11	120.40(17)
C4	C3	C2	117.69(17)
C2	C3	C11	121.90(17)
C24	C23	C25	111.89(19)
C22	C23	C24	111.00(18)
C22	C23	C25	110.80(18)
C5	C4	C3	121.42(18)
C9	C8	C10	111.15(17)
C7	C8	C9	111.53(17)
C7	C8	C10	110.59(16)
C20	C21	C22	121.17(19)
C5	C6	C7	121.06(18)
C16	C15	C14	109.87(16)
C18	C26	C28	113.2(2)
C27	C26	C18	111.25(18)
C27	C26	C28	110.0(2)
C4	C5	C6	119.80(18)
N2	C16	C15	109.75(16)
C20	C19	C18	120.69(19)
C21	C20	C19	120.56(19)
N1	C14	C15	109.85(16)
C3	C11	C12	111.08(19)
C3	C11	C13	111.96(18)
C12	C11	C13	110.65(19)
N3	C29	Cu1	120.40(16)
N3	C30	C31	112.21(19)
C32	C31	C30	120.7(2)
C32	C31	C36	117.9(2)
C36	C31	C30	121.4(2)
C33	C34	C35	119.0(2)
C33	C32	C31	121.0(2)
C34	C35	C36	120.8(2)
C34	C33	C32	120.8(2)
C3	C2	N1	118.76(16)
C7	C2	N1	119.13(15)
C7	C2	C3	122.11(17)
C21	C22	C23	119.80(18)
C21	C22	C17	117.26(18)
C17	C22	C23	122.94(17)
C18	C17	N2	118.42(17)
C22	C17	N2	118.67(17)
C22	C17	C18	122.81(18)
N1	C1	Cu1	120.27(13)
N2	C1	Cu1	121.94(13)
N2	C1	N1	117.61(16)
C6	C7	C8	119.87(17)
C2	C7	C8	122.19(16)
C2	C7	C6	117.91(17)
C35	C36	C31	120.5(2)

2.5 References

[1] Deutsch, C.; Krause, N.; Lipshutz, B. H. *Chem. Rev.* **2008**, *108*, 2916-2927.

[2] Churchill, M. R.; Bezman, S. A.; Osborn, J. A.; Wormald, J. *J. Amer. Chem. Soc.* **1971**, *93*, 2063-2065

[3] Mahoney, W. S.; Brestensky, D. M.; Stryker, J. M. *J. Am. Chem. Soc.* **1988**, *110*, 291-293.

[4] Brestensky, D. M.; Stryker, J. M. *Tetrahedron Lett.* **1989**, *30*, 5677-5680.

[5] Koenig, T. M.; Daeuble, J. F.; Brestensky, D. M.; Stryker, J. M. *Tetrahedron Lett.* **1990**, *31*, 3237-3240.

[6] Eberhart, M. S.; Norton, J. R.; Zuzek, A.; Sattler, W.; Ruccolo, S. *J. Am. Chem. Soc.* **2013**, *135*, 17262-17265.

[7] Grigg, R. D.; Van Hoveln, R.; Schomaker, J. M. *J. Am. Chem. Soc.* **2012**, *134*, 16131-16134.

[8] Tani, Y.; Kuga, K.; Fujihara, T.; Terao, J.; Tsuji, Y. *Chem. Commun.* **2015**, *51*, 13020-13023.

[9] Van Hoveln, R. J.; Schmid, S. C.; Tretbar, M.; Buttke, C. T.; Schomaker, J. M. *Chem. Sci.* **2014**, *5*, 4763-4767.

[10] Wang, Y.-M.; Bruno, N. C.; Placeres, A. L.; Zhu, S.; Buchwald, S. L. *J. Am. Chem. Soc.* **2015**, *137*, 10524-10527.

[11] Yang, Y.; Shi, S.-L.; Niu, D.; Liu, P.; Buchwald, S. L. *Science* **2015**, *349*, 62-66.

[12] Goeden, G. V.; Huffman, J. C.; Caulton, K. G. *Inorg. Chem.* **1986**, *25*, 2484-2485.

[13] Jurkauskas, V.; Sadighi, J. P.; Buchwald, S. L. *Org. Lett.* **2003**, *5*, 2417-2420.

[14] Kaur, H.; Zinn, F. K.; Stevens, E. D.; Nolan, S. P. *Organometallics* **2004**, *23*, 1157-1160.

[15] Schmid, S. C.; Van Hoveln, R.; Rigoli, J. W.; Schomaker, J. M. *Organometallics* **2015**, *34*, 4164-4173.

[16] Uehling, M. R.; Rucker, R. P.; Lalic, G. *J. Am. Chem. Soc.* **2014**, *136*, 8799-8803.

[17] Whittaker, A. M.; Lalic, G. *Org. Lett.* **2013**, *15*, 1112-1115.

[18] Mankad, N. P.; Laitar, D. S.; Sadighi, J. P. *Organometallics* **2004**, *23*, 3369-3371.

[19] Frey, G. D.; Donnadieu, B.; Soleilhavoup, M.; Bertrand, G. *Chem. - Asian J.* **2011**, *6*, 402-405.

[20] Page, M. J.; Lu, W. Y.; Poulten, R. C.; Carter, E.; Algarra, A. G.; Kariuki, B. M.; MacGregor, S. A.; Mahon, M. F.; Cavell, K. J.; Murphy, D. M.; Whittlesey, M. K. *Chem. - Eur. J.* **2013**, *19*, 2158-2167.

[21] Tate, B. K.; Nguyen, J. T.; Bacsa, J.; Sadighi, J. P. *Chem. - Eur. J.* **2015**, *21*, 10160-10169

[22] Phillips, N.; Dodson, T.; Tirfoin, R.; Bates, J. I.; Aldridge, S. *Chem. - Eur. J.* **2014**, *20*, 16721-16731.

[23] Collins, L. R.; Riddlestone, I. M.; Mahon, M. F.; Whittlesey, M. K. *Chem. - Eur. J.* **2015**, *21*, 14075-14084.

[24] This ligand is usually abbreviated as SIPr or SIDipp. We have chosen to keep notation consistent between NHCs of different ring sizes.

[25] Uehling, M. R.; Suess, A. M.; Lalic, G. *J. Am. Chem. Soc.* **2015**, *137*, 1424-1427.

[26] Chen, Z.; Wannere, C. S.; Corminboeuf, C.; Puchta, R.; Schleyer, P. v. R. *Chem. Rev.* **2005**, *105*, 3842-3888.

[27] Lu, W. Y.; Cavell, K. J.; Wixey, J. S.; Kariuki, B. *Organometallics* **2011**, *30*, 5649-5655.

[28] Tsui, E. Y.; Muller, P.; Sadighi, J. P. *Angew. Chem., Int. Ed.* **2008**, *47*, 8937-8940.

[29] Vergote, T.; Nahra, F.; Merschaert, A.; Riant, O.; Peeters, D.; Leyssens, T. *Organometallics* **2014**, *33*, 1953-1963.

[30] Milder, S. J.; Goldbeck, R. A.; Kliger, D. S.; Gray, H. B. *J. Am. Chem. Soc.* **1980**, *102*, 6761-6764

[31] Che, C.-M.; Atherton, S. J.; Butler, L. G.; Gray, H. B. *J. Am. Chem. Soc.* **1984**, *106*, 5143-5145.

[32] Stiegman, A. E.; Rice, S. F.; Gray, H. B.; Miskowski, V. M. *Inorg. Chem.* **1987**, *26*, 1112-1116.

[33] Harvey, P. D.; Adar, F.; Gray, H. B. *J. Am. Chem. Soc.* **1989**, *111*, 1312-1315.

[34] Shintani, R.; Nozaki, K. *Organometallics* **2013**, *32*, 2459-2462.

[35] Wyss, C. M.; Tate, B. K.; Bacsa, J.; Gray, T. G.; Sadighi, J. P. *Angew. Chem., Int. Ed.* **2013**, *52*, 12920-12923.

[36] Zhang, L.; Cheng, J.; Hou, Z. *Chem. Commun.* **2013**, *49*, 4782-4748.

[37] Santoro, O.; Lazreg, F.; Minenkov, Y.; Cavallo, L.; Cazin, C. S. J. *Dalton Trans.* **2015**, *44*, 18138-18144.

[38] Zhu, S.; Buchwald, S. L. *J. Am. Chem. Soc.* **2014**, *136*, 15913-15946.

[39] Mankad, N. P.; Gray, T. G.; Laitar, D. S.; Sadighi, J. P. *Organometallics* **2004**, *23*, 1191-1193.

[40] Goj, L. A.; Blue, E. D.; Munro-Leighton, C.; Gunnoe, T. B.; Petersen, J. L. *Inorg. Chem.* **2005**, *44*, 8647-8649.

[41] Rucker, R. P.; Whittaker, A. M.; Dang, H.; Lalic, G. *J. Am. Chem. Soc.* **2012**, *134*, 6571-6574.

[42] Ueno, A.; Takimoto, M.; O, W. W. N.; Nishiura, M.; Ikariya, T.; Hou, Z. *Chem. - Asian J.* **2015**, *10*, 1010-1016.

[43] Tobisu, M.; Fujihara, H.; Koh, K.; Chatani, N. *J. Org. Chem.* **2010**, *75*, 4841-4847.

[44] Boyarskiy, V. P.; Bokach, N. A.; Luzyanin, K. V.; Kukushkin, V. Y. *Chem. Rev.***2015**, *115*, 2698-2779

[45] Christian, D. F.; Clark, G. R.; Roper, W. R.; Waters, J. M.; Whittle, K. R. *J. Chem. Soc., Chem. Commun.* **1972**, 458-459.

[46] Duckett, S. B.; Lowe, J. P.; Mawby, R. J. *Dalton Trans.* **2006**, 2661-2670.

[47] Kuhn K.M.; Grubbs R.H. *Org. Lett.* **2008**, *10*, 2075

[48] Laitar, D. S. Ph.D. Thesis, Massachusetts Institute of Technology, **2006**. https://dspace.mit.edu/handle/1721.1/36268 (Accessed June 2019)

[49] Kolychev E. L.; Portnyagin I. A.; Shuntikov V. V.; Khrustalev V. N.; Nechaev M. S. *J. Organomet. Chem.* **2009**, *694*, 2454

[50] Fluegge, S.; Anoop, A.; Goddard, R.; Thiel, W.; Fuerstner, A. *Chem. - Eur. J.* **2009**, *15*, 8558

[51] Yoo, W.-J.; Nguyen, T. V. Q.; Kobayashi, S. *Angew. Chem. Int. Ed.* **2014**, *53*, 10213

[52] Sheldrick, G.M. *Acta Cryst.* **2014**, *A71*, 3-8.

[53] Dolomanov, O. V.; Bourhis L. J.; Gildea, R. J.; and. Howard, J. A. K.; Puschmann, H. *J. Appl. Cryst.* **2009**, *42*, 339-341

[54] Sheldrick, G.M. *Acta Cryst.* **2008**, *A64*, 339-341

CHAPTER 3. COPPER(I)-MEDIATED BOROFLUORINATION OF ALKYNES

Part of this thesis chapter has been adapted with permission from an article co-written by the author:

Jordan, A. J.; Thompson, P. K.; Sadighi, J. P. Copper(I)-Mediated Borofluorination of Alkynes. *Org. Lett.* **2018**, *20*, 5242-5246.

3.1 Background

Applications of fluorinated organic compounds in pharmaceuticals,[1] materials[2] and agrochemicals[3] are ever increasing due to the unique properties engendered by carbon-fluorine bonds. Much effort has been dedicated to furthering synthetic access to fluorine containing organics.[4] Transition-metal-catalyzed and -mediated processes provide synthetic methods to construct C–F bonds while avoiding the use of harsh fluorination reagents;[5] the coinage metals, copper[6] and silver[7] and gold[8] have proven notably useful in these efforts. For example, C(sp^2)–(main group element) bonds can be converted to C–F bonds using electrophilic fluorine sources in the presence of copper or silver salts (Scheme 3.1a).[6b,6d,7c-f,7h] Additionally, gold(I) fluorides catalyze the *trans*-hydrofluorination of alkynes using Et_3N•3HF or DMPU•HF (Scheme 3.1b).[8a,8c,8d] Gold(III) fluorides have been shown to form alkyl-fluoride bonds through reductive elimination (Scheme 3.1c).[9]

The significant utility of fluorinated alkenes has spurred substantial advances in their synthesis during the past decade.[4b,10] Despite these advances, limitations in the scope, selectivity or safety of the fluorine source remain. The reductive functionalization of alkynes represents an appealing approach to fluorinated alkenes due to the synthetic accessibility of alkynes. Gold hydrofluorination catalysis[8] is a useful approach to alkyne fluorination chemistry, but copper- and silver-catalyzed hydrofluorination is limited to

ynamides.[11] In these systems, the C–F bond forming step occurs by *trans*-addition of the metal and fluoride across an alkyne (Scheme 3.1b).

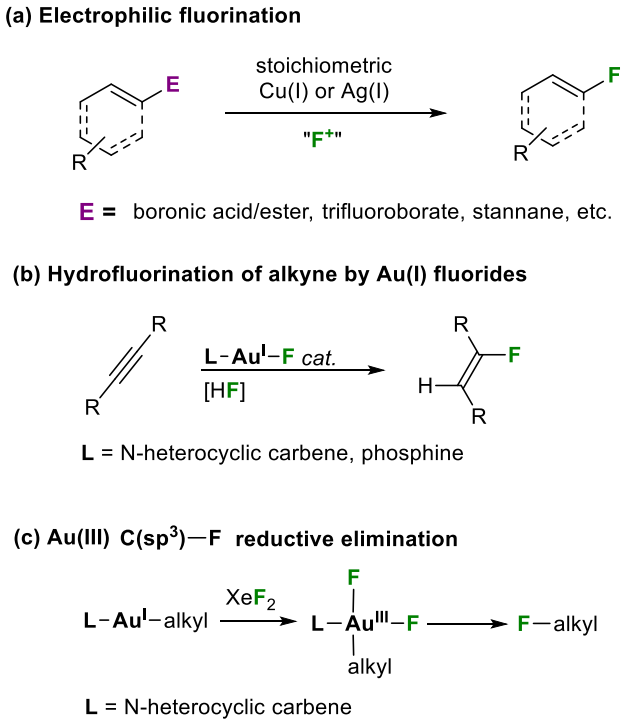

Scheme 3.1 Coinage metals in C–F bond formation.

3.2 Results and Discussion

3.2.1 Fluorination of (NHC)Copper(I) Vinyls

The few methods developed for the fluorination of terminal alkynes yield internal fluorination products, and a direct transformation of terminal alkynes to terminal fluorinated alkenes remains elusive.[7c] The anti-Markovnikov hydrobromination of alkynes has been developed by Lalic and coworkers to afford terminal bromoalkenes,[12] and Buchwald and coworkers recently demonstrated the oxidative anti-Markovnikov hydroamination of alkynes.[13] We envisioned an analogous sequence involving alkyne

insertion to form a copper-carbon bond, followed by oxidative cleavage. This chapter presents a new sequence for alkene C–F bond construction which occurs by the electrophilic fluorination of alkyne derived copper(I) vinyls.

Addition of NFSI to (IDipp)Cu[(*E*)-3-hexynyl], (IDipp = 1,3-bis(2,6-diisopropylphenyl)imidazole-2-ylidene), generated from $[(IDipp)CuH]_2$,[14] resulted in the formation of (*E*)-3-fluorohex-3-ene (**8**), determined by the quartet in the ^{19}F NMR at δ –108.3 ppm, in 35% yield (Scheme 3.2) The insertion of phenylacetylene into $[(IDipp)CuH]_2$ results in the formation of both 1- and 2-phenylvinylcopper intermediates, thus yielding both 1- and (*E*)-2-(fluorovinyl)benzene after reaction with NFSI. Using the more sterically demanding ligand 6Dipp, [1,3-bis(2,6-diisopropylphenyl)-3,4,5,6-tetrahydropyrimidin-2-ylidene],[15] we observed only the terminal copper vinyl. Fluorination of this intermediate with NFSI affords (*E*)-(2-fluorovinyl) benzene (**9**) in 30% yield; analysis by GC-MS shows the major product to be the divinyl formed by oxidative coupling (Scheme 3.2). This is the sole pathway reported for the reaction of gold(I) vinyls with NFSI.[16]

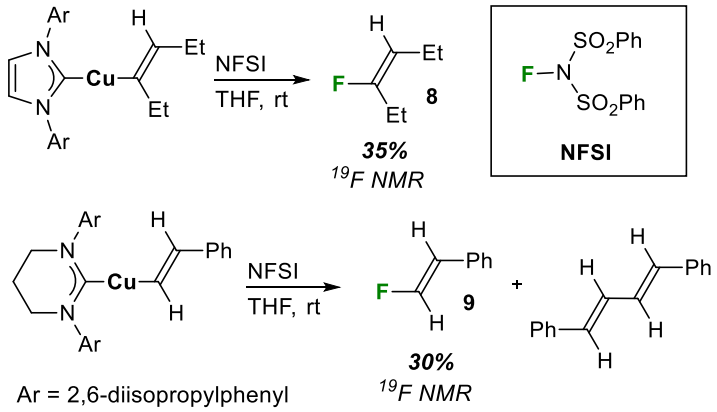

Scheme 3.2 Fluorination of (NHC)copper(I) vinyls.

3.2.2 Borofluorination of Alkynes

Encouraged by these results, we then considered the fluorination of (NHC)copper(I) borovinyls due to the synthetic utility of boronates. Initially, (IDipp)CuO-*t*-Bu, bis(pinacolato)diboron [$B_2(pin)_2$][17] and 3-hexyne were combined in THF before N-fluorobenzenesulfonimide (NFSI) was added to the solution. Gratifyingly, the ^{19}F NMR showed a triplet at δ –90.5 ppm, consistent with the formation of the (*E*)-(4-fluoro-3-hexen-3-yl) boronic acid pinacol ester, albeit in only 19% yield. This ^{19}F NMR chemical shift is similar to those of related *cis*-(β-fluorovinyl)boronate esters synthesized by Hara and coworkers' from (2-fluoro-1-alkenyl)iodonium salts (Scheme 3.3a).[18] This motif could be further functionalized to a variety of fluorinated products. Recently, several groups synthesized *gem*-borylfluoroalkenes, which also could be functionalized further, by copper-catalyzed borylation/defluorination of *gem*-difluoroalkenes (Scheme 3.3b).[19] The present method introduces, rather than removes, a carbon-fluorine bond while avoiding the use of hydrofluoric acid.

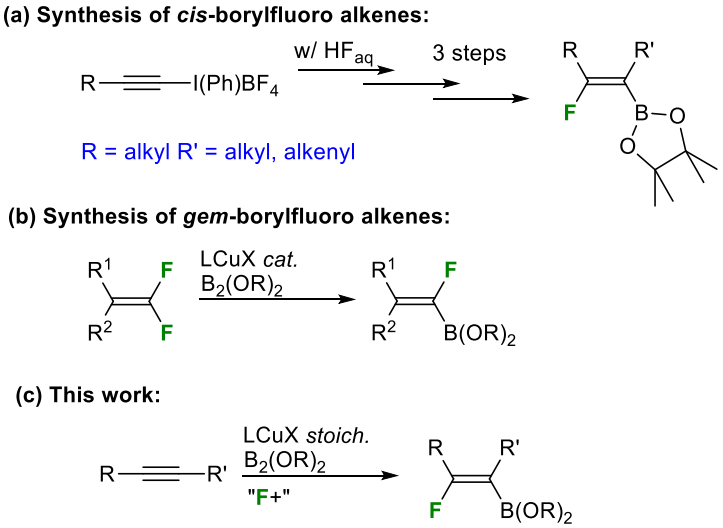

Scheme 3.3 Synthesis of fluorovinyl-boronate esters.

With 3-hexyne as the substrate, reaction conditions were then screened, and these results are summarized in Table 3.1. The common electrophilic fluorinating reagent, SelectFluor®, also resulted in considerable product formation (Table 2.1), but NFSI resulted in higher yields.[20] Using (IDipp)CuO-*t*-Bu as the copper(I) source, bis(neopentyl glycolato)diboron [$B_2(neo)_2$], and NFSI in toluene solution, the yield of the borofluorination product of 3-hexyne was 84% as judged by ^{19}F NMR spectroscopy. The copper-based product (IDipp)CuN($SO_2Ph)_2$ (**11**) can be isolated in good yield (*vide infra*).

To confirm the formation of **10**, a protiodeborylation of **10** was carried out to generate (*E*)-3-fluoro-3-hexene (**8**). Addition of aqueous potassium carbonate following the fluorination step readily yields (*E*)-3-fluoro-3-hexene, judged by ^{19}F NMR spectroscopy (Scheme 3.4). Replacement of the boryl substituent with a proton results in an upfield shift of the fluorine resonance from δ –88.7 ppm to δ –108.3 ppm; the additional coupling between the fluorine and the newly installed vicinal proton turns the triplet resonance to a pseudo-quartet.

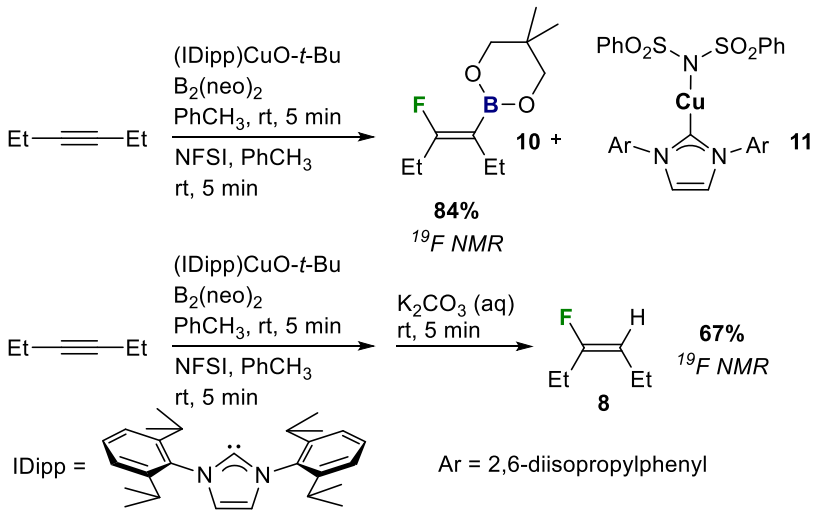

Scheme 3.4 Borofluorination and protiodeborylation.

3.2.3 Elementary Steps of the Borofluorination of Alkynes

As hypothesized, (IDipp)CuO-*t*-Bu quickly reacts with $B_2(neo)_2$ to yield a copper boryl,[17] judged by ^{1}H NMR spectroscopy (Scheme 3.5). The resulting copper boryl may be observed in solution at ambient temperature, but decomposition is substantial after 20 minutes. In the presence of an alkyne, the Cu–B bond readily adds across the C≡C bond of the alkyne to generate the copper (2-borovinyl).[21] This 1,2-insertion must occur in a *cis* fashion, setting the geometry between B and F. The copper borovinyls are stable at room temperature, and the product of diphenylacetylene insertion can be isolated cleanly. Subsequent addition of NFSI to the (2-borovinyl) copper species yields (*E*)-(2-fluoro-1,2-diphenylvinyl)boronic acid neopentyl glycolato ester (**12**) and the (NHC)copper benzenesulfonimide (**11**), which can be isolated in 93% yield. In addition to the fluorinated product and (IDipp)CuN$(SO_2Ph)_2$, diphenylacetylene is reformed. The formation of this byproduct implies the formation of a strong B–F bond, competitively with the desired C–F bond formation, during the reaction of the (2-borovinyl)copper intermediate with NFSI. The nature of the C–F bond forming step is unknown, but one could envision a concerted σ-bond metathesis, or an oxidative-addition/reductive-elimination mechanism via a transient Cu(III) intermediate. Compound **12** was generated in 75% yield according to ^{19}F NMR spectroscopy, and could be isolated in 55% yield following recrystallization from pentane at –20 ^{o}C.

During the fluorinations of copper(I) vinyls in THF solution, we observed the formation of 2-fluorotetrahydrofuran as a minor byproduct, resulting in a complex multiplet at δ –112.2 ppm in the ^{19}F NMR spectra. Originally assigned as a copper(III) fluoride complex in the copper(I)-mediated fluorination of aryl-boron and aryl-tin

bonds,[6b,d] this resonance is consistent with that reported by Vincent and coworkers for the NFSI-mediated fluorination of THF.[22]

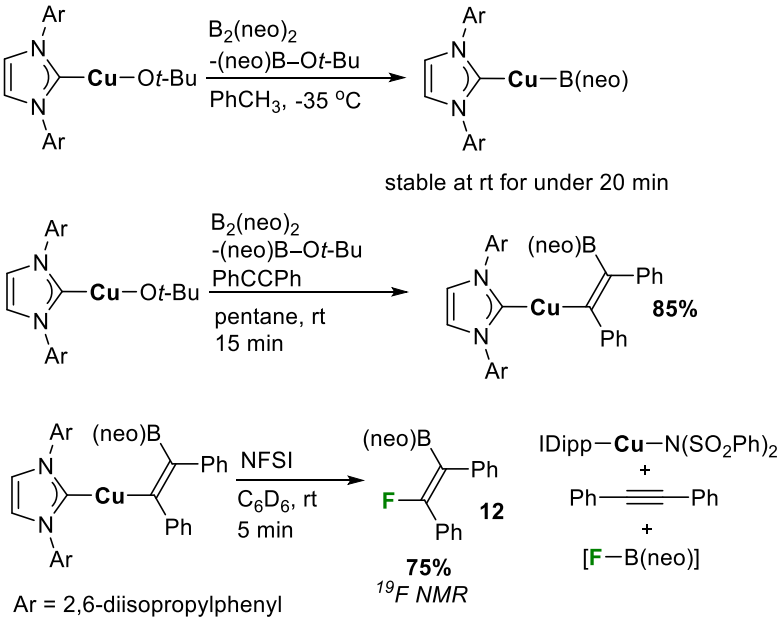

Scheme 3.5 Isolation and determination of intermediates.

We have examined potential turnover steps for this reaction, but have not yet found conditions conducive to catalysis. Complex **11** does not react with $B_2(neo)_2$ to regenerate a copper boryl, but does undergo ligand exchange with potassium or sodium *tert*-butoxide to regenerate the copper alkoxide (Scheme 3.6). Unfortunately, both (IDipp)CuO-*t*-Bu and (IDipp)CuB(neo) react with NFSI to generate multiple vibrant colors, which we suspect is due to formation of Cu(II) species, and ^{1}H NMR spectra show multiple sets of ligand resonances. Furthermore, addition of (IDipp)CuO-*t*-Bu to **12** results in transmetalation to copper, forming a copper β-fluorovinyl. Subsequent loss of diphenylacetylene is observed by ^{1}H NMR spectroscopy. We suspect the concomitant formation of (IDipp)CuF but could not detect it by ^{19}F NMR spectroscopy. Although (IDipp)CuF is poorly soluble in C_6D_6, we hypothesize it reacts readily with (neo)B–O-*t*-Bu based on the disappearance of the

(neo)B–O-*t*-Bu resonances in the ^{1}H NMR spectra.[23] The copper β-fluorovinyl continues to lose diphenylacetylene over the course of 24 hours (Scheme 3.6).

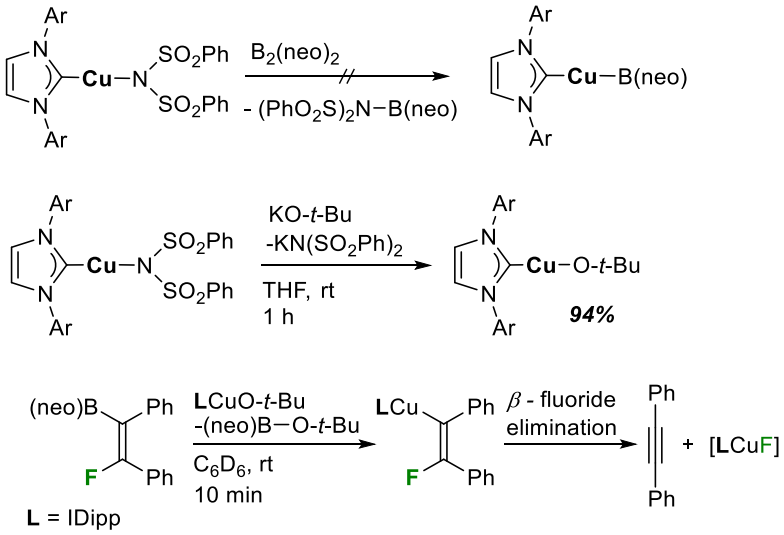

Scheme 3.6 Cu–F elimination from copper cis-β-fluorovinyl.

3.2.4 Scope of the Borofluorination of Alkynes

Although **12** could be isolated in good yield, some decomposition was evident over the course of a day on the benchtop. In light of the stability and synthetic utility of potassium trifluoroborate salts,[24] we converted the boronic ester products to the corresponding potassium trifluoroborate salts as shown by Sakaguchi and coworkers.[19b] Extraction of the crude reaction mixture with pentane separates the desired product and organic byproducts from complex **11**; treatment of the concentrated extract with KHF_2 in methanol converts the boronate ester to the trifluoroborate salt, which is easily separated from glycol and re-formed alkyne.[19b] Generally, the borofluorination of internal alkynes was more effective than that of terminal alkynes, and alkyl alkynes gave higher yields than

that of aryl (Scheme 3.7). In the case of terminal alkynes, only the terminal fluoroalkene was generated, but (IDipp)CuB(neo) must be generated prior to addition of the terminal alkyne to avoid deprotonation by the copper(I) alkoxide to form a copper(I) acetylide.[25] Addition of excess terminal alkyne can also lead to formation of a copper(I) acetylide, as the vinylcopper(I) intermediate can deprotonate the alkyne.[25] Interestingly, the borofluorination of phenylpropyne yielded a 5:1 mixture of the β- and α-*cis*-fluorovinyl boronic esters, but following conversion to the trifluoroborate salt the ratio of isolated product increased to a 20:1 mixture of β- to α-*cis*-fluorovinyl boronate, presumably due to differential solubility. The borofluorination of the doubly propargylic substrate 1,4-dimethoxy-2-butyne resulted in multiple products, and conversion to potassium trifluoroborate salts was quite low. Additionally, no product was detected when dimethyl acetylenedicarboxylate was used under normal conditions.

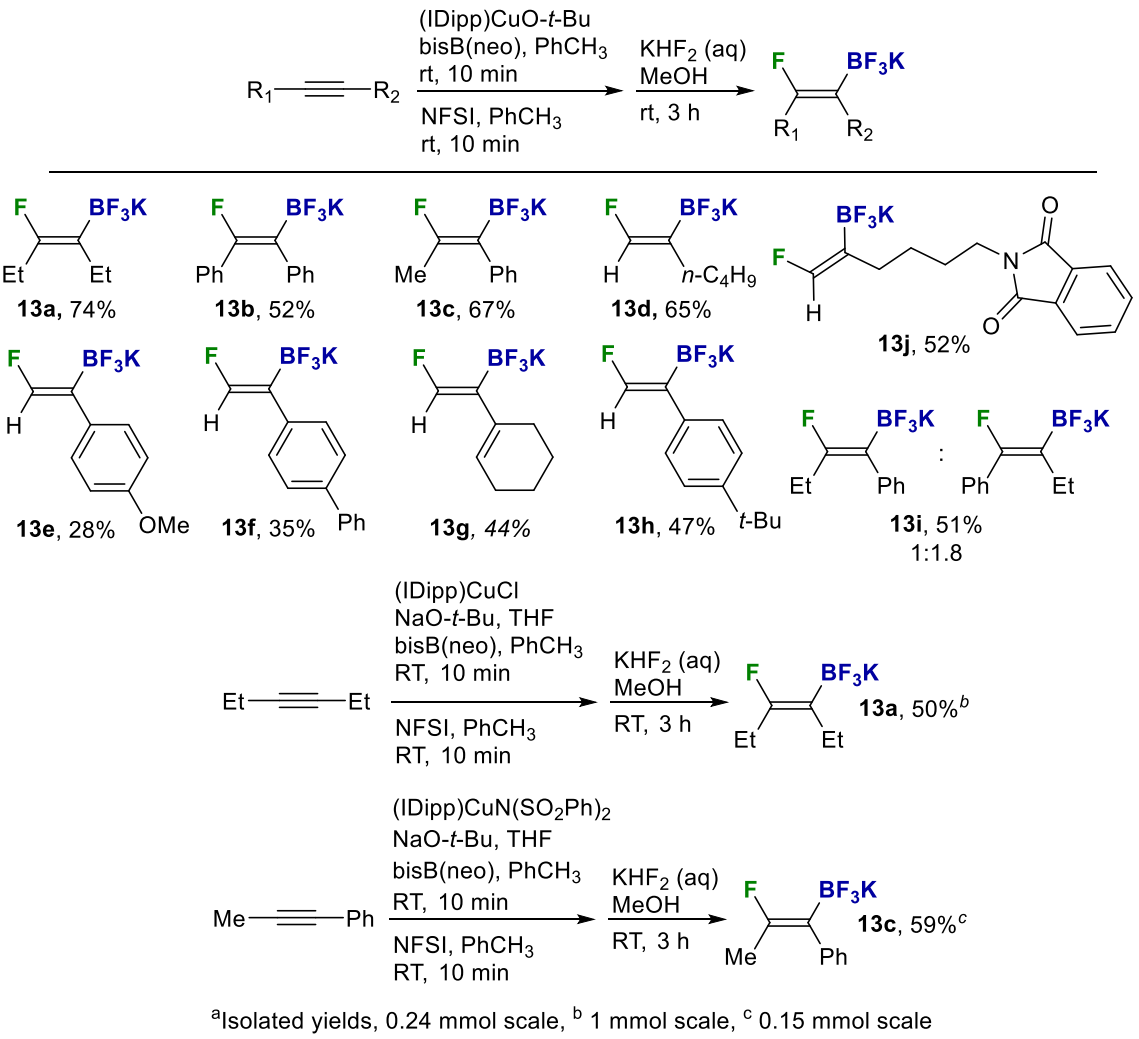

Scheme 3.7 Scope of alkynes converted to cis-(β-fluorovinyl) trifluoroboronates.

Knowing that the byproduct (IDipp)CuN(SO_2Ph)$_2$ (**11**) can undergo anion exchange to yield (IDipp)CuO-*t*-Bu, we explored the possibility of reusing **11** as our initial copper source. Sodium *tert*-butoxide and **11** were mixed in tetrahydrofuran solvent prior to addition of a solution of alkyne and diboron reagent in toluene. Following the standard conditions after the addition of the alkyne and $B_2(neo)_2$, the potassium *cis*-(β-fluorovinyl)trifluoroboronate product of phenylpropyne was isolated in good yield (Scheme 3.7). In addition, the borofluorination of 3-hexyne was also achieved at a 1 mmol

scale starting with a combination of (IDipp)CuCl and sodium *tert*-butoxide to generate (IDipp)CuO-*t*-Bu in situ. The byproduct **11** was isolated in 71% yield from this reaction.

3.2.5 Derivatization of cis-(β-Fluorovinyl)trifluoroboronates.

With the *cis*-(β-fluorovinyl)trifluoroboronates in hand, various methods for carbon-carbon bond functionalization were examined to gauge the synthetic utility of these compounds. To date, we have not observed successful conversion to vinylaldehydes using established rhodium catalysis,[26] nor to vinylamines via Chan-Evans-Lam coupling. [27] This may be in part due to β-fluoride elimination from the metal *cis*-(2-fluorovinyl) intermediate (*vide supra*). The potentially vulnerable C–F bond is retained, however, through other elaborations. Initial attempts to oxidize the *cis*-(2-fluorovinyl)trifluoroboronates following the established routes[28] resulted in slow reaction times and a mixture of products. Addition of silica gel to the common oxidizing mixture of aqueous $NaOH/H_2O_2$ led to the formation of the α-fluoroketone in good yield (Scheme 3.8). Presumably, the trifluoroborate is first converted to the boronic acid which is more susceptible to oxidation, allowing a clean transformation.

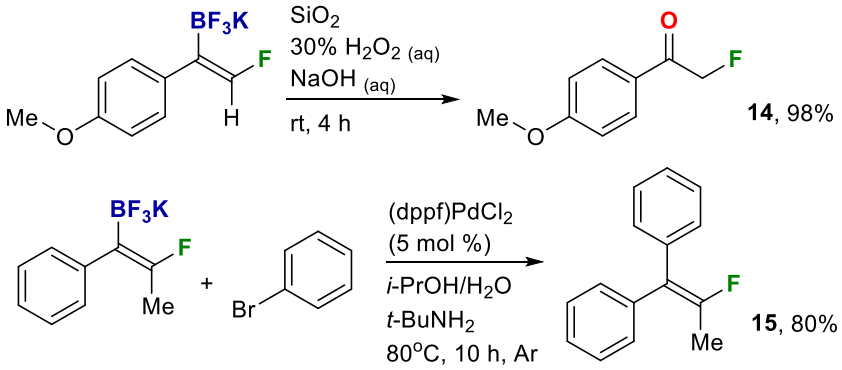

Scheme 3.8 Derivatization of cis-(β-fluorovinyl) trifluoroboronates.

In contrast to the attempted Cu- or Rh-catalyzed couplings, a Pd-catalyzed Suzuki-Miyuara coupling proceeded effectively. Under conditions established by Molander and coworkers,[29] phenylation of a *cis*-(β-fluorovinyl)trifluoroboronate afforded corresponding the tetra-substituted fluoroalkene.

3.3 Conclusion

We have explored the formation of fluorovinyl products by the reaction of an electrophilic fluorine source with copper(I) vinyl complexes, which are readily generated by 1,2-insertion of alkynes into copper(I) hydrides or boryls. The sequence of alkyne insertion, followed by electrophilic fluorination enables a one-pot synthesis of *cis*-(β-fluorovinyl)boronates that can be readily isolated as their potassium trifluoroborate salts. This method affords potential nucleophiles for the construction of more elaborate fluorovinyl-containing systems.

3.4 Experimental

3.4.1 *General Considerations*

Unless otherwise indicated, manipulations were performed in an MBraun glovebox under an inert atmosphere of nitrogen, or in sealable glassware on a Schlenk line under an atmosphere of argon. Glassware and magnetic stir bars were dried in a ventilated oven at 160°C and were allowed to cool under vacuum. Tetrahydrofuran (THF, EMD Millipore Omnisolv), and toluene (EMD Millipore Omnisolv) were sparged with ultra-high purity argon (NexAir) for 30 minutes prior to first use, dried using an MBraun solvent purification system, transferred to Straus flasks, degassed using three freeze-pump-thaw cycles, and

stored under nitrogen or argon. Anhydrous benzene (EMD Millipore Drisolv), anhydrous *N*,*N*-dimethylformamide (EMD Millipore Drisolv), anhydrous acetonitrile (EMD Millipore Drisolv) and, anhydrous pentane (EMD Millipore Drisolv, sealed under a nitrogen atmosphere) were used as received and stored in a glovebox. Tap water was purified in a Barnstead International automated still prior to use. Dichloromethane (VWR), acetone (VWR), methanol (VWR), diethyl ether (EMD Millipore), and isopropanol (VWR) were used as received.

Benzene-d_6 (Cambridge Isotope Laboratories) and tetrahydrofuran-*d8* (THF-*d8*, Cambridge Isotope Laboratories) was dried over sodium benzophenone ketyl, vacuum-transferred into oven-dried resealable flasks, and degassed by successive freeze-pump-thaw cycles. Dichloromethane-d_2 (Cambridge Isotope Laboratories) and acetonitrile-d_3 (Cambridge Isotope Laboratories) were dried over calcium hydride overnight, vacuum-transferred to an oven-dried resealable Schlenk flask, and degassed by successive freeze-pump-thaw cycles. Chloroform-*d* (Cambridge Isotope Laboratories) was used as received.

Sodium metal (Alfa-Aesar), benzophenone (Alfa-Aesar), nitrogen (NexAir), argon (both industrial and ultra-high purity grades, NexAir), *N*-fluorobenzenesulfonimide (Oakwood), bis(catecholato)diboron [$B_2(cat)_2$] (Alfa-Aesar), bis(pinacolato)diboron [$B_2(pin)_2$] (Alfa-Aesar), F-TEDA-BF_4 (Sigma-Aldrich), *N*-fluoropyridinium tetrafluoroborate (Sigma-Aldrich), and potassium hydrogen fluoride (Alfa-Aesar) were used as received. Bis(neopentylglycolato)diboron [$B_2(neo)_2$] (Frontier Scientific) was dissolved in THF, passed through activated basic alumina and concentrated *in vacuo* prior to use. The solid alkynes diphenylacetylene (Alfa-Aesar), 4-ethynylbiphenyl (Oakwood), and 6-pthalimido-1-hexyne (Sigma-Aldrich) were pumped into the glovebox overnight

before use. The liquid alkynes 3-hexyne (Alfa-Aesar), 1-hexyne (Alfa-Aesar), 1-phenylpropyne (Alfa-Aesar), 1-phenylbutyne (Alfa-Aesar), phenylacetylene (Sigma-Aldrich), 4-ethynylanisole (Oakwood), 1-ethynylcyclohexene (Sigma-Aldrich), and 4-*tert*-butylphenylacetylene (Sigma-Aldrich), were sparged with Ar for 20 min and stored over molecular sieves under inert atmosphere prior to use. Bromobenzene (Alfa-Aesar), (dppf)$PdCl_2$•CH_2Cl_2 (Sigma-Aldrich), *tert*-butylamine (Alfa-Aesar) were used as received. (IDipp)CuO-*t*-Bu,[14] [(IDipp)CuH]$_2$,[14] (IDipp)Cu[(*E*)-3-hexynyl],[14] (6Dipp)CuO-*t*-Bu,[15] [(6Dipp)CuH]$_2$,[15] (5Dipp)CuO-*t*-Bu,[23] (^{Cl}IDipp)CuO-*t*-Bu,[30] and (ICy)CuO-*t*-Bu[23] were synthesized according to literature protocols and were characterized by ^{1}H NMR spectroscopy.

3.4.2 *Spectroscopic Measurements*

^{1}H, ^{11}B, ^{13}C, and ^{19}F spectra were obtained using Bruker Avance IIIHD 700 MHz, Bruker DSX 400 MHz and Varian Vx 400 MHz spectrometers. ^{1}H and ^{13}C NMR chemical shifts are referenced with respect to solvent signals and reported relative to tetramethylsilane. A capillary insert of α,α,α-trifluorotoluene (-63.72 ppm) was used to determine ^{19}F chemical shifts. Unless otherwise stated, infrared spectra were collected using microcrystalline samples on a Bruker Alpha-P infrared spectrometer equipped with an attenuated total reflection (ATR) attachment. Samples were exposed to air as briefly as possible prior to data collection.

The *cis*-(β-fluorovinyl)trifluoroboronates contained KBF_4 as a minor impurity, typically under 5%, evident in the ^{19}F (–152 ppm) and ^{11}B NMR (–1.5 ppm) spectra. The carbon atoms bearing boronic ester and trifluoroborate groups did not give rise to discernible resonances in the ^{13}C NMR spectra, consistent with previous findings.[31]

3.4.3 *Elemental Analyses*

Elemental analyses were performed by Atlantic Microlab, Inc. in Norcross, Georgia.

3.4.4 *Synthetic Procedures*

3.4.4.1 Determination of ^{19}F NMR yields for electrophilic fluorinations

(NHC)CuO-*t*-Bu (0.038 mmol), diboron reagent (0.038 mmol), and 3-hexyne (0.015 g, 0.19 mmol, 5 eq) were combined in a 20-mL vial and dissolved in solvent (3 mL). After 10 min a solution of fluorinating agent (0.038 mmol) in 1.5 mL of the chosen solvent

was added. After 10 min, $PhCF_3$ (4.7 μL, 0.038 mmol) was added as an internal standard. The yields were determined by the relative ratios of the product and $PhCF_3$ in the ^{19}F NMR spectrum.

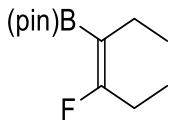

Figure 3.1 (*E*)-2-(4-fluorohex-3-en-3-yl)boronic acid pinacol ester

^{19}F NMR (376 MHz, $PhCH_3$) δ –85.30 ppm (t, $^3J_{FH}$ = 22.2 Hz, 1F, C=C*F*)

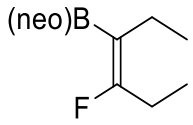

Figure 3.2 (*E*)-2-(4-fluorohex-3-en-3-yl)boronic acid neopentylglycol ester

^{19}F NMR (376 MHz, $PhCH_3$) δ –88.72 ppm (t, $^3J_{FH}$ = 22.0 Hz, 1F, C=C*F*)

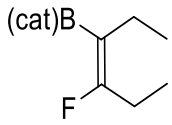

Figure 3.3 (*E*)-2-(4-fluorohex-3-en-3-yl)boronic acid catechol ester

^{19}F NMR (376 MHz, $PhCH_3$) δ –80.74 ppm (t, $^3J_{FH}$ = 23.0 Hz, 1F, C=C*F*)

3.4.4.2 Optimization of *cis*-borofluorination

Table 3.1. Optimization of *cis*-borofluorination conditions

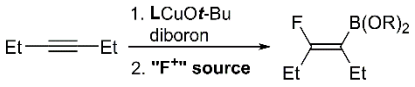

Entry	Ligand (L)	Solvent (0.02M)	Diboron Reagent	"F^+" Source	Yield[a] (%)
1	IDipp	THF	$B_2(pin)_2$	NFSI	19
2	IDipp	THF	$B_2(cat)_2$	NFSI	15
3	IDipp	THF	$B_2(neo)_2$	NFSI	72
4	IDipp	DMF	$B_2(neo)_2$	NFSI	42
5	IDipp	DMF	$B_2(neo)_2$	F-TEDA[b]	38
6	IDipp	DMF	$B_2(neo)_2$	$(F\text{-py})BF_4$	37
7	IDipp	CH_3CN	$B_2(neo)_2$	NFSI	32
8	IDipp	$PhCH_3$	$B_2(neo)_2$	NFSI	84
9	^{Cl}IDipp	$PhCH_3$	$B_2(neo)_2$	NFSI	78
10	ICy	$PhCH_3$	$B_2(neo)_2$	NFSI	trace
11	5Dipp	$PhCH_3$	$B_2(neo)_2$	NFSI	71
12	6Dipp	$PhCH_3$	$B_2(neo)_2$	NFSI	26
13	IDipp	$PhCH_3$	$B_2(neo)_2$	NFSI	50
14	IDipp	$PhCH_3$	$B_2(neo)_2$	NFSI	45

[a] Yields were determined by ^{19}F NMR compared to $PhCF_3$ as an internal standard.
[b] Commonly known as Selectfluor®

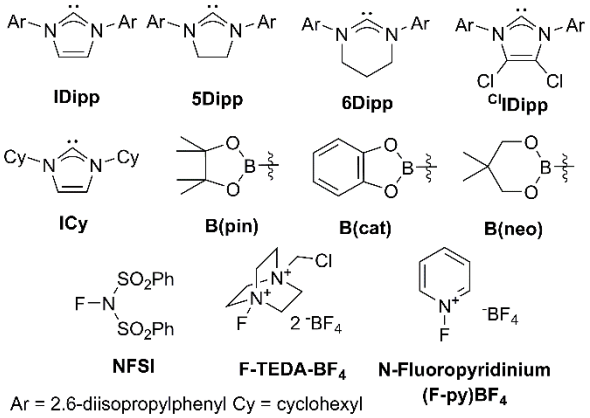

3.4.4.3 ^{1}H NMR of (IDipp)CuB(neo)

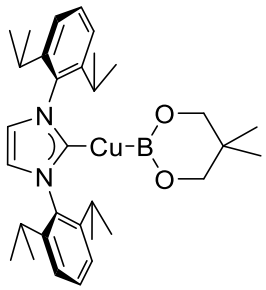

Figure 3.4 (IDipp)CuB(neo)

$B_2(neo)_2$ (0.017 g, 0.076 mmol), was added to a solution of (IDipp)CuO-*t*-Bu (0.040 g, 0.076 mmol), in toluene (2 mL) at –35^{o} C. After 15 min, the solution was layered with pentane (4 mL) and remained at –35^{o} C for 16h. The supernatant was decanted by pipette, toluene (1 mL) and pentane (2 mL) were added and the mixture was placed back in the freezer for 16h. The resulting crystals were dried *in vacuo* at room temperature for 5 min to afford the title complex (0.028 g, 68% yield). ^{1}H NMR (400 MHz, C_6D_6): 7.13 (t, $^{3}J_{HH}$ = 7.6 Hz, 2H, *para*-C*H*), 7.06 (d, $^{3}J_{HH}$ = 7.6 Hz, 4H, *meta*-C*H*), 6.22 (s, 2H, NC*H*), 3.27 (s, 4H, OCH_2), 2.67 (sept, $^{3}J_{HH}$ = 6.8 Hz, 4H, C*H*$(CH_3)_2$), 1.54 (d, $^{3}J_{HH}$ = 6.8 Hz, 12H, CH(CH_3)$_2$), 1.10 (d, $^{3}J_{HH}$ = 6.8 Hz, 12H, CH(CH_3)$_2$ 0.60 (s, 6H, BOCH$_2$CCH_3). The low thermal stability complicated efforts to further characterize this compound.

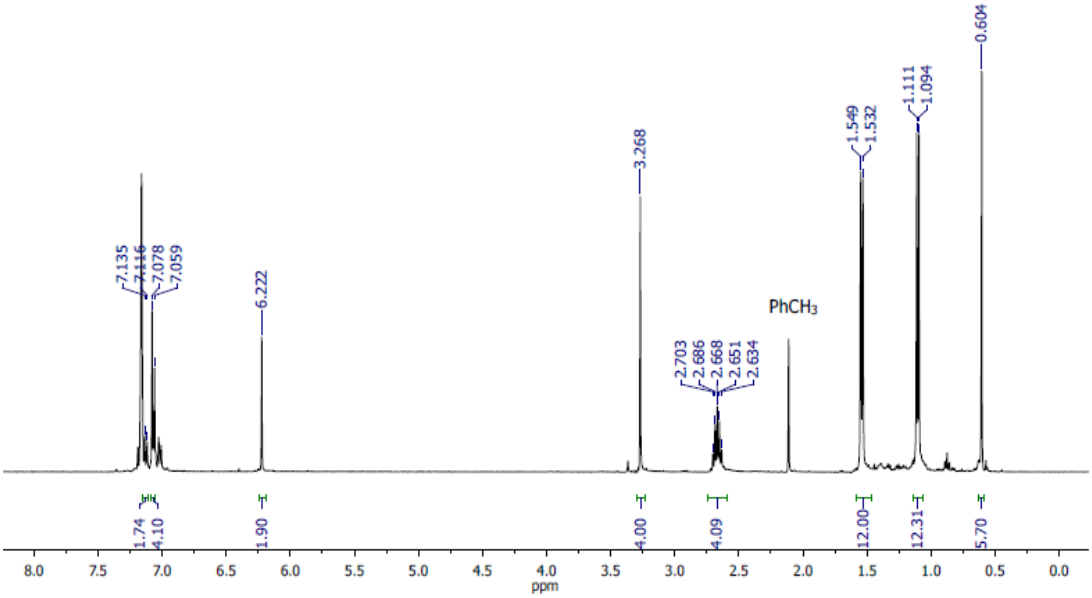

Figure 3.5 ^{1}H NMR of (IDipp)CuB(neo) in C_6D_6.

3.4.4.4 Synthesis of (IDipp)copper (1,2-diphenyl-2-borovinyl)

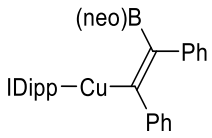

Figure 3.6 (IDipp)copper (1,2-diphenyl-2-borovinyl)

(IDipp)CuO-*t*-Bu (0.057 g, 0.11 mmol), $B_2(neo)_2$ (0.025 g, 0.11 mmol), and diphenylacetylene (0.019 g, 0.11 mmol) were combined in a 20-mL vial before pentane (5 mL) was added. The mixture was allowed to stir for 3h before the pentane was decanted. The resulting solid was washed with pentane (2 x 3 mL) to afford the product as a pale-yellow solid (0.068 g, 85% yield). ^{1}H NMR (400 MHz, C_6D_6): 7.27 (d, $^3J_{HH}$ = 7.2 Hz, 2H, phenyl-C*H*), 7.18 (t, $^3J_{HH}$ = 7.6 Hz, 2H, *para*-C*H*, IDipp), 7.04-7.00 (m, 6H, *meta*-C*H* IDipp, phenyl-C*H*), 6.85-6.80 (m, 3H, phenyl-C*H*), 6.74 (t, $^3J_{HH}$ = 7.2 Hz, 2H, phenyl-C*H*), 6.53 (d, $^3J_{HH}$ = 7.2 Hz, 2H, phenyl-C*H*), 6.23 (s, 2H, NC*H*), 2.87 (s, 4H, BOCH_2), 2.67 (sept, $^3J_{HH}$ = 6.8 Hz, 4H, C*H*(CH_3)$_2$), 1.34 (d, $^3J_{HH}$ = 6.8 Hz, 12 H, CH(CH_3)$_2$), 1.08 (d, $^3J_{HH}$ = 6.8 Hz, 12 H, CH(CH_3)$_2$, 0.66 (s, 6H, BOCH$_2$CCH_3). ^{13}C{^{1}H} NMR (100 MHz, C_6D_6): δ (ppm) 196.8 (C_α), 186.5 (N*C*Cu), 156.1 (C_β), 146.8, 145.7, 136.2, 131.4, 130.3, 127.3, 126.8, 126.6, 124.3, 123.4, 122.6, 120.4, 71.7 (BO*C*H$_2$), 31.2 (BOCH$_2$*C*), 29.0 (*C*H(CH_3)$_2$), 28.4 (CH(*C*H$_3$)$_2$), 23.7 (CH(*C*H$_3$)$_2$), 22.0 (BOCH$_2$C*C*H$_3$). ^{11}B NMR (128 MHz, C_6D_6) 28.5 (br s, *B*neo). IR: *v* (cm^{-1}) 3126, 3069, 2962, 2927, 1541, 1474, 1405, 1305, 1245, 1201, 1176, 1090, 1061, 936, 802, 756, 720, 522, 451.

Note: We have been unable to obtain satisfactory elemental analysis for (IDipp)copper (1,2-diphenyl-2-borovinyl). Although the presence of NMR-silent impurities cannot be ruled out, we believe the ^{1}H and ^{13}C NMR spectra reflect the purity of the sample.

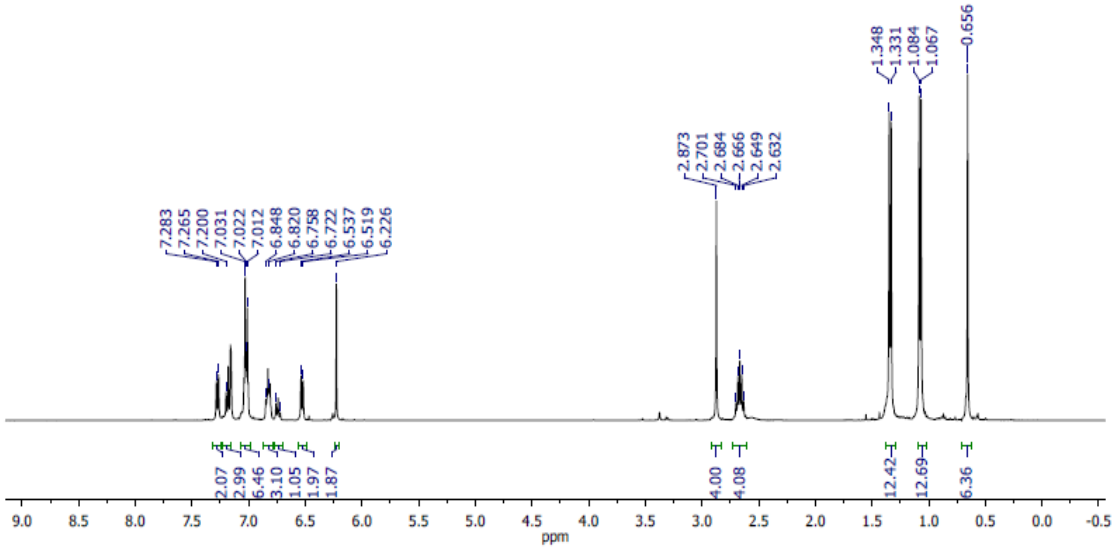

Figure 3.7 ^{1}H NMR of (IDipp)copper (1,2-diphenyl-2-borovinyl) in C_6D_6.

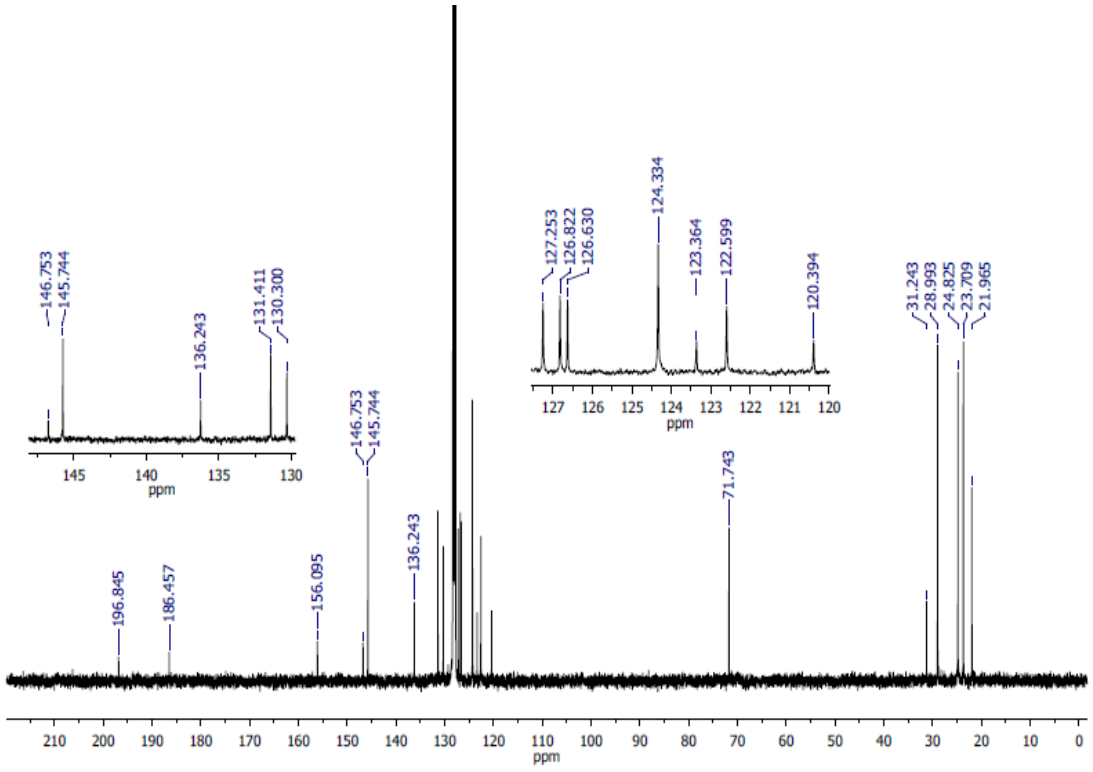

Figure 3.8 ^{13}C NMR of (IDipp)copper (1,2-diphenyl-2-borovinyl) in C_6D_6.

3.4.4.5 Regeneration of diphenylacetylene during electrophilic fluorination.

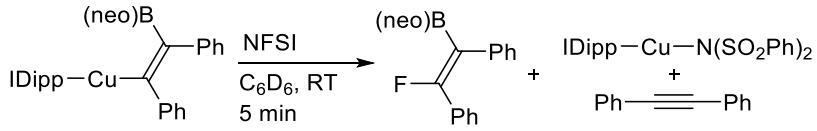

Figure 3.4 Regeneration of diphenylacetylene during electrophilic fluorination.

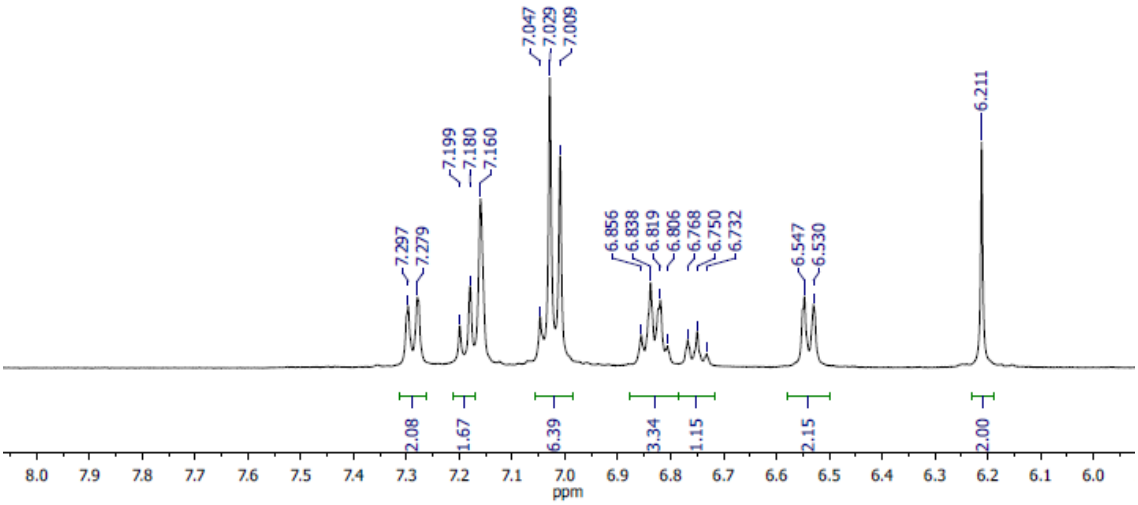

Figure 3.10 ^{1}H NMR of (IDipp)copper (1,2-diphenyl-2-borovinyl) in C_6D_6 before addition of NFSI.

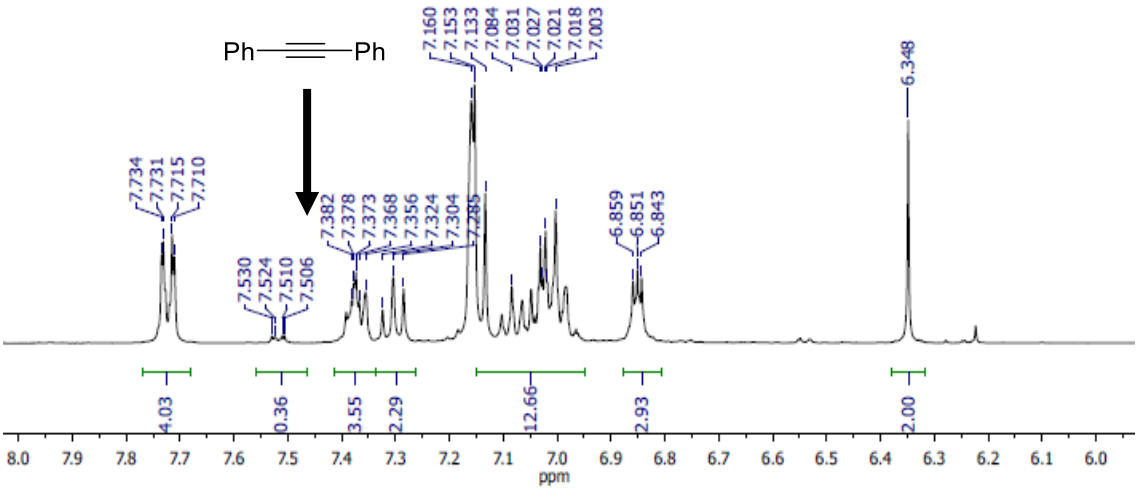

Figure 3.11 ^{1}H NMR of (IDipp)copper (1,2-diphenyl-2-borovinyl) in C_6D_6 after addition of NFSI.

3.4.4.6 Synthesis of (IDipp)CuN(SO_2Ph)$_2$

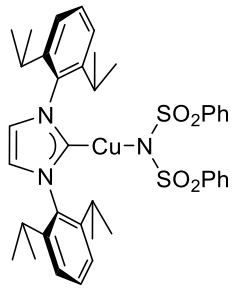

Figure 3.12 (IDipp)CuN(SO_2Ph)$_2$ (**11**)

(IDipp)CuO-*t*-Bu (0.151 g, 0.288 mmol), $B_2(neo)_2$ (0.065 g, 0.29 mmol), diphenylacetylene (0.051 g, 0.29 mmol) were combined in a 20-mL vial and dissolved in THF (6 mL). After 10 min a solution of NFSI (0.091 g, 0.29 mmol) in THF (3 mL) was added. After another 10 min, the mixture was concentrated *in vacuo* and the organic products were extracted with pentane to leave a colorless solid (0.200 g, 93% yield). ^{1}H NMR (400 MHz, $CDCl_3$): 7.63 (t, $^3J_{HH}$ = 7.6 Hz, 2H, *para*-C*H*, IDipp), 7.41 (d, $^3J_{HH}$ = 7.6 Hz, 4H, *meta*-C*H*, IDipp), 7.35 (t, $^3J_{HH}$ = 7.2 Hz, 2H, *para*-C*H*), 7.29 (d, $^3J_{HH}$ = 7.2 Hz, 4H, *ortho*-C*H*), 7.24 (s, 2H, NC*H*), 7.21 (t, $^3J_{HH}$ = 7.2 Hz, 4H, *meta*-C*H*), 2.62 (sept, $^3J_{HH}$ = 6.8 Hz, 4H, C*H*(CH_3)$_2$), 1.30 (d, $^3J_{HH}$ = 6.8 Hz, 12H, CH(C*H*$_3$)$_2$), 1.24 (d, $^3J_{HH}$ = 6.8 Hz, 12H, CH(C*H*$_3$)$_2$, ^{13}C{^{1}H} NMR (176 MHz, $CDCl_3$): δ (ppm) 180.6 (N*C*Cu), 146.3 (*ipso* -C), 143.5 (*ipso-C*), 134.6 (*ortho-C*, IDipp), 131.2 (*para-C*), 130.6 (*para-C*, IDipp), 128.1 (meta-*C*), 127.2 (*ortho-C*), 124.3 (*meta-C*, IDipp), 123.5 (NC*H*), 29.0 (*C*H(CH_3)$_2$, 24.5 (CH(*C*H$_3$)$_2$. IR: ν (cm^{-1}) 3122, 2960, 2696, 2867, 1461, 1445, 1327, 1310, 1287, 1146, 1084, 1003, 936, 883, 806, 744, 720, 684, 638, 590, 557 Anal. Calcd for $C_{39}H_{46}CuN_3O_4S_2$: C, 62.58; H, 6.19; N, 5.61 Found C, 62.77 H, 6.00; N, 5.72.

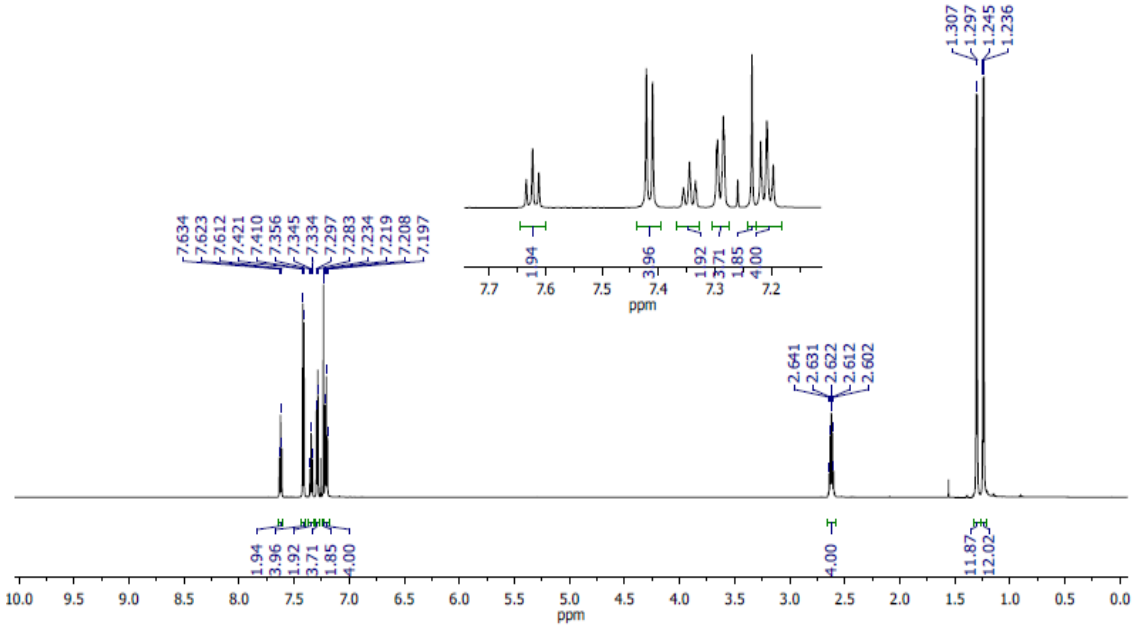

Figure 3.13 ^{1}H NMR of (IDipp)CuN(SO_2Ph)$_2$ (**11**) in $CDCl_3$.

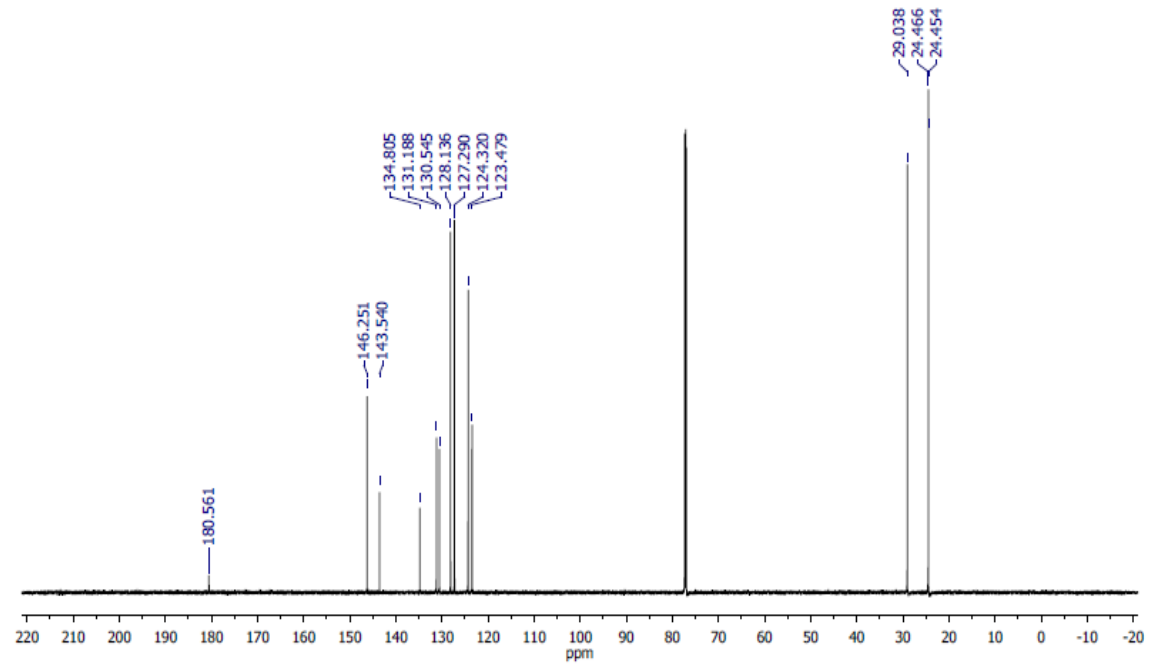

Figure 3.14 ^{13}C NMR of (IDipp)CuN(SO_2Ph)$_2$ (**11**) in $CDCl_3$.

3.4.4.7 Synthesis of (*E*)-(2-fluoro-1,2-diphenylvinyl)boronic acid neopentyl glycolato ester

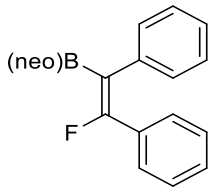

Figure 3.15 (*E*)-(2-fluoro-1,2-diphenylvinyl)boronic acid neopentyl glycolato ester (**12**)

(IDipp)CuO-*t*-Bu (0.100 g, 0.19 mmol), $B_2(neo)_2$ (0.043 g, 0.19 mmol), diphenylacetylene (0.034 g, 0.19 mmol) were combined in a 20-mL vial and dissolved $PhCH_3$ (6 mL). After 10 min a solution of NFSI (0.60 g, 0.19 mmol) in $PhCH_3$ (3 mL) was added. After another 10 min, the mixture was concentrated *in vacuo* and the products were extracted with pentane, filtered through a Celite plug, and concentrated *in vacuo* to give an oil. Crystallization, followed by recrystallization from pentane (3 mL each time), at –20°C afforded a colorless solid (0.031 g, 52% yield). ^{1}H NMR (400 MHz, C_6D_6): δ (ppm) 7.37 (m, 4H, phenyl C*H*), 7.08 (t, $^3J_{HH}$ = 7.6 Hz, 2H, phenyl C*H*), 6.98 (tt, 1H, $^3J_{HH}$ = 7.6 Hz, 1.6 Hz, phenyl C*H*), 6.85 (m, 3H, phenyl C*H*), 3.35 (s, 4H, BOCH_2), 0.59 (s, 6H, C(CH_3)$_2$), ^{13}C{^{1}H} NMR (100 MHz, C_6D_6): δ (ppm) 162.4 (d, $^1J_{FC}$ = 249 Hz, C=*C*F), 139.0 (d, $^3J_{FC}$ = 15 Hz, C=C(B)-*ipso*-*C*), 133.4 (d, $^2J_{FC}$ = 31 Hz, C=C(F)-*ipso*-*C*), 130.1 (d, $^4J_{FC}$ = 11 Hz, C=C(F)-*ortho*-*C*), 129.1 (d, $^4J_{FC}$ = 4 Hz, C=C(F)-*meta*-*C*), 129.0 (d, $^3J_{FC}$ = 22 Hz, C=C(F)-*ortho*-*C*), 128.9 (d, $^5J_{FC}$ = 2 Hz, C=C(B)-*meta*-*C*), 128.1 (d, $^5J_{FC}$ = 2 Hz, C=C(F)-*para*-*C*), 126.6 (C=C(B)-*para*-*C*), 72.3 (BO*C*H_2), 31.4 (*C*(CH_3)$_2$), 21.6 (C(*C*H_3)$_2$). ^{19}F NMR (376 MHz, C_6D_6): δ (ppm) –88.9 ^{11}B NMR (128 MHz, C_6D_6) δ (ppm) 26.8 (br s, *B*neo) IR: *v* (cm^{-1}) 3055, 2962, 2931, 1479, 1418, 1384, 1371, 1309, 1290, 1256, 1051, 996, 756, 692, 665, 659, 527, 420.

Note: We have been unable to obtain satisfactory elemental analysis for (*E*)-(2-fluoro-1,2-diphenylvinyl)boronic acid neopentyl glycolato ester. The compound is prone to protiodeborylation while standing. Although NMR-silent impurities cannot be ruled out, we believe the ^{1}H, ^{13}C, ^{19}F and ^{11}B and NMR spectra reflect the purity of the sample.

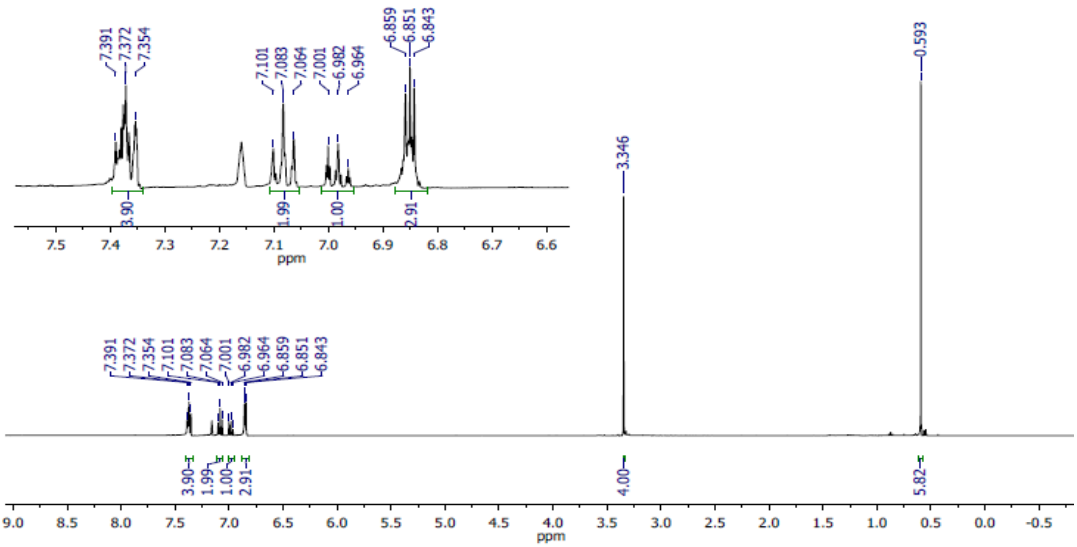

Figure 3.16 ^{1}H NMR of (*E*)-(2-fluoro-1,2-diphenylvinyl)boronic acid neopentyl glycolato ester (**12**) in C_6D_6.

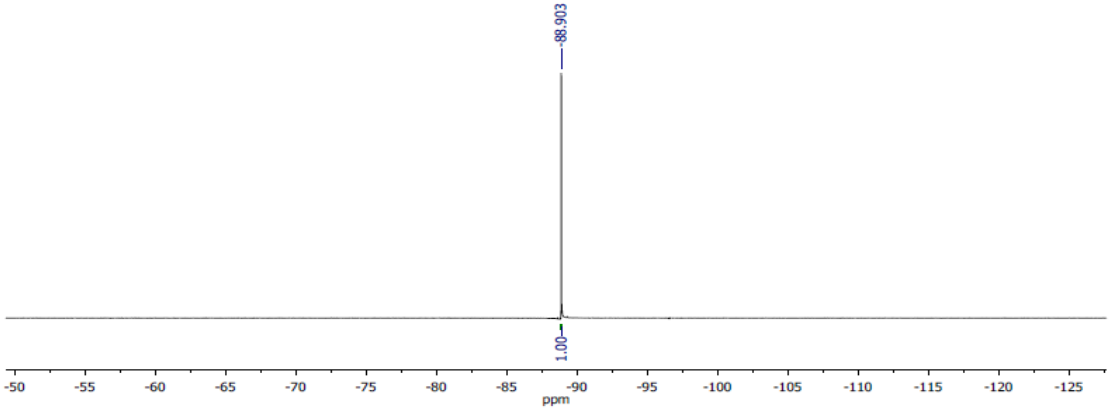

Figure 3.17 ^{19}F NMR of (*E*)-(2-fluoro-1,2-diphenylvinyl)boronic acid neopentyl glycolato ester (**12**) in C_6D_6.

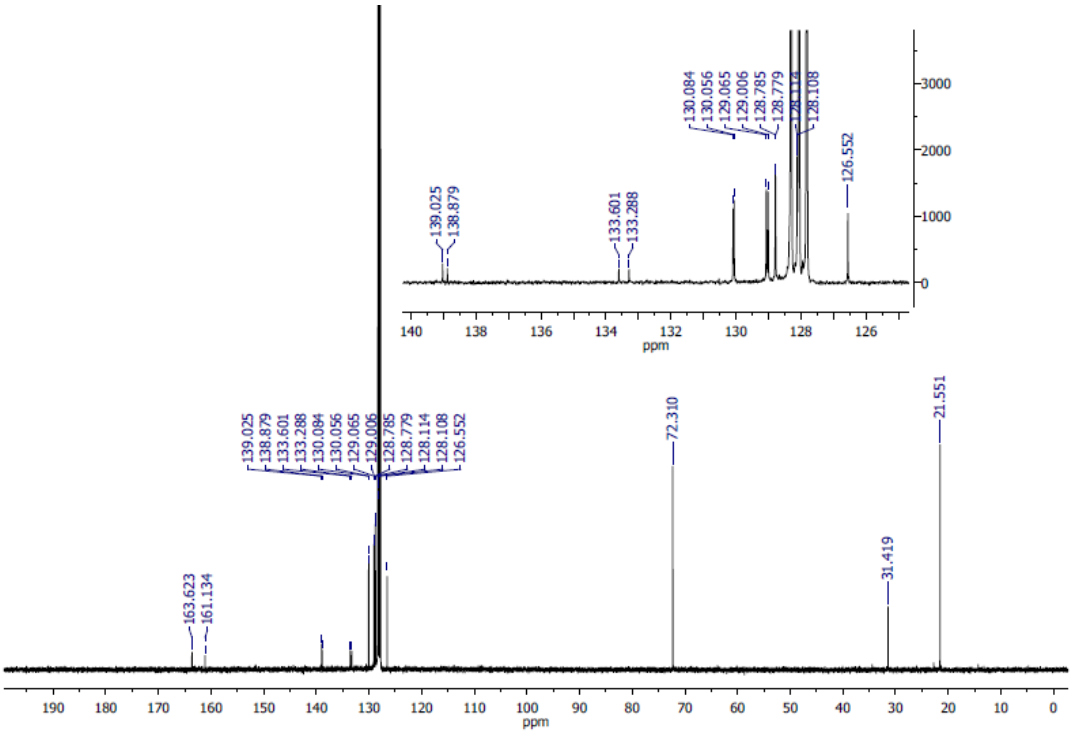

Figure 3.18 ^{13}C NMR of (*E*)-(2-fluoro-1,2-diphenylvinyl)boronic acid neopentyl glycolato ester (**12**) in C_6D_6.

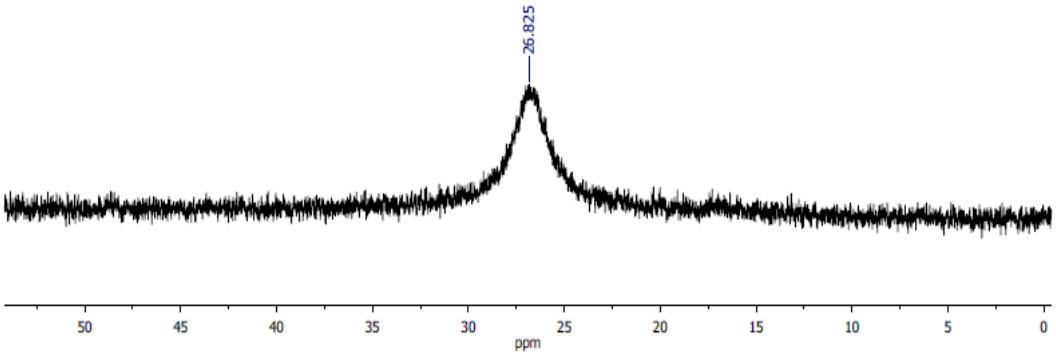

Figure 3.19 ^{11}B NMR of (*E*)-(2-fluoro-1,2-diphenylvinyl)boronic acid neopentyl glycolato ester (**12**) in C_6D_6.

3.4.4.8 Synthesis of potassium (*E*)-(4-fluorohex-3-en-3-yl)trifluoroborate

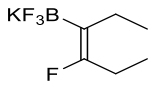

Figure 3.20 Potassium (*E*)-(4-fluorohex-3-en-3-yl)trifluoroborate (**13a**)

(IDipp)CuO-*t*-Bu (0.125 g, 0.238 mmol), $B_2(neo)_2$ (0.054 g, 0.24 mmol), 3-hexyne (0.028 g, 0.34 mmol) were combined in a 20-mL vial and dissolved in toluene (6 mL). After 10 min a solution of NFSI (0.075 g, 0.24 mmol) in toluene (3 mL) was added. After another 10 min, the mixture was concentrated *in vacuo* and the products were extracted with pentane, filtered through a Celite plug and concentrated in vacuo to give an oil. The oil was dissolved in MeOH (10 mL) with stirring before a solution of KHF_2 (0.186 g, 2.38 mmol) in H_2O (5 mL) was added and stirred for 3h. This mixture was then concentrated and the products were extracted with acetone (3 x 5 mL), filtered through a Celite plug and concentrated to give a colorless solid. This was washed with Et_2O (5 mL) and DCM (5 mL) and the residue was dried for 12h under vacuum, affording the product as a colorless powder (0.037 g, 74% yield). ^{1}H NMR (400 MHz, CD_3CN): δ (ppm) 2.18 (dq, $^3J_{FH}$ = 24.0 Hz, $^3J_{HH}$ = 7.6 Hz, 2H, C=C(F)CH_2CH$_3$), 1.86 (q, $^3J_{HH}$ = 7.6 Hz, 2H, C=C(BF_3K)CH_2CH$_3$), 1.02 (t, $^3J_{HH}$ = 7.6 Hz, 3H, C=C(BF_3K)CH$_2$CH_3), 0.90 (td, $^3J_{HH}$ = 7.6 Hz, $^4J_{FH}$ = 1.6 Hz, C=C(F)CH$_2$CH_3), ^{13}C{^{1}H} NMR (176 MHz, CD_3CN): δ (ppm) 161.5 (d, $^1J_{FC}$ = 238 Hz, C=*C*F), 23.1 (d, $^3J_{FC}$ = 16 Hz, C=C(BF_3K)*C*H$_2$CH$_3$), 22.5 (d, $^3J_{FC}$ = 35 Hz, C=C(F)*C*H$_2$CH$_3$), 15.8 (d, $^4J_{FC}$ = 3 Hz, C=C(F)CH$_2$*C*H$_3$), 12.4 (C=C(BF_3K)CH$_2$*C*H$_3$), ^{19}F NMR (376 MHz, CD_3CN): δ (ppm) –107.26 (br s, 1F, C=C*F*), –138.42 to –138.80 (br m, 3F, C=C(B*F*$_3$K) ^{11}B NMR (128 MHz, CD_3CN) δ (ppm) 2.51 (q, $^1J_{FB}$ = 52 Hz C=C(*B*F_3K) IR: *v* (cm^{-1}) 2962, 2932, 2872, 1664, 1474, 1320, 1130, 1130, 1048, 1020, 985, 925, 738, 697, 534, 522. Anal. Calcd for $C_6H_{10}BF_4K$: C, 34.64; H, 4.85. Found C, 34.84; H, 4.85.

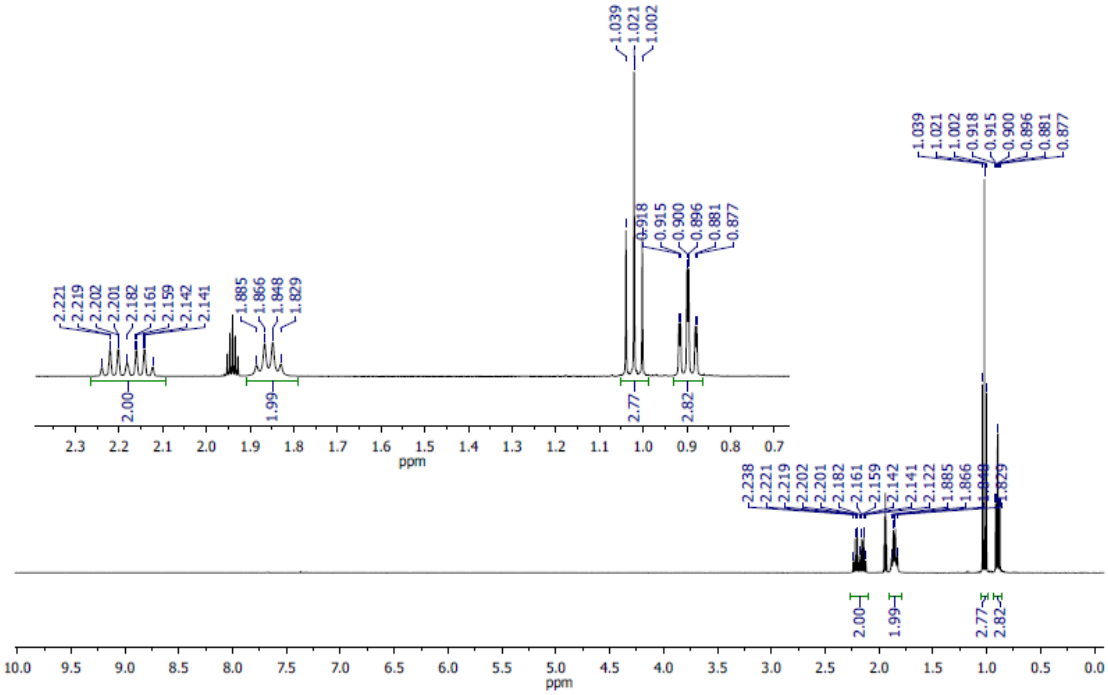

Figure 3.21 ^{1}H NMR of potassium (*E*)-(4-fluorohex-3-en-3-yl)trifluoroborate (**13a**) in CD_3CN.

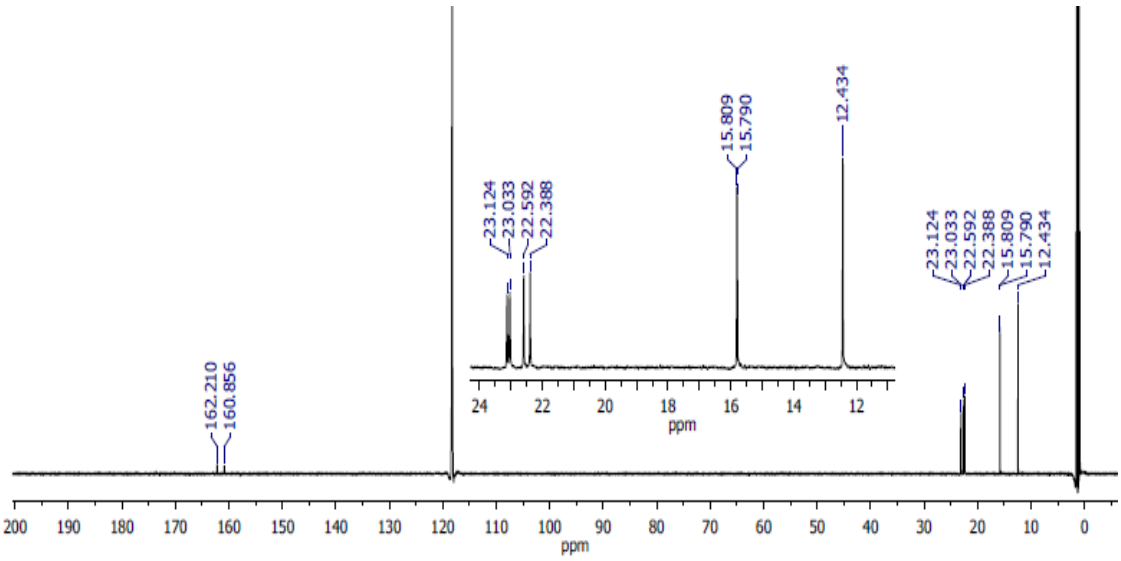

Figure 3.22 ^{13}C NMR of potassium (*E*)-(4-fluorohex-3-en-3-yl)trifluoroborate (**13a**) in CD_3CN.

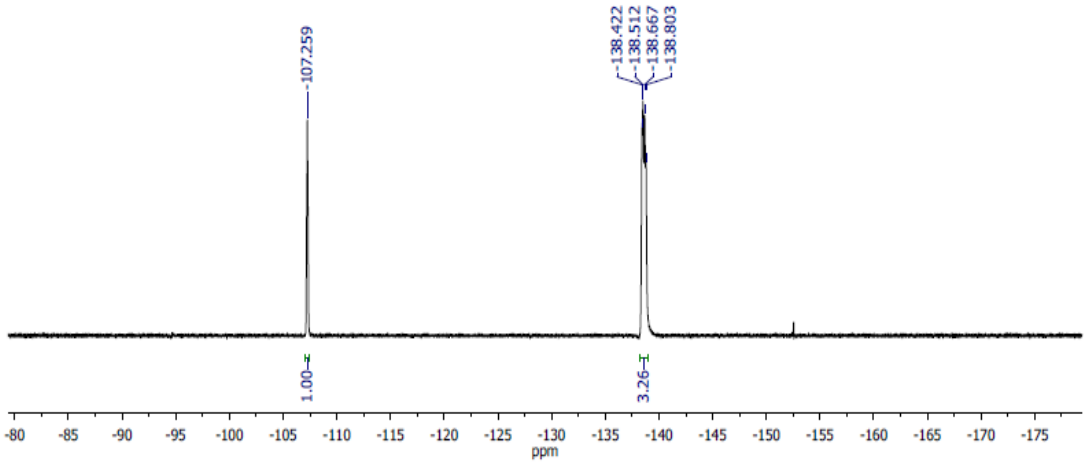

Figure 3.23 ^{19}F NMR of potassium (*E*)-(4-fluorohex-3-en-3-yl)trifluoroborate (**13a**) in

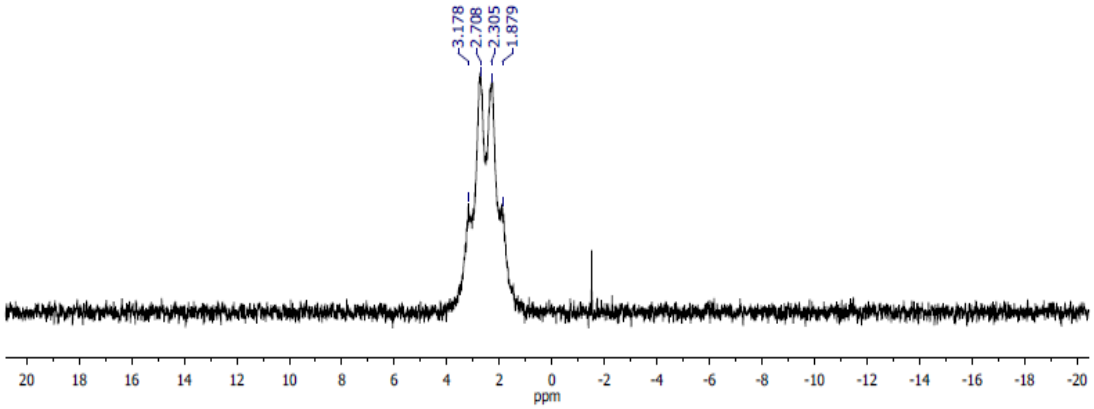

CD_3CN.

Figure 3.24 ^{11}B NMR of potassium (*E*)-(4-fluorohex-3-en-3-yl)trifluoroborate (**13a**) in CD_3CN.

3.4.4.9 Synthesis of potassium (*E*)-(2-fluoro-1,2-diphenylvinyl)trifluoroborate

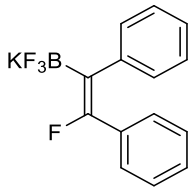

Figure 3.25 potassium (*E*)-(2-fluoro-1,2-diphenylvinyl)trifluoroborate (**13b**)

(IDipp)CuO-*t*-Bu (0.050 g, 0.095 mmol), $B_2(neo)_2$ (0.022 g, 0.096 mmol), diphenylacetylene (0.017 g, 0.096 mmol) were combined in a 20-mL vial and dissolved in toluene (6 mL). After 10 min, a solution of NFSI (0.030 g, 0.095mmol) in toluene (3 mL) was added. After another 10 min, the mixture was concentrated *in vacuo* and the products were extracted with pentane, filtered through a Celite plug and concentrated in vacuo to give an oil. The oil was then dissolved in MeOH (10 mL) with stirring before a solution of KHF_2 (0.074 g, 0.95 mmol) in H_2O (5 mL) was added and stirred for 12h. This mixture was then concentrated and the products were extracted with acetone (3 x 5 mL), filtered through a Celite plug and concentrated to give a colorless solid. This was washed with Et_2O (5 mL) and DCM (5 mL) and the residue was dried for 12h under vacuum, affording the product as a colorless powder (0.0147 g, 51% yield). ^{1}H NMR (400 MHz, CD_3CN): δ (ppm) 7.19-7.04 (m, 10H, phenyl-*C*). $^{13}C\{^1H\}$ NMR (100 MHz, CD_3CN): δ (ppm) 157.0 (d, $^1J_{FC}$ = 235 Hz, C=*C*F), 144.0 (d, $^3J_{FC}$ = 15 Hz, C=C(B)-*ipso*-*C*), 136.1 (d, $^3J_{FC}$ = 34 Hz, C=C(F)-*ipso*-*C*), 130.2 (d, $^3J_{FC}$ = 3 Hz, C=C(F)-*ortho*-*C*), 129.2 (d, $^3J_{FC}$ = 6 Hz, C=C(F)-*ortho*-*C*), 128.4 (C=C(F)-*meta*-*C*), 128.4 (C=C(B)-*meta*-*C*), 128.2 (d, $^3J_{FC}$ = 1 Hz, C=C(F)-*para*-*C*), 125.4 (C=C(B)-*para*-*C*). ^{19}F NMR (376 MHz, CD_3CN): δ (ppm) –99.96 (s, 1F, C=C*F*), –137.24 to –137.59 (br m, 3F, C=C(B*F*$_3$K), ^{11}B NMR (128 MHz, CD_3CN) δ (ppm)

2.10 (q, $^{1}J_{FB}$ = 48 Hz C=C(*B*F_3K) IR: *v* (cm^{-1}) 3053, 3023, 2959, 1640, 1493, 1443, 1280, 1212, 1116, 1071, 1005, 979, 893, 769, 750, 693, 638, 602.

Note: We have been unable to obtain satisfactory elemental analysis for potassium (*E*)-(2-fluoro-1,2-diphenylvinyl)trifluoroborate. Although NMR-silent impurities cannot be ruled out, we believe the ^{1}H, ^{13}C, ^{19}F and ^{11}B and NMR spectra reflect the purity of the sample.

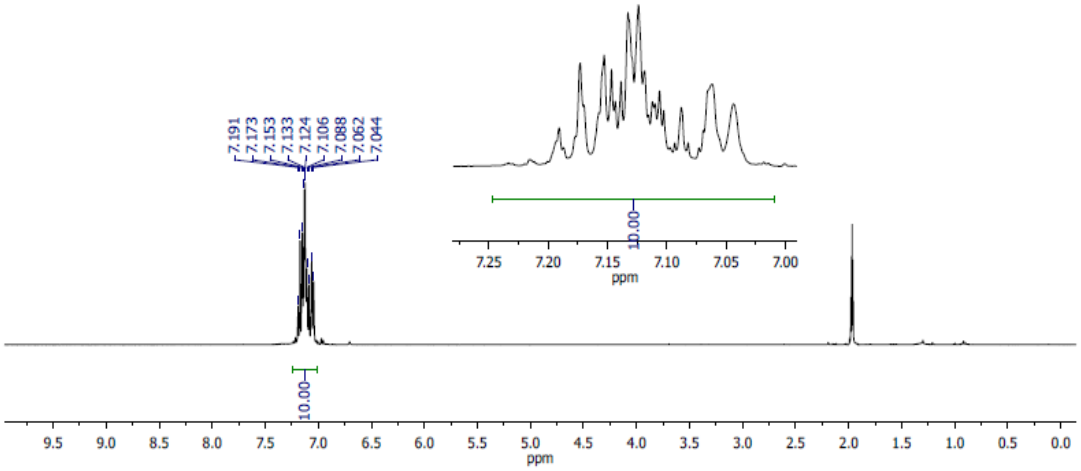

Figure 3.26 ^{1}H NMR of Potassium (*E*)-(2-fluoro-1,2-diphenylvinyl)trifluoroborate (**13b**) in CD_3CN.

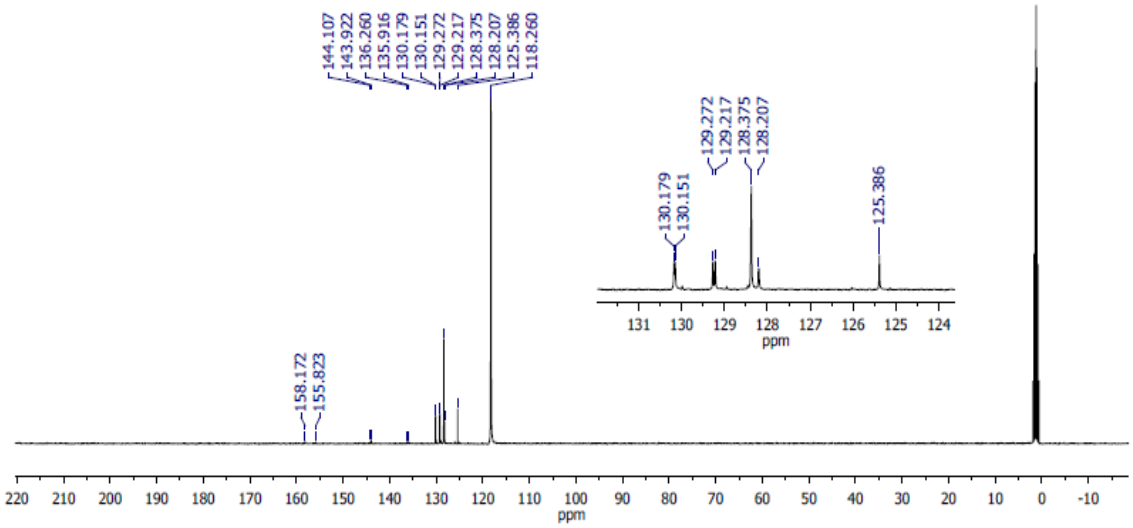

Figure 3.27 ^{13}C NMR of Potassium (*E*)-(2-fluoro-1,2-diphenylvinyl)trifluoroborate (**13b**) in CD_3CN.

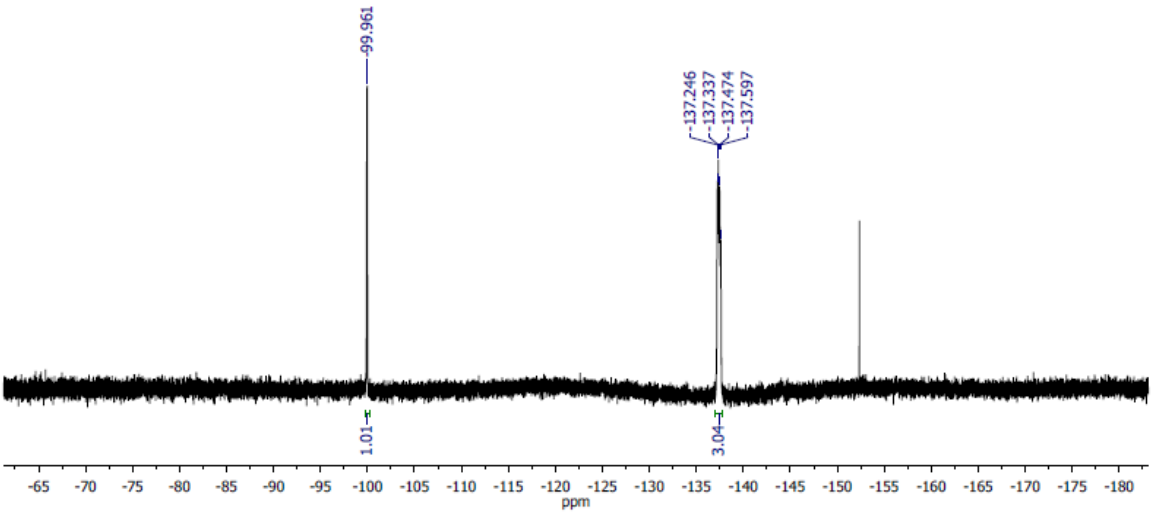

Figure 3.28 ^{19}F NMR of Potassium (*E*)-(2-fluoro-1,2-diphenylvinyl)**t**rifluoroborate (**13b**) in CD_3CN.

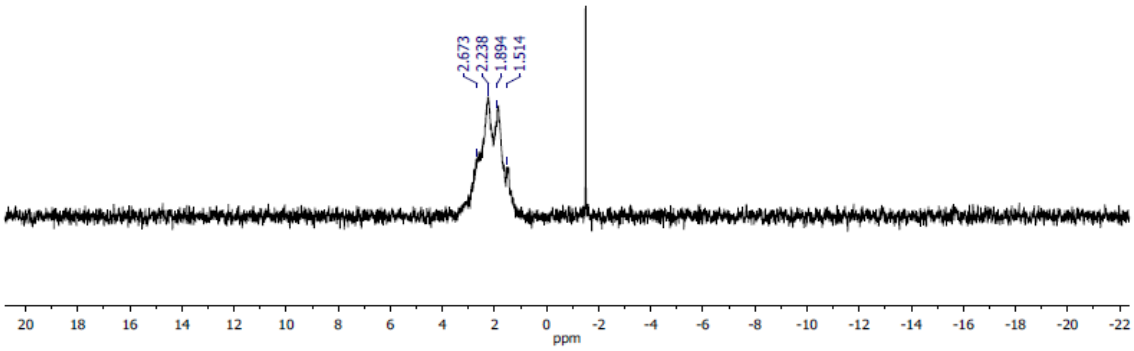

Figure 3.29 ^{11}B NMR of Potassium (*E*)-(2-fluoro-1,2-diphenylvinyl)trifluoroborate (**13b**) in CD_3CN.

3.4.4.10 Synthesis of potassium (*E*)-(2-fluoro-1-phenylprop-1-en-1-yl)trifluoroborate

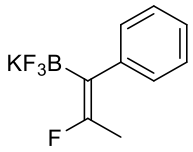

Figure 3.30 Potassium (*E*)-(2-fluoro-1-phenylprop-1-en-1-yl)trifluoroborate (**13c**)

(IDipp)CuO-*t*-Bu (0.124 g, 0.236 mmol), $B_2(neo)_2$ (0.054 g, 0.24 mmol), 1-phenyl-1-propyne (0.028 g, 0.24 mmol) were combined in a 20-mL vial and dissolved in toluene (6 mL). After 10 min, a solution of NFSI (0.075 g, 0.238 mmol) in toluene (3 mL) was added. After another 10 min, the mixture was concentrated *in vacuo* and the products were extracted with pentane, filtered through a Celite plug and concentrated in vacuo to give an oil. The oil was then dissolved in MeOH (10 mL) with stirring before a solution of KHF_2 (0.186 g, 2.38 mmol) in H_2O (5 mL) was added and stirred for 3h. This mixture was then concentrated and the products were extracted with acetone (3 x 5 mL), filtered through a Celite plug and concentrated to give a colorless solid. This was washed with Et_2O (5 mL) and DCM (5 mL) and the residue was dried for 12h under vacuum, affording the product as a colorless powder (0.038 g, 67% yield). ^{1}H NMR (400 MHz, CD_3CN): δ (ppm) 7.24-7.21 (m, 2H, *meta*-C*H*), 7.12-7.05 (m, 3H, *ortho*- and *para*-CH), 1.70 (dq, 3H, $^3J_{FH}$ = 17.6 Hz, , $^4J_{FH}$ = 1.2 Hz, C=C(F)CH_3), ^{13}C{^{1}H} NMR (176 MHz,CD_3CN): δ (ppm) 158.0 (d, $^1J_{FC}$ = 239 Hz, C=*C*F), 148.7 (d, $^3J_{FC}$ = 20 Hz, *ipso-C*), 129.9 (d, $^4J_{FC}$ = 3 Hz, *ortho-C*), 128.2 (*para-C*) 125.2 (*meta-C*), 16.2 (d, $^2J_{FC}$ = 37 Hz, C=C(F)CH_3),) ^{19}F NMR (376 MHz, CD_3CN): δ (ppm) –94.12 (br s, 1F, C=C*F*), –136.97 to –137.35 (br m, 3F, C=C(B*F*$_3$K), ^{11}B NMR (128 MHz, CD_3CN) δ (ppm) 2.00 (q, $^1J_{FB}$ = 51 Hz C=C(*B*F$_3$K) Anal. Calcd for $C_9H_8BF_4K$: C, 44.66; H, 3.33. Found C, 44.53 H, 3.30.

Note: Product contains about 5% potassium (*E*)-(1-fluoro-1-phenylprop-1-en-2-yl)trifluoroborate, evident in the ^{19}F NMR spectrum.

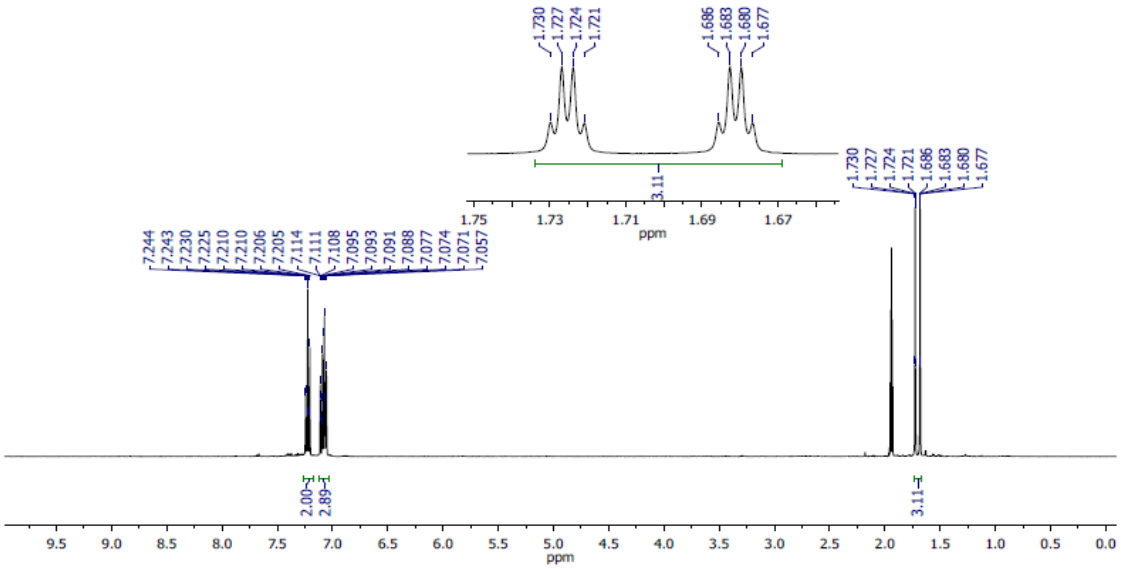

Figure 3.31 ^{1}H NMR of potassium (*E*)-(2-fluoro-1-phenylprop-1-en-1-yl)trifluoroborate (**13c**) in CD_3CN.

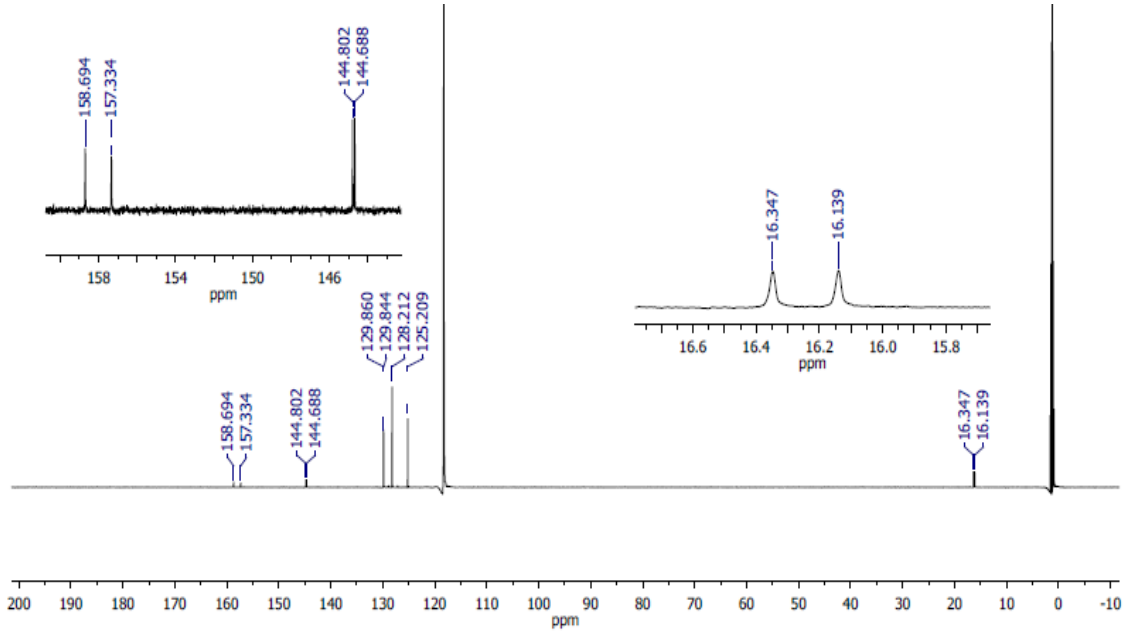

Figure 3.32 ^{13}C NMR of potassium (*E*)-(2-fluoro-1-phenylprop-1-en-1-yl)trifluoroborate (**13c**) in CD_3CN.

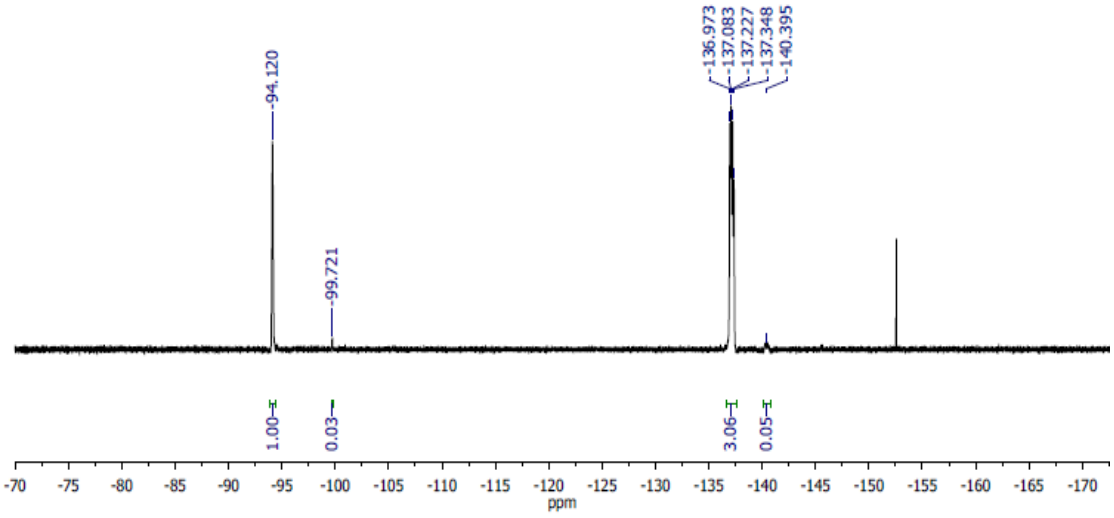

Figure 3.33 ^{19}F NMR of potassium (*E*)-(2-fluoro-1-phenylprop-1-en-1-yl)trifluoroborate (**13c**) in CD_3CN.

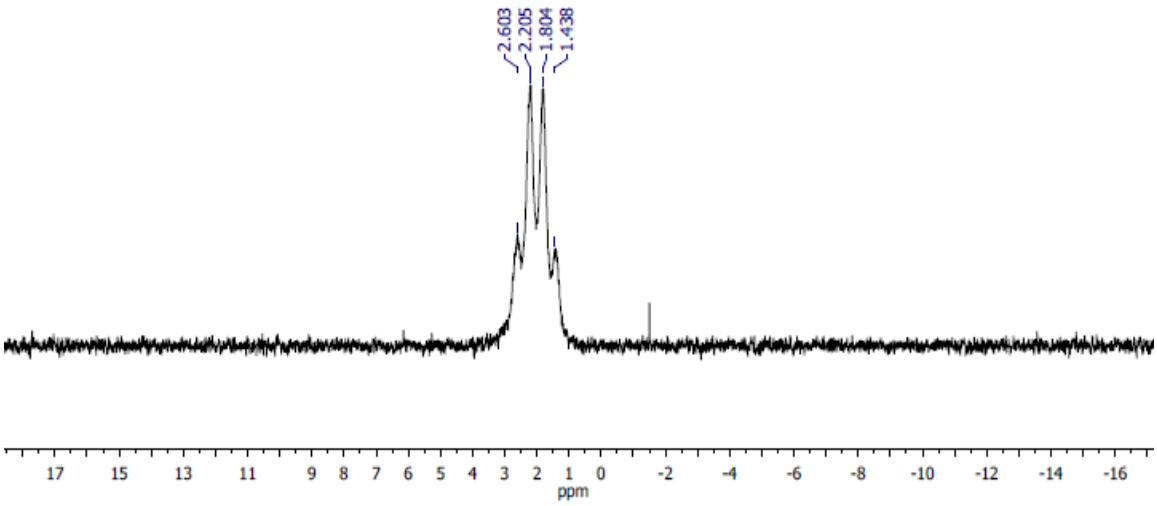

Figure 3.34 ^{11}B NMR of potassium (*E*)-(2-fluoro-1-phenylprop-1-en-1-yl)trifluoroborate (**13c**) in CD_3CN.

3.4.4.11 Synthesis of Potassium (*E*)-(1-fluorohex-1-en-2-yl)trifluoroborate

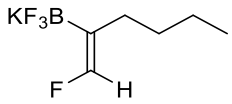

Figure 3.35 Potassium (*E*)-(1-fluorohex-1-en-2-yl)trifluoroborate (**13d**)

IDipp)CuO-*t*-Bu (0.130 g, 0.248 mmol), $B_2(neo)_2$ (0.056 g, 0.250 mmol) were combined in a 20-mL vial and dissolved in toluene (6 mL) before 1-hexyne (0.0285 μL, 0.248 mmol) was added via syringe. After 10 min, a solution of NFSI (0.078 g, 0.25 mmol) in toluene (3 mL) was added. After another 10 min, the mixture was concentrated *in vacuo* and the products were extracted with pentane, filtered through a Celite plug and concentrated in vacuo to give an oil. The oil was then dissolved in MeOH (10 mL) with stirring before a solution of KHF_2 (0.193 g, 2.48 mmol) in H_2O (5 mL) was added and stirred for 3h. This mixture was then concentrated and the products were extracted with acetone (3 x 5 mL), filtered through a Celite plug and concentrated to give a colorless solid. This was washed with Et_2O (5 mL) and DCM (5 mL) and the residue was dried for 12h under vacuum, affording the product as a colorless powder (0.034 g, 66% yield). ^{1}H NMR (400 MHz, CD_3CN): δ (ppm) 6.41 (d, $^2J_{FH}$ = 97.6 Hz, 1H, C=C(F)*H*), 1.79 (t, $^3J_{HH}$ = 6.8 Hz, 2H, C=C(BF_3K)CH_2), 1.36-1.21 (m, 4H, CH_2–CH_2CH), 0.87 (t, $^3J_{HH}$ = 7.2 Hz, 3H, CH_3), ^{13}C{^{1}H} NMR (176 MHz,$CDCl_3$): δ (ppm) 148.4 (d, $^1J_{FC}$ = 242 Hz, C=*C*F), 33.0 (d, $^4J_{FC}$ = 3 Hz, C=C(BF_3K)CH_2*C*H_2), 30.2 (d, $^3J_{FC}$ = 17 Hz, C=C(BF_3K)*C*H_2), 23.4 (*C*H_2CH_3), 14.3 (CH_2*C*H_3), ^{19}F NMR (376 MHz, CD_3CN): δ (ppm) –128.82 (d, $^2J_{HF}$ = 97.8 Hz 1F, C=C*F*), –138.66 to –139.07 (br m, 3F, C=C(B*F*$_3$K), ^{11}B NMR (128 MHz, CD_3CN) δ (ppm) 2.14 (q, $^1J_{FB}$ = 52 Hz C=C(*B*F_3K). IR: *ν* (cm^{-1}) 2957, 2929, 2854, 1465, 1345, 1187, 1175, 1044, 982, 938, 818, 649, 631, 499, 458. Anal. Calcd for $C_6H_{10}BF_4K$: C, 34.64; H, 4.85. Found C, 34.92 H, 4.71.

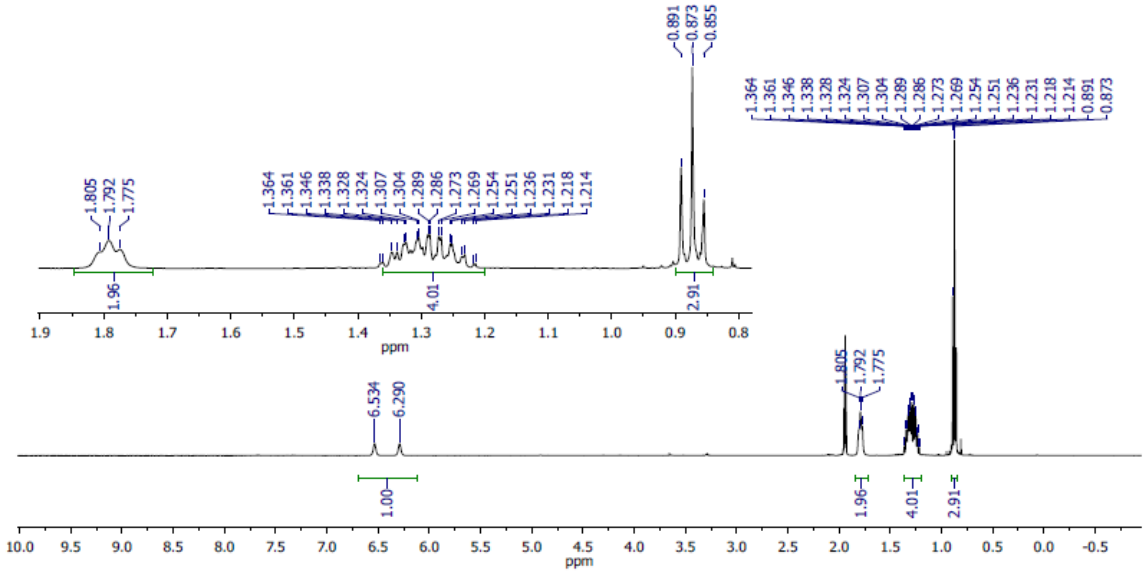

Figure 3.36 ^{1}H NMR of potassium (*E*)-(1-fluorohex-1-en-2-yl)trifluoroborate (**13d**) in CD_3CN.

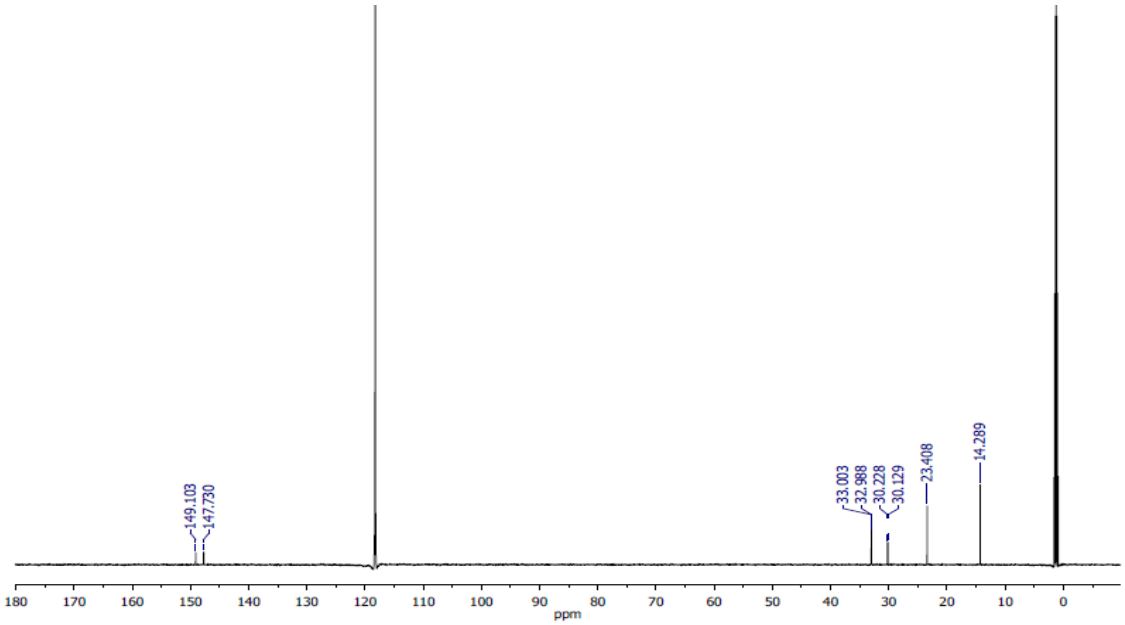

Figure 3.37 ^{13}C NMR of potassium (*E*)-(1-fluorohex-1-en-2-yl)trifluoroborate (**13d**) in CD_3CN.

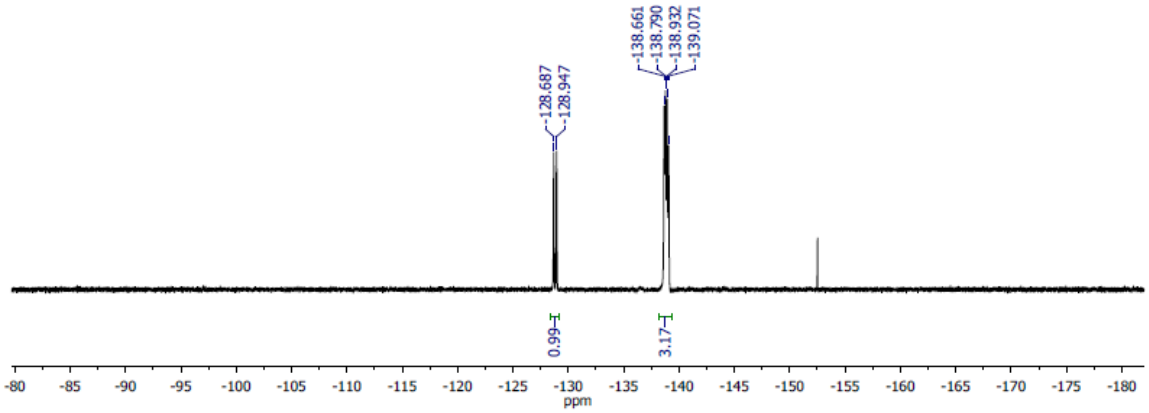

Figure 3.38 ^{19}F NMR of potassium (*E*)-(1-fluorohex-1-en-2-yl)trifluoroborate (**13d**) in CD_3CN.

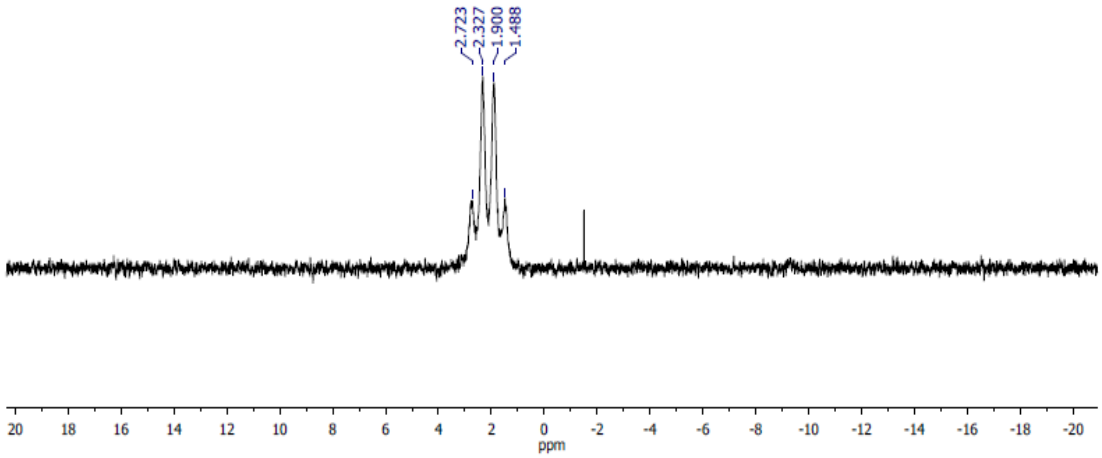

Figure 3.39 ^{11}B NMR of potassium (*E*)-(1-fluorohex-1-en-2-yl)trifluoroborate (**13d**) in CD_3CN.

3.4.4.12 Synthesis of potassium (*E*)-[2-fluoro-1-(4-methoxyphenyl)vinyl]trifluoroborate

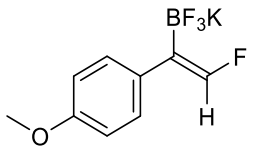

Figure 3.40 Potassium (*E*)-[2-fluoro-1-(4-methoxyphenyl)vinyl]trifluoroborate (**13e**)

Potassium (*E*)-[2-fluoro-1-(4-methoxyphenyl)vinyl]trifluoroborate (**13e**) (IDipp)CuO-*t*-Bu (0.123 g, 0.234 mmol), $B_2(neo)_2$ (0.053 g, 0.23 mmol), were combined in a 20-mL vial and dissolved in toluene (6 mL), before 4-ethynylanisole (0.030 mL, 0.23 mmol) was added via syringe. After 10 min, a solution of NFSI (0.075 g, 0.24 mmol) in toluene (3 mL) was added. After another 10 min, the mixture was concentrated *in vacuo* and the products were extracted with pentane, filtered through a Celite plug and concentrated in vacuo to give an oil. This was then dissolved in MeOH (10 mL) with stirring before a solution of KHF_2 (0.186 g, 2.38 mmol) in H_2O (5 mL) was added and stirred for 3h. This mixture was then concentrated and the products were extracted with acetone (3 x 5 mL), filtered through a Celite plug and concentrated to give a colorless solid. This was washed with Et_2O (5 mL) and DCM (5 mL) and the residue was dried for 12h under vacuum, affording the product as a colorless powder (0.017 g, 28% yield). ^{1}H NMR (700 MHz, CD_3CN): δ (ppm) 7.16 (d, $^3J_{HH}$ = 8.4 Hz, 2H, *meta*-C*H*) 6.79 (d, $^3J_{HH}$ = 8.4 Hz, 2H, *ortho*-C*H*) 6.63 (d, $^2J_{FH}$ = 94.5 Hz, 1H, C=C(F)*H*), 3.74 (s, 3H, OCH_3), ^{13}C{^{1}H} NMR (176 MHz,$CDCl_3$): δ (ppm) 158.6 (*para*-C), 150.4 (d, $^1J_{FC}$ = 251.2 Hz, C=*C*F), 134.8 (d, $^3J_{FC}$ = 20.8 Hz, *ipso*-*C*), 129.8 (*meta*-*C*), 114.0 (*ortho*-*C*), 55.6 (O*C*H_3), ^{19}F NMR (376 MHz, CD_3CN): δ (ppm) –124.27 (d, $^2J_{HF}$ = 94.8 Hz 1F, C=C*F*), –136.98 to –137.36 (br m, 3F, C=C(B*F*$_3$K), ^{11}B NMR (128 MHz, CD_3CN) δ (ppm) 2.02 (q, $^1J_{FB}$ = 50 Hz C=C(*B*F_3K) IR: *v* (cm^{-1}) 2959, 2837, 1607,

1511, 1407, 1284, 1245, 1130, 1112, 978, 956, 897, 827, 590, 537 Anal. Calcd for $C_9H_8BF_4KO$: C, 41.89; H, 3.12. Found C, 42.13 H, 3.04.

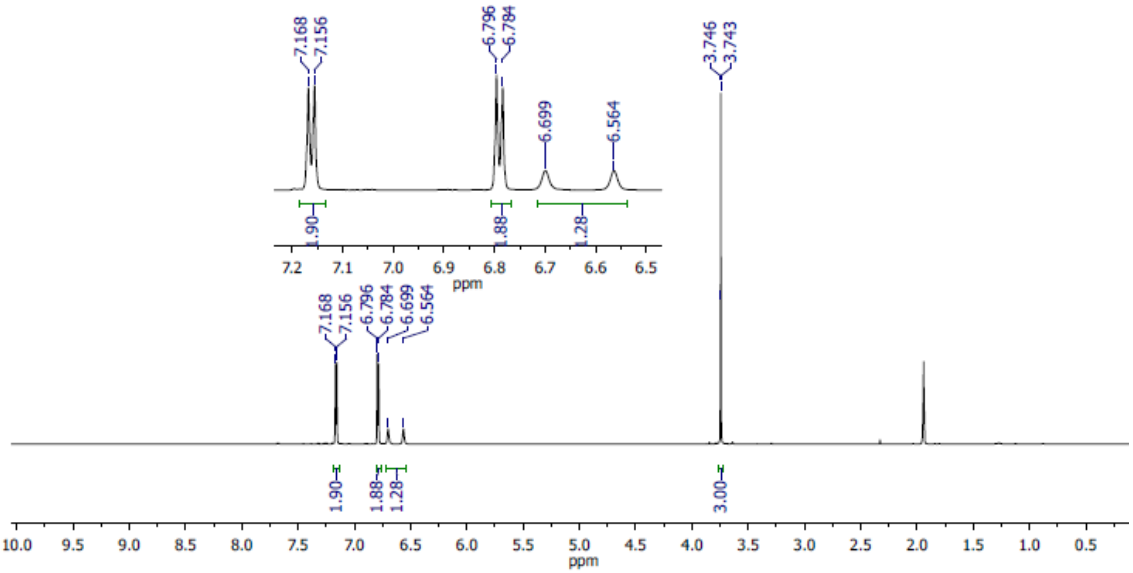

Figure 3.41 ^{1}H NMR of potassium (*E*)-[2-fluoro-1-(4-methoxyphenyl)vinyl] trifluoroborate (**13e**) in CD_3CN.

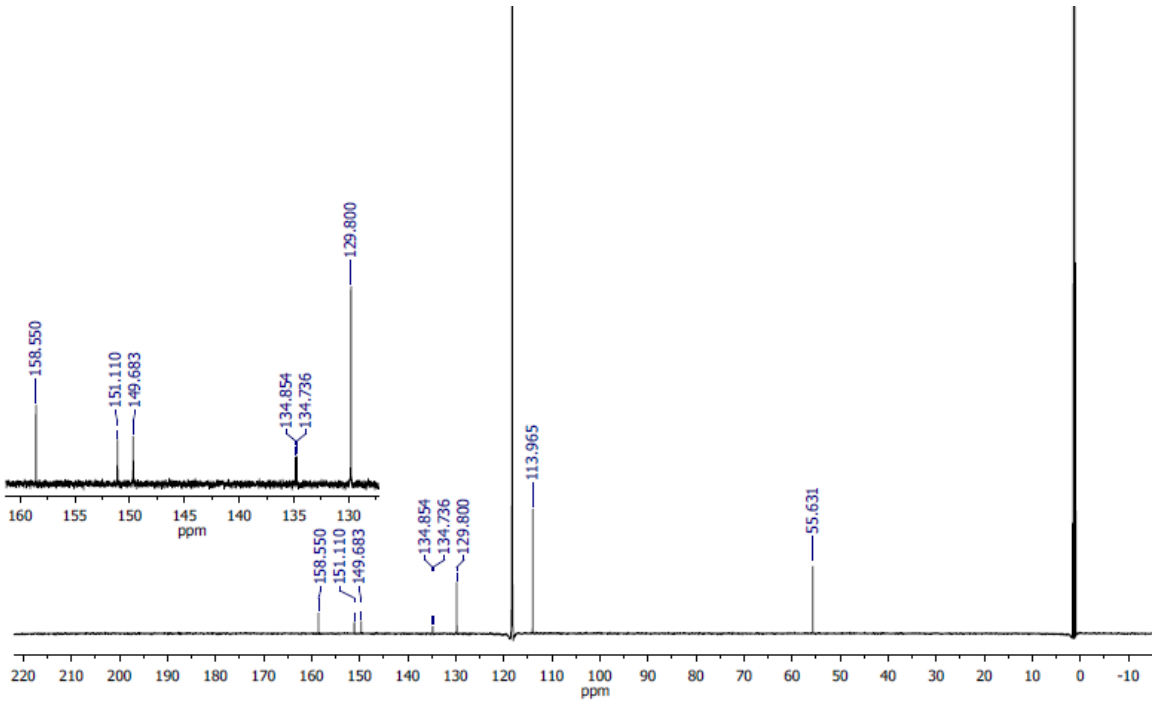

Figure 3.42 ^{13}C NMR of potassium (*E*)-[2-fluoro-1-(4-methoxyphenyl)vinyl] trifluoroborate (**13e**) in CD_3CN.

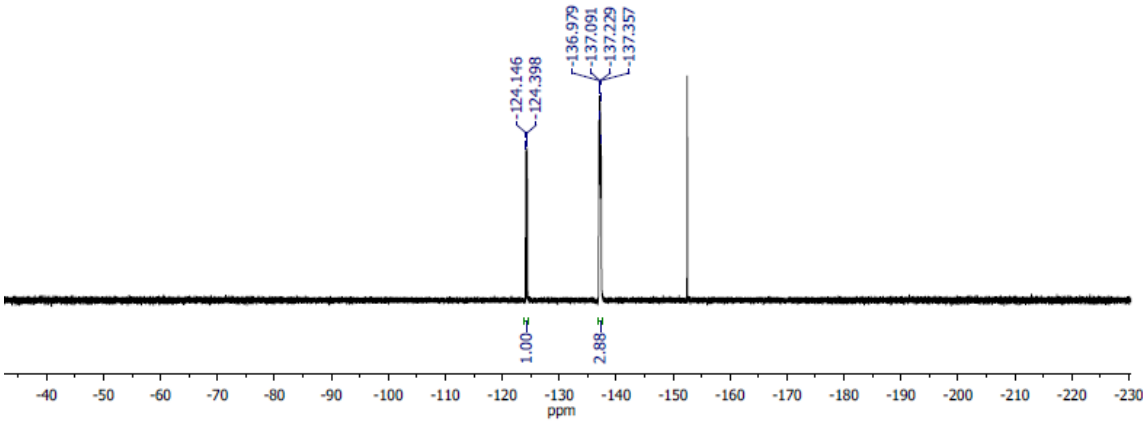

Figure 3.43 ^{19}F NMR of potassium (*E*)-[2-fluoro-1-(4-methoxyphenyl)vinyl] trifluoroborate (**13e**) in CD_3CN.

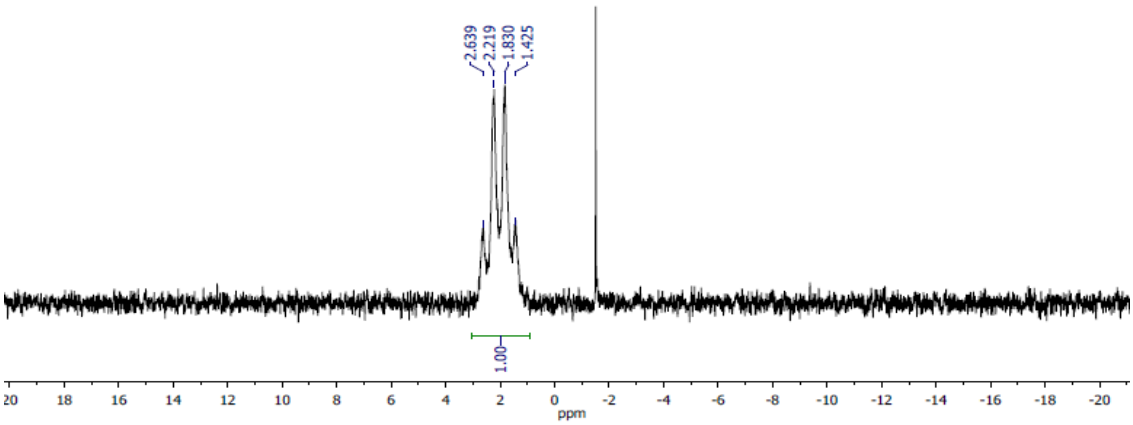

Figure 3.44 ^{11}B NMR of potassium (*E*)-[2-fluoro-1-(4-methoxyphenyl)vinyl] trifluoroborate in (**13e**) CD_3CN.

3.4.4.13 Synthesis of potassium (*E*)-[1-([1,1'-biphenyl]-4-yl)-2-fluorovinyl]trifluoroborate

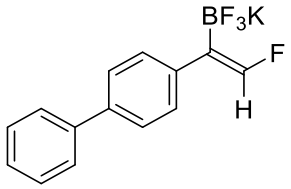

Figure 3.45 Potassium (*E*)-[1-([1,1'-biphenyl]-4-yl)-2-fluorovinyl]trifluoroborate (**13f**)

(IDipp)CuO-*t*-Bu (0.125 g, 0.238 mmol), $B_2(neo)_2$ (0.054 g, 0.24 mmol) were combined in a 20-mL vial and dissolved in toluene (6 mL) before a solution of 4-ethynylbiphenyl (0.042 g, 0.24 mmol) in toluene (1.5 mL) was added. After 10 min, a solution of NFSI (0.075 g, 0.24 mmol) in toluene (3 mL) was added. After another 10 min, the mixture was concentrated *in vacuo* and the products were extracted with pentane, filtered through a Celite plug and concentrated in vacuo to give an oil. The oil was then dissolved in MeOH (10 mL) with stirring before a solution of KHF_2 (0.186 g, 2.48 mmol) in H_2O (5 mL) was added and stirred for 3h. This mixture was then concentrated and the products were extracted with acetone (3 x 5 mL), filtered through a Celite plug and concentrated to give a colorless solid. This was washed with Et_2O (5 mL) and DCM (5 mL) and the residue was dried for 12h under vacuum, affording the product as a colorless powder (0.025 g, 35% yield). ^{1}H NMR (400 MHz, CD_3CN): δ (ppm) 7.63 (dd, $^3J_{HH}$ = 8.4 Hz, 1.6 Hz, 2H, *ortho*-C*H* phenyl), 7.51 ((d, $^3J_{HH}$ = 8.0 Hz, 2H, *meta*-C*H* aryl), 7.44 (t, $^3J_{HH}$ = 8.0 Hz, 2H, *meta*-C*H* phenyl), 7.35-7.30 (m, 3H, *ortho*-C*H* aryl, *para*-C*H* phenyl), 6.72 (d, $^2J_{FH}$ = 94.4 Hz, 1H, C=C(F)*H*), ^{13}C{^{1}H} NMR (176 MHz, CD_3CN): δ (ppm) 150.9 (d, $^1J_{FC}$ = 233 Hz, C=*C*F), 142.0 (d, $^3J_{FC}$ = 21 Hz, *ipso*-C aryl), 142.0 (*ipso*-C phenyl), 138.5 (*para*-C aryl), 129.7 (*meta*-C phenyl), 129.4 (*meta*-C aryl), 127.8 (*ortho*-C phenyl), 127.6 (*para*-C phenyl), 127.1 (*ortho*-C aryl), ^{19}F NMR (376 MHz, CD_3CN): δ (ppm) –122.58

(d, $^{2}J_{HF}$ = 94.7 Hz 1F, C=C*F*), –136.78 to –137.14 (br m, 3F, C=C(B*F*$_3$K), ^{11}B NMR (128 MHz, CD_3CN) δ (ppm) 2.02 (q, $^{1}J_{FB}$ = 49 Hz C=C(*B*F$_3$K) IR: *v* (cm^{-1}) 3074, 3028, 1612, 1514, 1366, 1254, 1120, 966, 954, 893, 832, 762, 728, 690, 561, 530. Anal. Calcd for $C_{14}H_{10}BF_4K$: C, 55.29; H, 3.31. Found C, 55.41; H, 3.34.

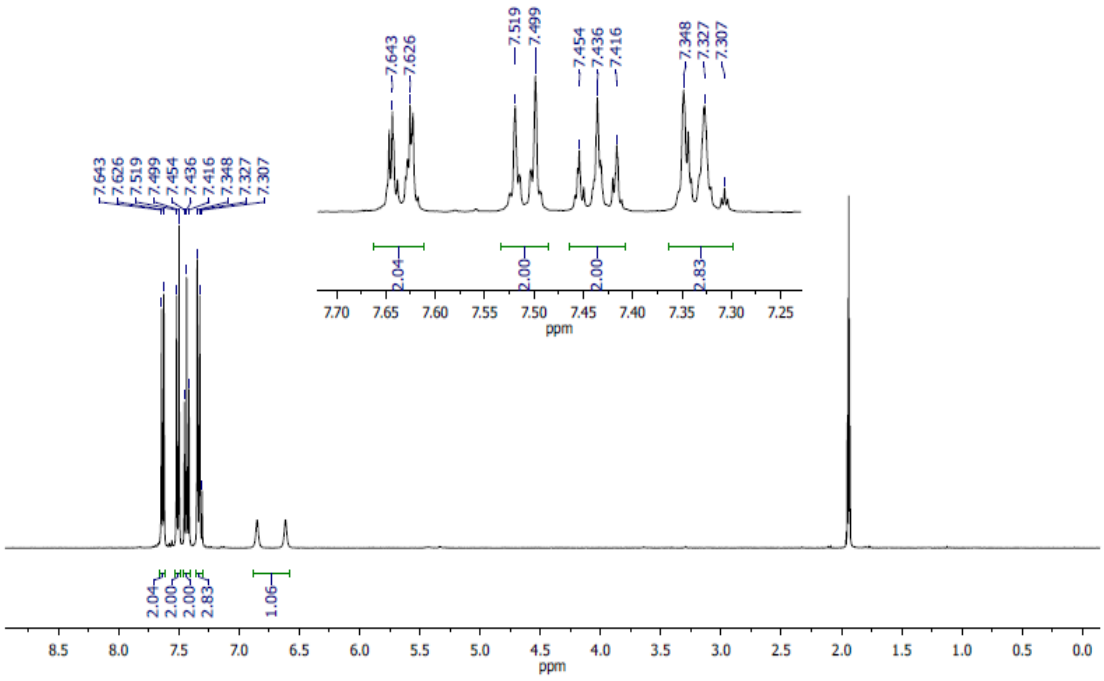

Figure 3.46. ^{1}H NMR of potassium (*E*)-[1-([1,1'-biphenyl]-4-yl)-2-fluorovinyl]trifluoroborate (**13f**) in CD_3CN.

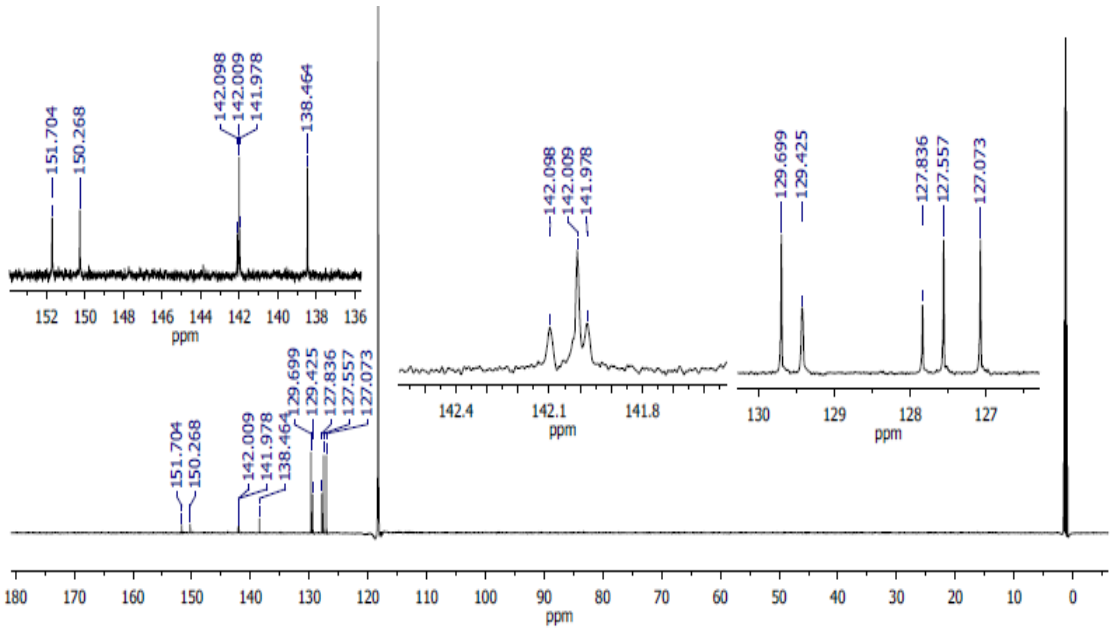

Figure 3.47 ^{13}C NMR of potassium (*E*)-[1-([1,1'-biphenyl]-4-yl)-2-fluorovinyl]trifluoroborate (**13f**) in CD_3CN.

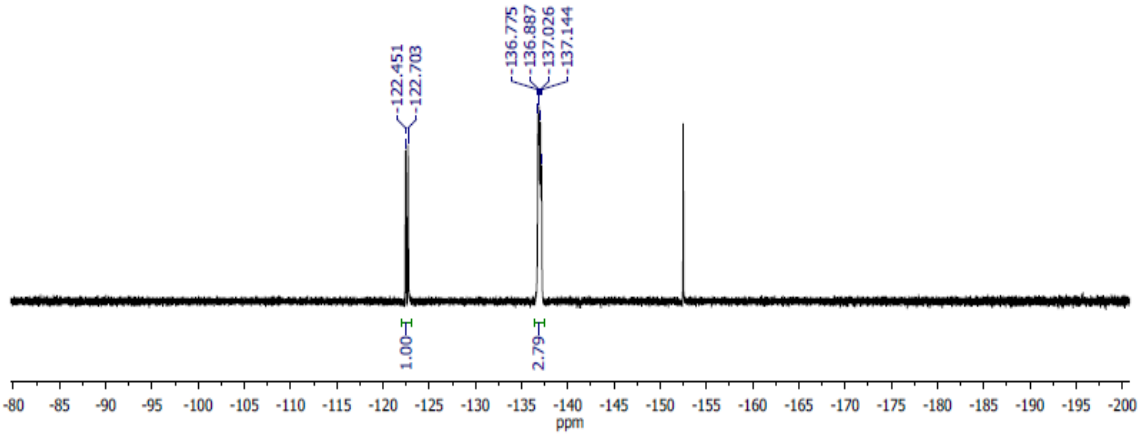

Figure 3.48 ^{19}F NMR of potassium (*E*)-[1-([1,1'-biphenyl]-4-yl)-2-fluorovinyl]trifluoroborate (**13f**) in CD_3CN.

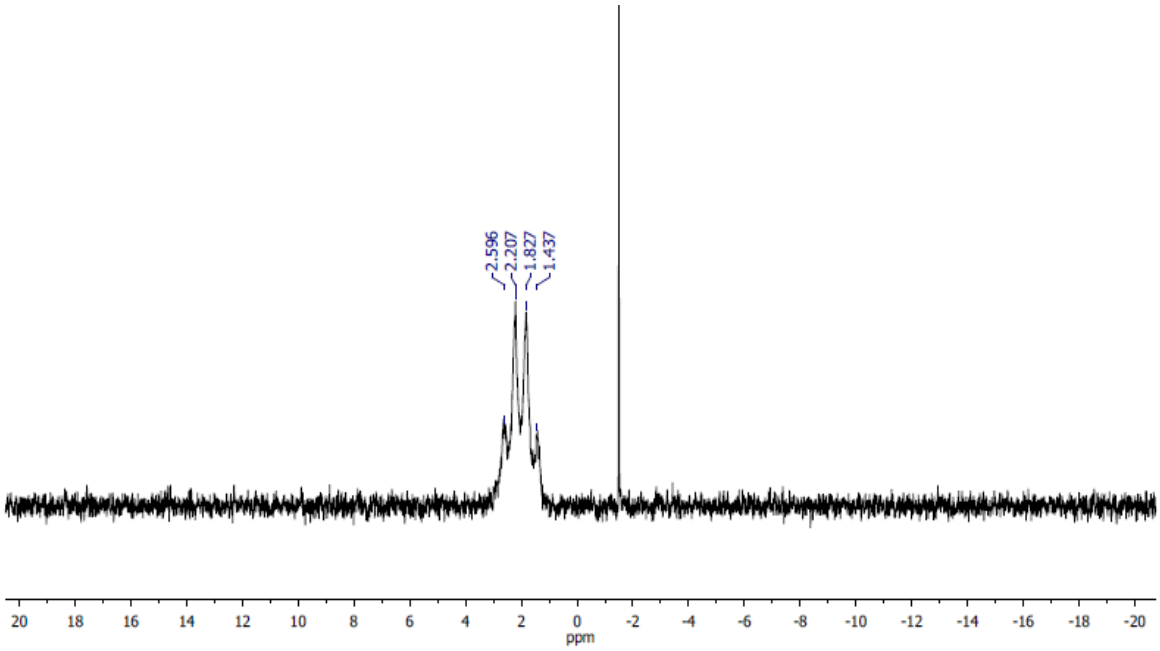

Figure 3.49 ^{11}B NMR of potassium (*E*)-[1-([1,1'-biphenyl]-4-yl)-2-fluorovinyl]trifluoroborate (**13f**) in CD_3CN.

3.4.4.14 Synthesis of potassium (*E*)-(1-(cyclohex-1-en-1-yl)-2-fluorovinyl)trifluoroborate

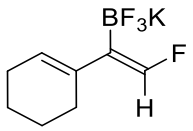

Figure 3.50 Potassium (*E*)-(1-(cyclohex-1-en-1-yl)-2-fluorovinyl)trifluoroborate (**13g**)

(IDipp)CuO-*t*-Bu (0.125 g, 0.238 mmol), $B_2(neo)_2$ (0.054 g, 0.23 mmol), were combined in a 20-mL vial and dissolved in toluene (6 mL), before 1-ethynylcyclohexene (0.028 mL, 0.24 mmol) was added via syringe. After 10 min, a solution of NFSI (0.075 g, 0.24 mmol) in toluene (3 mL) was added. After another 10 min, the mixture was concentrated *in vacuo* and the products were extracted with pentane, filtered through a Celite plug and concentrated in vacuo to give an oil. This was then dissolved in MeOH (10 mL) with stirring before a solution of KHF_2 (0.186 g, 2.38 mmol) in H_2O (5 mL) was added and stirred for 3h. This mixture was then concentrated and the products were extracted with acetone (3 x 5 mL), filtered through a Celite plug and concentrated to give a colorless solid. This was washed with Et_2O (5 mL) and DCM (5 mL) and the residue was dried for 12h under vacuum, affording the product as a colorless powder (0.024 g, 44% yield). ^{1}H NMR (400 MHz, CD_3CN): δ (ppm) 6.52 (d, $^2J_{FH}$ = 96.8 Hz, 1H, C=C(F)*H*), 5.41 (sept, $^3J_{HH}$ = 2.0 Hz, 1H, C=C(CH_2)*H*), 2.06-1.99 (m, 4H, (C*H*$_2$)C=C(C*H*$_2$), 1.61-1.49 (m, 4H, C*H*$_2$–C*H*$_2$), ^{13}C{^{1}H} NMR (176 MHz,$CDCl_3$): δ (ppm) 148.8 (d, $^1J_{FC}$ = 251 Hz, C=*C*F), 138.8 (d, $^3J_{FC}$ = 19 Hz, C=*C*(CH_2)C=C), 120.8 (*C*=C(CH_2)C=C), 29.3 (C*H*$_2$)C=C), 26.3 (*C*H_2)C=C), 23.9 *C*H_2–CH_2), 23.2 *C*H_2–CH_2), ^{19}F NMR (376 MHz, CD_3CN): δ (ppm) –128.42 (d, $^2J_{HF}$ = 96.6 Hz 1F, C=C*F*), –135.96 to –136.36 (br m, 3F, C=C(B*F*$_3$K), ^{11}B NMR (128 MHz, CD_3CN) δ (ppm) 1.90 (q, $^1J_{FB}$ = 54 Hz C=C(*B*F_3K) IR: *v* (cm^{-1}) 2931, 2854,

2844, 1625, 1319, 1213, 1104, 982, 960, 960, 881, 822, 815, 717, 588, 474, 451. Anal. Calcd for $C_8H_{10}BF_4K$: C, 41.40; H, 4.34. Found C, 41.16 H, 4.70.

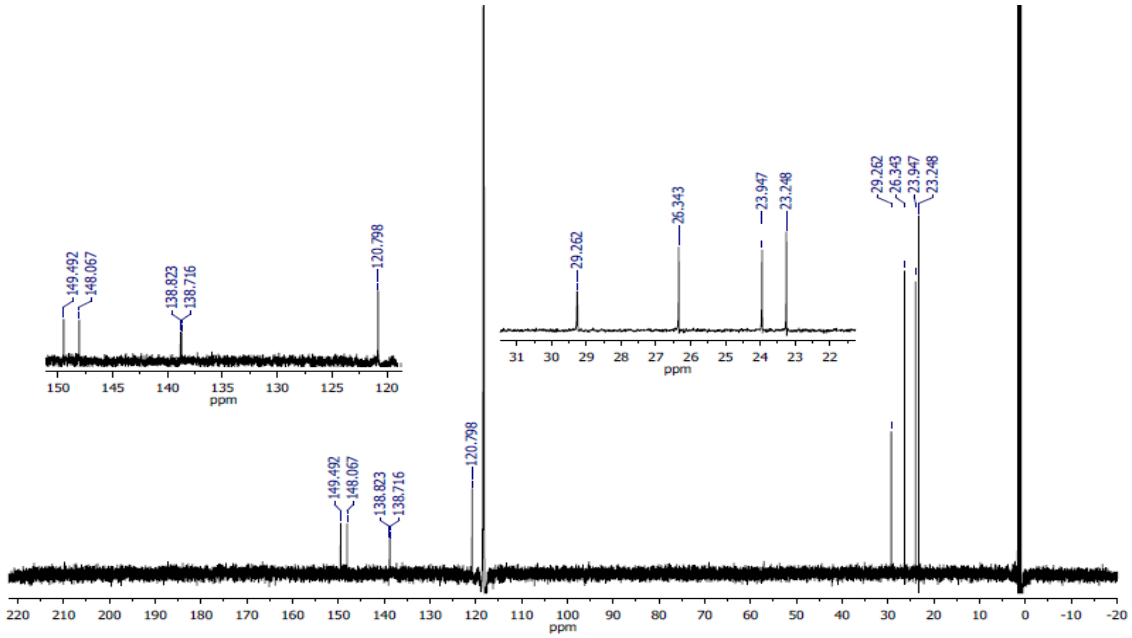

Figure 3.51. ^{1}H NMR of Potassium (*E*)-(1-(cyclohex-1-en-1-yl)-2-fluorovinyl)trifluoroborate (**13g**) in CD_3CN.

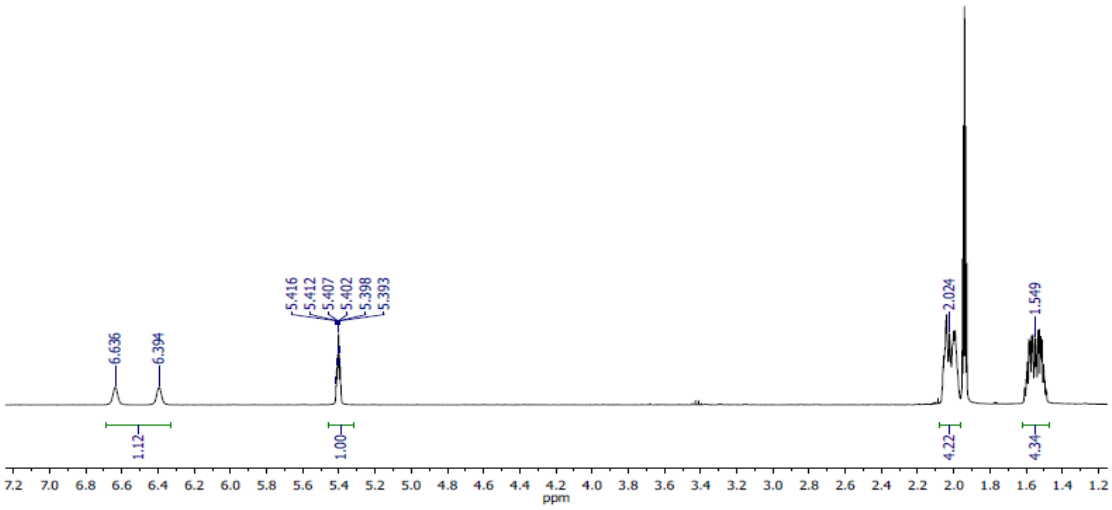

Figure 3.52 ^{13}C NMR of potassium (*E*)-(1-(cyclohex-1-en-1-yl)-2-fluorovinyl)trifluoroborate (**13g**) in CD_3CN.

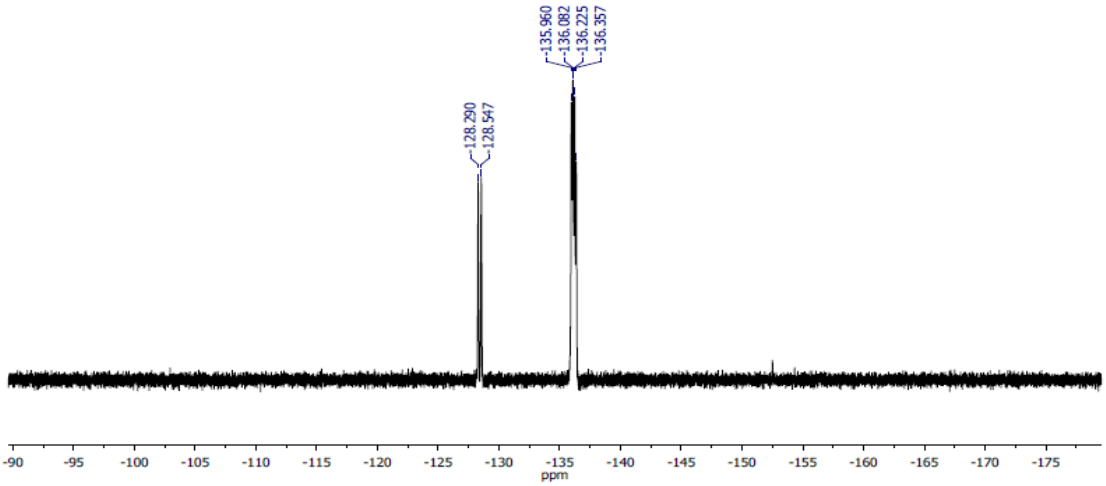

Figure 3.53 ^{19}F NMR of potassium (*E*)-(1-(cyclohex-1-en-1-yl)-2-fluorovinyl)trifluoroborate (**13g**) in CD_3CN.

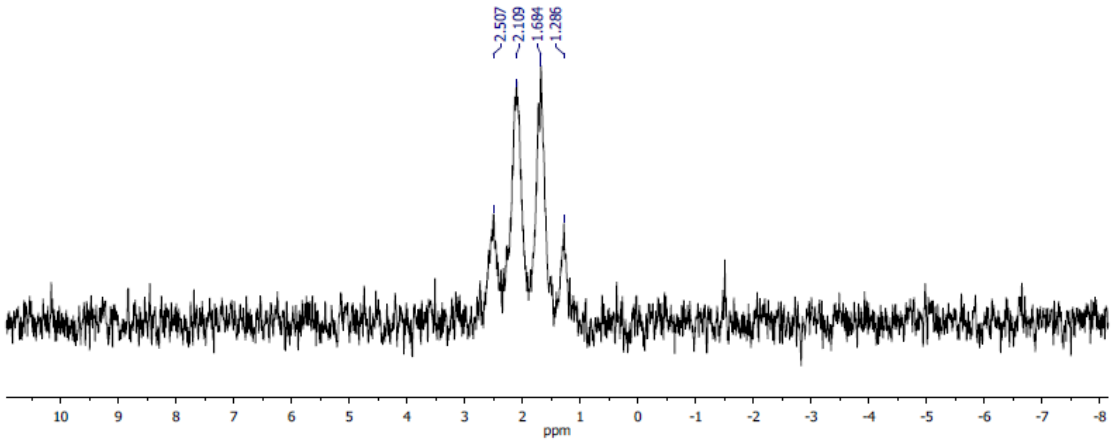

Figure 3.54 ^{11}B NMR of potassium (*E*)-(1-(cyclohex-1-en-1-yl)-2-fluorovinyl)trifluoroborate (**13g**)in CD_3CN.

3.4.4.15 Synthesis of potassium (*E*)-[1-(4-(tert-butyl)phenyl)-2-fluorovinyl]trifluoroborate

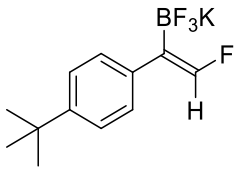

Figure 3.55 Potassium (*E*)-[1-(4-(tert-butyl)phenyl)-2-fluorovinyl]trifluoroborate (**13h**)

IDipp)CuO-*t*-Bu (0.128 g, 0.244 mmol), $B_2(neo)_2$ (0.055 g, 0.24 mmol), were combined in a 20-mL vial and dissolved in toluene (6 mL), before 4-*tert*-butylphenylacetylene (0.044 mL, 0.24 mmol) was added via syringe. After 10 min, a solution of NFSI (0.077 g, 0.24 mmol) in toluene (3 mL) was added. After another 10 min, the mixture was concentrated *in vacuo* and the products were extracted with pentane, filtered through a Celite plug and concentrated in vacuo to give an oil. The oil was then dissolved in MeOH (10 mL) with stirring before a solution of KHF_2 (0.190 g, 2.44 mmol) in H_2O (5 mL) was added and stirred for 3h. This mixture was then concentrated and the products were extracted with acetone (3 x 5 mL), filtered through a Celite plug and concentrated to give a colorless solid. This was washed with Et_2O (5 mL) and DCM (5 mL) and the residue was dried for 12h under vacuum, affording the product as a colorless powder (0.033 g, 47% yield). ^{1}H NMR (700 MHz, CD_3CN): δ (ppm) 7.28 (d, $^3J_{HH}$ = 8.4 Hz, 2H, *meta*-C*H*) 7.16 (d, $^3J_{HH}$ = 8.4 Hz, 2H, *ortho*-C*H*) 6.65 (d, $^2J_{FH}$ = 94.8 Hz, 1H, C=C(F)*H*), 1.29(s, 9H, C(CH_3)$_3$), ^{13}C{^{1}H} NMR (176 MHz, CD_3CN): δ (ppm) 150.7 (d, $^1J_{FC}$ = 251.5 Hz, C=*C*F), 148.7 (*para*-C), 139.4 (d, $^3J_{FC}$ = 20.6 Hz, *ipso*-*C*), 128.6 (*meta*-*C*), 125.4 (*ortho*-*C*), 34.8 *C*(CH_3)$_3$), 31.6 (C(*C*H_3)$_3$), ^{19}F NMR (376 MHz, CD_3CN): δ (ppm) –123.72 (d, $^2J_{HF}$ = 97.8 Hz 1F, C=C*F*), –136.93 to –137.30 (br m, 3F, C=C(B*F*$_3$K), ^{11}B NMR (128 MHz, CD_3CN) δ (ppm) 2.08 (q, $^1J_{FB}$ = 51 Hz C=C(*B*F_3K). IR: *v* (cm^{-1})

3063, 2956, 2902, 2865, 1664, 1376, 1263, 1129, 1104, 983, 955, 898, 819, 718, 564, 522, 453.

Note: We have been unable to obtain satisfactory elemental analysis for potassium (*E*)-[1-(4-(tert-butyl)phenyl)-2-fluorovinyl]trifluoroborate. Although NMR-silent impurities cannot be ruled out, we believe the ^{1}H, ^{13}C, ^{19}F and ^{11}B and NMR spectra reflect the purity of the sample.

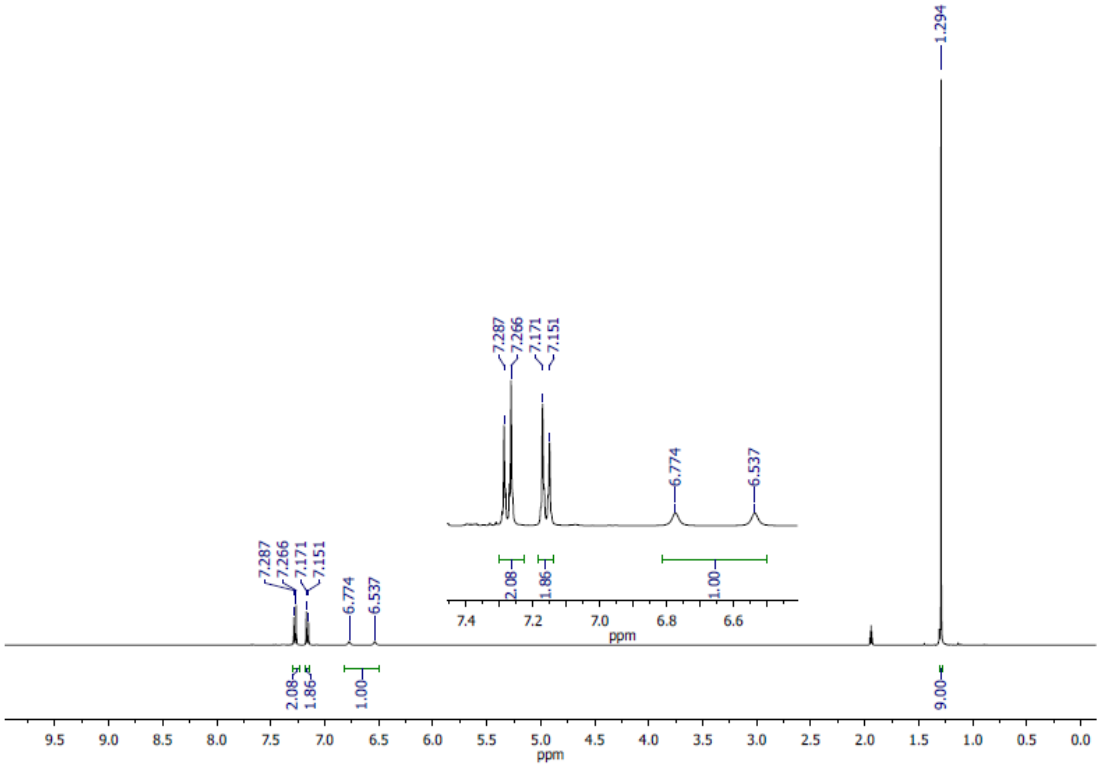

Figure 3.56 ^{1}H NMR of potassium (*E*)-[1-(4-(tert-butyl)phenyl)-2-fluorovinyl]trifluoroborate (**13h**) in CD_3CN.

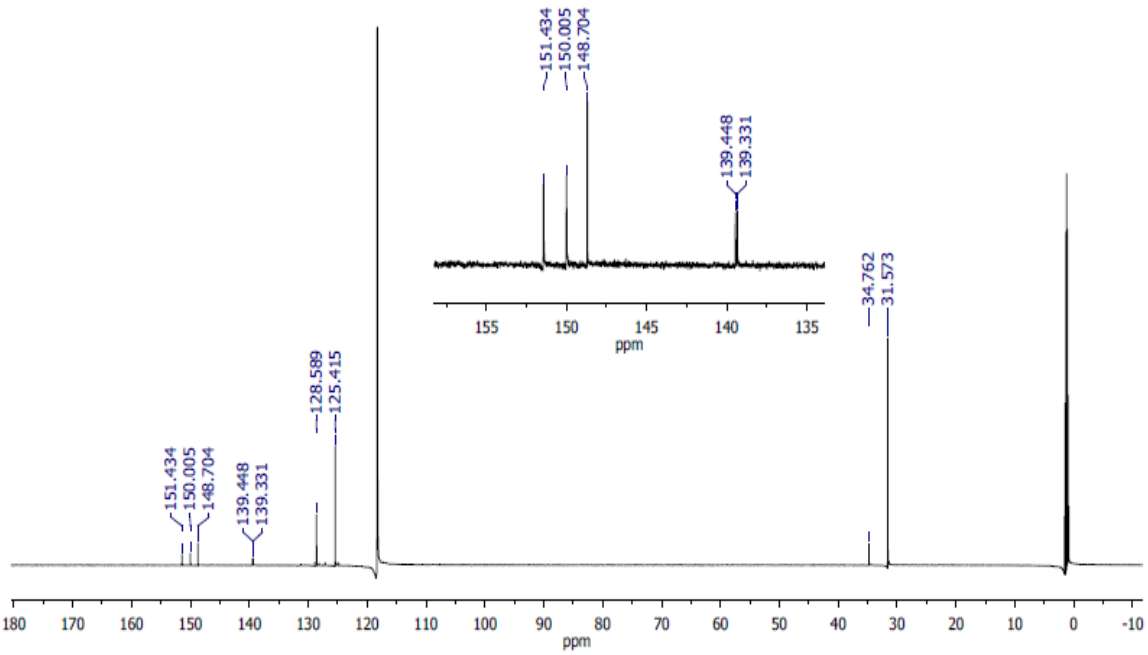

Figure 3.57 ^{13}C NMR of potassium (*E*)-[1-(4-(tert-butyl)phenyl)-2-fluorovinyl]trifluoroborate (**13h**) in CD_3CN.

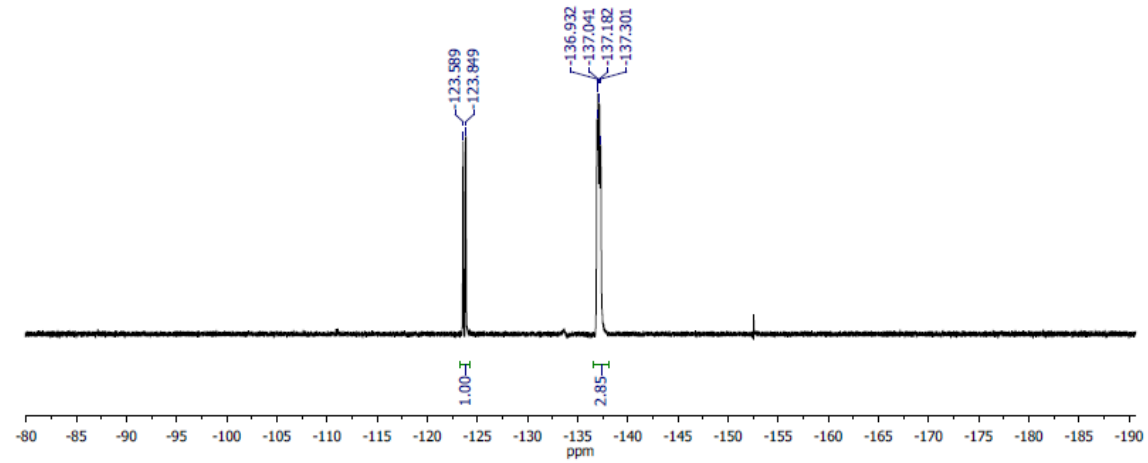

Figure 3.58 ^{19}F NMR of potassium (*E*)-[1-(4-(tert-butyl)phenyl)-2-fluorovinyl]trifluoroborate (**13h**) in CD_3CN.

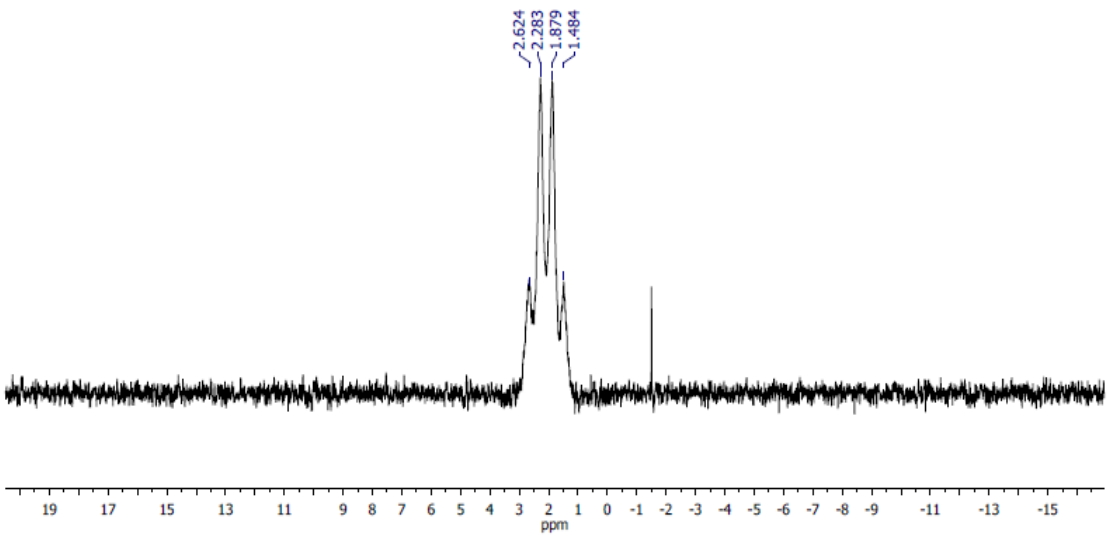

Figure 3.59 ^{11}B NMR of potassium (*E*)-[1-(4-(tert-butyl)phenyl)-2-fluorovinyl]trifluoroborate (**13h**) in CD_3CN.

3.4.4.16 Synthesis of Potassium (*E*)-(1-fluoro-1-phenylbut-1-en-2-yl)trifluoroborate, potassium (*E*)-(2-fluoro-1-phenylbut-1-en-1-yl)trifluoroborate

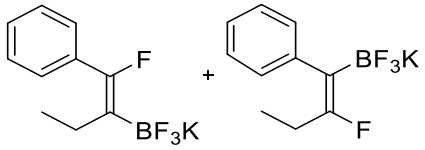

Figure 3.60 Potassium (*E*)-(1-fluoro-1-phenylbut-1-en-2-yl)trifluoroborate (1-fl), potassium (*E*)-(2-fluoro-1-phenylbut-1-en-1-yl)trifluoroborate (2-fl) (**13i**)

(IDipp)CuO-*t*-Bu (0.125 g, 0.238 mmol), $B_2(neo)_2$ (0.054 g, 0.24 mmol), 1-phenyl-1-butyne (0.031 g, 0.24 mmol) were combined in a 20-mL vial and dissolved in toluene (6 mL). After 10 min, a solution of NFSI (0.075 g, 0.24 mmol) in toluene (3 mL) was added. After another 10 min, the mixture was concentrated *in vacuo* and the products were extracted with pentane, filtered through a Celite plug and concentrated in vacuo to give an oil. The oil was then dissolved in MeOH (10 mL) with stirring before a solution of KHF_2 (0.186 g, 2.38 mmol) in H_2O (5 mL) was added and stirred for 3h. This mixture was then concentrated and the products were extracted with acetone (3 x 5 mL), filtered through a Celite plug and concentrated to give a colorless solid. This was washed with Et_2O (5 mL) and DCM (5 mL) and the residue was dried for 12h under vacuum, affording the product as a colorless powder (0.031 g, 51% yield). ^{1}H NMR (700 MHz, CD_3CN): δ (ppm) 7.40-7.36 (m, 4H, *meta*-C*H*, *ortho*-C*H*, 2-fl) 7.31 (t, $^3J_{HH}$ = 7.7Hz, 1H, *para*-C*H*, 2-fl), 7.22 (t, $^3J_{HH}$ = 7.7Hz, 2H, *meta*-C*H*, 1-fl), 7.09 (tt, $^3J_{HH}$ = 7.7Hz, $^4J_{HH}$ = 1.4Hz, 1H, *para*-C*H*, 1-fl), 7.06 (d, $^3J_{HH}$ = 7.7Hz, 2H, *ortho*-C*H*, 1-fl) 2.04-1.93 (m, C=CCH_2), 1.02 (td, $^3J_{HH}$ = 7.7Hz, $^4J_{FH}$ = 1.4Hz, 3H, C=C(F)CH_2CH_3), 0.99 (t, $^3J_{HH}$ = 7.7Hz, 3H, C=C(BF_3)CH_2CH_3), $^{13}C\{^1H\}$ NMR (176 MHz,CD_3CN): δ (ppm) 162.5 (d, $^1J_{CF}$ = 243 Hz, F*C*=C 1-fl), 156.9 (d, $^1J_{CF}$ = 230 Hz, F*C*=C 2-fl), 144.6 (d, $^3J_{CF}$ = 20 Hz, *ipso-C*, 2-fl), 136.0 (d, $^3J_{CF}$ = 36 Hz,

ipso-C, 1-fl), 129.7 (d, $^{4}J_{CF}$ = 3 Hz, *ortho-C*, 2-fl), 129.0 (d, $^{3}J_{CF}$ = 4 Hz, *ortho-C*, 1-fl), 128.9 (*para-C*, 2-fl), 128.6 (d, $^{4}J_{CF}$ = 2 Hz, *meta-C*, 2-fl), 128.2 (*para-C*, 1-fl) 125.2 (*meta-C*, 2-fl), 23.9 (d, $^{2}J_{CF}$ = 34 Hz, CH_2 2-fl), 23.7 ($^{3}J_{CF}$ = 14 Hz, CH_2 1-fl), 15.4 (d, $^{4}J_{CF}$ = 3 Hz, CH_3 2-fl), 12.2 (CH_3 2-fl). ^{19}F NMR (376 MHz, CD_3CN): δ (ppm) –97.97 (br s, 1F, 2-fl), –106.37 (br s, 1F, 1-fl), –136.92 to –137.26 (br m, 3F, (BF_3K), 2-fl), –138.48 to –138.78 (br m, 3F, (BF_3K), 2-fl), ^{11}B NMR (128 MHz, CD_3CN) δ (ppm) 2.02 (q, $^{1}J_{FB}$ = 49 Hz C=C(BF_3K) IR: *v* (cm^{-1}) 3057, 3003, 2924, 2852, 1599, 1493, 1429, 1219, 1170, 1092, 970, 889, 856, 775, 700, 668, 624, 523. Anal. Calcd for $C_{10}H_{10}BF_4K$: C, 46.90; H, 3.94. Found C, 46.76 H, 4.07.

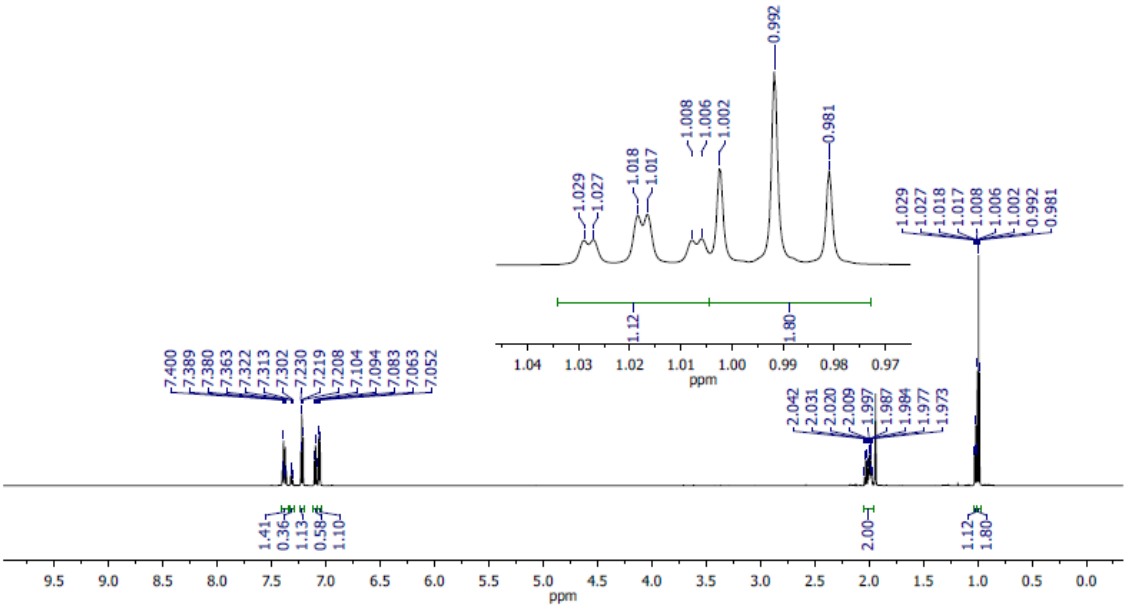

Figure 3.61 ^{1}H NMR of potassium (*E*)-(1-fluoro-1-phenylbut-1-en-2-yl)trifluoroborate and potassium (*E*)-(2-fluoro-1-phenylbut-1-en-1-yl)trifluoroborate (**13i**) in CD_3CN.

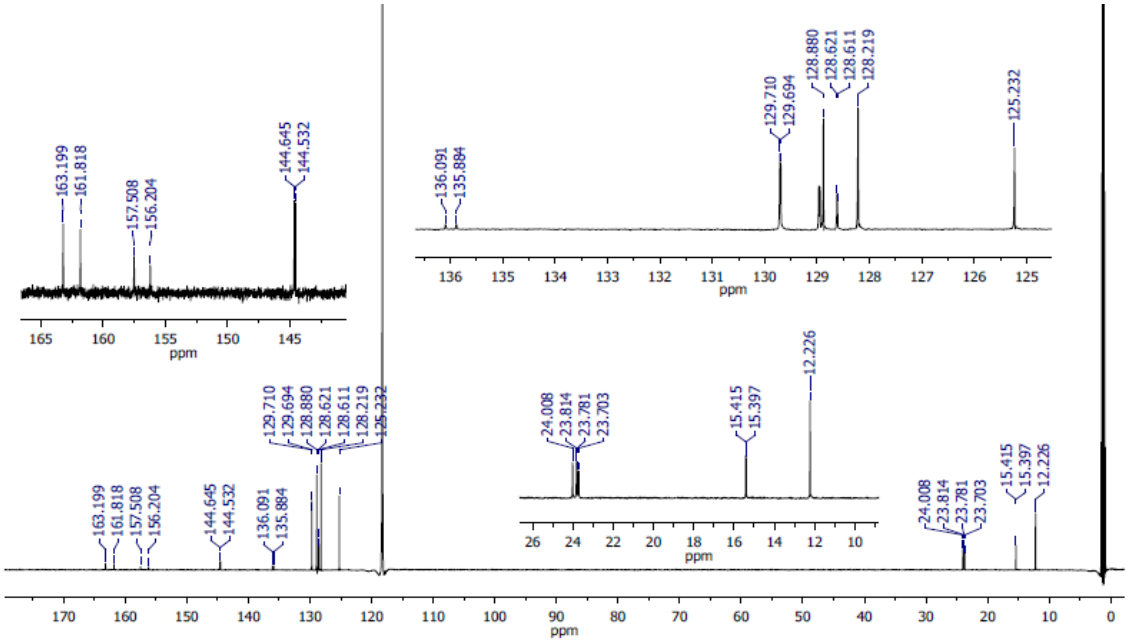

Figure 3.62 ^{13}C NMR of potassium (*E*)-(1-fluoro-1-phenylbut-1-en-2-yl)trifluoroborate and potassium (*E*)-(2-fluoro-1-phenylbut-1-en-1-yl)trifluoroborate (**6i**) in CD_3CN.

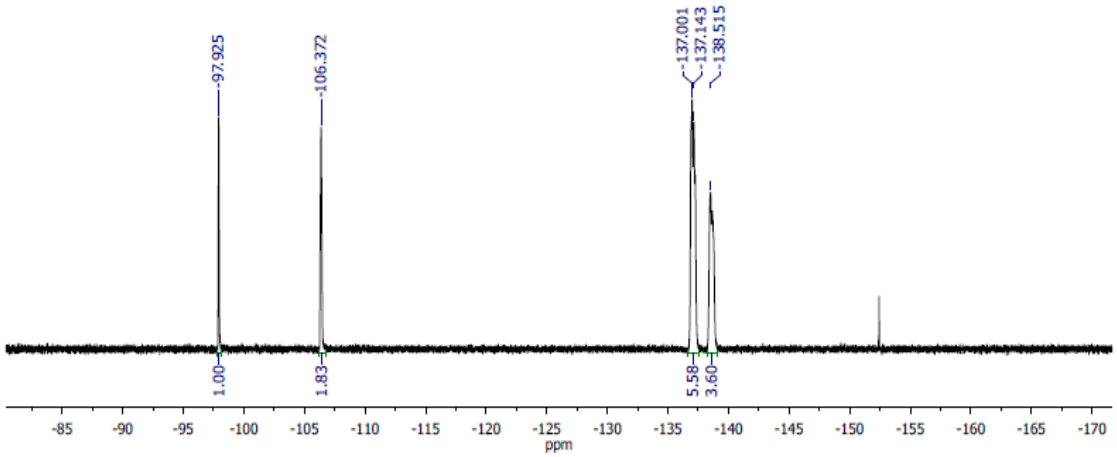

Figure 3.63 ^{19}F NMR of potassium (*E*)-(1-fluoro-1-phenylbut-1-en-2-yl)trifluoroborate and potassium (*E*)-(2-fluoro-1-phenylbut-1-en-1-yl)trifluoroborate (**13i**) in CD_3CN.

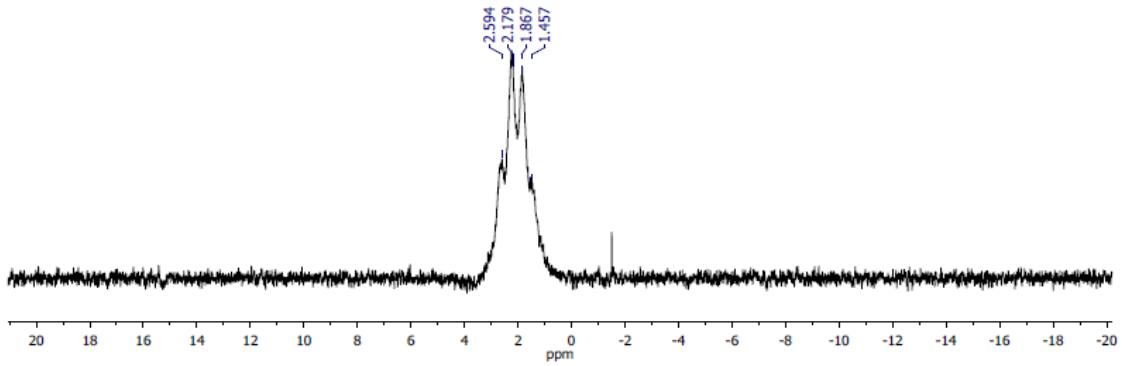

Figure 3.64 ^{11}BNMR of potassium (*E*)-(1-fluoro-1-phenylbut-1-en-2-yl)trifluoroborate and potassium (*E*)- (2-fluoro-1-phenylbut-1-en-1-yl)trifluoroborate (**13i**) in CD_3CN.

3.4.4.17 Synthesis of potassium (*E*)-(6-pthalimido-1-fluorohex-1-en-2-yl)trifluoroborate

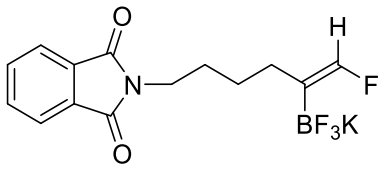

Figure 3.65 Potassium (*E*)-(6-pthalimido-1-fluorohex-1-en-2-yl)trifluoroborate (**13j**)

(IDipp)CuO-*t*-Bu (0.053 g, 0.10 mmol), $B_2(neo)_2$ (0.023 g, 0.10 mmol) were combined in a 20-mL vial and dissolved in toluene (5 mL) before a solution of 6-pthalimido-1-hexyne (0.023 g, 0.10 mmol) in toluene (1.5 mL) was added. After 10 min, a solution of NFSI (0.032 g, 0.10 mmol) in toluene (3 mL) was added. After another 10 min, the mixture was concentrated *in vacuo* and the products were extracted with pentane, filtered through a Celite plug and concentrated in vacuo to give an oil. The oil was then dissolved in MeOH (10 mL) with stirring before a solution of KHF_2 (0.100 g, 1.28 mmol) in H_2O (5 mL) was added and stirred for 3h. This mixture was then concentrated and the products were extracted with acetone (3 x 5 mL), filtered through a Celite plug and

concentrated to give a colorless solid. This was washed with Et_2O (5 mL) and DCM (5 mL) and the residue was dried for 12h under vacuum, affording the product as a colorless powder (0.0183 g, 51% yield). ^{1}H NMR (400 MHz, CD_3CN): δ (ppm) 7.82-7.75 (m, 4H, aryl C-*H*), 6.40 (d, $^2J_{FH}$ = 97.2 Hz, 1H, C=C(F)*H*), 3.58 (t, $^3J_{HH}$ = 7.2 Hz, 2H, NCH_2), 1.82 (t, $^3J_{HH}$ = 7.2 Hz, 2H, $C=C(BF_3)CH_2$), 1.58 (t, $^3J_{HH}$ = 7.2 Hz, 2H, NCH_2CH_2), 1.38 (t, $^3J_{HH}$ = 7.2 Hz, 2H, $C=C(BF_3)CH_2CH_2$), $^{13}C\{^1H\}$ NMR (176 MHz,CD_3CN): δ (ppm) 169.4 (C=O), 148.6 (d, $^1J_{FC}$ = 242.9 Hz, C=*C*F), 134.9 (*ortho*-C), 133.2 (*ipso*-C), 123.6 (*meta*-*C*), 38.6 (NCH_2), 30.0 (d, $^3J_{FC}$ = 17.6 Hz, $C=C(BF_3)CH_2$), 29.0 (NCH_2CH_2), 27.8 (d, $^4J_{FC}$ = 2.4 Hz, $C=C(BF_3)CH_2$), ^{19}F NMR (376 MHz, CD_3CN): δ (ppm) –128.82 (d, $^2J_{HF}$ = 100.4 Hz, 1F, C=C*F*), –139.18 to –139.58 (br m, 3F, $C=C(BF_3K)$, ^{11}B NMR (128 MHz, CD_3CN) δ (ppm) 2.01 (q, $^1J_{FB}$ = 57 Hz $C=C(BF_3K)$. IR: ν (cm^{-1}) 2981, 2949, 2927, 2857, 1770, 1638, 1464, 1437, 1396, 1363, 1326, 1177, 1114, 1061, 1040, 949, 917, 718, 633, 529. Anal. Calcd for $C_{14}H_{13}BF_4KNO_2$: C, 47.61; H, 3.71; N, 3.97 Found C, 47.60 H, 3.82; N, 3.89.

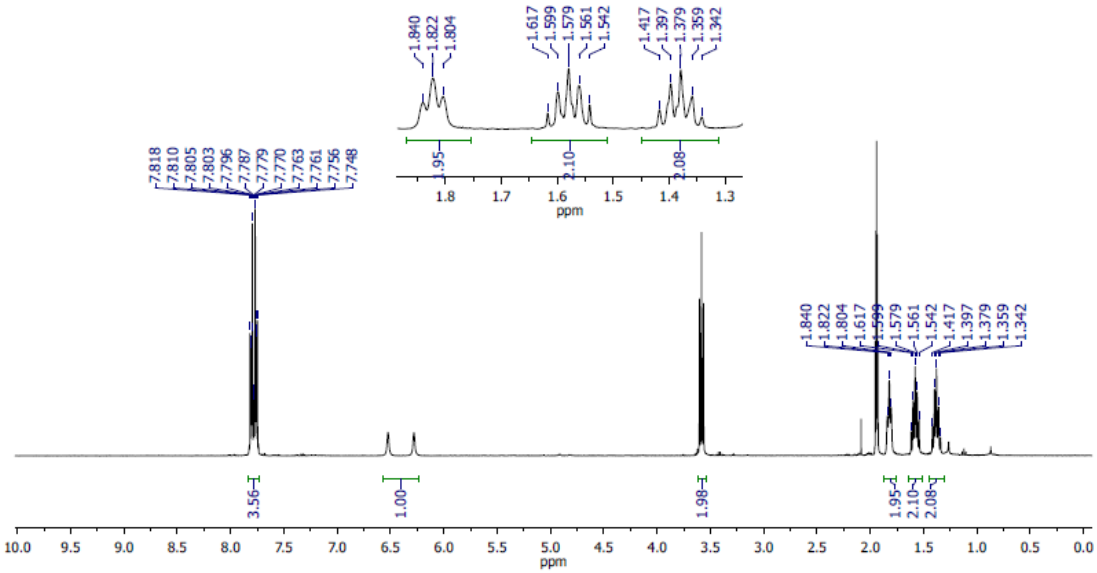

Figure 3.66 ^{1}H NMR of potassium (*E*)-(6-pthalimido-1-fluorohex-1-en-2-yl)trifluoroborate (**13j**) in CD_3CN.

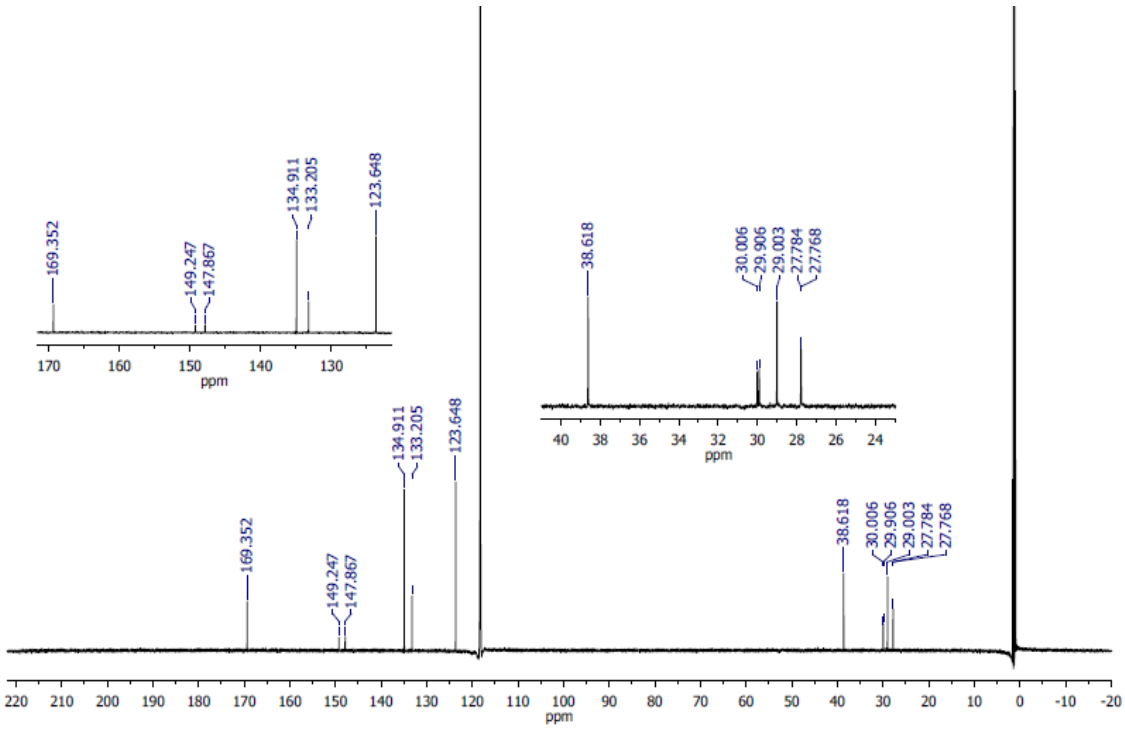

Figure 3.67 ^{13}C NMR of potassium (*E*)-(6-pthalimido-1-fluorohex-1-en-2-yl)trifluoroborate (**13j**) in CD_3CN.

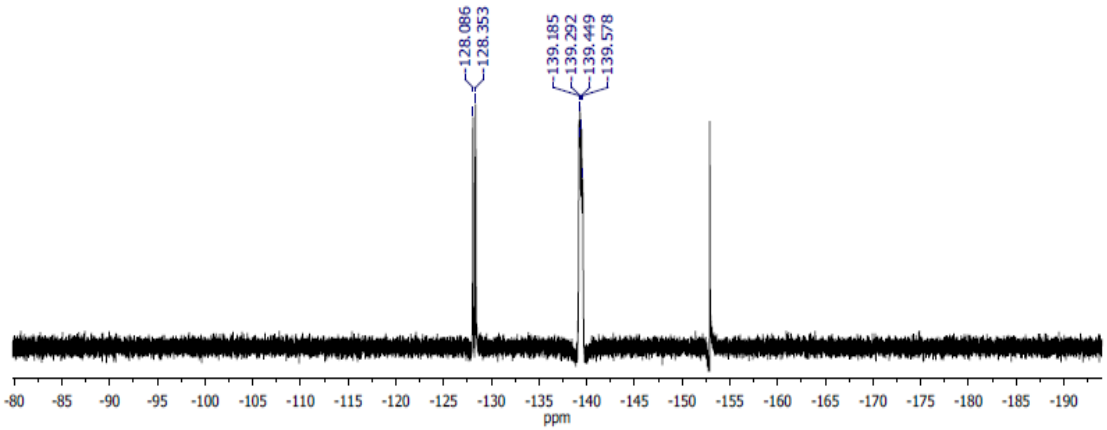

Figure 3.68 ^{19}F NMR of potassium (*E*)-(6-pthalimido-1-fluorohex-1-en-2-yl)trifluoroborate (**13j**) in CD_3CN.

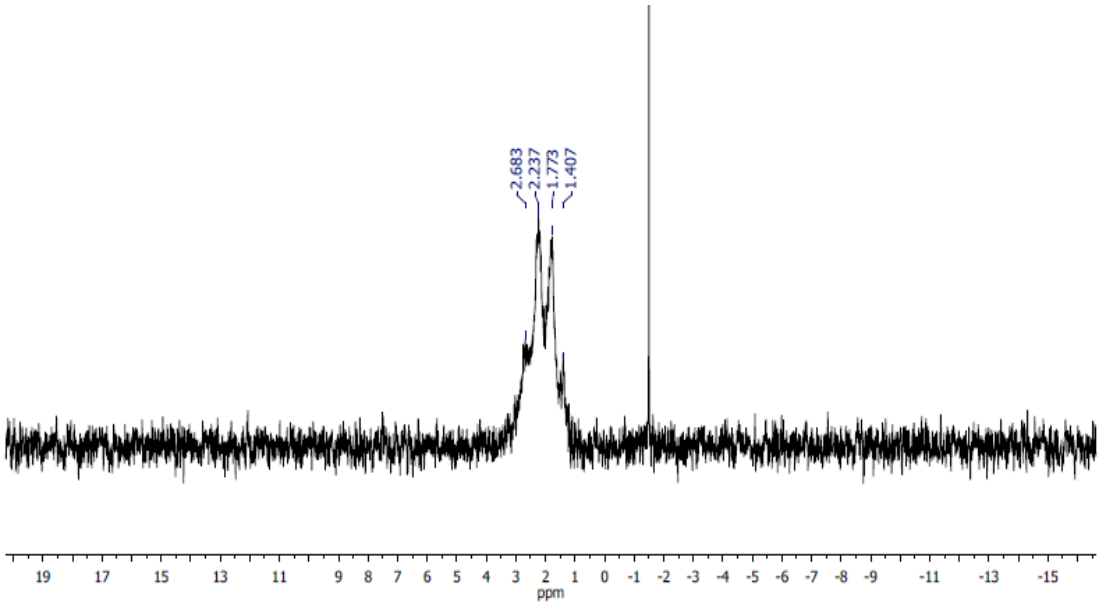

Figure 3.69 ^{11}B NMR of potassium (*E*)-(6-pthalimido-1-fluorohex-1-en-2-yl)trifluoroborate (**13j**) in CD_3CN.

3.4.4.18 Synthesis of **13c**

Potassium (*E*)-(2-fluoro-1-phenylprop-1-en-1-yl)trifluoroborate (13c)

(IDipp)CuN($SO_2Ph)_2$ (0.115 g, 0.154 mmol) and NaO-*t*-Bu (0.015 g, 0.16 mmol) were combined in a 20-mL vial and dissolved in THF (4 mL) with stirring for 15 min. $B_2(neo)_2$ (0.35 g, 0.16 mmol), phenylpropyne (0.036 g, 0.31 mmol) and toluene (4 mL) were added and allowed to stir for 10 min. After 10 min, a solution of NFSI (0.049 g, 0.16 mmol) in toluene (3 mL) was added. After another 10 min, the mixture was concentrated *in vacuo* and the products were extracted with pentane, filtered through a Celite plug and concentrated in vacuo to give an oil. The oil was then dissolved in MeOH (10 mL) with stirring before a solution of KHF_2 (0.180 g, 2.31 mmol) in H_2O (5 mL) was added and stirred for 3h. This mixture was then concentrated and the products were extracted with acetone (3 x 5 mL), filtered through a Celite plug and concentrated to give a colorless solid. This was washed with Et_2O (5 mL) and DCM (5 mL) and the residue was dried for 12h under vacuum, affording the product as a colorless powder (0.0220 g, 59% yield). The product was confirmed by ^{1}H NMR (pg. 89).

3.4.4.19 Synthesis of **13a** on 1 mmol scale

Potassium (*E*)-(4-fluorohex-3-en-3-yl)trifluoroborate (**13a**) (IDipp)CuCl (0.486 g, 1.00 mmol) and NaO-*t*-Bu (0.096 g, 1.0 mmol) were combined in a 20-mL vial and dissolved in THF (8 mL) with stirring for 15 min. $B_2(neo)_2$ (0.223 g, 1.0 0mmol), 3-hexyne (0.100 g, 1.22 mmol) and toluene (10 mL) were added and allowed to stir for 10 min. NFSI (0.315 g, 1.00 mmol) was then added and the mixture was concentrated *in vacuo* after 15 min of stirring. The products were extracted with pentane, filtered through a Celite plug and concentrated in vacuo to give an oil. The oil was dissolved in MeOH (30 mL) with stirring before a solution of KHF_2 (0.781 g, 10.0 mmol) in H_2O (15 mL) was added and stirred for 3h. This mixture was then concentrated and the products were extracted with acetone (3 x 10 mL), filtered through a Celite plug and concentrated to give a colorless solid. This was washed with Et_2O (10 mL) and DCM (10 mL) and the residue was dried for 12h under vacuum, affording the product as a colorless powder (0.104 g, 50% yield). The product was confirmed by ^1H NMR. (see page 85) After removal of the organic products, (IDipp)CuN$(SO_2Ph)_2$ was collected following extraction with DCM and filtration through Celite (0.529 g, 71% yield) (see page 80).

3.4.4.20 Synthesis of (IDipp)CuO-*t*-Bu from **11**

(IDipp)CuO-*t*-Bu Potassium *tert*-butoxide (0.011 g, 0.098 mmol) was added to a solution of (IDipp)CuN($SO_2Ph)_2$ (0.070 g, 0.094 mmol) in THF (4 mL) with stirring. After 1 hour, the reaction mixture was filtered through Celite, and the filter pad was washed with 1 portion of THF (1 mL). The filtrate was concentrated, and the residue was dried vacuum, affording the product at a colorless powder (0.046 g, 94%). ^{1}H NMR (400 MHz, C_6D_6): δ 7.22 (t, $^3J_{HH}$ = 7.6 Hz, 2H, *para*-C*H*), 7.08 (d, $^3J_{HH}$ = 7.6 Hz, 4H, *meta*-C*H*), 6.33 (s, 2H, NC*H*), 2.60 (sept, $^3J_{HH}$ = 6.8 Hz, 4H, C*H*$(CH_3)_2$), 1.41 (d, $^3J_{HH}$ = 6.8 Hz, 12 H, CH(C*H*$_3)_2$), 1.32 (s, 9H, OC(C*H*$_3)_3$), 1.08 (d, $^3J_{HH}$ = 6.8 Hz, 12H, CH(C*H*$_3)_2$).[14]

3.4.4.21 Synthesis of 2-Fluoro-1-(4-methoxyphenyl)ethenone

2-Fluoro-1-(4-methoxyphenyl)ethenone (**14**) Hydrogen peroxide (2 mL, 30% in H_2O) was added to a vial charged with Potassium (*E*)-2-fluoro-1-(4-methoxyphenyl)vinyl trifluoroborate (10.5 g, 0.0407 mmol) and SiO_2 (0.072 g). This mixture stirred for 5 min before $NaOH_{(aq)}$ (1 mL, 0.8 M) was added and stirred for 4h open to air, at which time the product was extracted with hexanes (3 x 3 mL), dried over Na_2SO_4, and concentrated *in vacuo* to afford a white solid (6.5 mg, 95% yield). ^{1}H NMR (400 MHz, $CDCl_3$) δ 7.89 (d, $^3J_{HH}$ = 8.6 Hz, 2H, *meta* CH), 6.96 (d, $^3J_{HH}$ = 8.7 Hz, 2H, *ortho* CH), 5.48 (d, $^2J_{HF}$ = 47.0 Hz, 2H, C(O)CH_2F), 3.88 (s, 3H, OCH_3), ^{13}C{^{1}H} NMR (176 MHz, $CDCl_3$) δ 192.1 (d, $^2J_{CF}$ = 15.6 Hz, *C*=O), 164.4 (*para*-*C*), 130.43 (d, $^3J_{CF}$ = 2.7 Hz, *ipso*-*C*), 126.9 (*meta*-*C*), 114.3 (*ortho*-*C*), 83.6 (d, $^1J_{CF}$ = 182.0 Hz, C(O)*C*H_2F), 55.7 (O*C*H_3), ^{19}F NMR (376 MHz, $CDCl_3$) δ –229.83 (t, $^2J_{FH}$ = 47.0 Hz, 1F, C(O)CH_2*F*).

3.4.4.22 Synthesis of (2-Fluoroprop-1-ene-1,1-diyl)dibenzene

(2-Fluoroprop-1-ene-1,1-diyl)dibenzene (**15)** Potassium (*E*)-(2-fluoro-1-phenylprop-1-en-1-yl) trifluoroborate (0.021 g, 0.087 mmol), bromobenzene (9.0 µL, 0.087 mmol), (dppf)$PdCl_2$•CH_2Cl_2 (3.5 mg, 0.0043 mmol), and *tert*-butyl amine (0.0270 mL, 0.261 mmol) were combined before being dissolved in a isopropanol/water mixture (1:1, 5 mL). This was heated to 80^o C and allowed to stir for 16h. The solvents were then removed *in vacuo* before the product was extracted with pentane (3 x 3 mL) and concentrated to give a yellow oil. The product was purified on a silica gel column using 30:1 pentane: dichloromethane to give a colorless oil (0.0148 g, 80 % yield). ^{1}H NMR (700 MHz, $CDCl_3$): 7.35-7.33 (m, 2H, aryl CH), 7.30-7.25 (m, 5H, aryl CH), 7.20-7.19 (m, 5H,

aryl CH), 2.05 (d, $^{3}J_{HF}$ = 17.5 Hz, 3H, C=C(C*H*$_3$)F). ^{13}C{^{1}H} NMR (176 MHz, $CDCl_3$) δ 155.0 (d, $^{1}J_{CF}$ = 257.8 Hz, C=*C*F), 139.4 (d, $^{3}J_{CF}$ = 8.1 Hz, aryl C), 137.8 (aryl C), 130.5 (d, $^{4}J_{CF}$ = 3.0 Hz, aryl C), 129.7 (d, $^{3}J_{CF}$ = 4.6 Hz, aryl C), 128.5 (aryl C), 128.1 (aryl C), 127.3 (aryl C), 126.9 (aryl C), 120.5 (d, $^{2}J_{CF}$ = 15.0 Hz, Ph$_2$*C*=CF), 17.2 (d, $^{2}J_{CF}$ = 29.9 Hz, C=C(*C*H$_3$)F). ^{19}F NMR (376 MHz, $CDCl_3$) δ –97.3 (q, $^{3}J_{FH}$ = 18.0 Hz, 1F, C=C(CH$_3$)*F*).

Note: The product contained (*Z*)-(1-fluoroprop-1-ene-1,2-diyl)dibenzene as judged by ^{1}H (δ 2.14 ppm d, $^{4}J_{HF}$ = 3.5 Hz) and ^{19}F NMR (δ –102.7 ppm, s) resulting from the coupling of potassium (*E*)-(1-fluoro-1-phenylprop-1-en-2-yl)trifluoroborate (~5%, *vide supra*, see page 93) contained in the starting potassium (*E*)-(2-fluoro-1-phenylprop-1-en-1-yl)trifluoroborate.

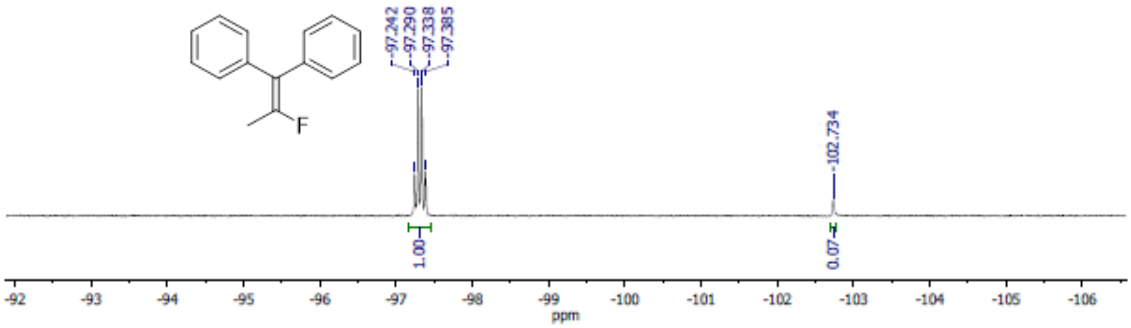

Figure 3.70 ^{19}F NMR of (2-fluoroprop-1-ene-1,1-diyl)dibenzene in $CDCl_3$.

3.4.4.23 Transmetalation of **12** to copper

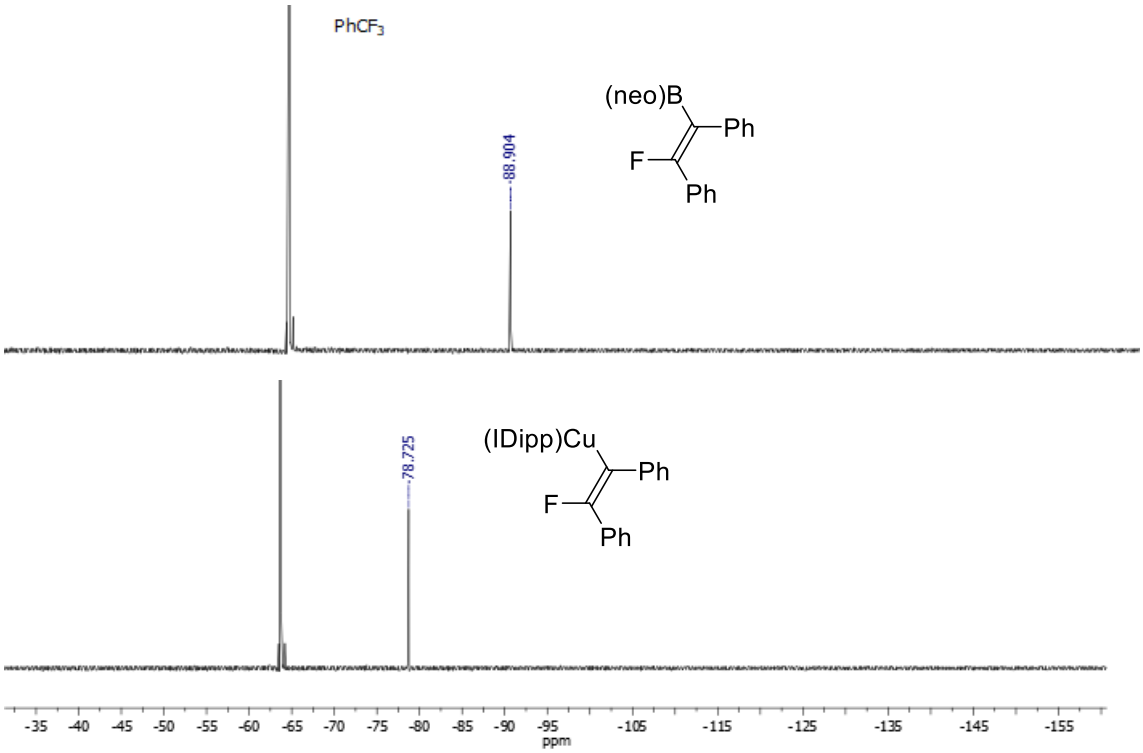

Figure 3.71 ^{19}F NMR of transmetalation of **12** to copper in C_6D_6.

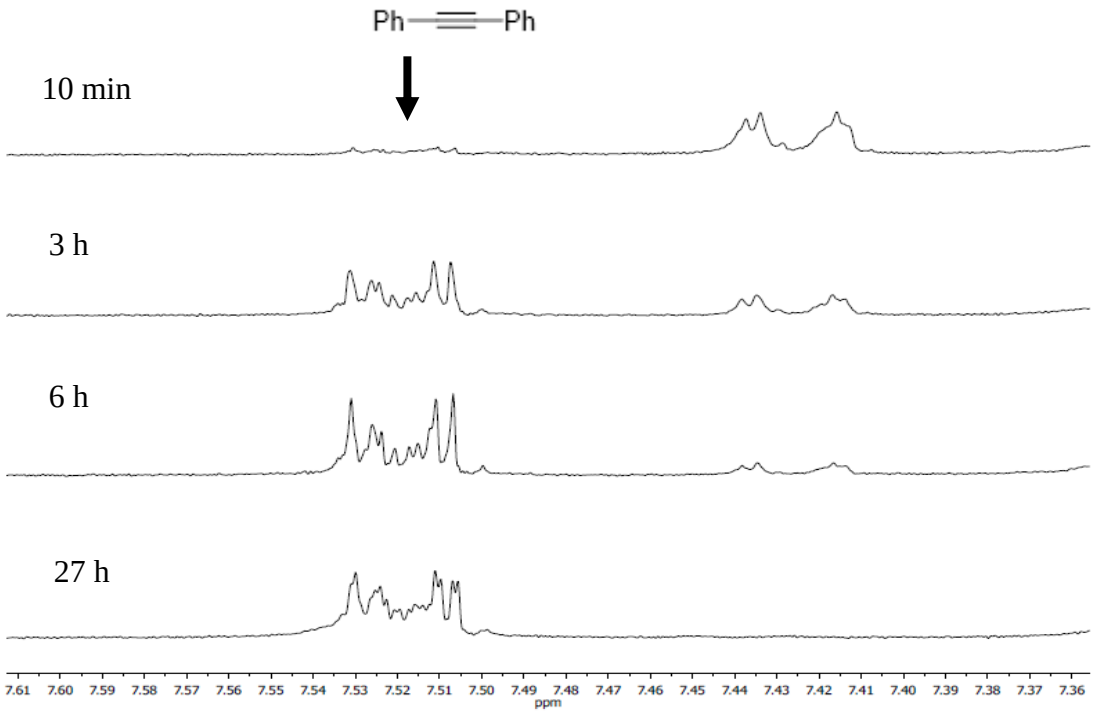

Figure 3.72 ^{1}H NMR of transmetalation of **12** to copper in C_6D_6 showing the loss of PhCCPh over time.

3.4.4.24 Fluorination of THF by NFSI

NFSI (0.051 g, 0.16 mmol) and Cs_2CO_3 (0.065 g, 0.20 mmol) were combined in a 20-mL vial before THF (0.75 mL), THF-*d8* (0.75 mL) and CH_3CN (1.0 mL) was added. The mixture was stirred for 16h before $PhCF_3$ (2.0 μL, 0.016 mmol) was added and an internal standard.

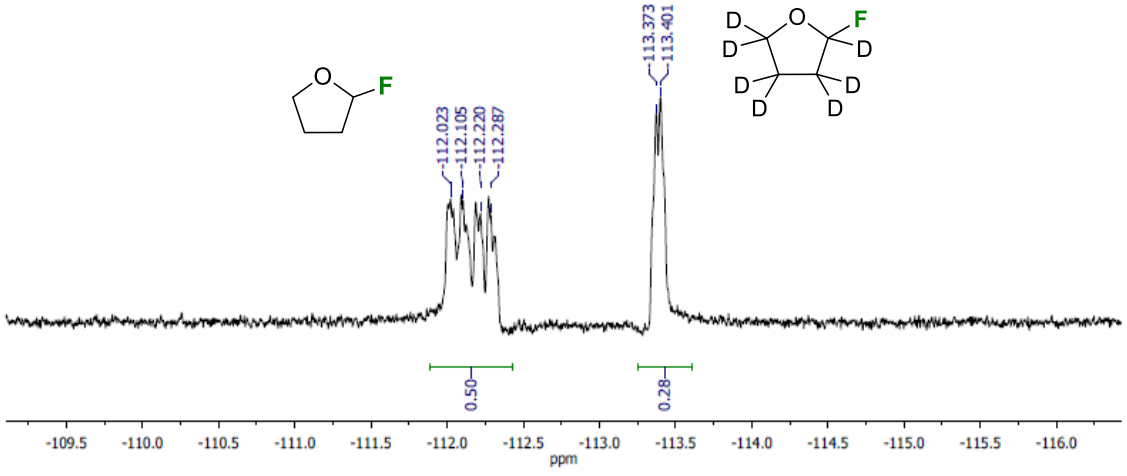

Figure 3.73 ^{19}F NMR of 2-fluoroTHF and 2-fluoroTHF-*d7* in THF and CH_3CN.

3.5 References

[1] (a) Mueller, K.; Faeh, C.; Diederich, F. *Science* **2007**, *317*, 1881-1886; (b) Wang, J.; Sanchez-Rosello, M.; Acena, J. L.; del Pozo, C.; Sorochinsky, A. E.; Fustero, S.; Soloshonok, V. A.; Liu, H. *Chem. Rev.* **2014**, *114*, 2432-2506.

[2] (a) Babudri, F.; Farinola, G. M.; Naso, F.; Ragni, R. *Chem. Commun.* **2007**, 1003-1022; (b) Berger, R.; Resnati, G.; Metrangolo, P.; Weber, E.; Hulliger, J. *Chem. Soc. Rev.* **2011**, *40*, 3496-3508; (c) Milian-Medina, B.; Gierschner, J. *J. Phys. Chem. Lett.* **2017**, *8*, 91-101.

[3] (a) Jeschke, P. *Pest Manage. Sci.* **2010**, *66*, 10-27; (b) Fujiwara, T.; O'Hagan, D. *J. Fluorine Chem.* **2014**, *167*, 16-29.

[4] (a) Liang, T.; Neumann, C. N.; Ritter, T. *Angew. Chem., Int. Ed.* **2013**, *52*, 8214-8264; (b) Champagne, P. A.; Desroches, J.; Hamel, J.-D.; Vandamme, M.; Paquin, J.-F. *Chem. Rev.* **2015**, *115*, 9073-9174; (c) Cresswell, A. J.; Davies, S. G.; Roberts, P. M.; Thomson, J. E. *Chem. Rev.* **2015**, *115*, 566-611; (d) Neumann, C. N.; Ritter, T. *Angew. Chem., Int. Ed.* **2015**, *54*, 3216-3221; (e) Ni, C.; Hu, M.; Hu, J. *Chem. Rev.* **2015**, *115*, 765-825; (f) Yang, X.; Wu, T.; Phipps, R. J.; Toste, F. D. *Chem. Rev.* **2015**, *115*, 826-870

[5] (a) Furuya, T.; Kamlet, A. S.; Ritter, T. *Nature* **2011**, *473*, 470-477; (b) Campbell, M. G.; Hoover, A. J.; Ritter, T. *Top. Organomet. Chem.* **2015**, *52*, 1-53; (c) Miro, J.; del Pozo, C. *Chem. Rev.* **2016**, *116*, 11924-11966; (d) Sather, A. C.; Buchwald, S. L. *Acc. Chem. Res.* **2016**, *49*, 2146-2157.

[6] (a) Fier, P. S.; Hartwig, J. F. *J. Am. Chem. Soc.* **2012**, *134*, 10795-10798; (b) Fier, P. S.; Luo, J.; Hartwig, J. F. *J. Am. Chem. Soc.* **2013**, *135*, 2552-2559; (c) Ichiishi, N.; Canty, A. J.; Yates, B. F.; Sanford, M. S. *Org. Lett.* **2013**, *15*, 5134-5137; (d) Ye, Y.; Sanford, M. S. *J. Am. Chem. Soc.* **2013**, *135*, 4648-4651; (e) Ye, Y.; Schimler, S. D.; Hanley, P. S.; Sanford, M. S. *J. Am. Chem. Soc.* **2013**, *135*, 16292-16295; (f) Ichiishi, N.; Canty, A. J.; Yates, B. F.; Sanford, M. S. *Organometallics* **2014**, *33*, 5525-5534; (g) Tredwell, M.; Preshlock, S. M.; Taylor, N. J.; Gruber, S.; Huiban, M.; Passchier, J.; Mercier, J.; Genicot, C.; Gouverneur, V. *Angew. Chem., Int. Ed.* **2014**, *53*, 7751-7755; (h) Mossine, A. V.; Brooks, A. F.; Makaravage, K. J.; Miller, J. M.; Ichiishi, N.; Sanford, M. S.; Scott, P. J. H. *Org. Lett.* **2015**, *17*, 5780-5783; (i) Gamache, R. F.; Waldmann, C.; Murphy, J. M. *Org. Lett.* **2016**, *18*, 4522-4525; (j) Makaravage, K. J.; Brooks, A. F.; Mossine, A. V.; Sanford, M. S.; Scott, P. J. H. *Org. Lett.* **2016**, *18*, 5440-5443; (k) Taylor, N. J.; Emer, E.; Preshlock, S.; Schedler, M.; Tredwell, M.; Verhoog, S.; Mercier, J.; Genicot, C.; Gouverneur, V. *J. Am. Chem. Soc.* **2017**, *139*, 8267-8276.

[7] (a) Tius, M. A.; Kawakami, J. K. *Synlett* **1993**, 207-208; (b) Tius, M. A.; Kawakami, J. K. *Tetrahedron* **1995**, *51*, 3997-4010; (c) Furuya, T.; Ritter, T. *Org. Lett.* **2009**, *11*, 2860-2863; (d) Tang, P.; Furuya, T.; Ritter, T. *J Am Chem Soc*

2010, *132*, 12150-12154; (e) Tang, P.; Ritter, T. *Tetrahedron* **2011**, *67*, 4449-4454; (f) Dubbaka, S. R.; Narreddula, V. R.; Gadde, S.; Mathew, T. *Tetrahedron* **2014**, *70*, 9676-9681; (g) Li, Z.; Wang, Z.; Zhu, L.; Tan, X.; Li, C. *J. Am. Chem. Soc.* **2014**, *136*, 16439-16443; (h) Sommer, H.; Fuerstner, A. *Chem. - Eur. J.* **2017**, *23*, 558-562.

[8] (a) Akana, J. A.; Bhattacharyya, K. X.; Mueller, P.; Sadighi, J. P. *J. Am. Chem. Soc.* **2007**, *129*, 7736-7737; (b) Gorske, B. C.; Mbofana, C. T.; Miller, S. J. *Org. Lett.* **2009**, *11*, 4318-4321; (c) Okoromoba, O. E.; Han, J.; Hammond, G. B.; Xu, B. *J. Am. Chem. Soc.* **2014**, *136*, 14381-14384; (d) Nahra, F.; Patrick, S. R.; Bello, D.; Brill, M.; Obled, A.; Cordes, D. B.; Slawin, A. M. Z.; O'Hagan, D.; Nolan, S. P. *ChemCatChem* **2015**, *7*, 240-244; (e) O'Conner, T. J.; Toste, F. D. *ACS Catal.* **2018**, *8*, 5947-5951.

[9] Mankad, N. P.; Toste, F. D. *Chem. Sci.* **2012**, *3*, 72-76.

[10] (a) Landelle, G.; Bergeron, M.; Turcotte-Savard, M.-O.; Paquin, J.-F. *Chem. Soc. Rev.* **2011**, *40*, 2867-2908; (b) Paquin, J.-F. *Synlett* **2011**, 289-293; (c) Yanai, H.; Taguchi, T. *Eur. J. Org. Chem.* **2011**, *2011*, 5939-5954; (d) Besset, T.; Poisson, T.; Pannecoucke, X. *Eur. J. Org. Chem.* **2015**, *2015*, 2765-2789; (e) Drouin, M.; Hamel, J.-D.; Paquin, J.-F. *Synthesis* **2018**, *50*, 881-955.

[11] (a) He, G.; Qiu, S.; Huang, H.; Zhu, G.; Zhang, D.; Zhang, R.; Zhu, H. *Org. Lett.* **2016**, *18*, 1856-1859; (b) Zhu, G.; Qiu, S.; Xi, Y.; Ding, Y.; Zhang, D.; Zhang, R.; He, G.; Zhu, H. *Org. Biomol. Chem.* **2016**, *14*, 7746-7753.

[12] Uehling, M. R.; Rucker, R. P.; Lalic, G. *J. Am. Chem. Soc.* **2014**, *136*, 8799-8803.

[13] Shi, S.-L.; Buchwald, S. L. *Nat. Chem.* **2015**, *7*, 38-44.

[14] Mankad, N. P.; Laitar, D. S.; Sadighi, J. P. *Organometallics* **2004**, *23*, 3369-3371.

[15] Jordan, A. J.; Wyss, C. M.; Bacsa, J.; Sadighi, J. P. *Organometallics* **2016**, *35*, 613-616

[16] Hashmi, A. S. K.; Ramamurthi, T. D.; Rominger, F. *J. Organomet. Chem.* **2009**, *694*, 592-597.

[17] Laitar, D. S.; Mueller, P.; Sadighi, J. P. *J. Am. Chem. Soc.* **2005**, *127*, 17196-17197.

[18] (a) Yoshida, M.; Hara, S. *Org. Lett.* **2003**, *5*, 573-574; (b) Hara, S.; Guan, T.; Yoshida, M. *Org. Lett.* **2006**, *8*, 2639-2641; (c) Guan, T.; Yoshida, M.; Hara, S. *J. Org. Chem.* **2007**, *72*, 9617-9621.

[19] (a) Hu, J. F.; Han, X. W.; Yuan, Y.; Shi, Z. Z. *Angew. Chem. Int. Ed.* **2017**, *56*, 13342-13346; (b) Sakaguchi, H.; Uetake, Y.; Ohashi, M.; Niwa, T.; Ogoshi, S.;

Hosoya, T. *J. Am. Chem. Soc.* **2017**, *139*, 12855-12862; (c) Zhang, J.; Dai, W.; Liu, Q.; Cao, S. *Org. Lett.* **2017**, *19*, 3283-3286.

[20] NFSI can be comparable to SelectFluor® or cheaper in price; for example, Oakwood Chemical, Inc. offers 500 g for $200 ($126/mol), compared to 500 g of SelectFluor® for $470 ($333/mol).

[21] Zhang, L.; Cheng, J.; Carry, B.; Hou, Z. *J. Am. Chem. Soc.* **2012**, *134*, 14314-14317.

[22] Beniazza, R.; Abadie, B.; Remisse, L.; Jardel, D.; Lastecoueres, D.; Vincent, J.-M. *Chem. Commun.* **2017**, *53*, 12708-12711.

[23] Laitar, D. S. Ph.D. Thesis, Massachusetts Institute of Technology, **2006**. https://dspace.mit.edu/handle/1721.1/36268 (Accessed June 2019)

[24] (a) Molander, G. A.; Ellis, N. *Acc. Chem. Res.* **2007**, *40*, 275-286; (b) Darses, S.; Genet, J.-P. *Chem. Rev.* **2008**, *108*, 288-325.

[25] Whittaker, A. M.; Lalic, G. *Org. Lett.* **2013**, *15*, 1112-1115.

[26] Batey, R. A.; Thadani, A. N.; Smil, D. V. *Org. Lett.* **1999**, *1*, 1683-1686.

[27] (a) Quach, T. D.; Batey, R. A. *Org. Lett.* **2003**, *5*, 4397-4400; (b) Shade, R. E.; Hyde, A. M.; Olsen, J.-C.; Merlic, C. A. *J. Am. Chem. Soc.* **2010**, *132*, 1202-1203.

[28] Molander, G. A.; Cavalcanti, L. N. *J. Org. Chem.* **2011**, *76*, 623-630.

[29] Molander, G. A.; Bernardi, C. R. *J. Org. Chem.* **2002**, *67*, 8424-8429.

[30] Fujihara, T.; Xu, T.; Semba, K.; Terao J.; Tsuji, Y. *Angew. Chem., Int. Ed.* **2011**, *50*, 523-527.

[31] Sakaguchi, H.; Uetake, Y.; Ohashi, M.; Niwa, T.; Ogoshi S.; Hosoya, T. *J. Am. Chem. Soc.* **2017**, *139*, 12855-12862.

CHAPTER 4. NITROSONIUM REACTIVITY OF (NHC)COPPER(I) SULFIDE COMPLEXES

Part of this thesis chapter has been adapted with permission from an article co-written by the author:

Jordan, A. J.; Walde, R. K; Schultz, K. M.; Bacsa, J.; Sadighi. J. P. Nitrosonium Reactivity of (NHC)Copper(I) Sulfide Complexes. *Inorg. Chem.* **2019**, *Article Accepted*

4.1 Background

Nitric oxide ($NO^{\bullet}$) and dihydrogen sulfide (H_2S) are important biological signaling molecules, whose chemistries are often linked due to proposed "cross-talk" products,[1,2] such as thionitrous acid (HSNO, and SNO^- species), nitroxyl (HNO) and perthionitrite ($SSNO^-$).[3-5] Many recent studies have shed light on the properties and reactivity of these transient, but much still remains unknown.[4-6] Of particular interest is their interaction with transition metals, but there are few studies relating well-defined transition-metal complexes and "cross-talk" products. Addition of HS^- to iron nitrosyl complexes (sodium nitroprusside or iron porphyrin) initially forms an iron bound HSNO complex, observable by mass spectrometry in the case of the iron porphyrin system, before HSNO decomposition products can be detected (Scheme 4.1a).[7-9] A "masked" terminal nickel sulfide reacts with $NO^{\bullet}$ to yield a nickel nitrosyl and SNO^- anion, reacts with further $NO^{\bullet}$ to yields $SSNO^-$ anion (Scheme 4.1b).[10] Lastly, an EDTA (ethylenediaminetetraacetate) supported diruthenium disulfide reacts with $NO^{\bullet}$ to yield the Ru–SNO complex, also observed by mass spectrometry (Scheme 4.1c).[11] Lastly, $SSNO^-$ and SNO^- anions have been isolated as the bis(triphenylphosphine)iminium salts.[12] Few studies have examined the reactivity of "cross-talk" products with copper.

Copper sulfide clusters have garnered much attention due to their prevalence in biological systems, particularly in the active site of nitrous oxide reductase[13] and carbon monoxide dehydrogenase.[14] A commonality in copper sulfide chemistry is in their tendency to form higher order complexes, featuring three or more copper centers;[15-25] copper/sulfur clusters with two metal centers are rare,[26] but include a number of dicopper(II) disulfide complexes[27-36] and a single dicopper(I) sulfide complex.[26,37] We envisioned that similar low-nuclearity sulfur-bound copper(I) complexes could shed light on the reactivity of various "cross-talk" products. Considering the sulfur atom(s) to be S^{2-} (or SS^{2-}) the addition of nitrosonium (NO^+) would formally lead to HSNO, SNO^-, $SSNO^-$, and HNO products.

Warren and coworkers have shown that a copper(II) thiolate reacts reversibly with $NO^{\bullet}$ at low-temperature to yield a bound thionitrite.[38] They have also shown that N-heterocyclic carbene (NHC) supported copper(I) thiolates react with NO^+ to cleanly generate a thiolate-bridged dicopper(I) cation and free organic thionitrites (Scheme 4.1d,e).[39] In this study we have examined the reactivity of NHC supported copper(I) sulfide, disulfide and hydrosulfide complexes with NO^+.

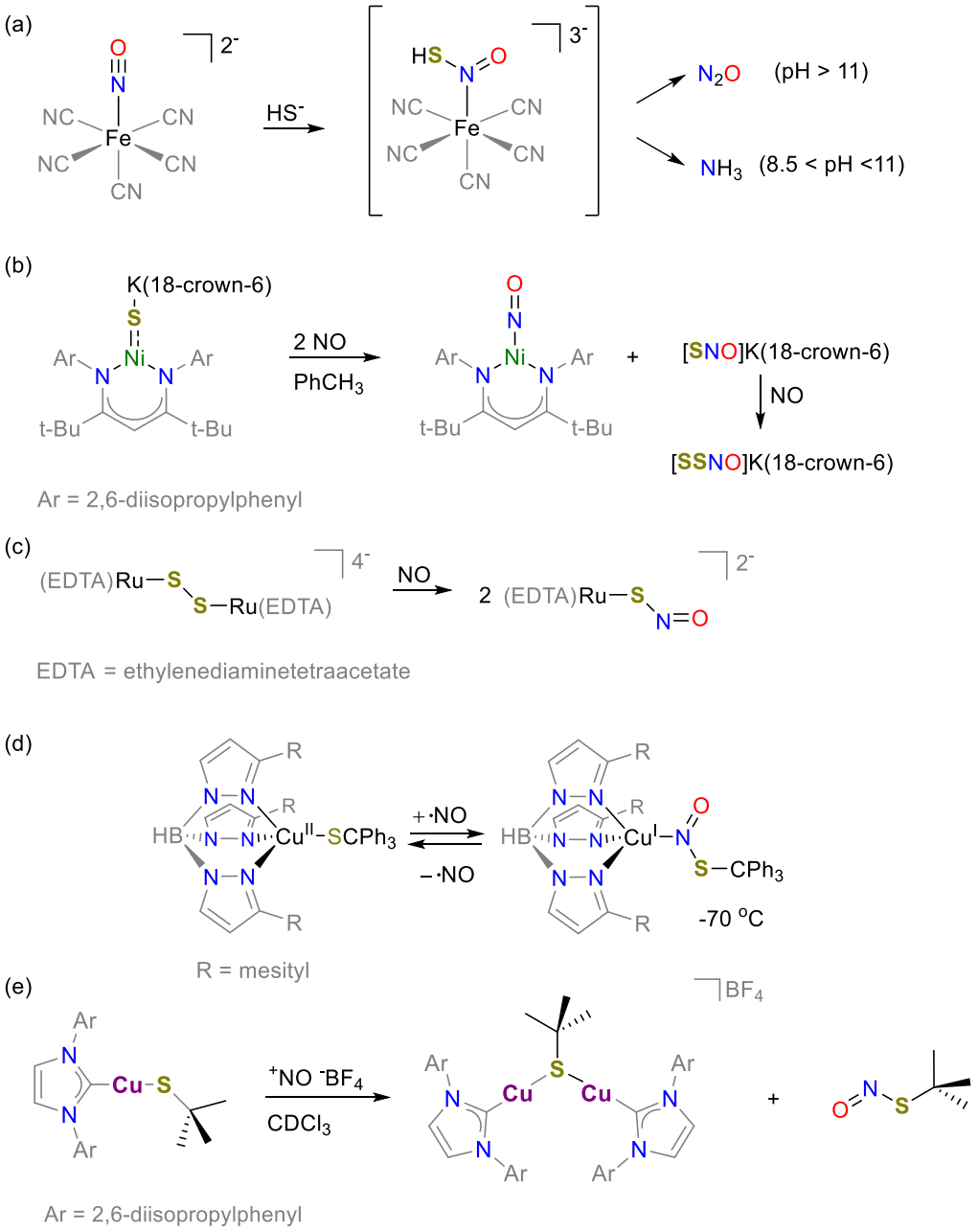

Scheme 4.1 Thionitrite-related compounds of transition-metals.

4.2 Results and Discussion

4.2.1 Synthesis of Bridging Sulfide and Disulfide Complexes

We initially set out to determine whether sterically encumbering expanded-ring NHCs stabilize a dicopper(I) sulfide core. We have previously shown that the expanded-ring NHC 7Dipp (1,3-bis(2,6-diisopropylphenyl)-4,5,6,7-tetrahydro-1,3-diazepin-2-ylidene) supports a stable copper(I) hydride dimer.[40] Gratifyingly, $(7DippCu)_2S$ (**16**) could be generated in good yield from the reaction of 7DippCuCl with excess Na_2S following an analogous procedure from Hillhouse and coworkers (Scheme 4.2).[26] The 7Dipp-supported copper(I) hydrosulfide (**17**) was readily synthesized from 7DippCuCl and potassium hydrosulfide. Another route to the sulfide-bridged dicopper(I) complex shown by Hillhouse and coworkers,[26] the deprotonation of a hydrosulfide complex by a copper(I) alkoxide, also proved viable with the 7Dipp ligands.

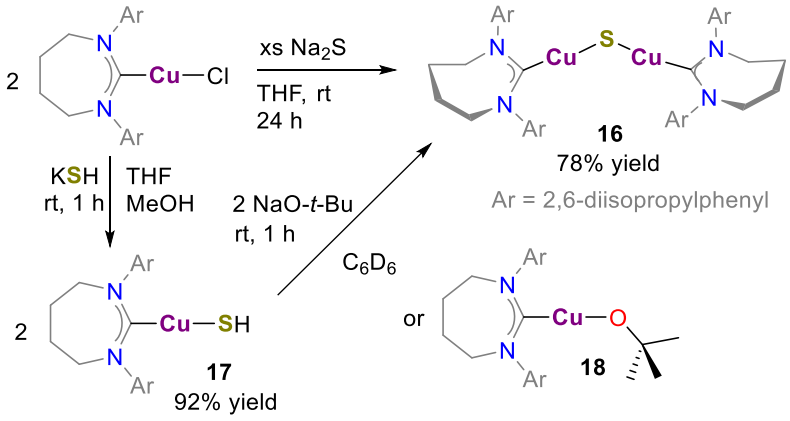

Scheme 4.2 Synthesis of a sulfide-bridged dicopper complex.

Interestingly, deprotonation of **17** by sodium *tert*-butoxide resulted in the formation of **16** as the major species with presumed loss of Na_2S, offering another avenue to the bridging sulfide complex. Rapid conversion of **17** by either deprotonation route was evident by the bright yellow color of **16**, and confirmed by ^{1}H NMR spectroscopy.

While there are numerous examples of dicopper(II) disulfides (*vide supra*) we have found no examples of dicopper(I) disulfides. Initial attempts to synthesize a 7Dipp-supported dicopper(I) disulfide by addition of elemental sulfur to **16** resulted in the formation of numerous products observed by ^{1}H NMR, regardless of stoichiometry, suggesting a tendency to form mixtures of higher-order copper oligosulfides. As an alternative, **18** reacts with bis(phenylacetyl) disulfide to give the 7Dipp-supported dicopper(I) disulfide (**19**), isolated as an orange-yellow solid. (Scheme 4.3). Addition of PPh_3 to a solution of **19** in C_6D_6 resulted in conversion to **16**, by sulfur abstraction with concomitant formation of $Ph_3P{=}S$, as confirmed by ^{1}H and ^{31}P NMR.

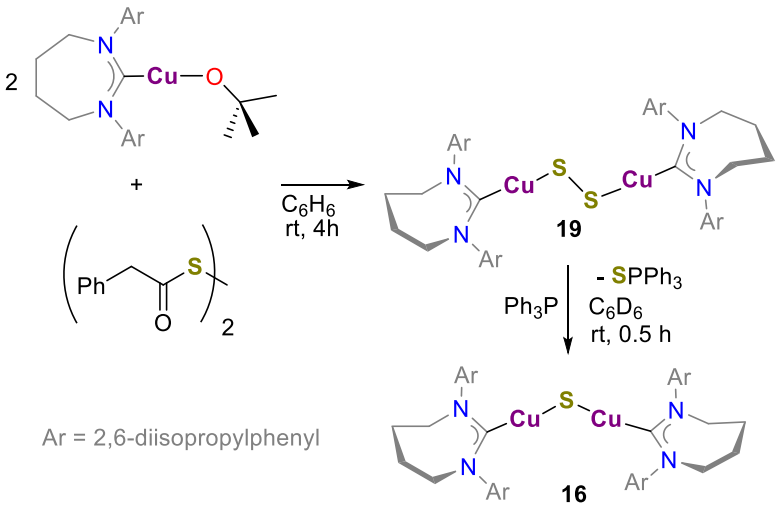

Scheme 4.3 Synthesis of a disulfide-bridged dicopper complex.

4.2.2 Structures of Bridging Sulfide and Disulfide Complexes

Recrystallization of **16** from CH_3CN (–35 °C) resulted in crystals suitable for X-ray diffraction. The structure is similar to that of the dicopper(I) sulfide reported by Hillhouse and coworkers.[26] Only one molecule of four in the asymmetric unit is shown in Figure 4.1. The Cu···Cu distances range from 3.475(2)–3.677(2) Å; the Cu–S–Cu angles, from 110.66(6)–120.68°. Crystals of **19** suitable for X-ray diffraction resulted after recrystallization from Et_2O (–35 °C). The structure of **19** features end-on binding of the disulfide unit to the copper(I) centers, analogous to that reported by Karlin and coworkers for a dicopper(II) disulfide.[29] Many side-on dicopper(II) disulfides have also been reported.[27-36] Complex **19** features a Cu–S distance of 2.132(1) Å, an S–S distance of 2.113(2) Å and a Cu–S–S angle of 99.80(7)°.

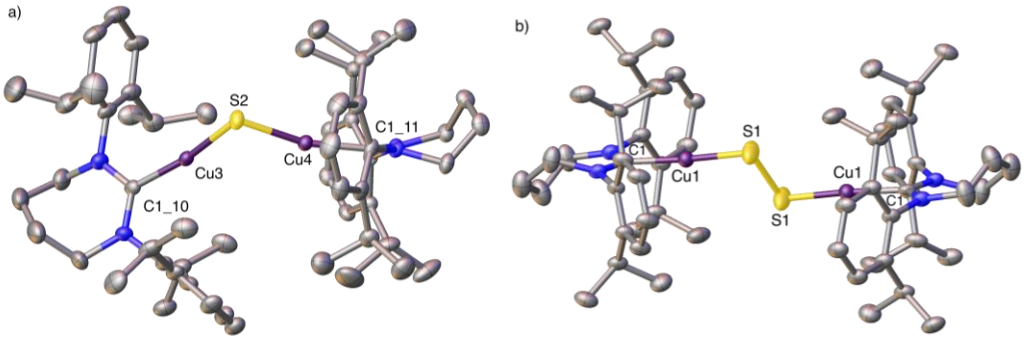

Figure 4.1 Thermal ellipsoid depiction (50% probability) of **16** and **19**. Selected bond lengths (Å) and angles (º): **16** (a, only one molecule of four in the asymmetric unit is shown) C1_10–Cu3 1.909(3), Cu3–S2 2.117(1), C1_11–Cu4 1.892(3), Cu4–S2 2.108(2), C1_10–Cu3–S2 163.94(9), C1_11–Cu4–S2 168.60(9), Cu3–S2–Cu4 110.66(6). **19** (b) Cu1–C1 1.906(3), Cu1–S1 2.132(1), S1–S1 2.113(2), C1–Cu1–S1 178.02(9), Cu1–S1–S1 99.80(7).

4.2.3 Nitrosylation of Copper(I) Hydrosulfide

Addition of NO^+ to a solution of **17** in CD_3CN results in the formation of $7DippCu^+$ as its acetonitrile adduct (**20**, Scheme 4.4a). Ammonium ion (NH_4^+) formation was evident by the appearance of a 1:1:1 triplet resonance, due to $^1H–^{14}N$ coupling, at δ 5.91 ppm, in the ^1H NMR spectrum. (Scheme 4.4a, Figure 4.21) Notably, NH_3 is observed from the decomposition of an Fe-bound HSNO complex in buffered solution,[7] whereas ammonium ion formation, shown herein, occurred in dried, deuterated solvent. Following addition of NO^+, the sample appeared cloudy, suggesting precipitation of elemental sulfur. Subsequent addition of PPh_3, generated a clear solution, and formation of $Ph_3P{=}S$ was confirmed by ^{31}P NMR. We thus suggest the formation of HSNO (copper-bound or free), which releases elemental sulfur generating HNO. Subsequent decomposition of HNO would form NH_4^+, and should generate N_2O. An analysis of the reaction headspace by GC-MS shows a peak at *m*/*z* 44, corresponding to N_2O. Based on this hypothesis, reaction of NO^+ with a copper(I) hydride would presumably generate HNO, with the Cu–H acting as source of $H^–$, and likewise lead to NH_4^+ formation. The ^1H NMR spectrum following dissolution of $(7DippCuH)_2$ and NO^+ in CD_3CN reveals formation of $[(7Dipp)Cu–NCCD_3]^+$, with a 1:1:1 triplet resonance corresponding to NH_4^+ (Scheme 4.4b).

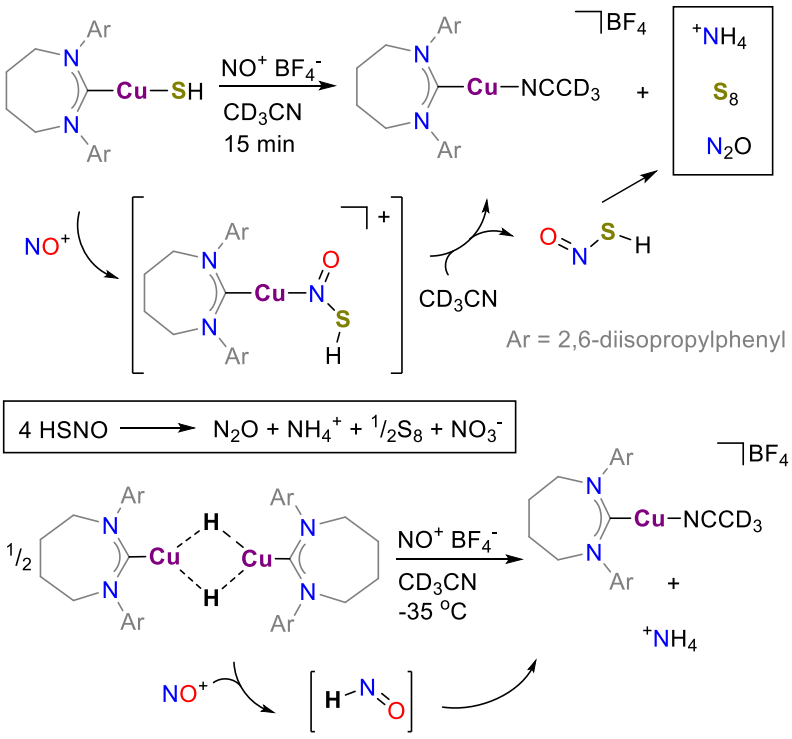

Scheme 4.4 Nitrosylation of copper(I) hydrosulfide.

4.2.4 Nitrosylation of Bridging Sulfide and Disulfide Complexes

Lastly, we investigated whether NO^+ would act as a Lewis acid or an oxidant toward **16** and **19**. Furthermore, we wondered whether oxidation would occur at the copper centers or the sulfur atom(s). Calculations by Hillhouse and coworkers show the HOMO consisting mainly of a non-bonding S p-orbital but with some Cu character (Ref. 10, Supp. Info.). Furthermore, oxidation of the dicopper(I) sulfide complex by CO_2 or N_2O to a dicopper(I) sulfate was recently reported.[37] Interestingly, the dicopper(I) sulfide and dicopper(I) disulfide react similarly with NO^+. Reactions in CD_3CN result in decomposition to Cu° while the ^1H NMR spectra show the presence of **20** (Scheme 4.5). Based on these findings, we inferred the formation of elemental sulfur, which was confirmed by the resonance for $Ph_3P{=}S$ in the ^{31}P NMR spectra after addition of Ph_3P. We thus conclude that an NHC-

coordinated Cu–SNO (or Cu–SSNO) complex is unstable, decomposing to form insoluble Cu^0, elemental sulfur and $NO^{\bullet}$. Knowing that organic thiols react with *t*-BuONO to yield organic thionitrites,[41] we added *t*-BuONO to 2 but saw no appreciable reaction after 24 h. After heating at 50 °C significant decomposition was evident.

Reaction of **16** with NO^+ in weakly coordinating fluorobenzene at –35 °C, with subsequent warming to room temperature, also resulted in decomposition to Cu^0, and a single set of resonances in the ^{1}H NMR spectrum (CD_2Cl_2). The ^{19}F NMR spectrum revealed a very broadened and upfield-shifted BF_4^- resonance (–160 ppm). Following addition of Ph_3P to the NMR sample, the ^{1}H and ^{31}P NMR spectra were consistent with formation of [7DippCu–PPh_3]$^+$. The ^{31}P spectrum showed the resonance for Ph_3P=S, confirming elemental sulfur had been formed. Furthermore, the ^{19}F NMR spectrum following Ph_3P showed a sharp BF_4^- resonance, no longer upfield-shifted. This finding suggests that weakly coordinating BF_4^- can interact with the copper(I) center. Labile BF_4^- complexes of (NHC)gold(I) cations have likewise been reported.[42] Reaction of 7DippCuCl and $AgBF_4$ in fluorobenzene solution resulted in the identical ^{1}H NMR shifts in addition to a broadened, upfield shift of the BF_4^- resonance. ^{1}H NMR spectra taken of mixtures kept at or below –35 °C showed 7DippCu$^+$ fragments as the major, or the only detectable species.

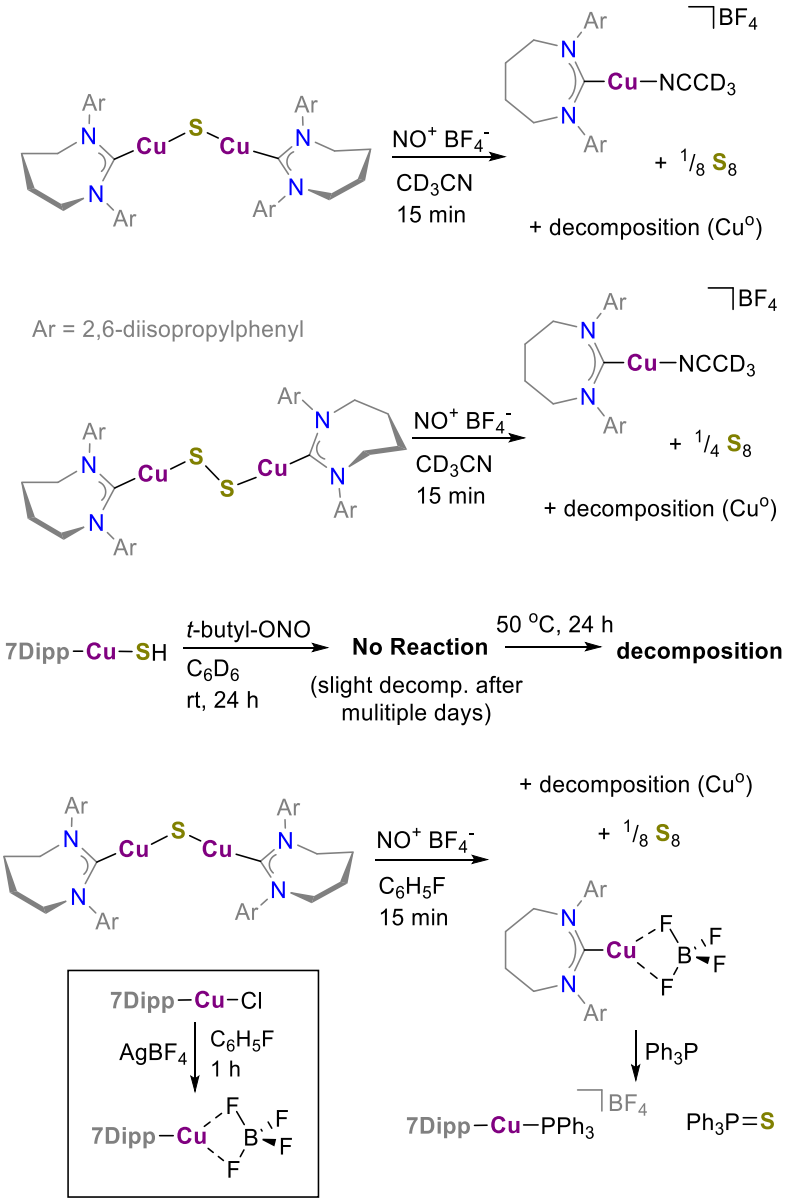

Scheme 4.5. Nitrosolation of dicopper(I) sulfides

4.3 Conclusion

We have outlined the nitrosonium reactivity of a series of NHC-supported copper(I) sulfide complexes. The syntheses and structures of new neutral sulfide- and disulfide-bridged dicopper(I) complexes in addition to their related hydrosulfide complex, show the

expanded-ring NHC 7Dipp to be a capable supporting ligand. Reaction with NO^+ results in oxidation at the sulfur atom(s) to elemental sulfur, and formation of (NHC)copper(I) cations. Despite the high oxidation potential of NO^+ (0.87 V vs. Fc in CH_3CN)[43], oxidation occurs only at the sulfur atom, leading to net reduction of a copper(I) center. Reaction of a 7Dipp-supported copper(I) hydrosulfide forms elemental sulfur, (NHC)copper(I) cation, N_2O and NH_4^+, possibly via decomposition of HSNO. Furthermore, the 7Dipp-supported copper(I) hydride dimer reacts with NO^+ to yield ammonium ion, suggesting formation and decomposition of HNO. These reactions model possible pathways in the generation and subsequent reactivity of molecules related to H_2S and $NO^{\bullet}$ signaling from copper(I) sulfide complexes.

4.4 Experimental

4.4.1 General Considerations

Unless otherwise indicated, manipulations were performed in an MBraun glovebox under an inert atmosphere of nitrogen, or in sealable glassware on a Schlenk line under an atmosphere of argon. Glassware and magnetic stir bars were dried in a ventilated oven at 160°C and were allowed to cool under vacuum. Dichloromethane (BDH), hexane (EMD Millipore Omnisolv), tetrahydrofuran (THF, EMD Millipore Omnisolv), toluene (EMD Millipore Omnisolv) were sparged with ultra-high purity argon (NexAir) for 30 minutes prior to first use, dried using an MBraun solvent purification system, transferred to Straus flasks, degassed using three freeze-pump-thaw cycles, and stored under nitrogen or argon. Anhydrous benzene (C_6H_6, EMD Millipore Drisolv) and, anhydrous pentane (EMD Millipore Drisolv, sealed under a nitrogen atmosphere) were used as received and stored

in a glovebox. Tap water was purified in a Barnstead International automated still prior to use.

Benzene-d_6 (Cambridge Isotope Laboratories) was dried over sodium benzophenone ketyl, vacuum-transferred into oven-dried resealable flasks, and degassed by successive freeze-pump-thaw cycles. Dichloromethane-d_2 (Cambridge Isotope Laboratories) and acetonitrile-d_3 (Cambridge Isotope Laboratories) were dried over calcium hydride overnight, vacuum-transferred to an oven-dried resealable Schlenk flask, and degassed by successive freeze-pump-thaw cycles. Chloroform-*d* (Cambridge Isotope Laboratories) was used as received.

Sodium *tert*-butoxide (TCI America), copper(I) chloride (Alfa-Aesar), 42,6-diisopropylaniline (Sigma-Aldrich), *N*,*N*-diisopropylethylamine (Alfa-Aesar), acetic acid, (Alfa-Aesar), sodium metal (Alfa-Aesar), benzophenone (Alfa-Aesar), calcium hydride (Alfa-Aesar), 1,4-dibromobutane (Sigma-Aldrich) triethyl orthoformate (Alfa-Aesar), sodium sulfide (Alfa-Aesar), potassium hydrosulfide (Strem), 2-phenylacetic dithioperxoyanhydride (Matrix), *tert*-butyl nitrite (Sigma-Aldrich) sodium bis(trimethylsilyl)amide (NaHMDS, Sigma-Aldrich or Strem Chemicals), nitrosonium tetrafluoroborate (NO^+ BF_4^-, Alfa-Aesar), silver tetrafluoroborate (Alfa-Aesar), nitrogen (NexAir), and argon (both industrial and ultra-high purity grades, NexAir) were used as received. (7Dipp)CuCl,[40] (7Dipp)CuO-*t*-Bu,[40] and $(7DippCuH)_2$[40] were prepared according to literature protocols and were characterized by ^{1}H NMR spectroscopy.

4.4.2 Spectroscopic Measurements

^{1}H, ^{13}C, ^{11}B ^{19}F, and ^{31}P spectra were obtained using Bruker Avance IIIHD 700 MHz, Bruker DSX 400 MHz and Varian Vx 400 MHz spectrometers. ^{1}H and ^{13}C NMR chemical shifts are referenced with respect to solvent signals and reported relative to tetramethylsilane. A capillary insert of α,α,α-trifluorotoluene (-63.72 ppm) was used to determine ^{19}F chemical shifts. Unless otherwise stated, infrared spectra were collected using microcrystalline samples on a Bruker Alpha-P infrared spectrometer equipped with an attenuated total reflection (ATR) attachment. Samples were exposed to air as briefly as possible prior to data collection.

4.4.3 Elemental Analyses

Elemental analyses were performed by Atlantic Microlab, Inc. in Norcross, Georgia.

4.4.4 Synthetic Procedures

4.4.4.1 Synthesis of $[(7Dipp)Cu]_2S$

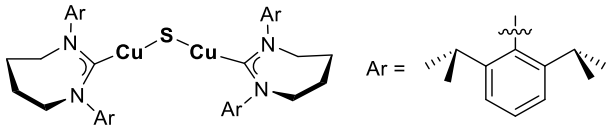

Figure 4.2 $[(7Dipp)Cu]_2S$ (**16**)

$[(7Dipp)Cu]_2S$ (**16**) 7DippCuCl (0.182 g, 0.352 mmol) and sodium sulfide (0.055 g, 0.70 mmol) were combined in a 20-mL vial, equipped with a stirbar, before THF (5 mL) was added. The mixture was allowed to stir for 24h before the THF was removed *in vacuo*. The product was extracted with C_6H_6 (3 x 3 mL) filtered through Celite and concentrated

in vacuo. The resulting yellow solid was washed with CH_3CN (2 x 3 mL), then dried *in vacuo* to afford the title complex as a yellow solid. (0.137 g, 78% yield) ^{1}H NMR (700 MHz, C_6D_6): δ (ppm) 7.15 (t, t, $^3J_{HH}$ = 7.7 Hz, 2H, para-C*H*), 7.06 (d, $^3J_{HH}$ = 7.7 Hz, 4H, *meta*-C*H*), 3.29 (m, 4H, NCH_2), 3.20 (sept, $^3J_{HH}$ = 7.0 Hz, 4H, C*H*$(CH_3)_2$), 1.62 (m, 4H, NCH_2CH_2), 1.48 (d, $^3J_{HH}$ = 7.0 Hz, 12H, $CH_2(CH_3)_2$), 1.27 (d, $^3J_{HH}$ = 7.0 Hz, 12H, $CH_2(CH_3)_2$). $^{13}C\{^1H\}$ NMR (176 MHz MHz, C_6D_6): δ (ppm) 212.6 (N*C*Cu), 145.0 (*ortho*-C), 144.7 (*ipso*-*C*), 128.4 (*para*-*C*), 124.6 (*meta*-*C*), 54.1 (NCH_2), 28.9 ($CH(CH_3)_2$), 25.9 ($CH(CH_3)_2$), 25.1 (NCH_2CH_2), 24.9 ($CH(CH_3)_2$). IR: ν (cm^{-1}) 2958, 2927, 2864, 1486, 1427, 1384, 1361, 1320, 1299, 1286, 1177, 1105, 1057, 999, 938, 799, 721, 550, 446, 434.

Note: We have been unable to obtain satisfactory elemental analysis for **16**. The complex is extremely air-and moisture-sensitive. While NMR-silent impurities cannot be ruled out, we believe the ^{1}H and ^{13}C NMR spectra provided reflect the purity of the sample. After addition of 1,4-dichlorobutane to a benzene solution of **16** and concentration *in vacuo*, to remove tetrahydrothiophene, and excess 1,4-dichlorobutane, the more stable (7Dipp)CuCl complex was isolated without further purification and the elemental analysis was obtained (see page 154). We reasoned that only a sufficiently pure sample of **16** would give rise to analytically pure 7DippCuCl**.**

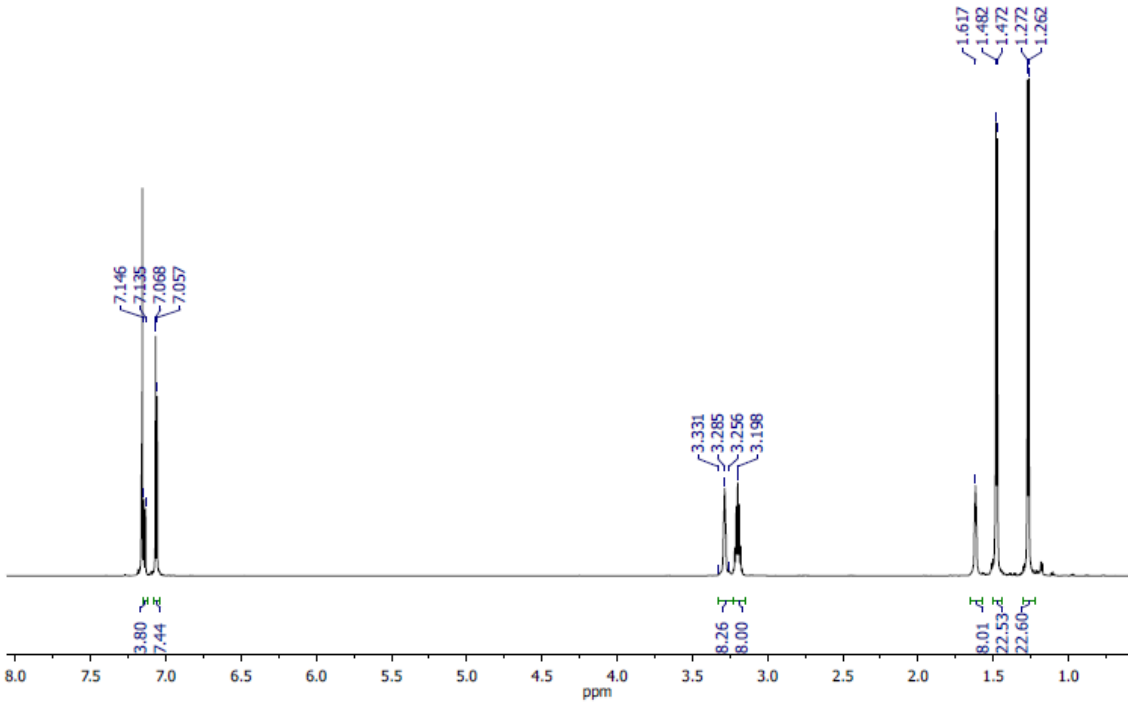

Figure 4.3 ^{1}H NMR spectrum of [(7Dipp)Cu]$_2$S in C_6D_6.

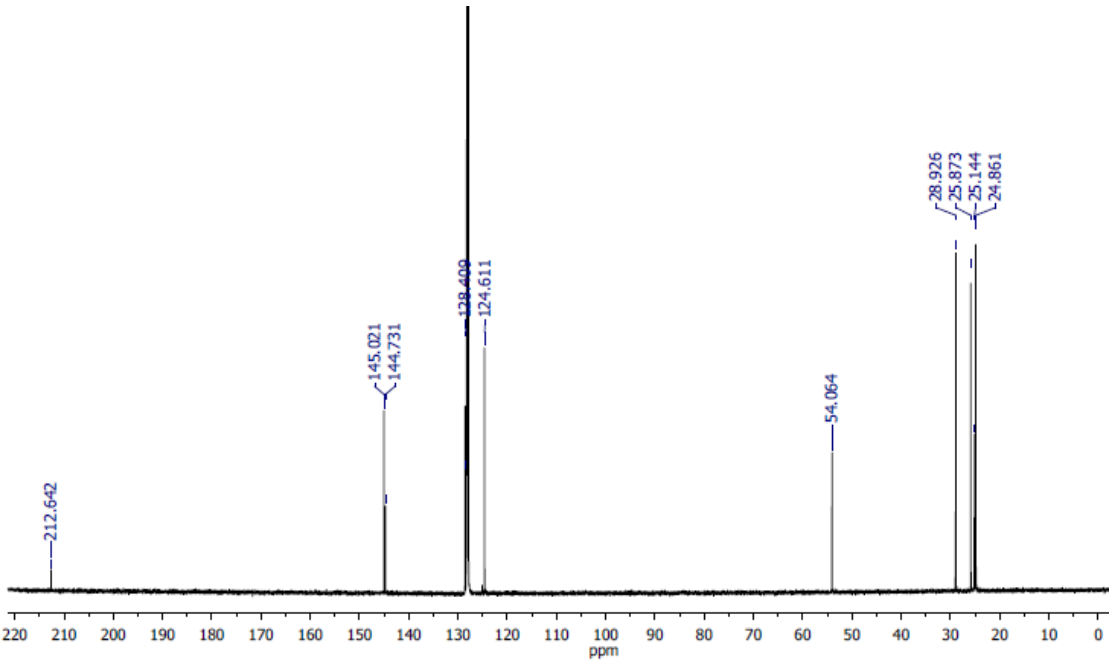

Figure 4.4 ^{13}C NMR spectrum of [(7Dipp)Cu]$_2$S in C_6D_6.

4.4.4.2 Synthesis of (7Dipp)CuSH

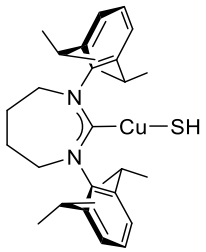

Figure 4.5 (7Dipp)CuSH

(7Dipp)CuSH (**17**) 7DippCuCl (0.202 g, 0.391 mmol) and potassium hydrosulfide (0.034 g, 0.47 mmol) were combined in a 20-mL vial, equipped with a stirbar, before MeOH (5 mL), and THF (10 mL) were added. The mixture was allowed to stir for 1h before the MeOH and THF were removed *in vacuo*. The product was extracted with CH_2Cl_2 (3 x 3 mL) filtered through Celite and concentrated *in vacuo* to afford the title complex as a colorless solid. (0.185 g, 92% yield) ^{1}H NMR (700 MHz, C_6D_6): δ (ppm) 7.15 (t, $^3J_{HH}$ = 7.7 Hz, 2H, para-C*H*), 7.04 (d, $^3J_{HH}$ = 7.7 Hz, 4H, *meta*-C*H*), 3.27 (m, 4H, NCH_2), 3.21 (sept, $^3J_{HH}$ = 7.0 Hz, 4H, C*H*(CH_3)$_2$), 1.63 (m, 4H, NCH_2CH_2), 1.52 (d, $^3J_{HH}$ = 7.0 Hz, 12H, $CH_2(CH_3)_2$), 1.19 (d, $^3J_{HH}$ = 7.0 Hz, 12H, $CH_2(CH_3)_2$) -2.17 (s, 1H, Cu–S*H*). ^{13}C{^{1}H} NMR (176 MHz MHz, C_6D_6): δ (ppm) 211.4 (N*C*Cu), 145.2 (*ortho*-C), 144.3 (*ipso*-*C*), 129.2 (*para*-*C*), 125.0 (*meta*-*C*), 53.4 (NCH_2), 29.0 (*C*H(CH_3)$_2$), 25.2(NCH_2CH_2), 25.1 (CH(*C*H_3)$_2$), 24.8 (CH(*C*H_3)$_2$). IR: ν (cm^{-1}) 2960, 2938, 2865, 1494, 1447, 1385, 1362, 1323, 1309, 1190, 1177, 1095, 1033, 1000, 936, 902, 786, 552, 457. Anal. Calcd for $C_{29}H_{43}CuN_2S$ C, 67.60; H, 8.41; N, 5.44. Found C, 67.60; H, 8.58; N, 5.40.

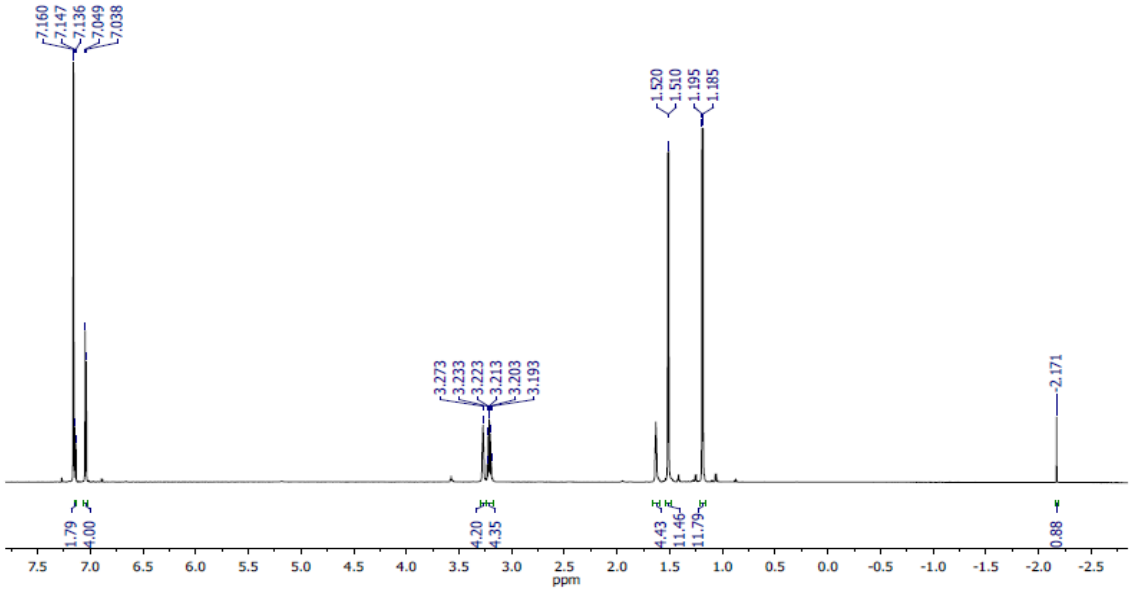

Figure 4.6 ^{1}H NMR spectrum of (7Dipp)CuSH in C_6D_6.

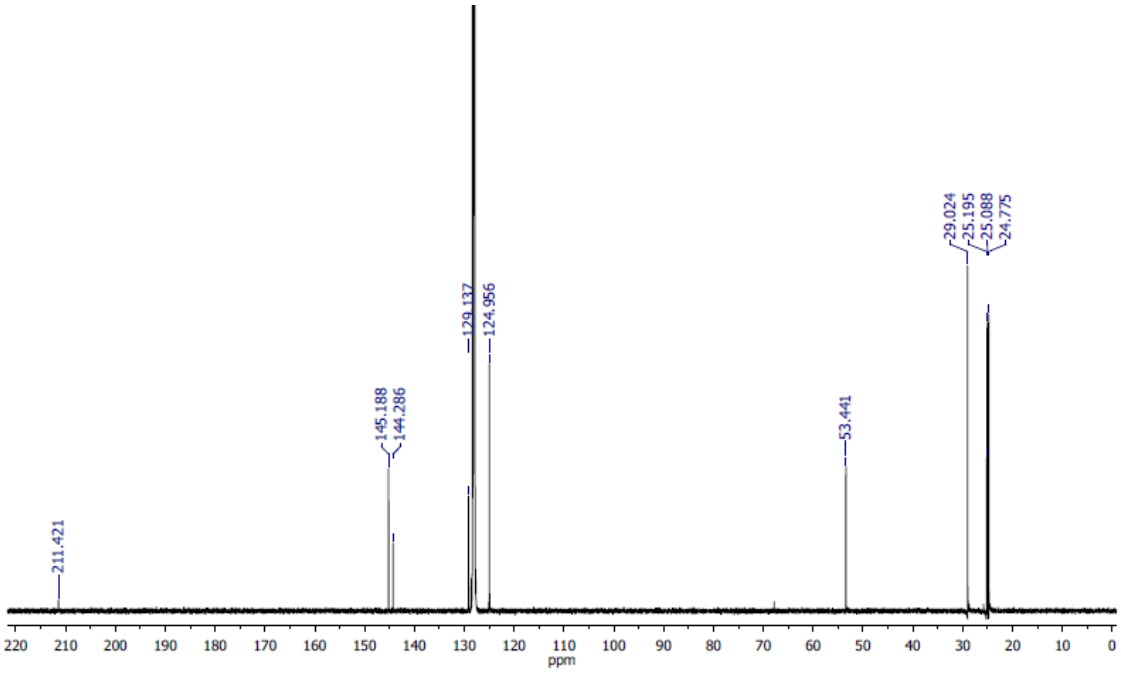

Figure 4.7 ^{13}C NMR spectrum of (7Dipp)CuSH in C_6D_6.

4.4.4.3 Synthesis of $[(7Dipp)CuS]_2$

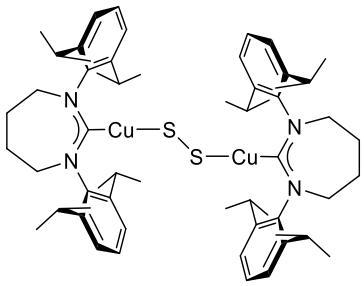

Figure 4.8 $[(7Dipp)CuS]_2$ (**19**)

[(7Dipp)CuS]$_2$ (**19**) (7Dipp)CuO-*t*-Bu (0.074 g, 0.13 mmol) and 2-phenylacetic dithioperxoyanhydride (0.020 g, 0.066 mmol) were combined in a 20-mL vial, equipped with a stirbar, before C_6H_6 (5 mL) was added. The mixture was allowed to stir for 1h before the C_6H_6 was removed *in vacuo*. The resulting yellow solid was washed with pentane (3 x 3 mL), the recrystallized from CH_3CN (5 mL) at –35 °C. The resulting solid was dried under *in vacuo* to afford the product as an orange solid. (0.040 g, 58% yield) ^{1}H NMR (700 MHz, C_6D_6): δ (ppm) 7.17 (t, $^3J_{HH}$ = 7.7 Hz, 4H, para-C*H*), 7.07 (d, $^3J_{HH}$ = 7.7 Hz, 8H, *meta*-C*H*), 3.32 (m, 8H, NCH_2), 3.23 (sept, $^3J_{HH}$ = 7.0 Hz, 8H, C*H*$(CH_3)_2$), 1.64 (m, 8H, NCH_2CH_2), 1.54 (d, $^3J_{HH}$ = 7.0 Hz, 24H, $CH_2(CH_3)_2$), 1.25 (d, $^3J_{HH}$ = 7.0 Hz, 24H, $CH_2(CH_3)_2$). ^{13}C{^{1}H} NMR (176 MHz MHz, C_6D_6): δ (ppm) 213.9 (N*C*Cu), 145.0 (*ortho*-C), 144.7 (*ipso*-*C*), 128.8 (*para*-*C*), 125.0 (*meta*-*C*), 53.6 (NCH_2), 29.1 (*C*H$(CH_3)_2$), 25.4 (CH$(CH_3)_2$), 25.2 (NCH_2CH_2), 25.0 (CH$(CH_3)_2$). IR: ν (cm^{-1}) 2957, 2926, 2865, 1498, 1446, 1385, 1363, 1312, 1290, 1222, 1096, 1055, 935, 899, 801, 756, 629, 504, 406.

Note: We have been unable to obtain satisfactory elemental analysis for **19**. The complex is extremely air-and moisture-sensitive. While NMR-silent impurities cannot be ruled out, we believe the ^{1}H and ^{13}C NMR spectra provided reflect the purity of the sample.

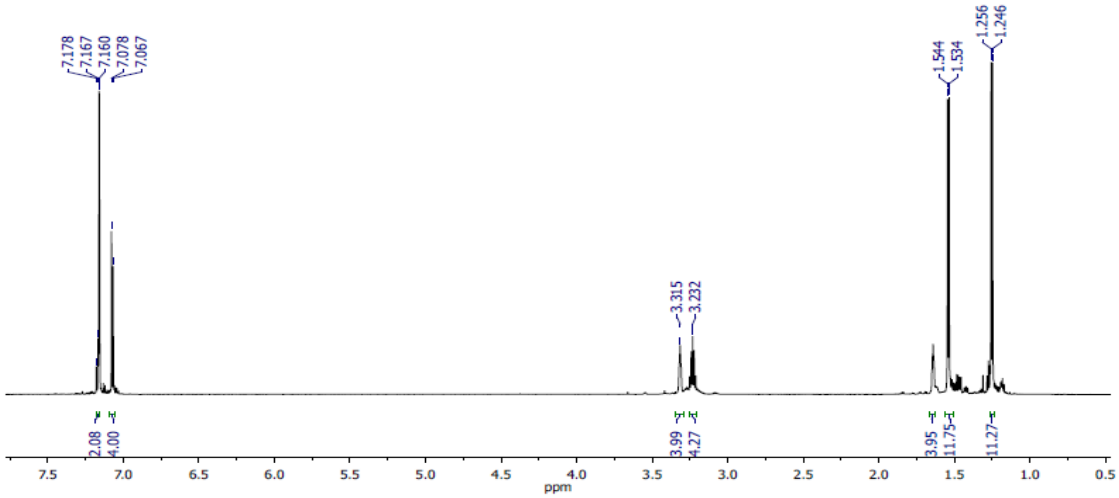

Figure 4.9 ^{1}H NMR spectrum of $[(7Dipp)CuS]_2$in C_6D_6.

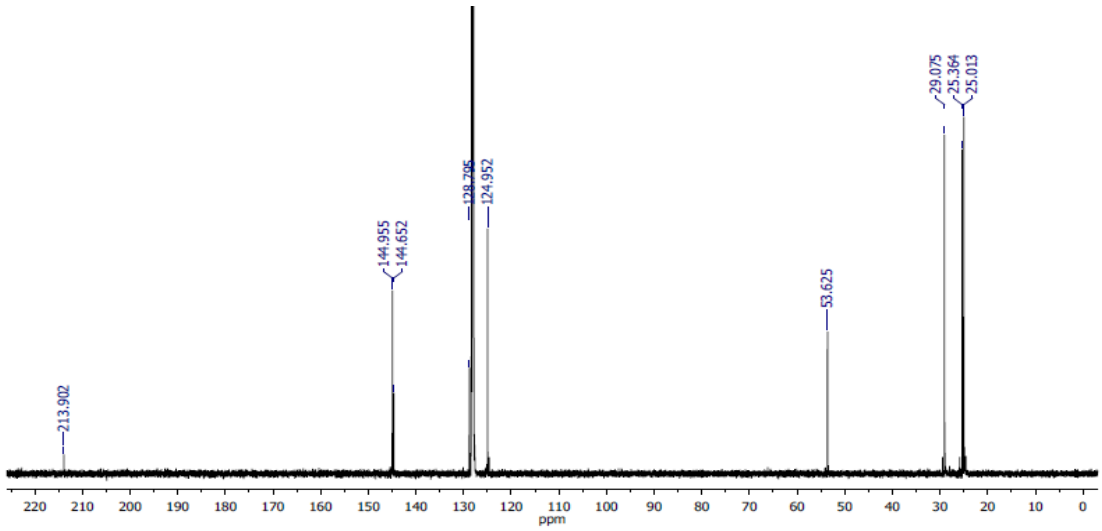

Figure 4.10 ^{13}C NMR spectrum of $[(7Dipp)CuS]_2$in C_6D_6.

4.4.4.4 Synthesis of (7Dipp)Cu(NCCD$_3$)BF$_4$

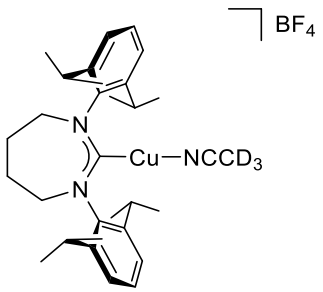

Figure 4.11 (7Dipp)Cu(NCCD$_3$)BF$_4$ (**20**)

(7Dipp)Cu(NCCD$_3$)BF$_4$ (**20**) **(**7Dipp)CuCl (0.059 g, 0.11 mmol) and silver tetrafluoroborate (0.022 g, 0.11 mmol) were combined in a 20-mL vial, equipped with a stirbar, before CD$_3$CN (0.1 mL) and DCM (3 mL) were added. The mixture was allowed to stir for 15 min, filtered through Celite, and concentrated *in vacuo*. The resulting colorless solid was dissolved in ethyl acetate (3 mL) layered with hexanes (5 mL) and placed in the freezer overnight. The resulting colorless solid was collected and, dried *in vacuo* to afford the title complex. (0.051 g, 74% yield) ^{1}H NMR (700 MHz, CD$_3$CN): δ (ppm) 7.33 (t, $^3J_{HH}$ = 7.7 Hz, 2H, para-C*H*), 7.26 (d, $^3J_{HH}$ = 7.7 Hz, 4H, meta-C*H*), 3.98 (m, 4H, NC*H*$_2$), 3.30 (sept, $^3J_{HH}$ = 7.0 Hz, 4H, C*H*(CH$_3$)$_2$), 2.29 (m, 4H, NCH$_2$C*H*$_2$), 1.29 (d, $^3J_{HH}$ = 7.0 Hz, 12H, CH$_2$(C*H*$_3$)$_2$) 1.27 (d, $^3J_{HH}$ = 7.0 Hz, 12H, CH$_2$(C*H*$_3$)$_2$) ^{13}C{^{1}H} NMR (176 MHz CD$_3$CN): δ (ppm) 213.2 (N*C*Cu), 146.4 (*ortho*-C), 146.2 (*ipso*-*C*), 129.4 (*para*-*C*), 125.5 (*meta*-*C*), 55.1 (N*C*H$_2$), 29.3 (*C*H(CH$_3$)$_2$), 26.0 (NCH$_2$*C*H$_2$), 25.1 (CH(*C*H$_3$)$_2$), 24.4 (CH(*C*H$_3$)$_2$). ^{19}F NMR (378 MHz, CD$_3$CN): δ (ppm) –152.4 (4F, B*F*$_4^-$). IR: ν (cm^{-1}) 2967, 2931, 2865, 1487, 1449, 1383, 1362, 1308, 1095, 1053, 1002, 934, 806, 790, 763, 612, 557, 518, 490.

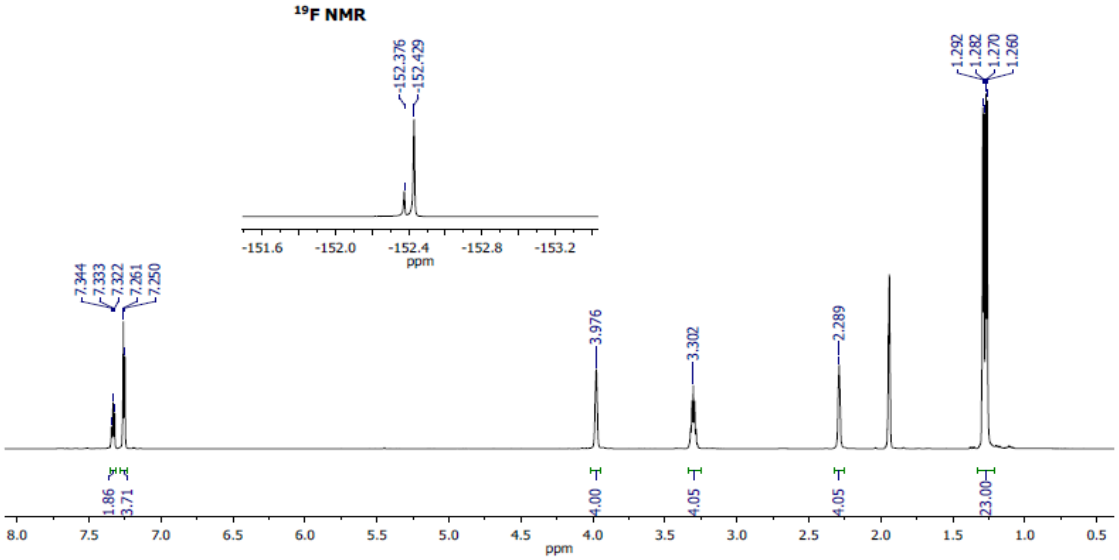

Figure 4.12 ^{1}H NMR spectrum of (7Dipp)Cu(NCCD$_3$)BF$_4$ overlaid with the BF$_4^-$ resonance in ^{19}F NMR spectrum in CD$_3$CN.

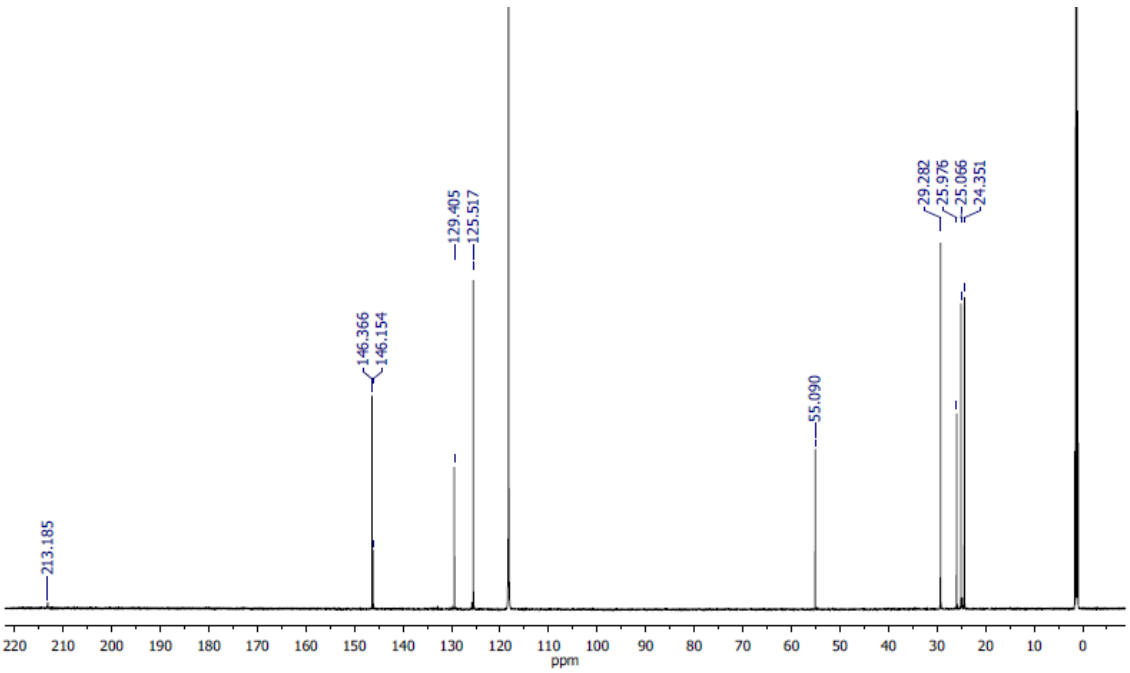

Figure 4.13 ^{13}C NMR spectrum of (7Dipp)Cu(NCCD$_3$)BF$_4$ in CD$_3$CN.

4.4.4.5 Synthesis of (7Dipp)Cu(PPh_3)BF_4

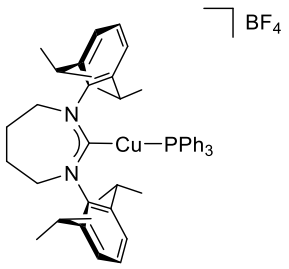

Figure 4.14 (7Dipp)Cu(PPh_3)BF_4

(7Dipp)Cu(PPh_3)BF_4 7DippCuCl (0.067 g, 0.13 mmol), triphenylphosphine (0.034, 0.13 mmol) and silver tetrafluoroborate (0.025 g, 0.13 mmol) were combined in a 20-mL vial, equipped with a stirbar, before DCM (5 mL) was added. The mixture was allowed to stir for 15 min, filtered thought Celite, before the resulting colorless solution was layered with pentane (8 mL) and placed in the freezer at –35 °C for 16h. The resulting crystals were dried *in vacuo* for 1h to afford the title complex. (0.090 g, 84 % yield) ^{1}H NMR (400 MHz, CD_2Cl_2): δ (ppm) 7.48-7.44 (m, 4H, dipp *para*-C*H*, PPh_3 *para*-C*H*), 7.32-7.26 (m, 10H, dipp *meta*-C*H*, PPh_3 *meta*-C*H*), 6.63-6.58 (m, PPh_3 *ortho*-CH), 4.07 (m, 4H, NCH_2), 3.27 (sept, $^3J_{HH}$ = 6.8 Hz, 4H, C*H*(CH_3)$_2$), 2.40 (m, 4H, NCH_2CH_2), 1.33 (d, $^3J_{HH}$ = 6.8 Hz, 12H, CH_2(CH_3)$_2$), 1.05 (d, $^3J_{HH}$ = 6.8 Hz, 12H, CH_2(CH_3)$_2$). ^{13}C{^{1}H} NMR (176 MHz CD_2Cl_2): δ (ppm) 206.1 (d, $^2J_{PC}$ = 60.2 Hz, N*C*Cu), 146.0 (dipp *ortho*-C), 143.8 (dipp *ipso*-*C*), 133.7 (d, $^2J_{PC}$ = 14.1 Hz**,** PPh_3 *ortho*-*C*), 131.9 (d, $^4J_{PC}$ = 2.1 Hz**,** PPh_3 *para*-*C*), 130.1 (*para*-*C*), 129.6 (d, $^3J_{PC}$ = 5.5 Hz**,** PPh_3 *para*-*C*), 127.8 (d, $^1J_{PC}$ = 45.9 Hz**,** PPh_3 *ipso*-*C*), 125.8 (dipp *meta*-*C*) 55.0 (NCH_2), 29.2 (*C*H(CH_3)$_2$), 25.5 (NCH_2CH_2), 25.2 (CH(*C*H_3)$_2$), 24.7 (CH(*C*H_3)$_2$). ^{31}P{^{1}H} NMR (162 MHz, CD_2Cl_2): δ (ppm) 7.65 (Cu–*P*Ph_3). ^{19}F NMR (378 MHz, CD_2Cl_2): δ (ppm) –152.7 (4F, B*F*$_4^-$). IR: ν (cm^{-1}) 2961, 2922, 2845, 1506, 1436,

1315, 1094, 1046, 998, 900, 807, 748, 675, 530, 506, 489, 451. Anal. Calcd for $C_{47}H_{57}CuN_2BF_4P$ C, 67.91; H, 6.91; N, 3.37. Found C, 67.45; H, 6.73; N, 3.47.

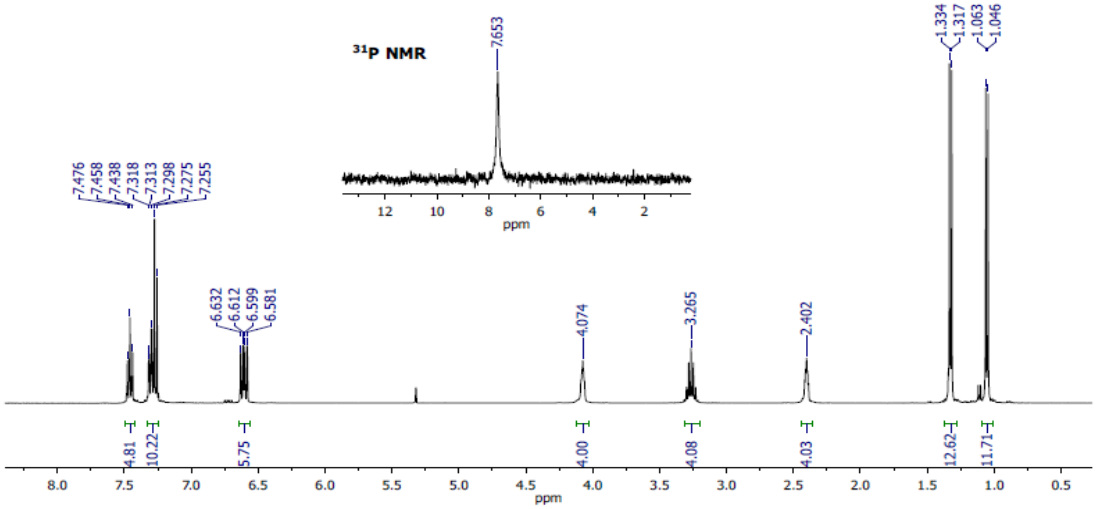

Figure 4.15 ^{1}H and ^{31}P NMR spectra of (7Dipp)Cu(PPh_3)BF_4 in CD_2Cl_2.

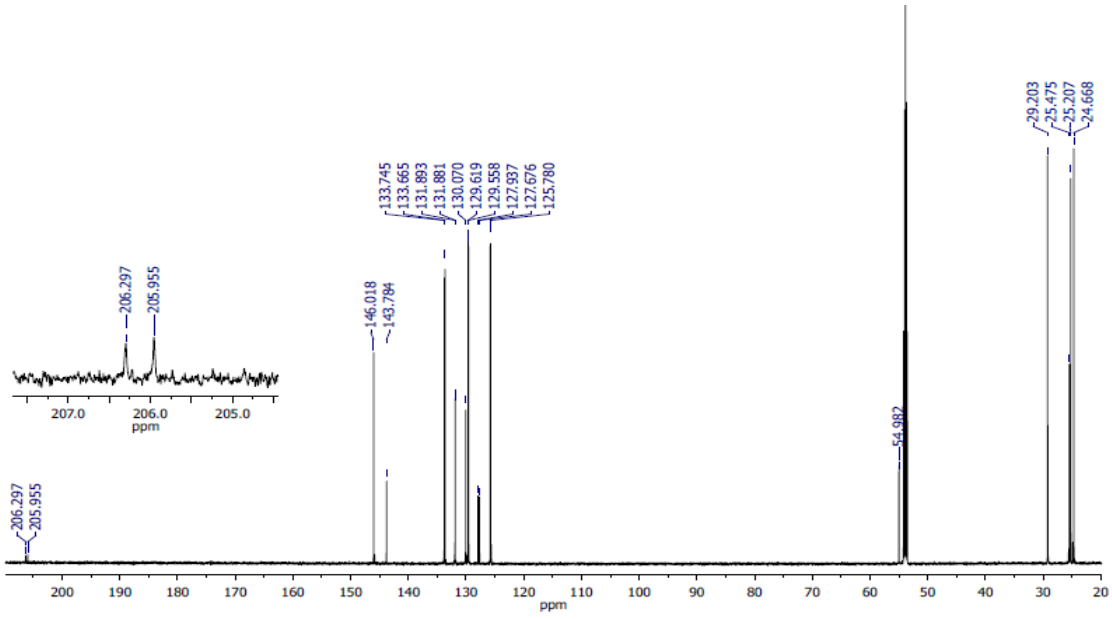

Figure 4.16 ^{13}C NMR spectrum of (7Dipp)Cu(PPh_3)BF_4 in CD_2Cl_2.

4.4.4.6 Deprotonation of **17** by **18**

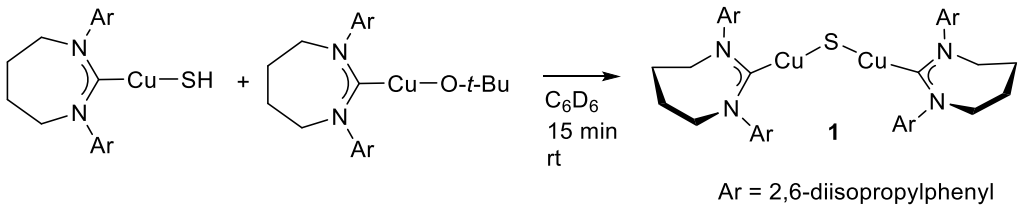

Scheme 4.6 Deprotonation of **17** by **18**.

(7Dipp)CuSH (**17**, 0.013 g, 0.025 mmol) and (7Dipp)CuO-*t*-Bu (**18**, 0.014 g, 0.025 mmol) were dissolved in C_6D_6 (0.75 mL) and mixed for 15 min before the ^{1}H NMR spectrum was recorded.

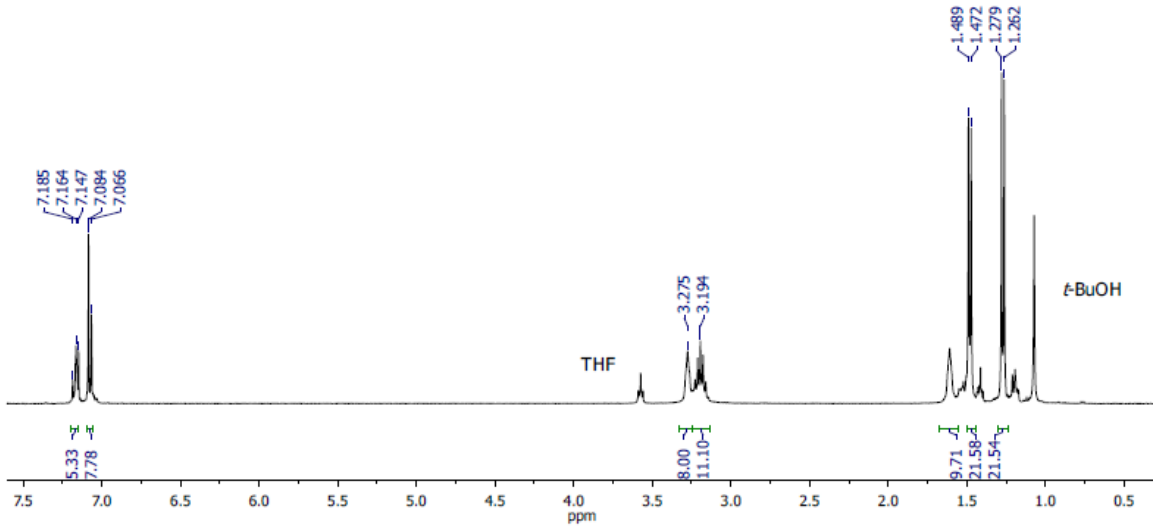

Figure 4.17 ^{1}H NMR spectrum of reaction of **17** and **18**.

4.4.4.7 Deprotonation of **17** by NaO-*t*-Bu

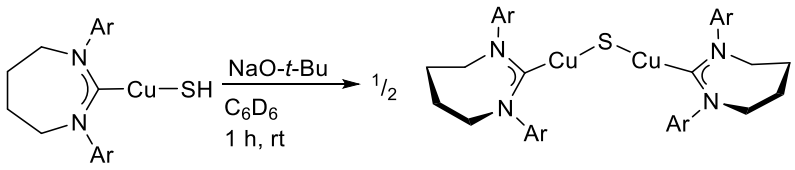

Scheme 4.7 Deprotonation of **17** by NaO-*t*-Bu.

(7Dipp)CuSH (**17**, 0.028 g, 0.054 mmol) and NaO-*t*-Bu (0.010 g, 0.010 mmol) were dissolved in C_6D_6 (0.75 mL) and mixed for 1 h before the ^{1}H NMR spectrum was recorded.

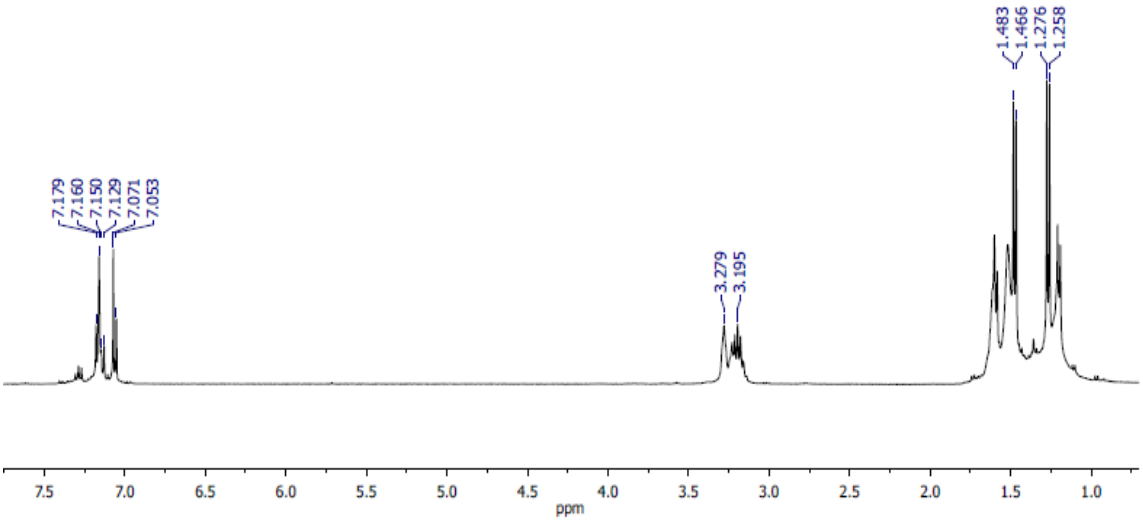

Figure 4.18. ^{1}H NMR spectrum of reaction of **17** and NaO-*t*-Bu.

4.4.4.8 Conversion of **16** to (7Dipp)CuCl and tetrahydrothiophene for elemental analysis

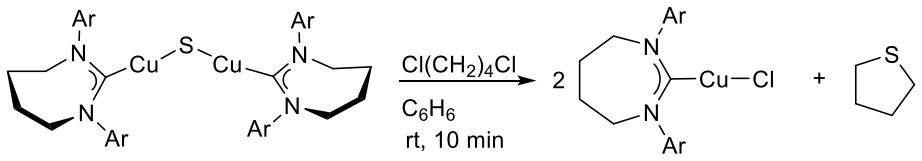

Ar = 2,6-diisopropylphenyl

Scheme 4.8 Conversion of **16** to (7Dipp)CuCl.

1,4-Dichlorobutane (11 μL, 0.10 mmol) was added to a solution of $(7DippCu)_2S$ (0.020 g, 0.020 mmol) in C_6D_6 (2 mL) and mixed for 10 min. The solution was then concentrated *in vacuo* and a small amount was dissolved in $CDCl_3$ and the ^1H NMR spectrum was recorded. The solid was dried under vacuum for 48 h to remove the excess 1,4-dichlorobutane. Anal. Calcd for $C_{29}H_{42}ClCuN_2$: C, 67.29; H, 8.18; N, 5.41. Found C, 67.19; H, 8.17; N, 5.28.

Note: Hillhouse and coworkers had previously shown the IPr* (IPr* = 1,3-bis(2,6-(diphenylmethyl)-4-methylphenyl)imidazol-2-ylidene) supported dicopper sulfide reacts with dibromoalkanes to generate the corresponding (NHC)copper(I) bromide and cyclic thioether.[37]

4.4.4.9 Conversion of **19** to **16**

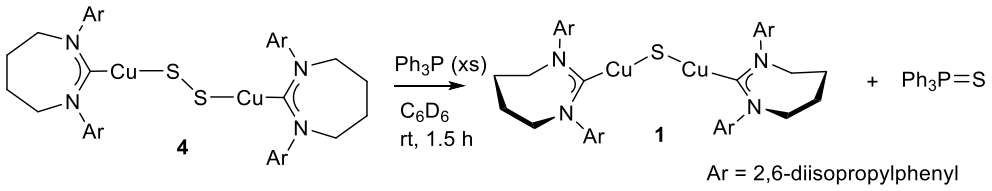

Scheme 4.9 Conversion of **19** to **16**

[(7Dipp)CuS]$_2$ (**19**, 0.010 g, 0.0097 mmol) was dissolved in C_6D_6 and a ^{1}H NMR spectrum was recorded. Triphenylphosphine (Ph_3P, 0.009 g, 0.03 mmol) was added and the ^{1}H and ^{31}P NMR spectra were recorded after 1.5 h.

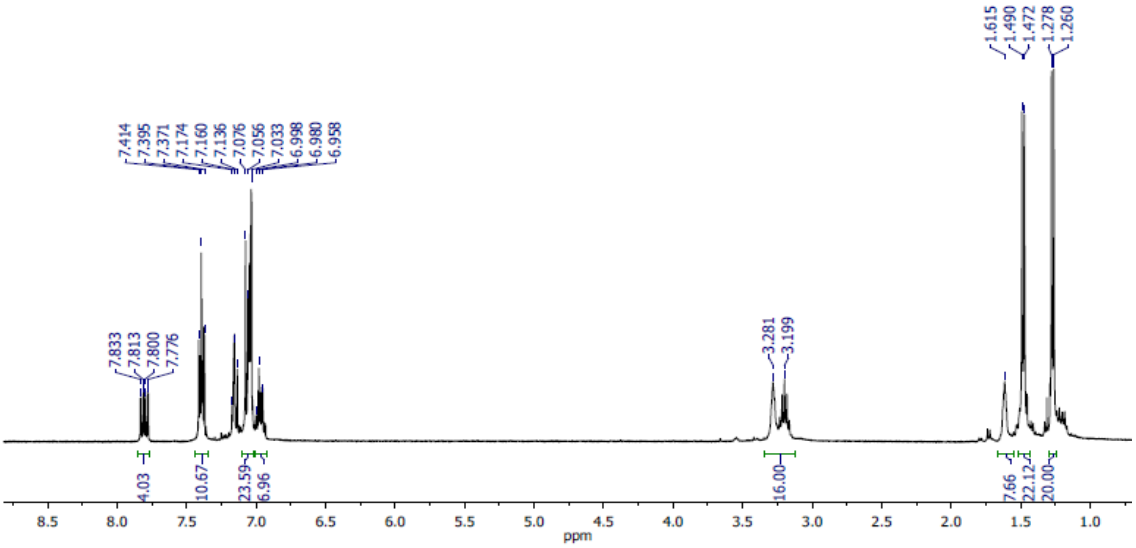

Figure 4.19 ^{1}H NMR spectrum after Ph_3P was added to **19**, generating **16** and Ph_3P=S.

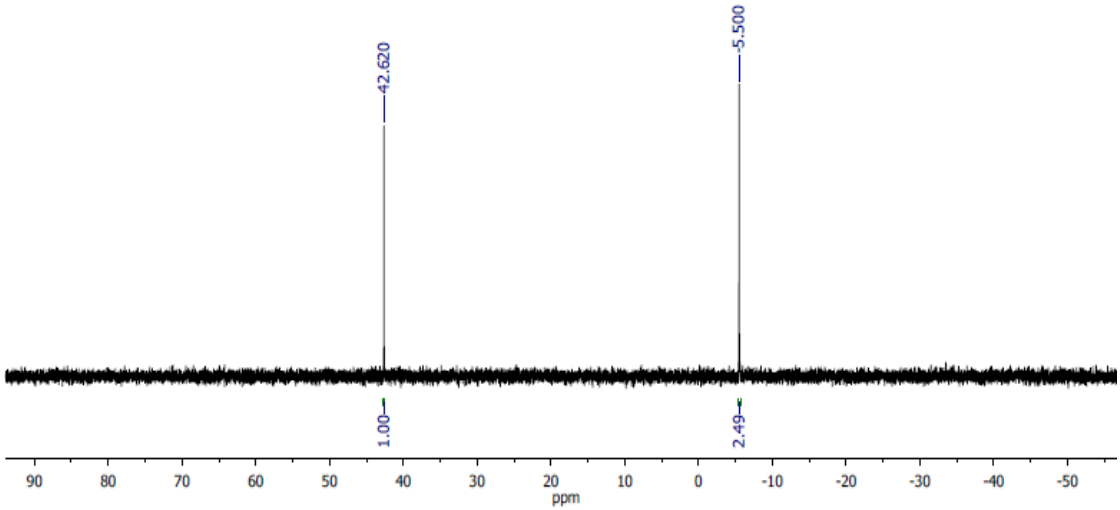

Figure 4.20 ^{31}P NMR spectrum after Ph_3P was added to **19**.

4.4.4.10 Nitrosonium reactivity of **17**

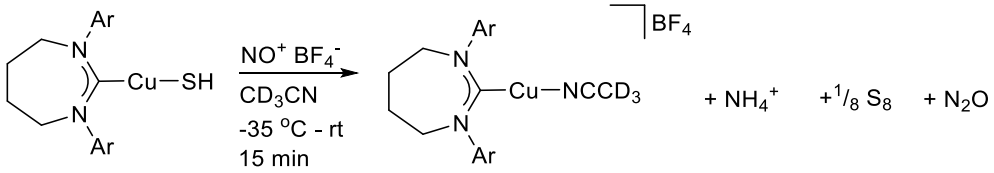

Scheme 4.10 Nitrosonium reactivity of **17**.

$NO^+BF_4^-$ (0.07 g, 0.060 mmol) was added to a solution of (7Dipp)CuSH (0.030 g, 0.060 mmol) in CD_3CN (1 mL) at –35 °C. The mixture was allowed to warm to room temperature with stirring before the ^{1}H NMR spectrum was recorded.

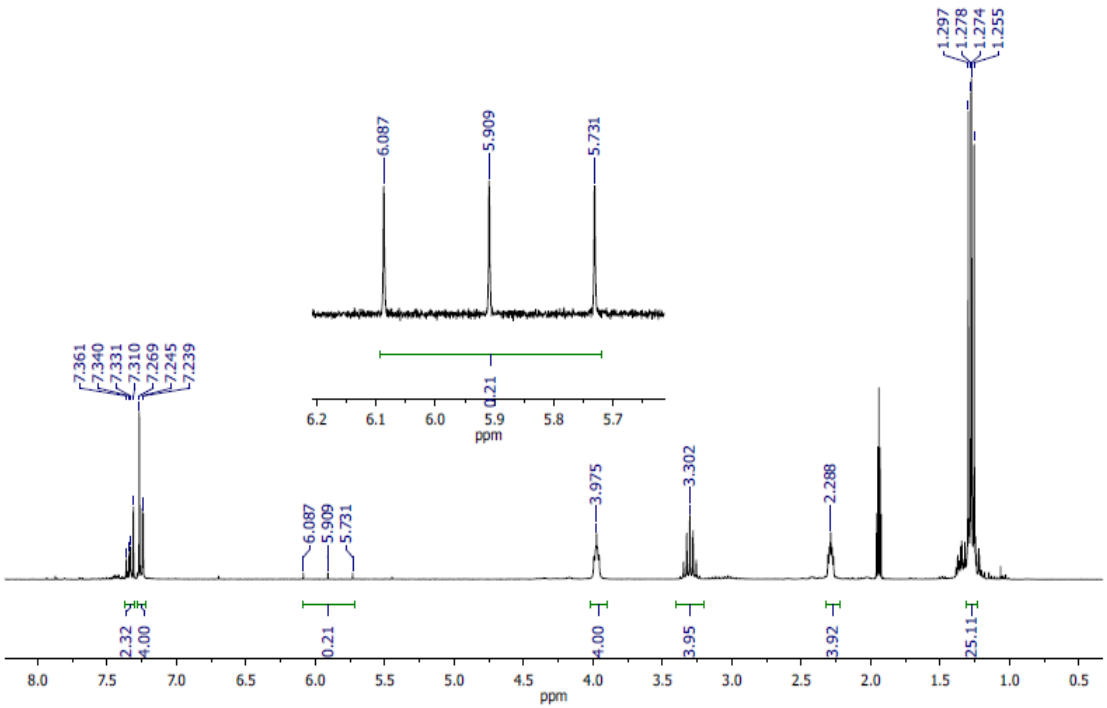

Figure 4.21 ^{1}H NMR spectrum following addition of NO^{+} BF_4^{-} to **17,** resulting in **20** in CD_3CN.

Triphenylphosphine (0.016 g, 0.060 mmol) was added and the ^{1}H and ^{31}P NMR spectra were recorded after 15 min.

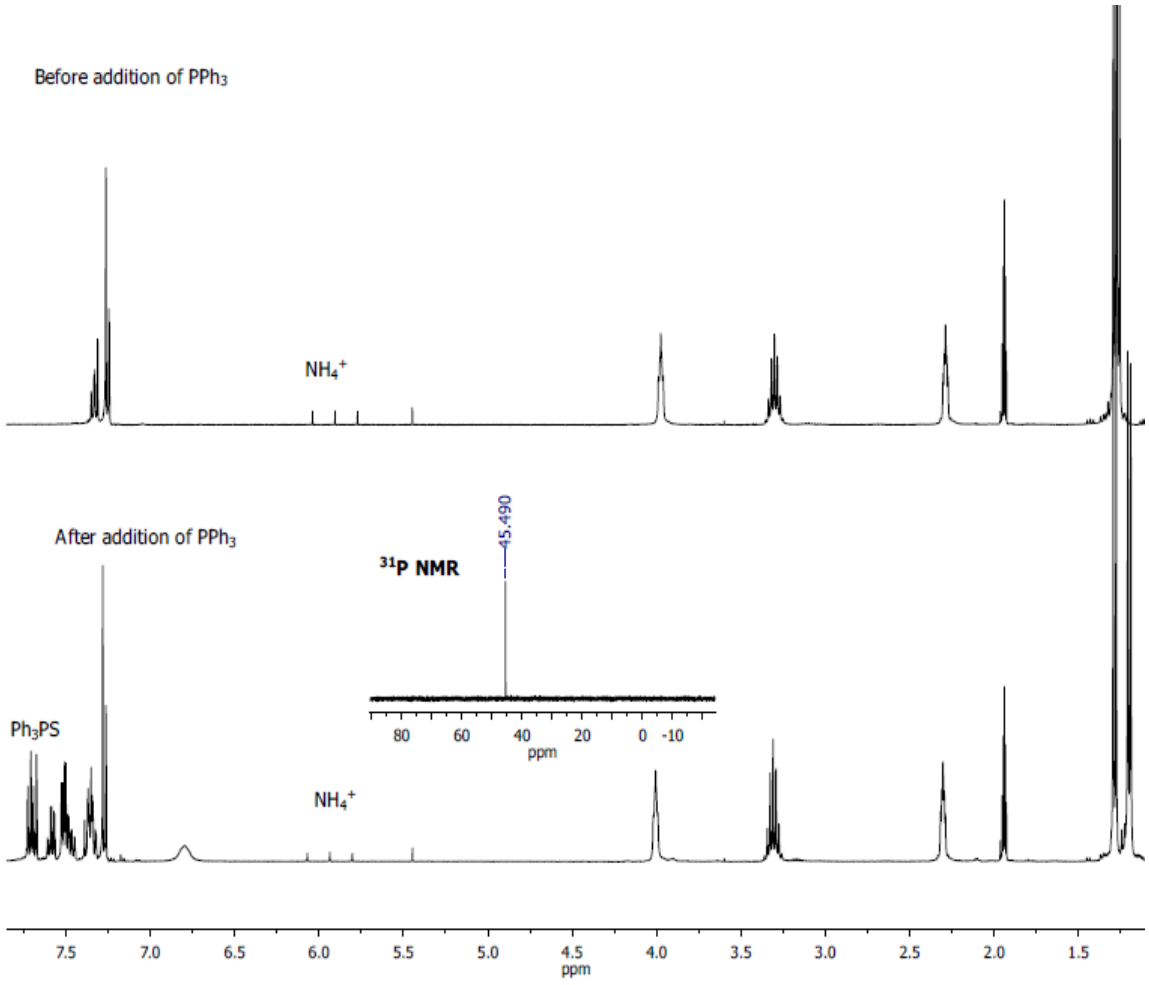

Figure 4.22 ^{1}H and ^{31}P spectrum following addition of Ph_3P in CD_3CN.

4.4.4.11 Nitrosonium Reactivity of **16**

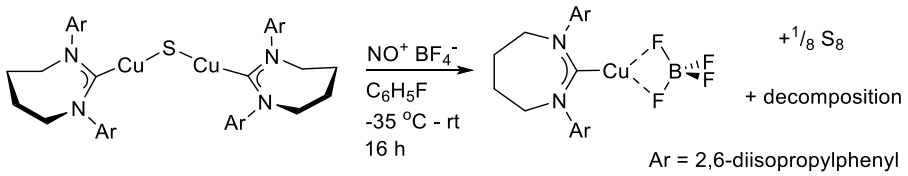

Scheme 4.11 Nitrosonium Reactivity of **16**.

A solution of $[(7Dipp)Cu]_2S$ (0.050 g, 0.050 mmol) in C_6H_5F (2 mL) was slowly added to solid $NO^+ BF_4^-$ (0.006 g, 0.052 mmol) at –40 °C. The mixture was allowed to stir at –40 °C for 4h before it was allowed to warm to room temperature while stirring for an additional 12h. The resulting mixture was filtered through Celite to remove the precipitate and concentrated *in vacuo*. The resulting colorless solid was taken up in CD_2Cl_2 and analyzed by NMR spectroscopy.

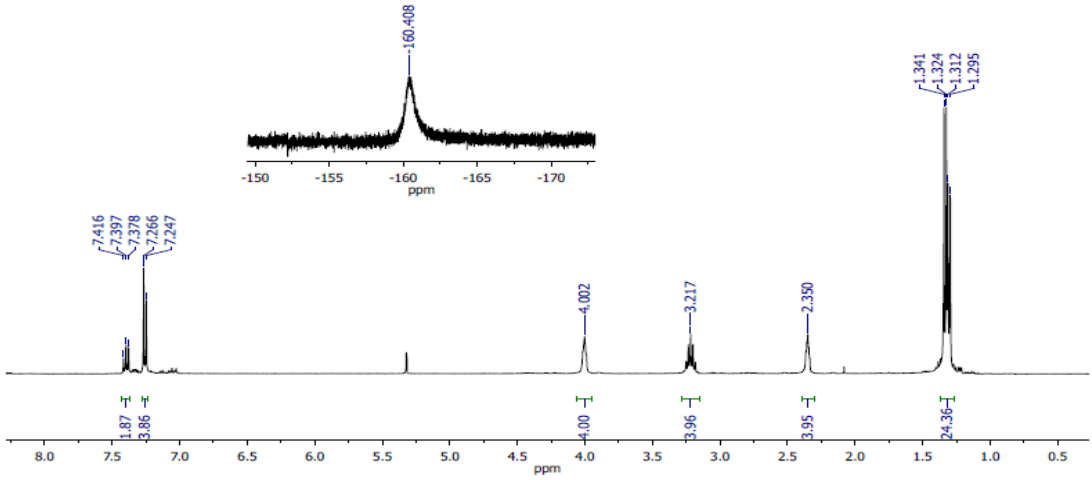

Figure 4.23 ^1H NMR spectrum in CD_2Cl_2 of **16** after reaction with $NO^+ BF_4^-$ with ^{19}F NMR spectra overlaid.

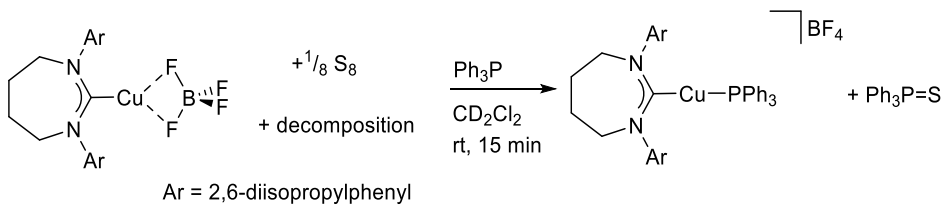

Scheme 4.12 Addition of triphenylphosphine.

Triphenylphosphine (0.026 g, 0.100 mmol) was then added, and the solution and reanalyzed by NMR spectroscopy.

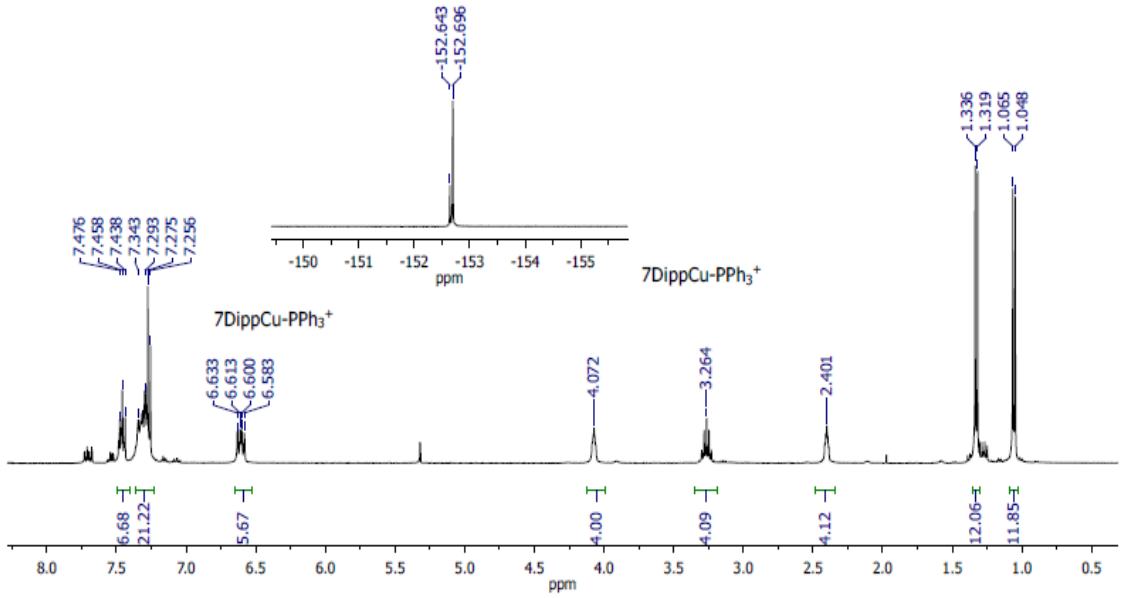

Figure 4.24 ^{1}H spectrum in CD_2Cl_2 following addition of PPh_3 with the ^{19}F NMR spectrum overlaid.

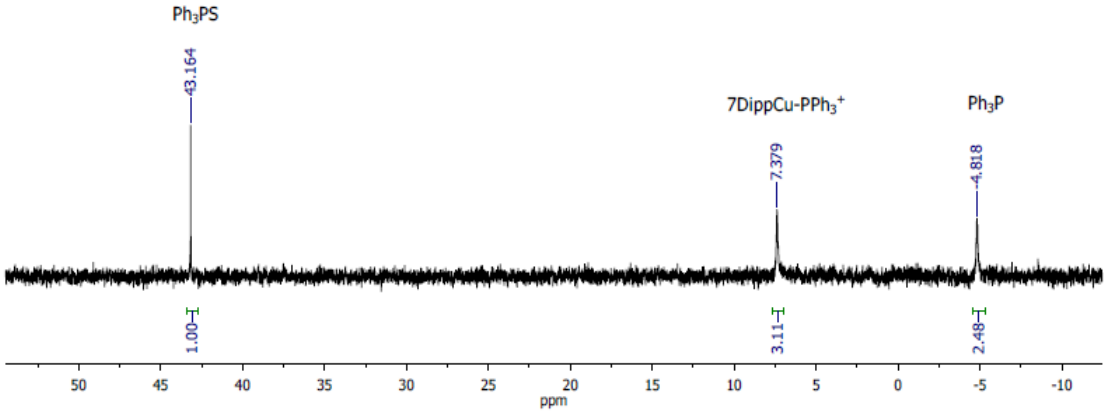

Figure 4.25 ^{31}P spectrum following addition of PPh_3 in CD_2Cl_2.

4.4.4.12 Nitrosonium Reactivity of **19**

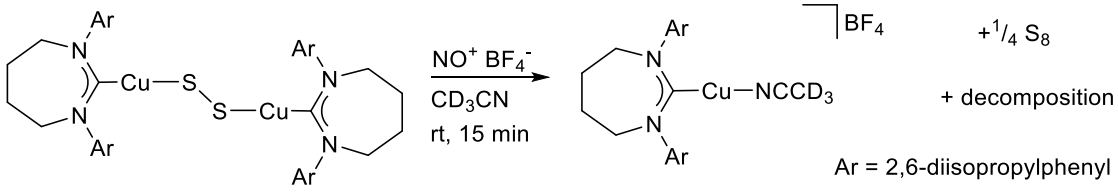

Scheme 4.13 Nitrosonium Reactivity of **19**.

$NO^+ BF_4^-$ (0.04 g, 0.034 mmol) was added to a solution of $(7DippCuS)_2$ (0.035 g, 0.034 mmol) in CD_3CN (1 mL) at room temperature. The mixture was allowed to stir for 15 min before the ^1H NMR spectrum was recorded.

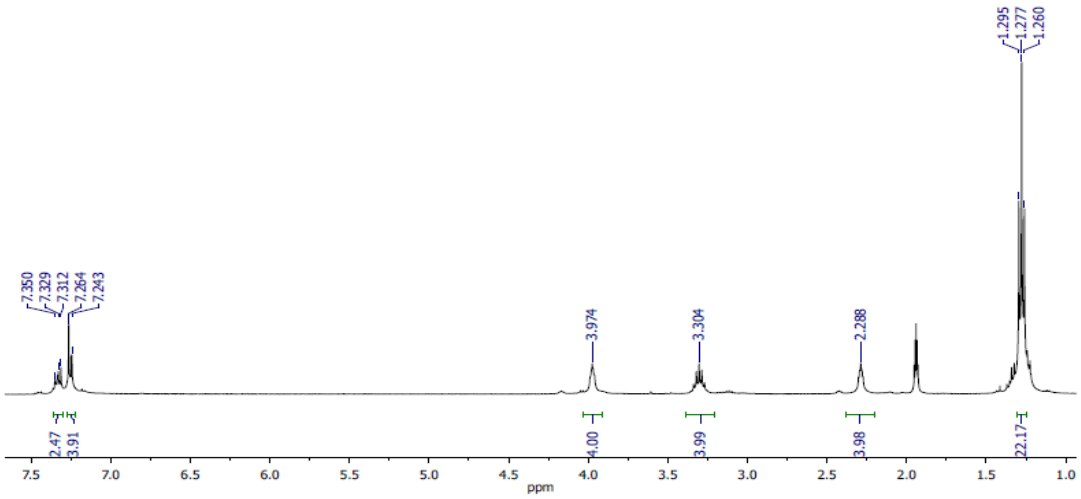

Figure 4.26. ^{1}H NMR spectrum following addition of $NO^{+}BF_4^{-}$ to **19,** resulting in **20** in CD_3CN.

Triphenylphosphine (0.026 g, 0.099 mmol) was added and the ^{1}H and ^{31}P NMR spectra were recorded after 15 min.

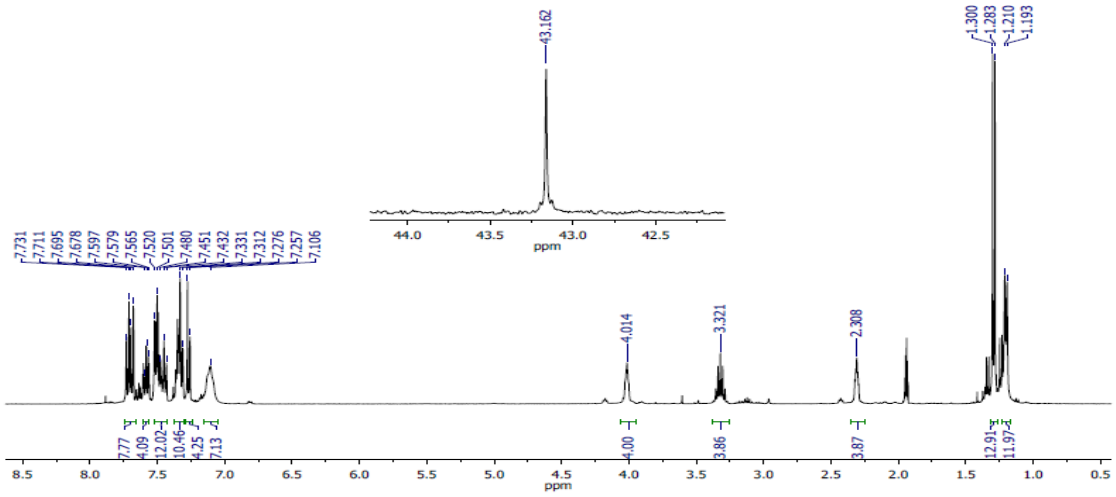

Figure 4.27 ^{1}H and ^{31}P NMR spectra following addition of Ph_3P, resulting in $Ph_3P{=}S$ in CD_3CN.

4.4.4.13 Generation of (7Dipp)CuBF$_4$

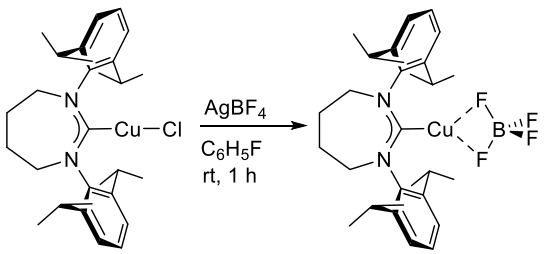

Scheme 4.14 Generation of (7Dipp)CuBF$_4$.

(7Dipp)CuBF$_4$ (7Dipp)CuCl (0.092 g, 0.18 mmol) and silver tetrafluoroborate (0.035 g, 0.18 mmol) were combined in a 20-mL vial, equipped with a stirbar, before C_6H_5F (5 mL) was added. The mixture was allowed to stir for 1h, filtered thought Celite, before the resulting colorless solution was concentrated *in vacuo* to afford the product as a colorless solid. (0.090 g, 89% yield) ^{1}H NMR (400 MHz, CD_2Cl_2): δ (ppm) 7.43 (t, $^3J_{HH}$ = 7.6 Hz, 2H, para-C*H*), 7.25 (d, $^3J_{HH}$ = 7.6 Hz, 4H, *meta*-C*H*), 4.00 (m, 4H, NCH_2), 3.21 (sept, $^3J_{HH}$ = 6.8 Hz, 4H, C*H*(CH_3)$_2$), 2.35 (m, 4H, NCH_2CH_2), 1.33 (d, $^3J_{HH}$ = 6.8 Hz, 12H, $CH_2(CH_3)_2$), 1.29 (d, $^3J_{HH}$ = 6.8 Hz, 12H, $CH_2(CH_3)_2$). ^{13}C{^{1}H} NMR (176 MHz CD_2Cl_2): δ (ppm) 145.4 (*ortho*-C), 144.3 (*ipso*-*C*), 129.6 (*para*-*C*), 125.4 (*meta*-*C*), 54.4 (N*C*H_2), 29.2 (*C*H(CH_3)$_2$), 25.5(NCH_2CH_2), 24.8 (CH(*C*H_3)$_2$). ^{11}B NMR (128 MHz, CD_2Cl_2): δ (ppm) –1.8 (s, 1B, *B*F_4^-). ^{19}F NMR (378 MHz, CD_2Cl_2): δ (ppm) –161.9 (br s, 4F, B*F*$_4^-$).

Note: The carbene-*C* resonance could not be resolved despite prolonged acquisition time. We suggest the signal is broadened by coupling to the BF_4^-. The complex is extremely air- and moisture-sensitive. A small amount of $HOBF_3^-$ (1:1:1:1 quartet, under 5%)[44] is typically observed in the ^{19}F NMR spectrum (see below) but continues to grow in over

time. In the solid-state, decomposition is observed within 24h at room-temperature while under an inert atmosphere.

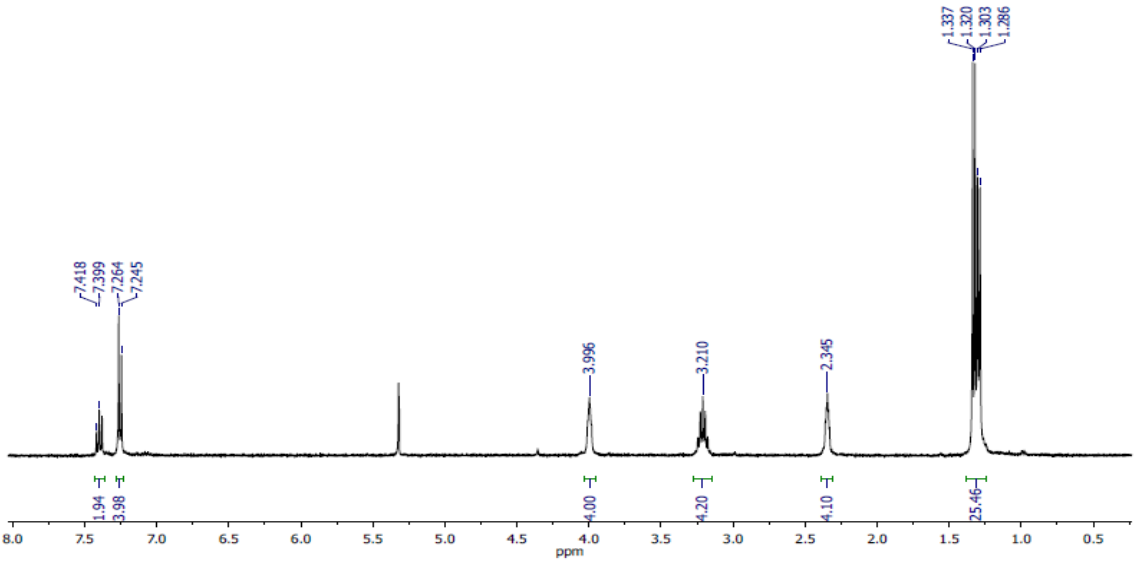

Figure 4.28 ^{1}H NMR spectrum of (7Dipp)CuBF$_4$ in CD_2Cl_2.

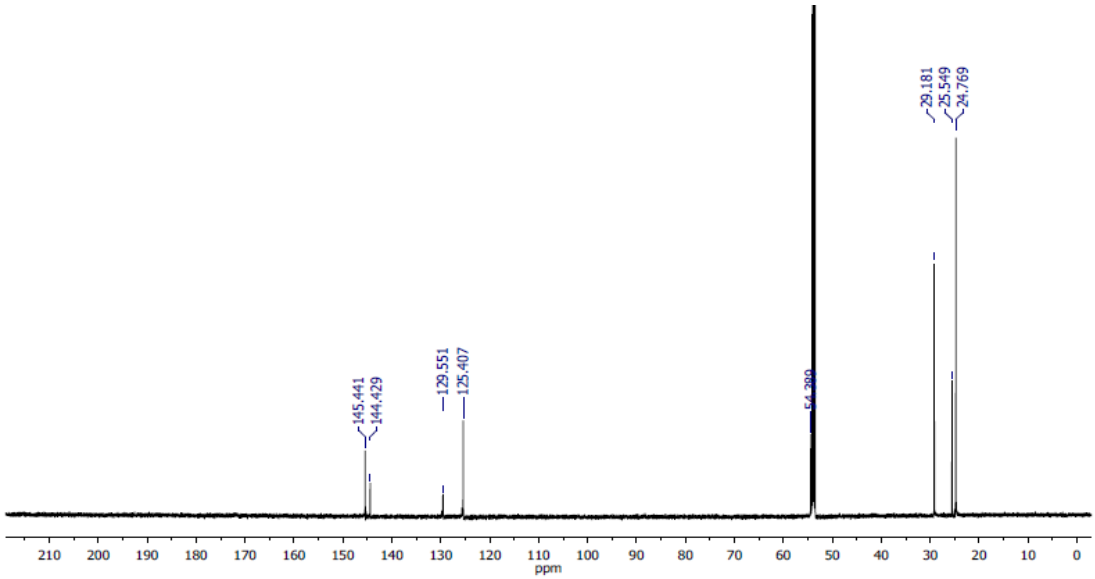

Figure 4.29 ^{13}C NMR spectrum of (7Dipp)CuBF$_4$ in CD_2Cl_2.

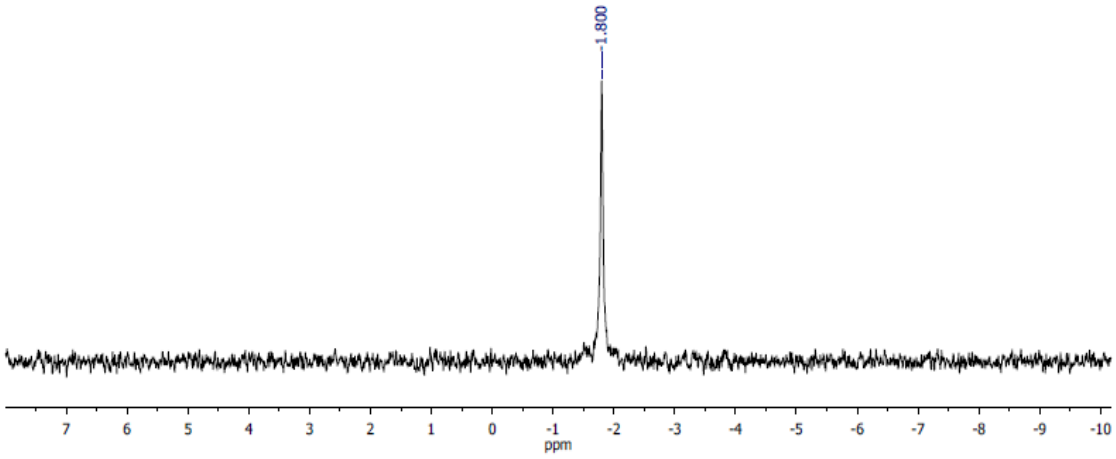

Figure 4.30 ^{11}B NMR spectrum of (7Dipp)$CuBF_4$ in CD_2Cl_2.

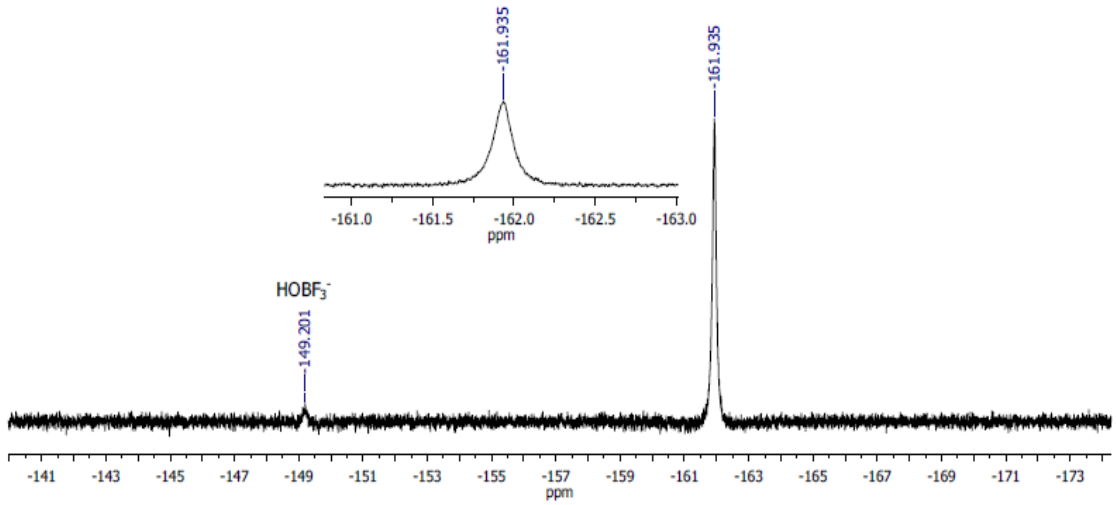

Figure 4.31 ^{19}F NMR spectrum of (7Dipp)$CuBF_4$ in CD_2Cl_2.

4.4.4.14 Nitrosonium Reactivity of $[(7Dipp)CuH]_2$

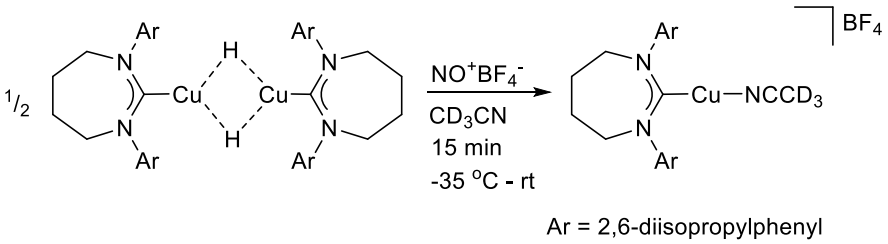

Scheme 4.15 Nitrosonium Reactivity of $[(7Dipp)CuH]_2$

$[(7Dipp)CuH]_2$ (0.015 g, 0.016 mmol) and $NO^+ BF_4^-$ (0.04 g, 0.034 mmol) were dissolved in CD_3CN (0.75 mL) at –35 °C and mixed for 15 min, allowing to warm to room temperature, before the ^1H NMR spectrum was recorded.

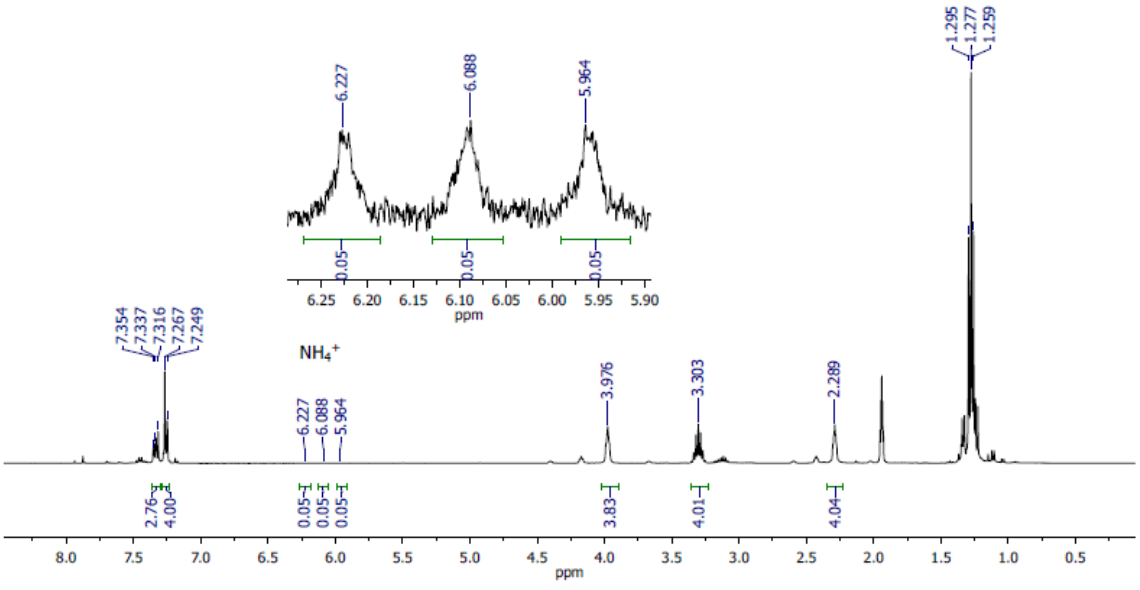

Figure 4.32. ^1H NMR spectrum following addition of $NO^+BF_4^-$ to $[(7Dipp)CuH]_2$.

4.4.5 X-ray Diffraction Studies

Compound **16**

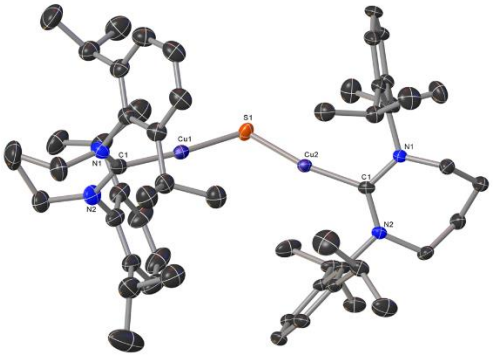

Figure 4.33 Thermal ellipsoid plot of **16**.

Experimental Single crystals of $C_{188}H_{273}Cu_6N_{19}S_3$ **16** were obtained from acetonitrile. A suitable crystal was selected, and the crystal was mounted on a loop with paratone oil on a Bruker D8 Venture diffractometer. The crystal was kept at 100(2) K during data collection. Using Olex2,[4] the structure was solved with the ShelXT[5] structure solution program using Intrinsic Phasing and refined with the ShelXL[6] refinement package using Least Squares minimization.

Crystal Data for $C_{188}H_{273}Cu_6N_{19}S_3$ (M =3276.75 g/mol): monoclinic, space group P2/n (no. 13), a = 24.8277(13) Å, b = 12.3758(7) Å, c = 62.737(3) Å, β = 97.108(3)°, V = 19128.6(17) Å^3, Z = 4, T = 100(2) K, μ(CuKα) = 1.424 mm^{-1}, $Dcalc$ = 1.138 g/cm^3, 142144 reflections measured (5.218° ≤ 2Θ ≤ 130.166°), 32605 unique (R_{int} = 0.0744, R_{sigma} = 0.0549) which were used in all calculations. The final R_1 was 0.0655 (I > 2σ(I)) and wR_2 was 0.1751 (all data).

Table 4.1 Crystal Data for **16**

Compound	**16**
Empirical formula	$C_{188}H_{273}Cu_6N_{19}S_3$
Formula weight	3276.75
Temperature/K	100(2)
Crystal system	monoclinic
Space group	P2/n
a/Å	24.8277(13)
b/Å	12.3758(7)
c/Å	62.737(3)
α/°	90
β/°	97.108(3)
γ/°	90
Volume/Å^3	19128.6(17)
Z	4
ρ_{calc}g/cm^3	1.138
μ/mm^{-1}	1.424
F(000)	7023.0
Crystal size/mm^3	0.257 × 0.228 × 0.146
Radiation	CuKα (λ = 1.54178)
2Θ range for data collection/°	5.218 to 130.166
Index ranges	$-26 \leq h \leq 29$, $-14 \leq k \leq 14$, $-73 \leq l \leq 73$
Reflections collected	142144
Independent reflections	32605 [R_{int} = 0.0744, R_{sigma} = 0.0549]
Data/restraints/parameters	32605/2766/2000
Goodness-of-fit on F^2	1.027
Final R indexes [I>=2σ (I)]	R_1 = 0.0655, wR_2 = 0.1647
Final R indexes [all data]	R_1 = 0.0828, wR_2 = 0.1751
Largest diff. peak/hole / e Å^{-3}	2.72/-1.27

Table 4.2 Bond Lengths (Å) for **16**

Atom	Atom	Length/Å	Atom	Atom	Length/Å
Cu1	Cu2	3.5816(7)	C27_10	C29_10	1.530(3)
Cu1	S1	2.1115(11)	N1_11	C1_11	1.345(2)
Cu1	C1_8	1.912(3)	N1_11	C2_11	1.479(2)
Cu2	S1	2.1236(10)	N1_11	C6_11	1.453(2)
Cu2	C1_9	1.916(2)	N2_11	C1_11	1.347(2)
Cu3	Cu4	3.4751(7)	N2_11	C5_11	1.484(2)
Cu3	S2	2.1171(10)	N2_11	C18_11	1.451(2)
Cu3	C1_10	1.909(2)	C2_11	C3_11	1.513(3)
Cu4	S2	2.1081(11)	C3_11	C4_11	1.531(3)
Cu4	C1_11	1.892(3)	C4_11	C5_11	1.520(3)
Cu5	Cu5[1]	3.5959(10)	C6_11	C7_11	1.398(3)
Cu5	S3	2.1128(10)	C6_11	C11_11	1.404(2)
Cu5	C1_13	1.900(2)	C7_11	C8_11	1.393(3)
Cu6	Cu6[2]	3.6774(11)	C7_11	C12_11	1.522(3)
Cu6	S4	2.1159(10)	C8_11	C9_11	1.394(3)
Cu6	C1_12	1.904(2)	C9_11	C10_11	1.374(3)
N1_8	C1_8	1.344(2)	C10_11	C11_11	1.393(3)
N1_8	C2_8	1.479(2)	C11_11	C15_11	1.519(3)
N1_8	C6_8	1.454(2)	C12_11	C13_11	1.532(3)
N2_8	C1_8	1.350(2)	C12_11	C14_11	1.530(3)
N2_8	C5_8	1.485(2)	C15_11	C16_11	1.526(3)
N2_8	C18_8	1.451(2)	C15_11	C17_11	1.542(3)
C2_8	C3_8	1.512(3)	C18_11	C19_11	1.398(2)
C3_8	C4_8	1.531(3)	C18_11	C23_11	1.401(2)
C4_8	C5_8	1.519(3)	C19_11	C20_11	1.401(3)
C6_8	C7_8	1.398(3)	C19_11	C24_11	1.516(2)
C6_8	C11_8	1.404(2)	C20_11	C21_11	1.384(3)
C7_8	C8_8	1.394(3)	C21_11	C22_11	1.385(3)
C7_8	C12_8	1.521(3)	C22_11	C23_11	1.395(3)
C8_8	C9_8	1.393(3)	C23_11	C27_11	1.527(3)
C9_8	C10_8	1.374(3)	C24_11	C25_11	1.528(3)
C10_8	C11_8	1.393(3)	C24_11	C26_11	1.534(3)
C11_8	C15_8	1.519(3)	C27_11	C28_11	1.527(3)
C12_8	C13_8	1.532(3)	C27_11	C29_11	1.528(3)
C12_8	C14_8	1.530(3)	N1_12	C1_12	1.344(2)
C15_8	C16_8	1.527(3)	N1_12	C2_12	1.476(2)
C15_8	C17_8	1.541(3)	N1_12	C6_12	1.456(2)
C18_8	C19_8	1.398(3)	N2_12	C1_12	1.348(2)

C18_8	C23_8	1.400(2)	N2_12	C5_12	1.486(2)
C19_8	C20_8	1.401(3)	N2_12	C18_12	1.448(2)
C19_8	C24_8	1.518(2)	C2_12	C3_12	1.511(3)
C20_8	C21_8	1.383(3)	C3_12	C4_12	1.532(3)
C21_8	C22_8	1.385(3)	C4_12	C5_12	1.520(3)
C22_8	C23_8	1.395(3)	C6_12	C7_12	1.397(3)
C23_8	C27_8	1.527(3)	C6_12	C11_12	1.403(2)
C24_8	C25_8	1.529(3)	C7_12	C8_12	1.393(3)
C24_8	C26_8	1.534(3)	C7_12	C12_12	1.520(3)
C27_8	C28_8	1.530(3)	C8_12	C9_12	1.393(3)
C27_8	C29_8	1.531(3)	C9_12	C10_12	1.373(3)
N1_9	C1_9	1.346(2)	C10_12	C11_12	1.393(3)
N1_9	C2_9	1.481(2)	C11_12	C15_12	1.518(3)
N1_9	C6_9	1.454(2)	C12_12	C13_12	1.531(3)
N2_9	C1_9	1.349(2)	C12_12	C14_12	1.529(3)
N2_9	C5_9	1.484(2)	C15_12	C16_12	1.527(3)
N2_9	C18_9	1.452(2)	C15_12	C17_12	1.543(3)
C2_9	C3_9	1.514(3)	C18_12	C19_12	1.400(3)
C3_9	C4_9	1.532(3)	C18_12	C23_12	1.400(2)
C4_9	C5_9	1.518(3)	C19_12	C20_12	1.401(3)
C6_9	C7_9	1.399(3)	C19_12	C24_12	1.517(3)
C6_9	C11_9	1.403(2)	C20_12	C21_12	1.383(3)
C7_9	C8_9	1.393(2)	C21_12	C22_12	1.385(3)
C7_9	C12_9	1.521(3)	C22_12	C23_12	1.396(3)
C8_9	C9_9	1.393(3)	C23_12	C27_12	1.527(3)
C9_9	C10_9	1.374(3)	C24_12	C25_12	1.529(3)
C10_9	C11_9	1.393(3)	C24_12	C26_12	1.534(3)
C11_9	C15_9	1.519(3)	C27_12	C28_12	1.529(3)
C12_9	C13_9	1.531(3)	C27_12	C29_12	1.532(3)
C12_9	C14_9	1.530(3)	N1_13	C1_13	1.344(2)
C15_9	C16_9	1.527(3)	N1_13	C2_13	1.479(2)
C15_9	C17_9	1.543(3)	N1_13	C6_13	1.453(2)
C18_9	C19_9	1.398(2)	N2_13	C1_13	1.349(2)
C18_9	C23_9	1.401(2)	N2_13	C5_13	1.484(2)
C19_9	C20_9	1.402(3)	N2_13	C18_13	1.450(2)
C19_9	C24_9	1.517(2)	C2_13	C3_13	1.512(3)
C20_9	C21_9	1.383(3)	C3_13	C4_13	1.531(3)
C21_9	C22_9	1.385(3)	C4_13	C5_13	1.518(3)
C22_9	C23_9	1.394(3)	C6_13	C7_13	1.399(3)
C23_9	C27_9	1.525(3)	C6_13	C11_13	1.404(2)
C24_9	C25_9	1.530(3)	C7_13	C8_13	1.394(3)
C24_9	C26_9	1.535(3)	C7_13	C12_13	1.520(3)

C27_9	C28_9	1.528(3)	C8_13	C9_13	1.393(3)
C27_9	C29_9	1.530(3)	C9_13	C10_13	1.374(3)
N1_10	C1_10	1.346(2)	C10_13	C11_13	1.393(3)
N1_10	C2_10	1.481(2)	C11_13	C15_13	1.520(3)
N1_10	C6_10	1.453(2)	C12_13	C13_13	1.533(3)
N2_10	C1_10	1.349(2)	C12_13	C14_13	1.531(3)
N2_10	C5_10	1.485(2)	C15_13	C16_13	1.527(3)
N2_10	C18_10	1.451(2)	C15_13	C17_13	1.543(3)
C2_10	C3_10	1.512(3)	C18_13	C19_13	1.397(3)
C3_10	C4_10	1.533(3)	C18_13	C23_13	1.401(2)
C4_10	C5_10	1.519(3)	C19_13	C20_13	1.402(3)
C6_10	C7_10	1.398(3)	C19_13	C24_13	1.517(3)
C6_10	C11_10	1.403(2)	C20_13	C21_13	1.383(3)
C7_10	C8_10	1.393(3)	C21_13	C22_13	1.385(3)
C7_10	C12_10	1.521(3)	C22_13	C23_13	1.395(3)
C8_10	C9_10	1.394(3)	C23_13	C27_13	1.526(3)
C9_10	C10_10	1.374(3)	C24_13	C25_13	1.529(3)
C10_10	C11_10	1.393(3)	C24_13	C26_13	1.536(3)
C11_10	C15_10	1.519(3)	C27_13	C28_13	1.529(3)
C12_10	C13_10	1.532(3)	C27_13	C29_13	1.530(3)
C12_10	C14_10	1.529(3)	N1S_2	C2S_2	1.128(3)
C15_10	C16_10	1.527(3)	C2S_2	C3S_2	1.440(3)
C15_10	C17_10	1.542(3)	N1S_3	C2S_3	1.128(3)
C18_10	C19_10	1.398(2)	C2S_3	C3S_3	1.441(3)
C18_10	C23_10	1.399(2)	N1S_4	C2S_4	1.128(3)
C19_10	C20_10	1.401(3)	C2S_4	C3S_4	1.440(3)
C19_10	C24_10	1.517(2)	N1S_5	C2S_5	1.128(3)
C20_10	C21_10	1.383(3)	C2S_5	C3S_5	1.440(3)
C21_10	C22_10	1.385(3)	N1S_6	C2S_6	1.129(3)
C22_10	C23_10	1.396(3)	C2S_6	C3S_6	1.439(3)
C23_10	C27_10	1.526(3)	N1S_7	C2S_7	1.128(3)
C24_10	C25_10	1.529(3)	C2S_7	C3S_7	1.441(3)
C24_10	C26_10	1.536(3)	N1S_1	C2S_1	1.129(3)
C27_10	C28_10	1.528(3)	C2S_1	C3S_1	1.441(3)

Table 4.3 Bond Angles (deg) for **16**

Atom	Atom	Atom	Angle/°	Atom	Atom	Atom	Angle/°
S1	Cu1	Cu2	32.36(3)	C22_10	C23_10	C27_10	119.62(19)
C1_8	Cu1	Cu2	154.64(10)	C19_10	C24_10	C25_10	111.8(2)
C1_8	Cu1	S1	172.83(10)	C19_10	C24_10	C26_10	110.98(19)
S1	Cu2	Cu1	32.15(3)	C25_10	C24_10	C26_10	109.8(2)
C1_9	Cu2	Cu1	163.25(8)	C23_10	C27_10	C28_10	110.7(2)
C1_9	Cu2	S1	164.29(9)	C23_10	C27_10	C29_10	111.8(2)
S2	Cu3	Cu4	34.58(3)	C28_10	C27_10	C29_10	110.9(2)
C1_10	Cu3	Cu4	161.23(8)	C1_11	N1_11	C2_11	125.3(2)
C1_10	Cu3	S2	163.95(9)	C1_11	N1_11	C6_11	117.61(19)
S2	Cu4	Cu3	34.75(3)	C6_11	N1_11	C2_11	115.60(19)
C1_11	Cu4	Cu3	156.32(9)	C1_11	N2_11	C5_11	129.56(19)
C1_11	Cu4	S2	168.61(10)	C1_11	N2_11	C18_11	117.00(19)
S3	Cu5	$Cu5^{1}$	31.68(4)	C18_11	N2_11	C5_11	113.40(18)
C1_13	Cu5	$Cu5^{1}$	160.01(9)	N1_11	C1_11	Cu4	119.86(16)
C1_13	Cu5	S3	168.27(10)	N1_11	C1_11	N2_11	118.3(2)
S4	Cu6	$Cu6^{2}$	29.66(4)	N2_11	C1_11	Cu4	121.62(17)
C1_12	Cu6	$Cu6^{2}$	161.01(9)	N1_11	C2_11	C3_11	113.5(2)
C1_12	Cu6	S4	168.98(11)	C2_11	C3_11	C4_11	111.4(2)
Cu1	S1	Cu2	115.49(4)	C5_11	C4_11	C3_11	112.1(2)
Cu4	S2	Cu3	110.67(4)	N2_11	C5_11	C4_11	113.7(2)
$Cu5^{1}$	S3	Cu5	116.63(8)	C7_11	C6_11	N1_11	118.69(18)
Cu6	S4	$Cu6^{2}$	120.68(8)	C7_11	C6_11	C11_11	122.30(18)
C1_8	N1_8	C2_8	125.7(2)	C11_11	C6_11	N1_11	118.99(19)
C1_8	N1_8	C6_8	118.22(19)	C6_11	C7_11	C12_11	122.82(19)
C6_8	N1_8	C2_8	115.26(19)	C8_11	C7_11	C6_11	117.73(19)
C1_8	N2_8	C5_8	129.18(19)	C8_11	C7_11	C12_11	119.4(2)
C1_8	N2_8	C18_8	116.62(19)	C7_11	C8_11	C9_11	120.8(2)
C18_8	N2_8	C5_8	113.46(19)	C10_11	C9_11	C8_11	120.2(2)
N1_8	C1_8	Cu1	122.19(16)	C9_11	C10_11	C11_11	121.2(2)
N1_8	C1_8	N2_8	117.8(2)	C6_11	C11_11	C15_11	122.2(2)
N2_8	C1_8	Cu1	120.01(16)	C10_11	C11_11	C6_11	117.7(2)
N1_8	C2_8	C3_8	114.1(2)	C10_11	C11_11	C15_11	120.0(2)
C2_8	C3_8	C4_8	111.2(2)	C7_11	C12_11	C13_11	112.0(2)
C5_8	C4_8	C3_8	112.2(2)	C7_11	C12_11	C14_11	110.3(2)
N2_8	C5_8	C4_8	114.6(2)	C14_11	C12_11	C13_11	110.5(2)
C7_8	C6_8	N1_8	118.47(18)	C11_11	C15_11	C16_11	111.8(2)
C7_8	C6_8	C11_8	122.28(18)	C11_11	C15_11	C17_11	110.9(2)
C11_8	C6_8	N1_8	119.22(19)	C16_11	C15_11	C17_11	110.9(2)

C6_8	C7_8	C12_8	122.29(19)	C19_11	C18_11	N2_11	119.24(18)
C8_8	C7_8	C6_8	118.07(19)	C19_11	C18_11	C23_11	122.92(18)
C8_8	C7_8	C12_8	119.6(2)	C23_11	C18_11	N2_11	117.77(19)
C9_8	C8_8	C7_8	120.4(2)	C18_11	C19_11	C20_11	117.20(19)
C10_8	C9_8	C8_8	120.3(2)	C18_11	C19_11	C24_11	122.94(19)
C9_8	C10_8	C11_8	121.5(2)	C20_11	C19_11	C24_11	119.9(2)
C6_8	C11_8	C15_8	122.5(2)	C21_11	C20_11	C19_11	120.8(2)
C10_8	C11_8	C6_8	117.4(2)	C20_11	C21_11	C22_11	120.7(2)
C10_8	C11_8	C15_8	120.1(2)	C21_11	C22_11	C23_11	120.5(2)
C7_8	C12_8	C13_8	111.6(2)	C18_11	C23_11	C27_11	121.54(19)
C7_8	C12_8	C14_8	110.5(2)	C22_11	C23_11	C18_11	117.71(19)
C14_8	C12_8	C13_8	110.7(2)	C22_11	C23_11	C27_11	120.47(19)
C11_8	C15_8	C16_8	111.5(2)	C19_11	C24_11	C25_11	112.5(2)
C11_8	C15_8	C17_8	111.4(2)	C19_11	C24_11	C26_11	111.7(2)
C16_8	C15_8	C17_8	111.0(2)	C25_11	C24_11	C26_11	110.0(2)
C19_8	C18_8	N2_8	118.62(18)	C23_11	C27_11	C28_11	110.5(2)
C19_8	C18_8	C23_8	122.69(19)	C23_11	C27_11	C29_11	112.3(2)
C23_8	C18_8	N2_8	118.69(19)	C28_11	C27_11	C29_11	111.1(2)
C18_8	C19_8	C20_8	117.57(19)	C1_12	N1_12	C2_12	128.63(18)
C18_8	C19_8	C24_8	122.59(19)	C1_12	N1_12	C6_12	116.54(19)
C20_8	C19_8	C24_8	119.8(2)	C6_12	N1_12	C2_12	114.64(18)
C21_8	C20_8	C19_8	120.6(2)	C1_12	N2_12	C5_12	126.73(19)
C20_8	C21_8	C22_8	120.6(2)	C1_12	N2_12	C18_12	118.43(19)
C21_8	C22_8	C23_8	120.8(2)	C18_12	N2_12	C5_12	114.22(18)
C18_8	C23_8	C27_8	121.8(2)	N1_12	C1_12	Cu6	120.95(15)
C22_8	C23_8	C18_8	117.7(2)	N1_12	C1_12	N2_12	118.11(19)
C22_8	C23_8	C27_8	120.3(2)	N2_12	C1_12	Cu6	120.90(16)
C19_8	C24_8	C25_8	111.7(2)	N1_12	C2_12	C3_12	115.2(2)
C19_8	C24_8	C26_8	111.6(2)	C2_12	C3_12	C4_12	111.6(2)
C25_8	C24_8	C26_8	110.0(2)	C5_12	C4_12	C3_12	112.09(19)
C23_8	C27_8	C28_8	111.3(2)	N2_12	C5_12	C4_12	113.6(2)
C23_8	C27_8	C29_8	111.4(2)	C7_12	C6_12	N1_12	118.05(19)
C28_8	C27_8	C29_8	110.0(2)	C7_12	C6_12	C11_12	122.73(18)
C1_9	N1_9	C2_9	124.90(18)	C11_12	C6_12	N1_12	119.20(19)
C1_9	N1_9	C6_9	118.38(18)	C6_12	C7_12	C12_12	122.21(19)
C6_9	N1_9	C2_9	115.15(18)	C8_12	C7_12	C6_12	117.76(19)
C1_9	N2_9	C5_9	129.36(18)	C8_12	C7_12	C12_12	120.0(2)
C1_9	N2_9	C18_9	117.35(18)	C9_12	C8_12	C7_12	120.4(2)
C18_9	N2_9	C5_9	113.23(17)	C10_12	C9_12	C8_12	120.6(2)
N1_9	C1_9	Cu2	118.24(14)	C9_12	C10_12	C11_12	121.3(2)
N1_9	C1_9	N2_9	117.74(19)	C6_12	C11_12	C15_12	122.73(19)
N2_9	C1_9	Cu2	123.59(16)	C10_12	C11_12	C6_12	117.2(2)

N1_9	C2_9	C3_9	113.5(2)	C10_12	C11_12	C15_12	120.0(2)
C2_9	C3_9	C4_9	110.95(19)	C7_12	C12_12	C13_12	111.7(2)
C5_9	C4_9	C3_9	112.4(2)	C7_12	C12_12	C14_12	110.4(2)
N2_9	C5_9	C4_9	114.71(19)	C14_12	C12_12	C13_12	111.1(2)
C7_9	C6_9	N1_9	118.22(18)	C11_12	C15_12	C16_12	111.5(2)
C7_9	C6_9	C11_9	122.19(18)	C11_12	C15_12	C17_12	111.3(2)
C11_9	C6_9	N1_9	119.50(18)	C16_12	C15_12	C17_12	110.5(2)
C6_9	C7_9	C12_9	122.34(18)	C19_12	C18_12	N2_12	118.90(19)
C8_9	C7_9	C6_9	118.05(19)	C23_12	C18_12	N2_12	118.63(19)
C8_9	C7_9	C12_9	119.59(19)	C23_12	C18_12	C19_12	122.25(19)
C9_9	C8_9	C7_9	120.5(2)	C18_12	C19_12	C20_12	117.6(2)
C10_9	C9_9	C8_9	120.2(2)	C18_12	C19_12	C24_12	122.59(19)
C9_9	C10_9	C11_9	121.5(2)	C20_12	C19_12	C24_12	119.5(2)
C6_9	C11_9	C15_9	122.68(18)	C21_12	C20_12	C19_12	120.9(2)
C10_9	C11_9	C6_9	117.41(19)	C20_12	C21_12	C22_12	120.3(2)
C10_9	C11_9	C15_9	119.89(19)	C21_12	C22_12	C23_12	120.7(2)
C7_9	C12_9	C13_9	112.0(2)	C18_12	C23_12	C27_12	122.3(2)
C7_9	C12_9	C14_9	110.0(2)	C22_12	C23_12	C18_12	118.0(2)
C14_9	C12_9	C13_9	110.7(2)	C22_12	C23_12	C27_12	119.6(2)
C11_9	C15_9	C16_9	111.8(2)	C19_12	C24_12	C25_12	111.3(2)
C11_9	C15_9	C17_9	111.1(2)	C19_12	C24_12	C26_12	111.8(2)
C16_9	C15_9	C17_9	110.5(2)	C25_12	C24_12	C26_12	110.1(2)
C19_9	C18_9	N2_9	119.15(18)	C23_12	C27_12	C28_12	110.7(2)
C19_9	C18_9	C23_9	122.60(18)	C23_12	C27_12	C29_12	111.5(2)
C23_9	C18_9	N2_9	117.98(18)	C28_12	C27_12	C29_12	110.7(2)
C18_9	C19_9	C20_9	117.46(19)	C1_13	N1_13	C2_13	125.74(19)
C18_9	C19_9	C24_9	123.16(19)	C1_13	N1_13	C6_13	118.13(18)
C20_9	C19_9	C24_9	119.37(19)	C6_13	N1_13	C2_13	115.25(18)
C21_9	C20_9	C19_9	120.9(2)	C1_13	N2_13	C5_13	129.43(18)
C20_9	C21_9	C22_9	120.5(2)	C1_13	N2_13	C18_13	116.95(19)
C21_9	C22_9	C23_9	120.8(2)	C18_13	N2_13	C5_13	113.41(18)
C18_9	C23_9	C27_9	122.13(19)	N1_13	C1_13	Cu5	119.60(15)
C22_9	C23_9	C18_9	117.75(19)	N1_13	C1_13	N2_13	117.66(19)
C22_9	C23_9	C27_9	120.12(19)	N2_13	C1_13	Cu5	122.74(15)
C19_9	C24_9	C25_9	111.6(2)	N1_13	C2_13	C3_13	113.7(2)
C19_9	C24_9	C26_9	111.3(2)	C2_13	C3_13	C4_13	111.06(19)
C25_9	C24_9	C26_9	109.8(2)	C5_13	C4_13	C3_13	112.5(2)
C23_9	C27_9	C28_9	111.0(2)	N2_13	C5_13	C4_13	114.5(2)
C23_9	C27_9	C29_9	112.2(2)	C7_13	C6_13	N1_13	118.56(18)
C28_9	C27_9	C29_9	110.5(2)	C7_13	C6_13	C11_13	122.25(18)
C1_10	N1_10	C2_10	124.89(18)	C11_13	C6_13	N1_13	119.04(19)
C1_10	N1_10	C6_10	118.17(18)	C6_13	C7_13	C12_13	122.71(19)

C6_10	N1_10	C2_10	115.20(18)	C8_13	C7_13	C6_13	117.91(19)
C1_10	N2_10	C5_10	129.37(18)	C8_13	C7_13	C12_13	119.32(19)
C1_10	N2_10	C18_10	117.29(18)	C9_13	C8_13	C7_13	120.6(2)
C18_10	N2_10	C5_10	113.25(17)	C10_13	C9_13	C8_13	120.3(2)
N1_10	C1_10	Cu3	117.79(14)	C9_13	C10_13	C11_13	121.3(2)
N1_10	C1_10	N2_10	117.73(19)	C6_13	C11_13	C15_13	122.39(19)
N2_10	C1_10	Cu3	124.01(16)	C10_13	C11_13	C6_13	117.59(19)
N1_10	C2_10	C3_10	113.5(2)	C10_13	C11_13	C15_13	119.78(19)
C2_10	C3_10	C4_10	110.90(19)	C7_13	C12_13	C13_13	112.0(2)
C5_10	C4_10	C3_10	111.9(2)	C7_13	C12_13	C14_13	110.2(2)
N2_10	C5_10	C4_10	114.32(19)	C14_13	C12_13	C13_13	110.6(2)
C7_10	C6_10	N1_10	118.57(18)	C11_13	C15_13	C16_13	112.0(2)
C7_10	C6_10	C11_10	121.98(18)	C11_13	C15_13	C17_13	110.7(2)
C11_10	C6_10	N1_10	119.45(19)	C16_13	C15_13	C17_13	110.8(2)
C6_10	C7_10	C12_10	122.36(19)	C19_13	C18_13	N2_13	119.38(19)
C8_10	C7_10	C6_10	118.08(19)	C19_13	C18_13	C23_13	122.52(18)
C8_10	C7_10	C12_10	119.5(2)	C23_13	C18_13	N2_13	118.03(19)
C7_10	C8_10	C9_10	120.6(2)	C18_13	C19_13	C20_13	117.58(19)
C10_10	C9_10	C8_10	120.1(2)	C18_13	C19_13	C24_13	123.23(19)
C9_10	C10_10	C11_10	121.4(2)	C20_13	C19_13	C24_13	119.2(2)
C6_10	C11_10	C15_10	122.91(19)	C21_13	C20_13	C19_13	120.7(2)
C10_10	C11_10	C6_10	117.6(2)	C20_13	C21_13	C22_13	120.7(2)
C10_10	C11_10	C15_10	119.51(19)	C21_13	C22_13	C23_13	120.5(2)
C7_10	C12_10	C13_10	111.6(2)	C18_13	C23_13	C27_13	121.8(2)
C7_10	C12_10	C14_10	110.3(2)	C22_13	C23_13	C18_13	117.9(2)
C14_10	C12_10	C13_10	110.9(2)	C22_13	C23_13	C27_13	120.1(2)
C11_10	C15_10	C16_10	111.7(2)	C19_13	C24_13	C25_13	111.6(2)
C11_10	C15_10	C17_10	110.9(2)	C19_13	C24_13	C26_13	111.2(2)
C16_10	C15_10	C17_10	110.4(2)	C25_13	C24_13	C26_13	109.9(2)
C19_10	C18_10	N2_10	119.04(18)	C23_13	C27_13	C28_13	110.4(2)
C19_10	C18_10	C23_10	122.36(18)	C23_13	C27_13	C29_13	112.3(2)
C23_10	C18_10	N2_10	118.43(18)	C28_13	C27_13	C29_13	110.7(2)
C18_10	C19_10	C20_10	117.69(19)	N1S_2	C2S_2	C3S_2	177.8(6)
C18_10	C19_10	C24_10	122.91(19)	N1S_3	C2S_3	C3S_3	179.3(6)
C20_10	C19_10	C24_10	119.39(19)	N1S_4	C2S_4	C3S_4	178.7(6)
C21_10	C20_10	C19_10	120.8(2)	N1S_5	C2S_5	C3S_5	178.0(6)
C20_10	C21_10	C22_10	120.5(2)	N1S_6	C2S_6	C3S_6	177.4(9)
C21_10	C22_10	C23_10	120.7(2)	N1S_7	C2S_7	C3S_7	179.8(8)
C18_10	C23_10	C27_10	122.36(19)	N1S_1	C2S_1	C3S_1	179.1(7)
C22_10	C23_10	C18_10	118.00(19)				

Compound **19**

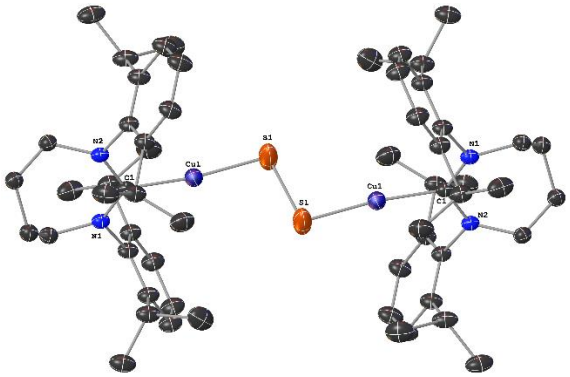

Figure 4.34 Thermal ellipsoid plot of **19**.

Experimental. Single yellow plate-shaped crystals of **19** were chosen from the sample. A suitable crystal 0.39×0.28×0.13 mm^3 was selected and mounted on a loop with paratone oil on a Bruker D8 VENTURE diffractometer. The crystal was kept at T = 100(2) K during data collection. The structure was solved with the ShelXT[5] structure solution program using the Intrinsic Phasing solution method and by using Olex2[4] as the graphical interface. The model was refined with version 2018/3 of ShelXL[7] using Least Squares minimisation.

Crystal Data. $C_{58}H_{84}Cu_2N_4S_2$, M_r = 1028.53, monoclinic, $P2_1/n$ (No. 14), a = 12.3238(9) Å, b = 23.592(2) Å, c = 12.3896(11) Å, β = 91.999(3)°, $\alpha = \gamma$ = 90°, V = 3600.0(5) $Å^3$, T = 100(2) K, Z = 2, Z' = 0.5, $\mu(MoK_\alpha)$ = 0.679 mm^{-1}, 62264 reflections measured, 8228 unique (R_{int} = 0.0389) which were used in all calculations. The final wR_2 was 0.2052 (all data) and R_1 was 0.0649 (I > 2σ(I)).

Table 4.4 Crystal Data for **19**

Compound	**19**
Formula	$C_{58}H_{84}Cu_2N_4S_2$
$D_{calc.}$/ g cm^{-3}	0.949
μ/mm^{-1}	0.679
Formula Weight	1028.53
Colour	yellow
Shape	plate
Size/mm^3	0.39×0.28×0.13
T/K	100(2)
Crystal System	monoclinic
Space Group	$P2_1/n$
a/Å	12.3238(9)
b/Å	23.592(2)
c/Å	12.3896(11)
α/°	90
β/°	91.999(3)
γ/°	90
V/Å^3	3600.0(5)
Z	2
Z'	0.5
Wavelength/Å	0.710730
Radiation type	MoK$_\alpha$
Θ_{min}/°	2.291
Θ_{max}/°	27.482
Measured Refl.	62264
Independent Refl.	8228
Reflections with I > 2(I)	7203
R_{int}	0.0389
Parameters	322
Restraints	302
Largest Peak	1.183
Deepest Hole	-0.628
GooF	1.036
wR_2 (all data)	0.2052
wR_2	0.1992
R_1 (all data)	0.0704
R_1	0.0649

Table 4.5 Bond Length (Å) for **19**

Atom	Atom	Length/Å
C2	C3	1.401(3)
C2	C10	1.396(4)
C2	N1_1	1.456(3)
C2	N1_2	1.454(3)
C3	C4	1.509(4)
C3	C7	1.396(4)
C4	C5	1.527(4)
C4	C6	1.516(4)
C7	C8	1.385(4)
C8	C9	1.383(4)
C9	C10	1.407(4)
C10	C11	1.517(4)
C11	C12	1.523(4)
C11	C13	1.546(5)
C18	C19	1.409(3)
C18	C26	1.393(4)
C18	N2_1	1.454(3)
C18	N2_2	1.458(3)
C19	C20	1.521(4)
C19	C23	1.389(4)
C20	C21	1.525(4)
C20	C22	1.523(4)
C23	C24	1.384(4)
C24	C25	1.396(4)
C25	C26	1.393(4)
C26	C27	1.522(4)
C27	C28	1.529(4)
C27	C29	1.526(5)
S1	$S1^{1}$	2.119(2)
S1	Cu1_1	2.1315(10)
S1	Cu1_2	2.1315(10)
Cu1_1	C1_1	1.899(2)
N1_1	C1_1	1.345(3)
N1_1	C14_1	1.487(3)
N2_1	C1_1	1.357(3)
N2_1	C17_1	1.475(3)
C14_1	C15_1	1.501(4)
C15_1	C16_1	1.543(4)
C16_1	C17_1	1.507(4)
Cu1_2	C1_2	1.899(2)
N1_2	C1_2	1.345(3)
N1_2	C14_2	1.487(3)
N2_2	C1_2	1.357(3)
N2_2	C17_2	1.475(3)
C14_2	C15_2	1.501(4)
C15_2	C16_2	1.543(4)
C16_2	C17_2	1.507(4)

Table 4.6 Bond Angle (deg) for **19**

Atom	Atom	Atom	Angle/°
C3	C2	N1_1	122.6(3)
C3	C2	N1_2	116.3(3)
C10	C2	C3	122.0(2)
C10	C2	N1_1	115.3(3)
C10	C2	N1_2	121.6(3)
C2	C3	C4	122.8(2)
C7	C3	C2	117.9(2)
C7	C3	C4	119.3(2)
C3	C4	C5	110.5(2)
C3	C4	C6	111.3(3)
C6	C4	C5	112.1(3)
C8	C7	C3	121.4(3)
C9	C8	C7	119.8(3)
C8	C9	C10	121.0(3)
C2	C10	C9	117.9(2)
C2	C10	C11	122.8(2)
C9	C10	C11	119.3(2)
C10	C11	C12	111.4(2)
C10	C11	C13	111.1(3)
C12	C11	C13	109.7(3)
C19	C18	N2_1	114.5(3)
C19	C18	N2_2	120.7(2)
C26	C18	C19	122.0(2)
C26	C18	N2_1	123.4(3)
C26	C18	N2_2	117.3(2)
C18	C19	C20	122.6(2)
C23	C19	C18	117.7(2)
C23	C19	C20	119.7(2)
C19	C20	C21	111.1(3)
C19	C20	C22	110.9(2)
C22	C20	C21	111.0(3)
C24	C23	C19	121.5(3)
C23	C24	C25	119.8(3)
C26	C25	C24	120.6(3)
C18	C26	C25	118.4(2)
C18	C26	C27	122.8(2)
C25	C26	C27	118.8(2)
C26	C27	C28	111.7(2)
C26	C27	C29	111.2(3)
C29	C27	C28	111.1(3)
S1[1]	S1	Cu1_1	99.66(6)
S1[1]	S1	Cu1_2	99.66(6)
C1_1	Cu1_1	S1	171.87(12)
C2	N1_1	C14_1	115.3(2)
C1_1	N1_1	C2	115.6(2)
C1_1	N1_1	C14_1	129.05(19)
C18	N2_1	C17_1	115.1(2)
C1_1	N2_1	C18	116.97(18)
C1_1	N2_1	C17_1	127.70(19)
N1_1	C1_1	Cu1_1	123.14(16)
N1_1	C1_1	N2_1	117.8(2)
N2_1	C1_1	Cu1_1	117.60(15)
N1_1	C14_1	C15_1	113.67(19)
C14_1	C15_1	C16_1	112.3(2)
C17_1	C16_1	C15_1	111.9(2)
N2_1	C17_1	C16_1	114.13(18)
C1_2	Cu1_2	S1	173.60(9)
C2	N1_2	C14_2	113.21(19)
C1_2	N1_2	C2	117.48(19)
C1_2	N1_2	C14_2	129.07(19)
C18	N2_2	C17_2	117.1(2)
C1_2	N2_2	C18	114.91(19)
C1_2	N2_2	C17_2	127.68(19)
N1_2	C1_2	Cu1_2	123.15(16)
N1_2	C1_2	N2_2	117.8(2)
N2_2	C1_2	Cu1_2	117.60(15)
N1_2	C14_2	C15_2	113.68(19)
C14_2	C15_2	C16_2	112.3(2)
C17_2	C16_2	C15_2	111.9(2)
N2_2	C17_2	C16_2	114.12(18)

4.5 References

[1] Moore, P. K.; Bhatia, M.; Moochhala, S. *Trends Pharmacol. Sci.* **2003**, *24*, 609-611.

[2] Yang, G.; Wu, L.; Jiang, B.; Yang, W.; Qi, J.; Cao, K.; Meng, Q.; Mustafa, A. K.; Mu, W.; Zhang, S.; Snyder, S. H.; Wang, R. *Science* **2008**, *322*, 587-590.

[3] Filipovic, M. R.; Miljkovic, J. L.; Nauser, T.; Royzen, M.; Klos, K.; Shubina, T.; Koppenol, W. H.; Lippard, S. J.; Ivanović-Burmazović, I. *J. Am. Chem. Soc.* **2012**, *134*, 12016-12027.

[4] Wedmann, R.; Zahl, A.; Shubina, T. E.; Dürr, M.; Heinemann, F. W.; Bugenhagen, B. E. C.; Burger, P.; Ivanovic-Burmazovic, I.; Filipovic, M. R. *Inorg. Chem.* **2015**, *54*, 9367-9380

[5] Ivanovic-Burmazovic, I.; Filipovic, M. R. *Inorg. Chem.* **2019**, *58*, 4039-4051

[6] Nava, M.; Martin-Drumel, M.-A.; Lopez, C. A.; Crabtree, K. N.; Womack, C. C.; Nguyen, T. L.; Thorwirth, S.; Cummins, C. C.; Stanton, J. F.; McCarthy, M. C. *J. Am. Chem. Soc.* **2016**, *138*, 11441-11444.

[7] Quiroga, S. L.; Almaraz, A. E.; Amorebieta, V. T.; Perissinotti, L. L.; Olabe, J. A. *Chem. Eur. J.* **2011**, *17*, 4145-4156

[8] Filipovic, M. R.; Eberhardt, M.; Prokopovic, V.; Mijuskovic, A.; Orescanin-Dusic, Z.; Reeh, P.; Ivanovic-Burmazovic, I. *J. Med. Chem.* **2013**, *56*, 1499-1508.

[9] Miljkovic, J. L.; Kenkel, I.; Ivanović-Burmazović, I.; Filipovic, M. R. A*ngew. Chem. Int. Ed.* **2013**, *52*, 12061-12064.

[10] Hartmann, N. J.; Wu, G.; Hayton, T. W. *J. Am. Chem. Soc.* **2016**, *138*, 12352-12355.

[11] Chatterjee, D.; Sarkar, P.; Oszajca, M.; van Eldik, R. *Inorg. Chem.* **2016**, *55*, 5037-5040.

[12] Seel, F.; Kuhn, R.; Simon, G.; Wagner, M.; Krebs, B.; Dartmann, M. *Z. Naturforsch., B: Anorg. Chem., Org. Chem.* **1985**, *40B*, 1607-1617.

[13] Pauleta, S. R.; Dell'Acqua, S.; Moura, I. *Coord. Chem. Rev.* **2013**, *257*, 332-349.

[14] Gourlay, C.; Nielsen, D. J.; White, J. M.; Knottenbelt, S. Z.; Kirk, M. L.; Young, C. G. *J. Am. Chem. Soc.* **2006**, *128*, 2164-2165.

[15] Dehnen, S.; Eichhofer, A.; Fenske, D. *Eur. J. Inorg. Chem.* **2002**, 279-317.

[16] Fuhr, O.; Dehnen, S.; Fenske, D. C. *Chem. Soc. Rev.* **2013**, *42*, 1871-1906.

[17] Di Francesco, G. N.; Gaillard, A.; Ghiviriga, I.; Abboud, K. A.; Murray, L. J. *Inorg. Chem.* **2014**, *53*, 4647-4654.

[18] Johnson, B. J.; Lindeman, S. V.; Mankad, N. P. *Inorg. Chem.* **2014**, *53*, 10611-10619.

[19] Johnson, B. J.; Antholine, W. E.; Lindeman, S. V.; Mankad, N. P. *Chem. Commun.* **2015**, *51*, 11860-11863.

[20] Zhai, J.; Hopkins, M. D.; Hillhouse, G. L. Synthesis and Structure of a CuI3S Cluster Unsupported by Other Bridging Ligands. *Organometallics* **2015**, *34*, 4637-4640.

[21] Johnson, B. J.; Antholine, W. E.; Lindeman, S. V.; Graham, M. J.; Mankad, N. P. *J. Am. Chem. Soc.* **2016**, *138*, 13107-13110.

[22] Maji, R. C.; Das, P. P.; Bhandari, A.; Mishra, S.; Maji, M.; Ghiassi, K. B.; Olmstead, M. M.; Patra, A. K. *Chem. Commun.* **2017**, *53*, 3334-3337.

[23] Polgar, A. M.; Weigend, F.; Zhang, A.; Stillman, M. J.; Corrigan, J. F. *J. Am. Chem. Soc.* **2017**, *139*, 14045-14048.

[24] Cook, B. J.; Di Francesco, G. N.; Abboud, K. A.; Murray, L. J. *J. Am. Chem. Soc.* **2018**, *140*, 5696-5700.

[25] Polgar, A. M.; Zhang, A.; Mack, F.; Weigend, F.; Lebedkin, S.; Stillman, M. J.; Corrigan, J. F. *Inorg. Chem.* **2019**, *58*, 3338-3348.

[26] Zhai, J.; Filatov, A. S.; Hillhouse, G. L.; Hopkins, M. D. *Chem. Sci.* **2016**, *7*, 589-595.

[27] Fujisawa, K.; Moro-oka, Y.; Kitajima, N. *J. Chem. Soc. Chem. Commun.* **1994**, 623-624.

[28] Chen, P.; Fujisawa, K.; Helton, M. E.; Karlin, K. D.; Solomon, E. I. *J. Am. Chem. Soc.* **2003**, *125*, 6394-6408.

[29] Helton, M. E.; Chen, P.; Paul, P. P.; Tyeklár, Z.; Sommer, R. D.; Zakharov, L. N.; Rheingold, A. L.; Solomon, E. I.; Karlin, K. D. *J. Am. Chem. Soc.* **2003**, *125*, 1160-1161.

[30] Brown, E. C.; Aboelella, N. W.; Reynolds, A. M.; Aullon, G.; Alvarez, S.; Tolman, W. B. *Inorg. Chem.* **2004**, *43*, 3335-3337.

[31] Brown, E. C.; Bar-Nahum, I.; York, J. T.; Aboelella, N. W.; Tolman, W. B. *Inorg. Chem.* **2007**, *46*, 486-496.

[32] Maiti, D.; Woertink, J. S.; Vance, M. A.; Millign, A. E.; Narducci Sarjeant, A. A.; Solomon, E. I.; Karlin, K. D. *J. Am. Chem. Soc.* **2007**, *129*, 8882-8892.

[33] Kajita, Y.; Matsumoto, J.; Takahashi, I.; Hirota, S.; Funahashi, Y.; Ozawa, T.; Masuda, H. *Eur. J. Inorg. Chem.* **2008**, 3977-3986.

[34] Sarangi, R.; York, J. T.; Helton, M. E.; Fujisawa, K.; Karlin, K. D.; Tolman, W. B.; Hodgson, K. O.; Hedman, B.; Solomon, E. I. *J. Am. Chem. Soc.* **2008**, *130*, 676-686.

[35] Yang, L.; Tehranchi, J.; Tolman, W. B. *Inorg. Chem.* **2011**, *50*, 2606-2612.

[36] Prabhakaran, R.; Kalaivani, P.; Renukadevi, S. V.; Huang, R.; Senthilkumar, K.; Karvembu, R.; Natarajan, K. *Inorg. Chem.* **2012**, *51*, 3525-3532.

[37] Bagherzadeh, S.; Mankad, N. P. *Chem. Commun.* **2018**, *54*, 1097-1100.

[38] Zhang, S.; Melzer, M. M.; Sen, S. N.; Celebi-Olcum, N.; Warren, T. H. *Nat. Chem.* **2016**, *8*, 663-669.

[39] Melzer, M. M.; Li, E.; Warren, T. H. *Chem. Commun.* **2009**, 5847-5849.

[40] Jordan, A. J.; Wyss, C. M.; Bacsa, J.; Sadighi, J. P. *Organometallics* **2016**, *35*, 613-616.

[41] Doyle, M. P.; Terpstra, J. W.; Pickering, R. A.; LePoire, D. M. *J. Org. Chem.* **1983**, *48*, 3379-3382.

[42] Veenboer, R. M. P.; Collado, A.; Dupuy, S.; Lebl, T.; Falivene, L.; Cavallo, L.; Cordes, D. B.; Slawin, A. M. Z.; Cazin, C. S. J.; Nolan, S. P. *Organometallics* **2017**, *36*, 2861-2869.

[43] Connelly, N. G.; Geiger, W. E. Chemical Redox Agents for Organometallic Chemistry. *Chem. Rev.* **1996**, *96*, 877-910.

[44] Stephen Hartman, J.; Shoemaker, J. A. W.; Janzen, A. F.; Ragogna, P. J.; Szerminski, W. R. *J. Fluorine Chem.* **2003**, *119*, 125-139.

CHAPTER 5. CONCLUSION

5.1 Thesis Overview

This thesis describes the synthesis, characterization and reactivity of a variety of N-heterocyclic carbene supported copper(I) complexes. The body of this work broadly provides advances in copper hydride and sulfide chemistries in addition to C–F bond forming processes. The use of sterically demanding, electron-rich expanded-ring NHCs proved vital to much to the chemistry discussed above.

The first section discusses the use of expanded-ring NHCs to stabilize copper(I) hydride dimers. The increased stability is imparted from the increased steric encumbrance around the $\{Cu_2(\mu\text{-}H_2)\}$ core. In addition to the increased stability, the expanded-ring NHC supported copper hydride dimers remain reactive towards CO_2, unactivated alkenes, and isonitriles. The 1,2-insertion of a copper(I) hydride is an important step in a number of copper-hydride-catalyzed transformations, particularly the hydroamination of alkenes.[1] The 1,1-insertion of an isonitrile has since been suggested as a key step, and the resulting copper(I) formidoyl to be an important intermediate, in the synthesis of quaternary formimides and aldehydes.[2] The expanded-ring NHC copper(I) hydrides presented in this chapter, $[(6Dipp)CuH]_2$ and $[(7Dipp)CuH]_2$, proved useful synthons in Chapters 3 and 4, respectively.

The following section described the copper-mediated *cis*-borofluorination of alkynes to monofluoroalkenes. This was achieved by a 1,2-insertion of an NHC supported copper(I) boryl across an alkyne to generate a *cis*-copper(I) borovinyl. Electrophilic

fluorination by NFSI releases the *cis*-borofluoroalkene, easily converted to and isolated as a potassium trifluoroborate salt. Particularly interesting is the ability of this system to selectively install the fluorine functionality at the terminal position, when starting with a terminal alkyne. The *cis*-borofluroalkenes could be further derivatized by palladium-catalyzed Suzuki-Miyuara coupling or simple oxidation to the α-fluoroketone. The catalytic conversion of terminal alkynes to terminal fluoroalkenes has yet to be realized, but this study has laid out much of the framework for that to occur.

Chapter 4 presented the synthesis and nitrosonium reactivity of NHC supported copper(I) sulfide, disulfide and hydrosulfide complexes. The sterically demanding expanded-ring NHC 7Dipp, proved capable of supporting the reactive low-nuclearity copper-sulfide clusters. Reaction of NO^+ with both the dicopper(I) sulfide and disulfide results in oxidation to the bridging sulfur to elemental sulfur and release of the (NHC)copper(I) cation. Conversely, elemental sulfur and ammonium ion formation results from the reaction of the copper(I) hydrosulfide and NO^+. These are suggested to form through the decomposition of HSNO. Similarly, ammonium ion formation is evident from reaction of the $[(7Dipp)CuH]_2$ with NO^+, proposed to occur through decomposition of HNO. These investigations suggested possible reactivity of NO and H_2S "cross-talk" products with copper(I) complexes.

5.2 Future Copper-Mediated Processes for Organic Transformations

5.2.1 Copper-Catalyzed C–O Bond Formation

The new organocopper chemistry presented above, particularly that described in Chapters 2 and 3, could lead to many potentially exciting catalytic transformations. First,

well-defined (NHC)copper(I) alkyl, vinyl and aryl complexes could serve as a platform to study reactivity with O_2, or an O-atom transfer reagent, to develop new C–O bond forming processes and better understand their oxidation chemistry. Molecular dioxygen would be the ideal oxidant, as it is abundant, inexpensive, and environmentally benign.[3] Insertion of an O-atom into the Cu–C bond would generate new copper(I) alkoxide, enolate or phenoxide species (Scheme 5.1). This route is perhaps most promising for the copper(I) vinyl or aryl species, because oxidative coupling or β-hydride elimination are likely for Cu(I) alkyl complexes.[4] The outcomes will provide valuable understanding of the reactivity of organocopper species under oxidizing conditions, and one can envision incorporating this reactivity into other catalytic cycles for the oxidation of saturated organic compounds or C–C bond formation.

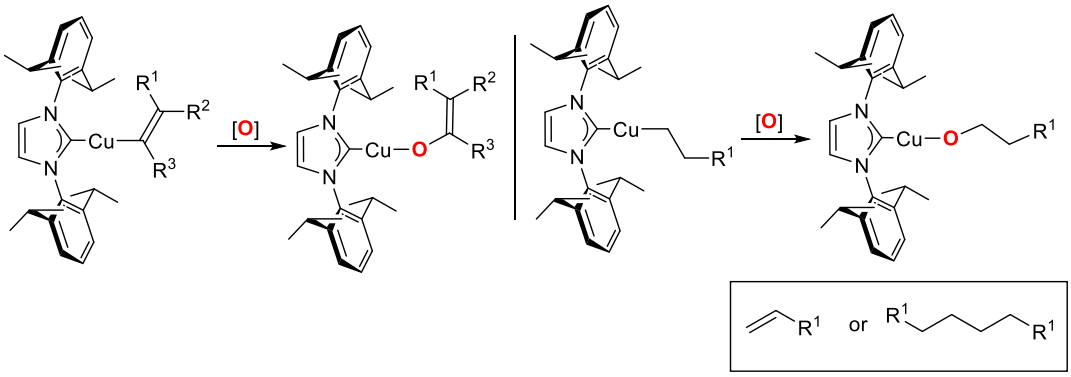

Figure 5.1 Oxidation of NHC supported organocopper species.

Following O-atom insertion, possibilities for incorporation as a key step in catalytic C–O bond forming processes become evident. Possible aryl or vinyl ether formations are outlined in Scheme 5.2. One such process of interest is the formation of silyl enol ethers from alkynes; Silyl enol ethers are useful and versatile reagents, often used in C–C bond-forming reactions.[5] The 1,2-insertion and transmetalation steps are well-studied

organometallic transformations described in Chapter 1, and Si–O or Cu–X bond formations are favorable.[6] Additionally, O-atom insertion from common O-atom transfer reagents such pyridine-*N*-oxide or trimethylamine *N*-oxide could also be studied.

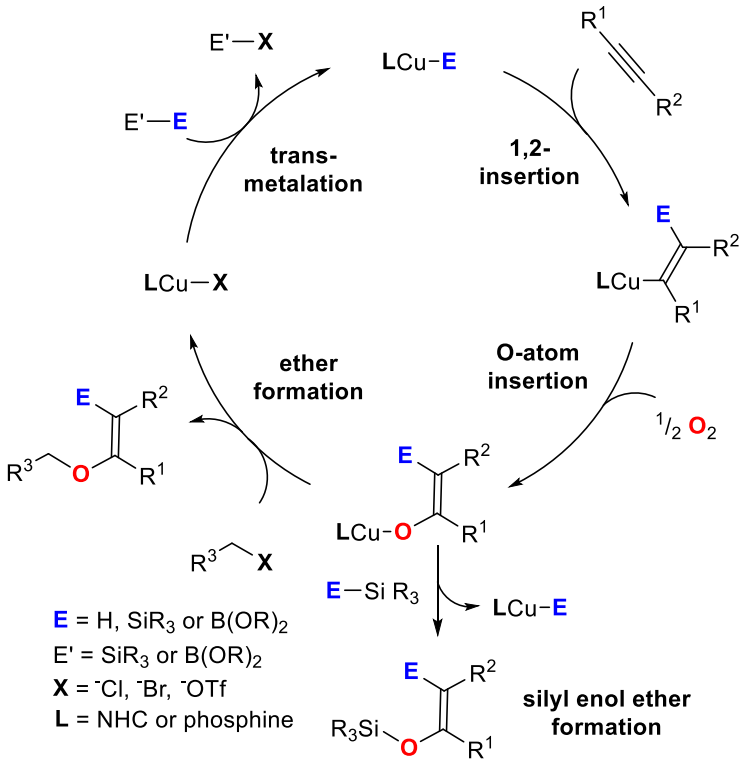

Scheme 5.2 Proposed copper-catalyzed synthesis of silyl-enol ethers from alkynes.

5.2.2 Copper-Catalyzed Functionalization of Donor-Acceptor Cyclopropanes

There continue to be tremendous advances in Donor-Acceptor (DA) cyclopropane chemistry,[7] and their reactivity with well-defined organocopper species could yield new organometallic transformations. Addition of NHC-supported copper(I) fluorides to DA cyclopropanes could provide valuable new avenues for C–F bond construction. Reaction with a DA cyclopropane could lead to fluorine installation α to the donor and the Cu α to the acceptor, thus creating new C–F and Cu–C bonds. The copper(I) alkyl could

conceivably undergo a number well-studied of transformation to yield new C–H, C–N or C–B bonds (Scheme 5.3). Conversely, a copper(I) hydride, boryl or alkyl could react similarly, first installing functionality, then followed by electrophilic functionalization. For example, NFSI could be used to generate a new C–F bond.

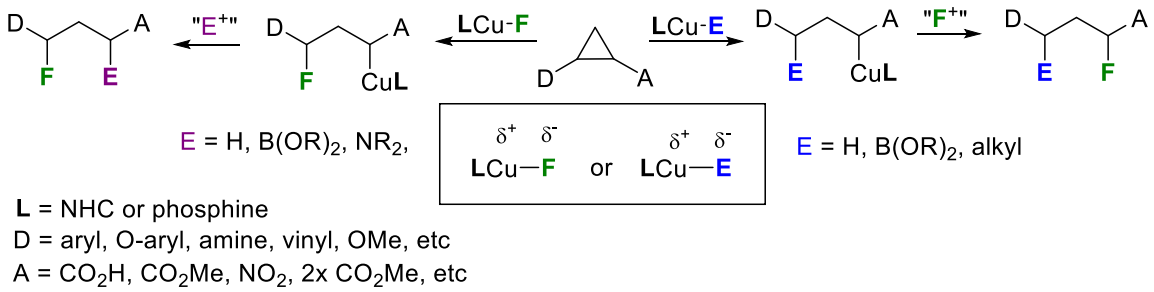

Scheme 5.3 Addition of copper(I) fluorides and organocopper complexes to cyclopropanes.

5.3 New Low-Nuclearity Copper(I) Complexes.

5.3.1 Towards Monomeric Copper(I) Hydrides

As mentioned in Chapter 1, Bertrand and coworkers recently provided spectroscopic evidence for a monomeric copper(I) hydride, in equilibrium with the dimer.[8] The extremely bulky ligand IPr** (IPr** = 1,3-bis[2,6-bis[di(4-*tert*-butylphenyl)methyl]-4-methylphenyl]imidazol-2-ylidene) was employed to achieve this. The related ligand IPr* (IPr* = 1,3-bis(2,6-(diphenylmethyl)-4-methylphenyl)imidazol-2-ylidene) was used by Hillhouse and coworkers to isolate the first dicopper(I) bridged-sulfide.[9] These both feature large N-aryl substituents that could be employed in combination with expanded-ring backbones, to yield extremely sterically demanding NHC ligands (Scheme 5.4). This could permit isolation of a monomeric copper(I) hydride. The proposed synthesis is outlined in Scheme 5.4 and is analogous to the synthesis of $[(6Dipp)CuH]_2$ and $[(7Dipp)CuH]_2$. Since

the active species in copper-hydride-catalyzed reaction is suggested to be the monomeric form, an isolable terminal copper(I) hydride should be highly reactive.

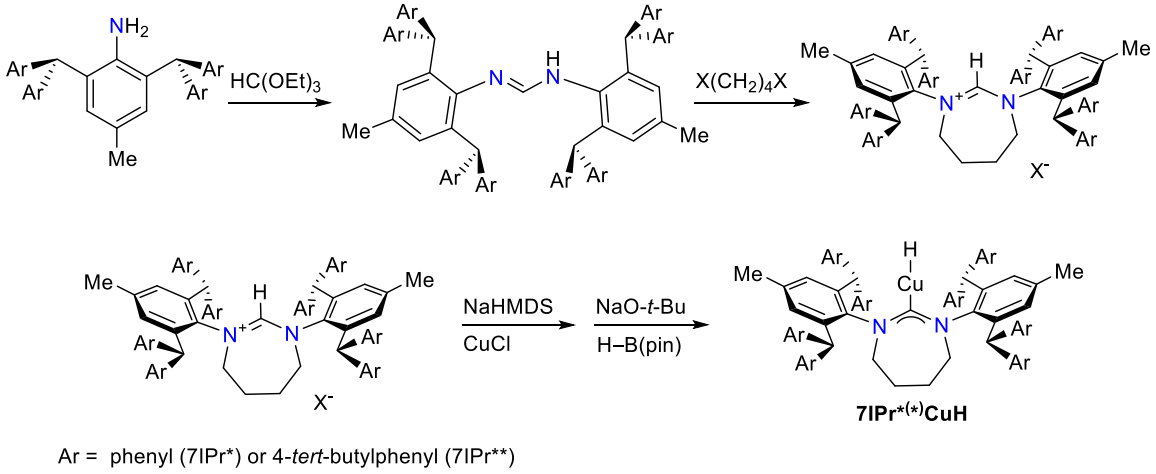

Scheme 5.4 Proposed Synthesis of mononuclear copper(I) hydride.

5.3.2 Low-Nuclearity Chalcogenide-Bridged Complexes

Although the reactivity of the low-nuclearity copper(I) sulfide compounds have been studied within this thesis, they remain an understudied class of molecules. Of specific interest would be to study of their material properties, optical properties particularly, to compare those to larger copper sulfide clusters. These studies could also include low-nuclearity congeners of copper-sulfide clusters. Other chalcogenide-bridged dicopper(I) complexes could be synthesized via analogous routes described in Chapter 4 and would be of much interest (Scheme 5.5). A dicopper(I) oxide has been invoked,[10] but not fully characterized or studied, and is presumed to be very nucleophilic. Conversely, the neutral dinuclear species bridged by chalcogenides heavier chalcogenides have not been studied, but many larger-nuclearity selenide and telluride clusters have garnered interest.[11] Furthermore, the related complexes with silver(I) and gold(I) could be compared. Lastly,

low-nuclearity chalcogenide-bridged complexes of other d^{10} metals, such as zinc(II) or cadmium(II) might show interesting optical properties. Such compounds could be realized with the use of sterically encumbering anionic ligands.

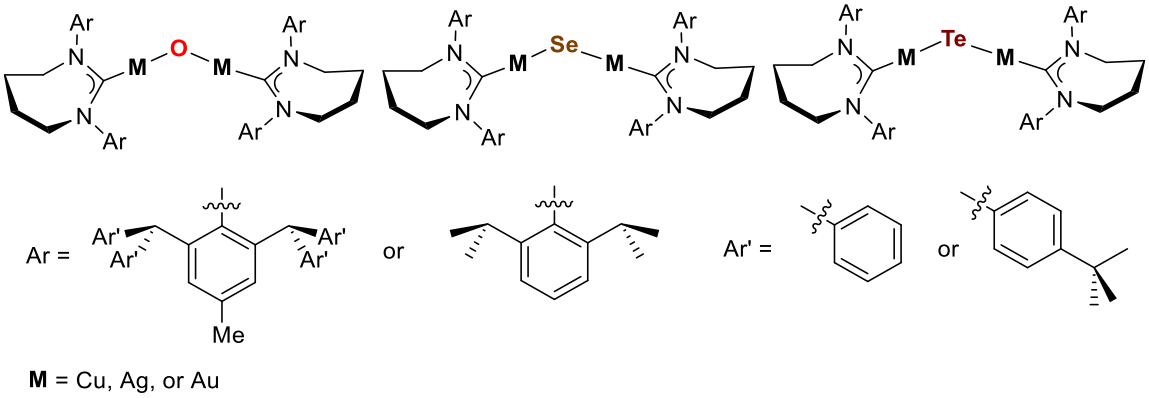

Figure 5.5 Proposed group 11 chalcogenide-bridged complexes.

5.4 References

[1] Yang, Y.; Shi, S.-L.; Niu, D.; Liu, P.; Buchwald, S. L. *Science* **2015**, *349*, 62-66

[2] Hojoh, K.; Ohmiya, H.; Sawamura, M. *J. Am. Chem. Soc.* **2017**, *139*, 2184-2187.

[3] Boisvert, L.; Goldberg, K. I. *Acc. Chem. Res.* **2012**, *45*, 899-910.

[4] Goj, L. A.; Blue, E. D.; Delp, S. A.; Gunnoe, T. B.; Cundari, T. R.; Petersen, J. L. *Organometallics* **2006**, *25*, 4097-4104.

[5] Pramanik, S.; Rej, S.; Kando, S.; Tsurugi, H.; Mashima, K. *J. Org. Chem.* **2018**, *83*, 2409-2417.

[6] Jordan, A. J.; Lalic, G.; Sadighi, J. P. *Chem. Rev.* **2016**, *116*, 8318-8372.

[7] (a) Ebner, C.; Carreira, E. M. *Chem. Rev.* **2017**, *117*, 11651-11679; (b) Cavitt, M. A.; Phun, L. H.; France, S. *Chem. Soc. Rev.* **2014**, *43*, 804-818; (c) Budynina, E. M.; Ivanov, K. L.; Sorokin, I. D.; Melnikov, M. Y. *Synthesis* **2017**, *49*, 3035-3068; (d) Schneider, T. F.; Kaschel, J.; Werz, D. B. *Angew. Chem., Int. Ed.* **2014**, *53*, 5504-5523.

[8] Romero, E. A.; Olsen, P. M.; Jazzar, R.; Soleilhavoup, M.; Gembicky, M.; Bertrand, G. *Angew. Chem., Int. Ed.* **2017**, *56*, 4024-4027.

[9] Zhai, J.; Filatov, A. S.; Hillhouse, G. L.; Hopkins, M. D. *Chem. Sci.* **2016**, *7*, 589-595.

[10] Bagherzadeh, S.; Mankad, N. P. *Chem. Commun.* **2018**, *54*, 1097-1100.

[11] Fuhr, O.; Dehnen, S.; Fenske, D. *Chem. Soc. Rev.* **2013**, *42*, 1871-1906.

APPENDIX A. COLLABORATOR CONTRIBUTIONS

Much of the research presented in this thesis was the result of collaborative efforts. This appendix serves to credit collaborators and their respective contributions.

A.1 Synthesis and Reactivity of New Copper(I) Hydride Dimers

Dr. Chelsea M. Wyss contributed significantly to the development of synthetic methods. Dr. John Bacsa performed all X-ray diffraction studies and solved all solid-state structures.

A.2 Copper(I)-Mediated Borofluorination of Alkynes

Ms. Percie K. Thompson performed several optimization and scope determining studies for this chapter under my guidance.

A.3 Nitrosonium Reactivity of (NHC)Copper(I) Sulfide Complexes

Ms. Rebecca K. Walde and Ms. Kelly M. Schultz performed several synthesis and reactivity studies for this chapter under my guidance. Dr. John Bacsa performed all X-ray diffraction studies and solved all solid-state structures.

APPENDIX B. PERMISSIONS TO REPRODUCE PUBLISHED MATERIAL

Part of these thesis chapters have been adapted with permission from articles co-written by the author:

B.1 Chapter 1. Introduction

Jordan, A. J.; Lalic, G.; Sadighi, J. P. Coinage Metal Hydrides: Synthesis, Characterization, and Reactivity. *Chem. Rev.* **2016**, *116*, 8318-8372.

https://pubs.acs.org/doi/abs/10.1021/acs.chemrev.6b00366 (accessed June 2019)

B.2 Chapter 2. Synthesis and Reactivity of New Copper(I) Hydride Dimers

Jordan, A. J.; Wyss, C. M.; Bacsa, J.; Sadighi, J. P. Synthesis and Reactivity of New Copper(I) Hydride Dimers. *Organometallics* **2016**, *35*, 613-616.

https://pubs.acs.org/doi/abs/10.1021/acs.organomet.6b00025 (accessed June 2019)

B.3 Chapter 3. Copper(I)-Mediated Borofluorination of Alkynes

Jordan, A. J.; Thompson, P. K.; Sadighi, J. P. Copper(I)-Mediated Borofluorination of Alkynes. *Org. Lett.* **2018**, *20*, 5242-5246.

https://pubs.acs.org/doi/abs/10.1021/acs.orglett.8b02195 (accessed June 2019)

B.4 Chapter 4. Nitrosonium Reactivity of (NHC)Copper(I) Sulfide Complexes

Jordan, A. J.; Walde, R. K; Schultz, K. M.; Bacsa, J.; Sadighi. J. P. Nitrosonium Reactivity of (NHC)Copper(I) Sulfide Complexes. *Inorg. Chem.* **2019**, *Article Accepted*

VITA

Abraham J. Jordan

Abe grew up in Weedsport, NY and graduated from Weedsport High School in 2010. He attended the Virginia Military Institute with the class of 2014, majoring in chemistry. While at VMI he conducted undergraduate research with Daren J. Timmons, and in the summer of 2012 worked in Daniel A. Clark's research group at Syracuse University. He attended graduate school at the Georgia Institute of Technology, where he conducted graduate research under the supervision of Joseph P. Sadighi and obtained his Ph.D. in chemistry in 2019.